

THESE TERMS GOVERN YOUR USE OF THIS DOCUMENT

Your use of this Ontario Geological Survey document (the “Content”) is governed by the terms set out on this page (“Terms of Use”). By downloading this Content, you (the “User”) have accepted, and have agreed to be bound by, the Terms of Use.

Content: This Content is offered by the Province of Ontario’s *Ministry of Northern Development and Mines* (MNDM) as a public service, on an “as-is” basis. Recommendations and statements of opinion expressed in the Content are those of the author or authors and are not to be construed as statement of government policy. You are solely responsible for your use of the Content. You should not rely on the Content for legal advice nor as authoritative in your particular circumstances. Users should verify the accuracy and applicability of any Content before acting on it. MNDM does not guarantee, or make any warranty express or implied, that the Content is current, accurate, complete or reliable. MNDM is not responsible for any damage however caused, which results, directly or indirectly, from your use of the Content. MNDM assumes no legal liability or responsibility for the Content whatsoever.

Links to Other Web Sites: This Content may contain links, to Web sites that are not operated by MNDM. Linked Web sites may not be available in French. MNDM neither endorses nor assumes any responsibility for the safety, accuracy or availability of linked Web sites or the information contained on them. The linked Web sites, their operation and content are the responsibility of the person or entity for which they were created or maintained (the “Owner”). Both your use of a linked Web site, and your right to use or reproduce information or materials from a linked Web site, are subject to the terms of use governing that particular Web site. Any comments or inquiries regarding a linked Web site must be directed to its Owner.

Copyright: Canadian and international intellectual property laws protect the Content. Unless otherwise indicated, copyright is held by the Queen’s Printer for Ontario.

It is recommended that reference to the Content be made in the following form:

Smith, L., Charbonneau, S.L. and Grimes, D.J. 1993. Karst episodes and permeability development, Silurian reef reservoirs, Southwestern Ontario, Ontario Geoscience Research Grant Program, Grant No. 295; Ontario Geological Survey, Open File Report 5850, 240p.

Use and Reproduction of Content: The Content may be used and reproduced only in accordance with applicable intellectual property laws. *Non-commercial* use of unsubstantial excerpts of the Content is permitted provided that appropriate credit is given and Crown copyright is acknowledged. Any substantial reproduction of the Content or any *commercial* use of all or part of the Content is prohibited without the prior written permission of MNDM. Substantial reproduction includes the reproduction of any illustration or figure, such as, but not limited to graphs, charts and maps. Commercial use includes commercial distribution of the Content, the reproduction of multiple copies of the Content for any purpose whether or not commercial, use of the Content in commercial publications, and the creation of value-added products using the Content.

Contact:

| FOR FURTHER INFORMATION ON | PLEASE CONTACT: | BY TELEPHONE: | BY E-MAIL: |
|-----------------------------------|---------------------------|--|--|
| The Reproduction of Content | MNDM Publication Services | Local: (705) 670-5691 Toll Free: 1-888-415-9845, ext. 5691 (inside Canada, United States) | pubsales.ndm@ontario.ca |
| The Purchase of MNDM Publications | MNDM Publication Sales | Local: (705) 670-5691 Toll Free: 1-888-415-9845, ext. 5691 (inside Canada, United States) | pubsales.ndm@ontario.ca |
| Crown Copyright | Queen’s Printer | Local: (416) 326-2678 Toll Free: 1-800-668-9938 (inside Canada, United States) | copyright@gov.on.ca |



Ministry of
Northern Development
and Mines

Ontario

**Ontario Geological Survey
Open File Report 5850**

**Ontario Geoscience Research
Grant Program
Grant No. 295**

**Karst Episodes and
Permeability Development,
Silurian Reef Reservoirs,
Southwestern Ontario**

1993



Ministry of
Northern Development
and Mines

Ontario

ONTARIO GEOLOGICAL SURVEY

Open File Report 5850

Karst Episodes and Permeability Development, Silurian Reef Reservoirs,
Southwestern Ontario

By

L. Smith, S.L. Charbonneau and D.J. Grimes

1993

Parts of this publication may be quoted if credit is given. It is recommended that reference to this publication be made in the following form:

Smith, L, Charbonneau, S.L. and Grimes, D.J. 1993. Karst episodes and permeability development, Silurian reef reservoirs, Southwestern Ontario, Ontario Geoscience Research Grant Program, Grant No. 295; Ontario Geological Survey, Open File Report 5850, 240p.

Ontario Geological Survey

OPEN FILE REPORT

Open File Reports are made available to the public subject to the following conditions:

This report is unedited. Discrepancies may occur for which the Ontario Geological Survey does not assume liability. Recommendations and statements of opinions expressed are those of the author or authors and are not to be construed as statements of government policy.

This Open File Report is available for viewing at the following locations:

Mines Library
Level A3, 933 Ramsey Lake Road
Sudbury, Ontario P3E 6B5

Mines and Minerals Information Centre (MMIC)
Rm. M2-17, Macdonald Block
900 Bay St.
Toronto, Ontario M7A 1C3

The office of the Resident Geologist whose district includes the area covered by this report.

Copies of this report may be obtained at the user's expense from:

OGS On-Demand Publications
Level B4, 933 Ramsey Lake Road
Sudbury, Ontario P3E 6B5
Tel. (705) 670-5691 Collect calls accepted.

Microfiche copies (42x reduction) of this report are available for \$2.00 each plus provincial sales tax at MMIC.

Handwritten notes and sketches may be made from this report. Check with MMIC, the Mines Library or the Resident Geologist's office whether there is a copy of this report that may be borrowed. A copy of this report is available for Inter-Library loan.

This report is available for viewing at the following Resident Geologists' offices:

Southwestern, Box 5463, 659 Exeter Rd., London N6A 4L6

The right to reproduce this report is reserved by the Ontario Ministry of Northern Development and Mines. Permission for other reproductions must be obtained in writing from the Director, Ontario Geological Survey - Geoscience Branch.

CONTENTS

| | |
|--|----|
| ABSTRACT..... | iv |
| INTRODUCTION..... | 2 |
| TECTONIC AND ENVIRONMENTAL CONTROLS..... | 2 |
| DEPOSITIONAL HISTORY..... | 4 |
| PINNACLE REEF FACIES..... | 4 |
| PLATFORM REEF FACIES..... | 6 |
| SUBAERIAL EXPOSURE..... | 6 |
| KARST FACIES IN BIOHERMS..... | 6 |
| INTER-REEF KARST FACIES..... | 7 |
| FACIES CHANGES—CAUSES..... | 9 |
| DIAGENETIC HISTORY..... | 9 |
| PINNACLE BIOHERMS..... | 10 |
| PLATFORM BIOHERMS..... | 10 |
| DOLOMITIZATION..... | 10 |
| ISOTOPE ANALYSIS..... | 11 |
| HYDROCARBON/STORAGE RESERVOIRS..... | 11 |
| POROSITY/PERMEABILITY..... | 12 |
| CONCLUSIONS..... | 13 |
| ACKNOWLEDGEMENTS..... | 14 |
| REFERENCES..... | 15 |
| APPENDIX I Plates showing karst features in Silurian reef bioherms, Southwestern Ontario..... | 18 |
| APPENDIX II M. Sc. Thesis Report of Steven L. Charbonneau..... | 25 |
| CONVERSION TABLE..... | |

FIGURES

| | |
|---|---|
| Figure 1 Location of reef bioherm reservoirs and inter-reef well, southwestern Ontario..... | 3 |
| Figure 2 Stratigraphic section of the Union Enniskillen 8-9-II A (Rosedale) core showing depositional, organic, and karstic features (from Grimes, 1987)..... (Back pocket) | |
| Figure 3 Stratigraphic section of the Ram 5, Sombra 2-24-IX (Terminus) core showing depositional, organic, and karstic features (from Charbonneau, 1990)..... | 5 |
| Figure 4 Stratigraphic section of the Corden et al. Moore 5 - I inter-reef core showing depositional and karstic features..... | 8 |

ABSTRACT

The Rosedale, Warwick, Terminus, Payne, Wilkesport, and Bayfield pinnacle reef bioherms and the Fletcher platform/bank bioherm are located in the southwestern Ontario subsurface. They are part of the Guelph Formation of Middle Silurian age, which is underlain by the Lockport Formation regional platform, and are enclosed by the evaporitic Salina Formation. Where the bioherms are not present, the Salina rests directly on the Lockport.

Development of these subsurface hydrocarbon reservoirs was governed by cyclic sea level fluctuations. Each rising sea level produced a reef growth episode, each falling sea level caused an episode of exposure with development of paleokarst on the Lockport platform, on the bioherm or on inter-bioherm units.

The bioherms are a succession of depositional facies that vary upward from the regional platform to local wackestone silt mound to reef core and flank complex to restricted algal cap and finally to algal mudstone/boundstone units. The strongest erosional episodes were followed by major changes in the bioherms' depositional facies, whereas other such changes were caused by regional variations in salinity. Thus, major changes in the reefs' organic communities was due to extrinsic factors.

There were eight major episodes of subaerial exposure, so that each pinnacle reef bioherm is a vertical succession of up to seven different biohermal units separated by erosional discontinuities. Each subaerial exposure created laterally-extensive leached zones of enhanced permeability and increased porosity in the then upper portion of each bioherm. Vertical seals were formed by crusts and paleosols, and by the formation of overlying impermeable limestone during the next sea level rise.

There is abundant evidence of diagenesis, in early marine, meteoric vadose and phreatic, post-karstic marine, and burial environments, resulting in different types and generations of pore-occluding calcite cements especially in the lower portion of each bioherm.

Only major karstic episodes could have created the zones of laterally-extensive permeability which constitute the hydrocarbon reservoirs in the middle and upper portions of each bioherm.

Karst Episodes and Permeability Development, Silurian Reef
Reservoirs, Southwestern Ontario

L. Smith, S.L. Charbonneau, and D.J. Grimes

Department of Geological Sciences, Queen's University, Kingston,
Ontario.

INTRODUCTION

Middle Silurian carbonate bioherms are present in the subsurface rocks of southwestern Ontario, within a broad area along the southeastern margin of the Michigan Basin. Over 70% of those that have been located contained hydrocarbon reserves. Some are now used for critical seasonal storage of natural gas. This study of several bioherms is to identify the origin and delineate the three-dimensional geometry of their commercially-useful porosity and permeability.

Figure 1 shows the location of the Rosedale and Terminus Fields in Lambton County and the Fletcher Field in Kent County. The first two reservoirs are contained within laterally-extensive permeable zones in limestone pinnacle-reef bioherms and the Fletcher reservoir is within a dolomitized platform or bank-reef complex. These reefs were chosen as examples of the two principal types of bioherm. All have continuous drill core records. The stratigraphic section of the Rosedale bioherm is given in Figure 2 and that of the Terminus bioherm in Figure 3. The Fletcher section is in Grimes (1987) and that of the Warwick pinnacle is in Smith and Charbonneau (1990). The lithologic columns of Rosedale, Terminus, Warwick, Payne, Wilkesport, and Bayfield are in Charbonneau (1990) (see Appendix II).

The overall purpose of this study is to understand the succession of depositional, karstic, and diagenetic environments that were responsible through time for the present state of the permeable zones and associated cements in the Middle Silurian reefal bioherms of southwestern Ontario.

TECTONIC AND ENVIRONMENTAL CONTROLS

Southwestern Ontario in the mid-Silurian was within the North American Bank - a large region with decreasing tectonic activity. Within this region was an oval area of very slightly differential--downsinking the incipient Michigan Basin. This basinal differential produced only very slight differences in sea water depth, but these were enough to have profound effects on reef location and development.

At the end of a long episode of subaerial exposure, community - reef growth was made possible by overall sea level rise and the end of westward dispersal of the substantial amounts of fine terrigenous sediment which had formed the Rochester Formation.

However, as with the type Wenlockian (Middle Silurian) of Shropshire, being in the midst of a huge regional bank was not ecologically optimal. The very slightly elevated salinities caused the production and dolomitization of the smaller - size brachiopod/crinoid - dominated sediment of the Lockport Formation. In contrast, in the Gotland region of the Baltic, reef bioherms developed at once and produced large skeletal sizes - showing an optimal environment for reef growth.

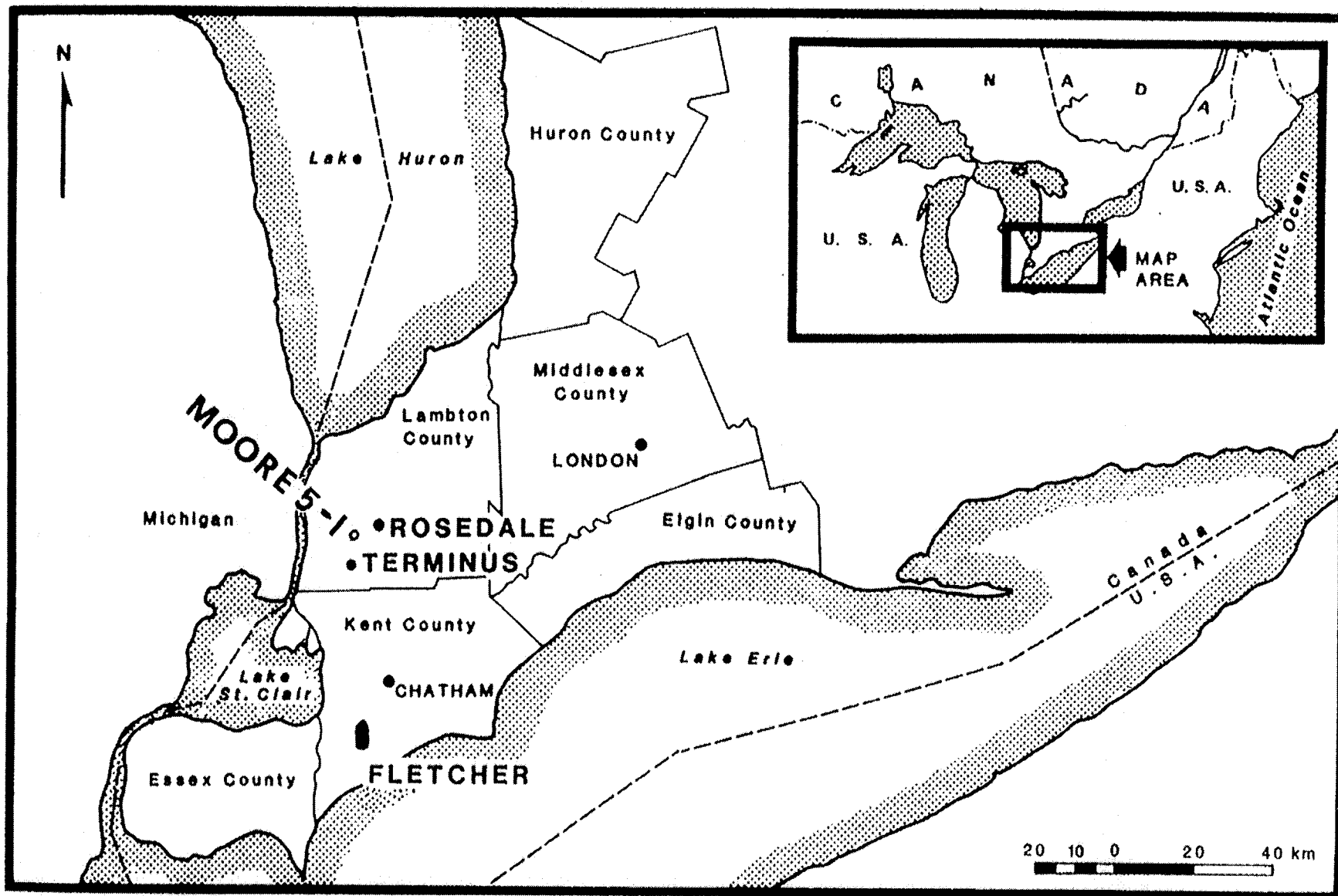


Figure 1. Location of reef bioherm reservoirs and inter-reef well, southwestern Ontario.

Deposition of the regionally-extensive Lockport carbonate platform provided a base for later reef development. Slight freshening of sea water was signalled by an end to dolomitization and by initiation of biohermal reef growth. Broad areas of bank-reef platforms developed over most of North America. Very slightly more rapid downwarping caused deposition of a thin section of the Lockport Formation in the incipient Michigan Basin, and the resulting very gentle slope around its margin allowed only patch reef development on top of slight and very local, crinoidal sand mounds - initiating pinnacle bioherm growth (Trevail and Smith, 1987).

The combined effect of this slightly differential tectonism and the differential bioherm growth that resulted caused the regional thickness variations in the Lockport and Guelph formations shown by Bailey (1986) and delineated in detail in Bailey and Cochrane (1990). Sanford et al. (1985) suggest that rejuvenation of basement fault-blocks controlled both the origin and development of these reservoir units, and this seems to be responsible for some of the platform/bank reef geometries. Prouty (1983) interprets a fault-block influence throughout southern Michigan. Effects on the pinnacle reefs are discussed in Charbonneau (1990) (see Appendix II).

DEPOSITIONAL HISTORY

Once begun, the development of these bioherms was governed by cyclical sea level fluctuations. Raising sea level allowed organic growth on the bioherms, and deposition off-reef of fine carbonate interbedded with storm layers of reef skeletal debris.

PINNACLE REEF FACIES

The first detailed description of the Rosedale bioherm was made by Bainbridge (1973). The fauna of the Warwick reef was studied by Pearson (1980). The present study uses specific and inclusive analyses of cores from these and other Guelph bioherms. With these, the bioherms have been subdivided into the five discrete depositional facies which overlie the regional Lockport platform (Figures 2 and 3).

The Lockport Formation platform facies consists of coalesced mounds and sand waves of abundant crinoid and brachiopod remains. This wackestone unit was regionally dolomitized.

The Guelph Formation pinnacle bioherms developed on this platform. Most began with the carbonate-silt wackestones and packstones of the crinoid-bryozoan-mound facies. The overlying reef mass proper is a complex of reef core facies mudstones and floatstones, with corals, bryozoans, algae, and stromatoporoids, intermingled with reef flank facies of bedded, bioclastic floatstones. This reef mass complex is topped by an algae-brachiopod-dominated wackestone unit, and then by a thin unit of laminated mudstone and algal boundstone, the upper part of which was subaerially (karstically) altered and brecciated. Above this major erosional discontinuity is the restricted cap facies of layered algal wackestone,

TERMINUS

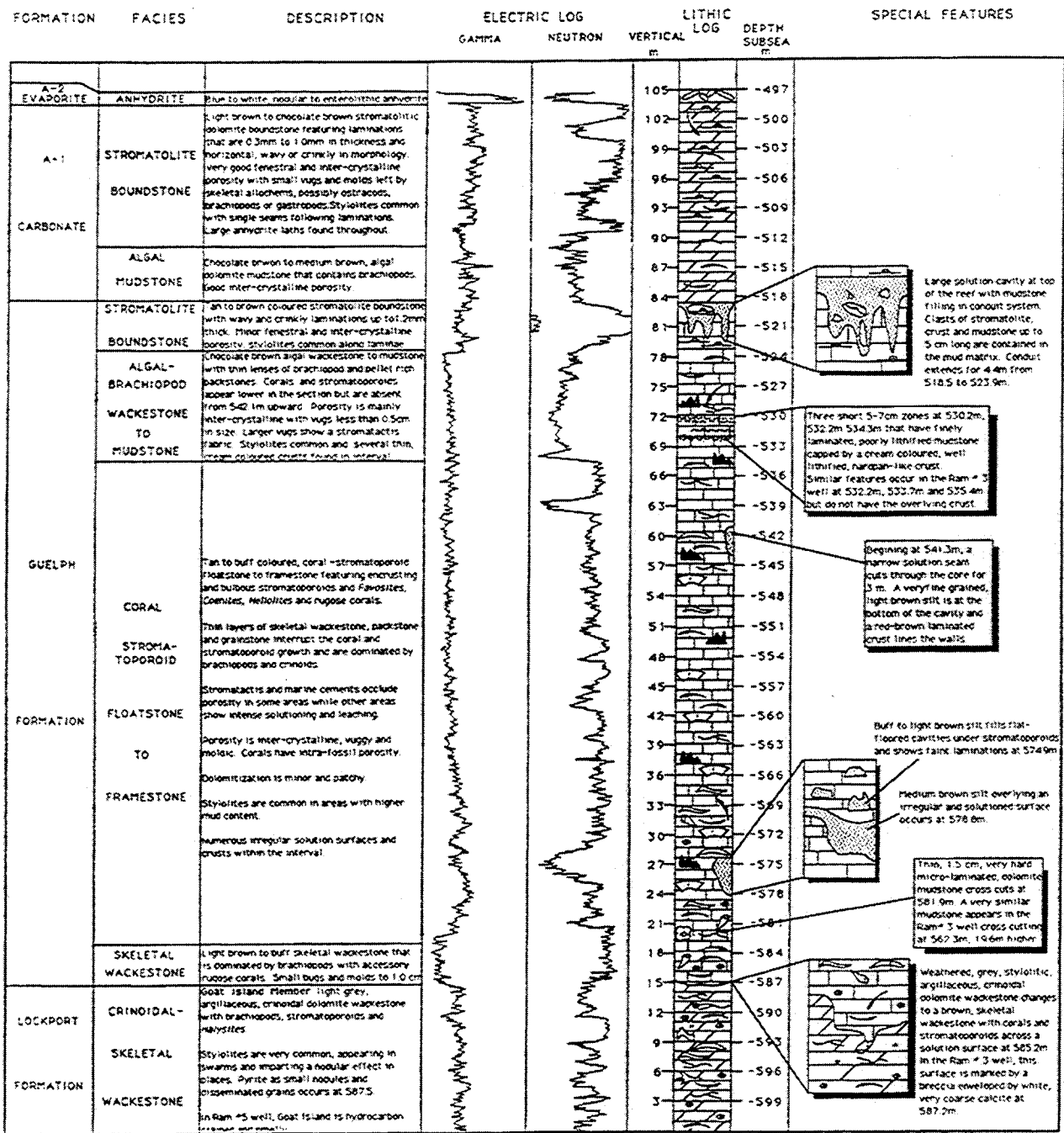


Figure 3. Stratigraphic section of the Ram 5, Sombra 2-24-IX (Terminus) core showing depositional, organic, and karstic features (from Charbonneau, 1990) (Appendix II). Lower 7 m and some karstic features are from the Ram 3, Sombra 4-23-IX core. Ram 3 = Core No. 818 and Ram 5 = Core No. 604.

mudstone and boundstone. This is overlain by the uppermost biohermal unit, of algal mudstone to stromatolitic boundstone. Some of the latter boundstone has "travertine"-like, very regular layering (not "caliche"). This unit was severely leached just after deposition.

These bioherms were sealed, overlain and laterally surrounded by impermeable carbonate and evaporite units of the lower part of the Salina Formation.

PLATFORM REEF FACIES

The structure of the Fletcher bioherm was first described by Chalkley (1983). This study found that the platform reef was deposited as a series of adjacent and superimposed patch reefs. As a result, only two biohermal facies were recognized above the Lockport Formation platform: reef core wackestone/floatstone with corals and stromatoporoids and the reef flank beds of bioclastic floatstone. The silt mound facies is absent (Grimes, 1987).

SUBAERIAL EXPOSURE

Most early workers thought that the Lockport Formation and Guelph Formation carbonate units and the succeeding Salina Formation evaporite units accumulated during one long, submarine episode. Mesolella et al. (1974) interpreted two episodes caused by sea level fluctuations, but thought a period of subaerial exposure to be only "possible". Sarg (1982) thought that the development of all reef porosity was due to salinity variation, without exposure. Huh et al. (1977), Sears and Lucia (1979), Petta (1980), and Cercone and Lohmann (1986) identified one exposure episode, mainly because of the general duality of off-reef Salina units. Bay (1983) saw two subaerial exposure episodes. Kahle (1974) early identified the many karstic features in a reef in northern Ohio. However, the idea that there was only one karstic episode at most and that it occurred after the growth of the entire bioherm has been a persistent misconception.

KARST FACIES IN BIOHERMS

This study has found that, during cyclic sea level fluctuations, lowering sea level produced reef exposure, creating soils, crusts, and laterally-extensive zones of enhanced porosity, along with either partial off-reef exposure, and deposition of evaporites and reef lithic debris, or full exposure, with sabkha formation. As a result, each growth phase of these Silurian bioherms was delineated by a period of major subaerial exposure (Smith, 1984). There were eight such episodes of subaerial exposure during development of the Guelph Formation bioherms (Figures 2 and 3, and Smith et al., 1988). Each episode created a new beginning for subsequent reef growth, so that each bioherm is a vertical succession of up to seven individual and different reefal units, separated by erosional discontinuities. All of these units were internally altered in part or in whole by rain water during subaerial exposure. Besides forming the karst breccias and causing the severe leaching of the overlying unit, these waters enlarged any residual depositional porosity in the reef mass or mud

mound facies and enlarged any joints or available conduits, and producing mini-caves or grikes. (Plates 1 to 11). Charbonneau (1990) (see Appendix II) places the top of the Lockport Formation at such strong erosional features found in each of the bioherms a few metres above the dolomitized portion of the unit (Plates 1 to 3).

In this way, each karstic episode formed a zone of notably increased permeability and enhanced porosity (Plates 4,6,8,11), that has extensive lateral interconnection but is vertically sealed by subaerial or later submarine cementation. Due to the original heterogeneity of the calcareous sediment and the different responses of the resulting limestones to the fresh-water and mixed-water subaerial environment, each of these leached, once-vadose zones is complex in internal detail (Plates 3,5,7,10). They are separated vertically from one another by impermeable intervals of karstically-unaltered (non-porous) carbonate (Plates 2,4,9), by karstic crusts and soils (Plate 10), by fills in karstic conduits (Plates 3,5,7), and by intervals plugged with precipitated anhydrite or halite (Plates 1,6). They possess, therefore, the best reservoir characteristics in each bioherm. These zones of enhanced porosity and permeability in the Rosedale pinnacle bioherm have been delineated and described in Figure 2 and those in the Terminus bioherms in Figure 3. Equivalent porosity zones in the Wilkesport, Payne and Bayfield reefs are delineated by Charbonneau (1990) (Appendix II).

These pinnacle bioherms are thus very similar to Holocene bioherms, such as Enewetok Atoll where Buddemeier and Oberdorfer (1986) found several "solution unconformities" in cores showing abundant karstic features.

INTER-REEF KARST FACIES

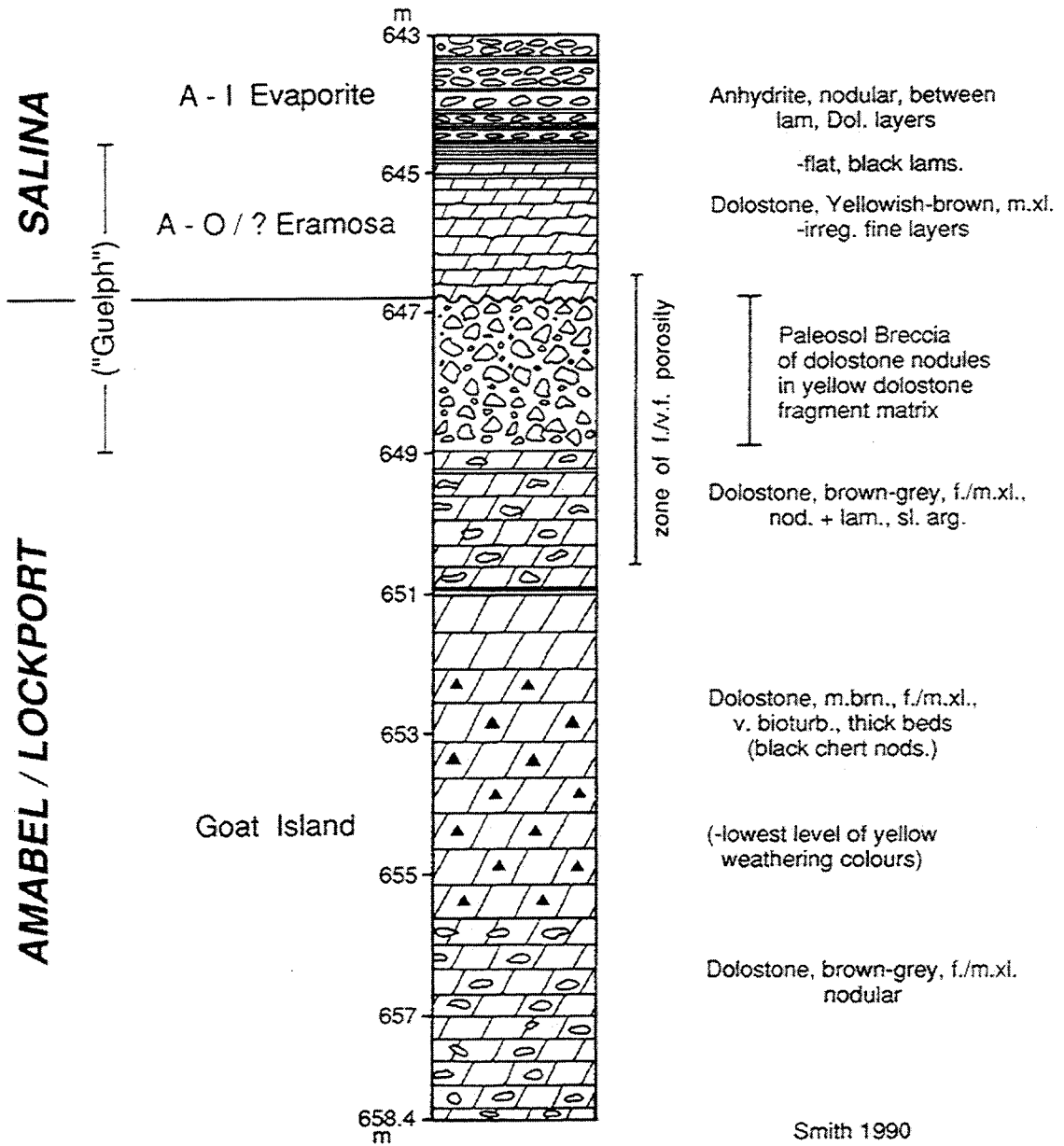
Several of these cyclic sea level fluctuations produced complete subaerial exposure in the areas between the reef bioherms, causing severe karstic weathering of exposed inter-reef units. One instance is shown in the Moore 5 - I core (Figure 4), located near two pinnacle bioherms (Figure 1), and in other cores. There, the top of the Lockport Formation is karstically gutted to a soil breccia. Of the original nodular dolostone only ragged fragments of the indurated nodules have survived (Plate 12). A zone of fine porosity was also created, needing only slight folding or faulting to create a reservoir.

The Salina A - O Carbonate/laminated "Eramosa" directly overlies the paleosol unit, showing the first effects of marine flooding during the rising sea level phase of that cycle.

Representing a common view, Gill (1977) saw the "conglomerate" (i.e. paleosol) as formed entirely of reef detritus, and called it a "Guelph" unit. The A - O unit is also included in the "Brown Niagaran", and is often included in the inter-reef "Guelph".

The cores show, however, that no Guelph Formation rocks are present in the inter-reef areas, where the Salina sits directly on the Lockport.

CORDEN et al. MOORE 5 - I



Smith 1990

Figure 4. Stratigraphic section of the Corden et al. Moore 5 -I inter-reef core showing depositional and karstic features. Core No. 382.

FACIES CHANGES-CAUSES

The development of Middle Silurian bioherms is the result of a series of subaerial exposures each followed by reef-growth episodes. Therefore, each bioherm is a vertical succession of seven, individual, reefal units separated by erosional discontinuities. Within this framework is a pattern of changes in the bioherm's depositional facies which only coincides with the erosional pattern in some places. Each karstic facies is directly related to the overlying erosional surfaces, as both are due to eustatic sea level change. However, some of the changes in depositional facies, due to change in the organic communities that produced them, appear to be due to inter-regional variation in salinity, apparently independent of sea level change.

The change from platform to silt mound deposition followed a slight salinity decrease (Plate 2), that from mound to reef mass complex occurred after subaerial exposures (Plates 4,7). Deposition of the reef complex was ended by a distinct salinity increase, well before the prolonged subaerial exposure that produced the karst breccia facies (Plate 10). This higher salinity remained afterward, to cause deposition of the algal shallow-marine facies (Plate 11).

Organic-reef biohermal development would have continued indefinitely if outside factors had not interfered. Thus, the apparent linear pattern of reef development was due to factors extrinsic to the reef's organic communities.

Overall, Middle Silurian bioherm growth was terminated by an general trend of lowering of sea level, causing more frequent and longer subaerial exposures. The reef communities were unable to re-establish themselves in the Late Silurian, due to an inter-regional rise in salinities over the North American Bank caused by the development of barrier reefs.

DIAGENETIC HISTORY

The pinnacle reef bioherms have undergone a complex and varied diagenesis. Considerable physical and chemical alteration of the original sediments was caused by submarine diagenesis and by changes during subaerial exposure and subsequent marine flooding. Petrographical, chemical and isotopic studies show that there were stages in the development of these diagenetic changes that were caused by variations in the chemistry of the pore fluids.

The results of each diagenetic stage are unevenly distributed throughout the bioherms. Some diagenetic effects were found to be spatially restricted and facies specific. This results from variations in the original carbonate sediment and its primary depositional porosity, from a resulting variability in karstic porosity enhancement, and from the variable residence times of any particular fluid in the pores. Original shelter porosities have partially survived in some places within the lower and middle portions of the bioherms, associated with bryozoa and stromatoporoids. Karstically-enhanced vuggy porosities are more

important in the reef complex portion, with fenestral porosities in the leached algal facies of the uppermost unit.

PINNACLE BIOHERMS

These reservoirs underwent early marine, meteoric, vadose, and phreatic, post-karstic marine, and burial diagenetic stages. Early marine cement in the form of isopachous, pore-lining, fibrous calcite is mainly restricted to the silt mound wackestone facies (Plate 3,8). It lines primary shelter porosity, initially associated with fenestrate bryozoan fragments but commonly enhanced by later vadose solution. Marine and/or later vadose silt deposition into each pore give it the flat base below a very irregular top surface characteristic of "stromatactis" (Plates 3,7). Many of these, and other types of karstically-enhanced pores, have an initial non-luminescent vadose cement. Most were then infilled by iron-poor blocky calcite of probable meteoric phreatic origin. This completed the formation of "stromatactis", and caused most of the loss of porosity in the lower portion of the bioherms (Plate 3). In the upper portions of the bioherms this cementation process was less efficient, and substantial porosity survived. Burial cements are not volumetrically significant. Euhedral white dolomite and euhedral calcite are found in a few vugs and fractures. Cercone and Lohmann (1986) found hydrocarbon inclusions in both the dolomite and the calcite in a Northern Michigan bioherm, which emphasizes their burial environment genesis. Simo and Lehmann (1988), however, found that hydrocarbon migration postdated such cements in central Indiana.

PLATFORM BIOHERMS

The Fletcher bioherm also contains much isopachous, pore-lining cement, but this cement has been thoroughly dolomitized along with the surrounding rocks. These cements also occur in karstically-altered zones partially or fully occluding the enhanced porosity. A burial phase of pore-lining, euhedral white dolomite post-dates the pervasive dolomitization of the bioherm (Grimes and Smith, 1987).

DOLOMITIZATION

The original tectonic background appears to have pre-determined the lack of pervasive dolomitization in isolated pinnacle bioherms, while platform/bank bioherms were thoroughly dolomitized. The regionally-extensive Lockport Formation platform was also well dolomitized. At those times when the region's marine waters were sufficiently enriched in magnesium to dolomitize the bioherms, the more widespread platform masses constricted sea water flow. This forced the magnesium-rich marine waters through the pores of the platform/bank especially if these had just been karstically-enhanced. The less-constrained water currents in the basin-slope environment flowed around the relatively small pinnacles, leaving them undolomitized except at their margins.

Mixed-water dolomitization, if it occurs at all, did not produce this pervasive dolomitization. It may have operated locally during a few of the

exposure episodes, at two levels in the Fletcher bioherm and at one level in the Warwick bioherm. The Rosedale bioherm was not affected at those times, even though it was also exposed.

ISOTOPE ANALYSIS

The results of analysis for the stable isotope ratios of $\delta^{18}\text{O}$ and $\delta^{13}\text{C}$ were given in Smith et al. (1988). The basic assumption behind this analysis is that the composition of the oxygen and carbon isotopes in the cements will reflect the composition of the pore fluids from which they precipitated and/or with which they later reacted. However, oxygen isotopic composition varies with temperature, salinity, and biological activity, while the carbon isotopic composition varies with organic matter content and any sediment/rock source of the bicarbonate ion. The isotope values distinguished the different cement phases in the pores of the bioherms and delineated the sequence of events in their history (as done, for example, by Dickson and Coleman, 1980).

It appears that some of the signatures obtained from fossil skeletal grains in the Rosedale bioherm give a close indication of normal sea water composition during Middle Silurian time. Comparison with the other signatures emphasizes how much the pore waters varied in other environments. The signature shift from the first phase isopachous cement (slightly mixed water?), to the second phase (closer to normal sea water), to the blocky cement (meteoric phreatic) shows that these cements were precipitated from different pore waters. This is significant, as the three cement types in each case were sampled from the same pore.

Very different signatures from calcites in laminated crusts and paleosols are important indicators of the more variable subaerial environments. The coarse euhedral calcites clearly show a burial environment.

The effect of the natural gas in enriching the ^{13}C of cements in the upper portion of the Rosedale pinnacle is noticeable. This can also be seen in a reef on the northern margin of the Basin (Cercione and Lohmann, 1986).

HYDROCARBON/STORAGE RESERVOIRS

This research has shown the presence of eight, major, subaerial, karstic episodes during development of the pinnacle reef bioherms. Each episode formed a laterally-extensive zone of increased permeability and vuggy or leached porosity. This permeability is laterally connected, but is vertically restricted beneath a zone of subaerial cementation or evaporite plugging and between sections of impermeable marine-cemented rock which were not affected by karstic processes. Some early zones of enhanced permeability were formed in the silt mound facies, lower in the bioherm. As these were later sealed by marine and phreatic cementation, their karstic affinity has not been recognized. The reservoir zones in the pinnacle bioherms occur in the middle and upper portions of each bioherm. They are laterally-extensive and vertically-separate, and are laterally enclosed by the impermeable carbonates and evaporites of the Salina Formation. Each zone can be expected to act as a separate reservoir.

POROSITY/PERMEABILITY

Figures 2 and 3 describe in general the variation in porosity in the Rosedale and Terminus bioherms. Both figures show the pre-eminent role of karstic processes in creating the reservoir zones. There are four main karstic vuggy zones in the middle portion of the bioherms (Plates 6 and 8), and leached porosity peaks in the upper portion of the reef mass and in the algal cap unit (Plate 11).

The seals to permeability which effectively separate the reservoir zones are evaporite plugging, submarine cements, karstic crusts and paleosols, a tight stromatolite unit and nodular anhydrite at the top. The evaporites appear to have been precipitated in two ways. The earlier sulphates and halites were apparently implaced during deposition in the inter-reef of the A-1 and A-2 evaporite units. The later phase, especially in fractures and larger vugs, seems to be the result of partial solution and re-precipitation of Salina evaporites on a regional scale. Geochemical studies by Dollar et al. (1988) of formation waters in Salina salt units and the Guelph bioherms show the Guelph fluids to be the product of halite dissolution that may have migrated into the bioherms after their deposition.

The persistent concept that there was only one karst episode at the end of bioherm construction has led to the assumption that the major permeability interconnections in the Guelph reefal bioherms are vertical. Instead there are laterally-extensive and separate zones of enhanced permeability within these bioherms. This has a major impact on exploration procedures, formation testing, well completions, enhanced recovery techniques, gas storage and retrieval methods, and techniques of subsurface waste disposal.

CONCLUSIONS

1. Development of the subsurface Silurian bioherm reservoirs of southwestern Ontario was governed by cyclic sea level fluctuations.
2. The succession of growth stages and depositional facies were identified in several pinnacle bioherms (e.g. Rosedale and Terminus) and in the Fletcher platform/bank bioherm.
3. There were eight major episodes of subaerial exposure during development of these pinnacle reef bioherms.
4. Each bioherm is a vertical succession of up to seven individual reefal units separated by erosional discontinuities.
5. The appearance of a linear pattern of reef development was not intrinsic to the reef communities, but was caused by the external controls of sea level change and salinity variation.
6. Each karst episode produced a zone of enhanced porosity and permeability, which is laterally-extensive and is vertically-restricted by karstic crusts and paleosols, evaporite plugging, and non-porous marine carbonates.
7. Each such zone can be expected to act as a separate reservoir.
8. Marine, meteoric vadose and phreatic, and burial diagenesis created pore-occluding cements, especially in the lower portions of each bioherm.
9. A paleosol (not a Guelph unit) was developed at the top of the inter-reef Lockport platform.
10. Only major karstic episodes, probably followed by relatively rapid sea level rise, seemed able to create lasting zones of enhanced permeability.

ACKNOWLEDGEMENTS

The Rosedale cores were given by Union Gas Limited, with the assistance of Thomas Bainbridge. The Fletcher cores were given by Consumers' Gas Co. Limited. We thank Steven Colquhoun of Telesis Oil and Gas for initiating the Fletcher study. The cores were slabbed by the Petroleum Resources Section Laboratory of the Ministry of Natural Resources. Other cores were available for study at the Laboratory's Core Library Facility. We wish to thank P.A. Palonen and T. Carter of the Ministry and R.A. Trevail of Telesis Oil and Gas for their considerable assistance to the project.

Major funding was given by the Ministry of Northern Development and Mines through Geoscience Research Grant 295. We thank Canterra Energy Limited for supplying thin sections; and K.C. Lohmann and his laboratory for stable isotope analyses. Field study of quarries in Ohio, Indiana and Illinois and further stable isotope analyses were funded by the Advisory Research Committee of Queen's University. Sarmistha Dey assisted with petrographic analysis. Linda Anderson typed the manuscript. Ela Rusak Mazur drafted three of the figures.

REFERENCES

- Bailey, S.M.B., 1986. A new look at the development, configuration and trapping mechanisms of the Silurian Guelph reefs of southwestern Ontario. Ontario Petroleum Institute, Twenty-fifth Annual Conference, Paper No. 14, 28p.
- Bailey Geological Services Ltd. and Cochrane R.O., 1990, Geology of selected oil and gas pools in the Silurian carbonates of southern Ontario. Ontario Geological Survey Open File Report 5722, 50 p.
- Bainbridge, T.W., 1973. The sedimentology of a Silurian pinnacle reef in the Michigan Basin. unpublished B.Sc. Thesis, Queen's University, Kingston, 62p.
- Bay, T.A., 1983. The Silurian of the northern Michigan Basin. p. 53-72 *in* Society Economic Paleontologists and Mineralogists, Carbonate Buildups, Core Workshop No. 4, 593p.
- Buddemeier, R.W., and Oberdorfer, J.A., 1986. Internal hydrology and geochemistry of coral reefs and atoll islands; Key to diagenetic variations. p. 94-111 *in* Schroeder, J.H. and Purser, B.H. eds., Reef Diagenesis; Springer, Berlin, 455 p.
- Cercone, K.R., and Lohmann, K.C., 1986. Diagenetic history of the Union 8 pinnacle reef (Middle Silurian), northern Michigan, U.S.A.. p. 381-398 *in* Schroeder, J.H. and Purser, B.H., eds., Reef Diagenesis; Springer, Berlin, 455p.
- Chalkley, P., 1983. The sedimentologic correlation and history of the Fletcher Silurian pinnacle reef, eastern Michigan Basin. unpublished B.Sc. Thesis, Queen's University, Kingston, 54p.
- Charbonneau, S.L., 1990. Subaerial exposure and meteoric diagenesis in Guelph Formation (Niagaran) pinnacle reef bioherms of the Michigan Basin, southwestern Ontario. unpublished M.Sc. Thesis, Queen's University, Kingston, 215 p.
- Dickson, J.A.D., and Coleman, M.L., 1980. Changes in carbon and oxygen isotope composition during limestone diagenesis. *Sedimentology*, v 27, p. 107-118.
- Dollar, P., Frappe, S.K., McNutt, R.H., Fritz, P., and Macqueen, R.W., 1988. Geochemical studies of formation waters, southwestern Ontario, Canada, and southern Michigan, U.S.A. p. 14-28 *in* Geoscience Research Grant Program Summary of Research 1987-1988, edited by V.G. Milne, Ontario Geological Survey Miscellaneous Paper 140, 251 p.
- Gill, D., 1977. Salina A - 1 sabkha cycles and the Late Silurian paleogeography of the Michigan Basin: *Journal of Sedimentary Petrology*, v. 47, p. 979-1017.
- Grimes, D.J., 1987. Depositional models, subaerial facies, and diagenetic histories of the Rosedale and Fletcher reefs, southwestern Ontario. unpublished M.Sc. Thesis, Queen's University, Kingston, 120p.

- Grimes, D.J., and Smith, L., 1987. Depositional and diagenetic history of the Fletcher reservoir, a platform reef in southwestern Ontario. p. 86 in Reef Research Symposium, Canadian Society of Petroleum Geologists, Banff, Abstracts Volume, 111 p.
- Huh, J.M., Briggs, L.I., and Gill, D., 1977. Depositional environments of pinnacle reefs, Niagara and Salina Groups, northern shelf, Michigan Basin. p. 1-21 in Fisher, J.H., ed., Reefs and Evaporites; American Association Petroleum Geologists, Studies in Geology 5, 196 p.
- Kahle, C.F., 1974. Nature and significance of Silurian rocks at Maumee Quarry, Ohio. p. 31-54 in Kesling, R.V., ed. Silurian Reef-Evaporite Relationships; Michigan Basin Geological Society, 111p.
- Mesolella, K.J., Robinson, J.D., McCormick, L.M., and Ormiston, A.R., 1974. Cyclic deposition of Silurian carbonates and evaporites in Michigan Basin. American Association Petroleum Geologists Bulletin, v. 58, p. 34-62.
- Pearson, E.M., 1980. Sedimentology and diagenesis of the Warwick reef (Silurian), Lambton County, southwestern Ontario. unpublished M.Sc. Thesis, University of Waterloo, 250p.
- Petta, T.J., 1980. Silurian pinnacle reef diagenesis - northern Michigan: Effects of evaporites on pore space distribution. p. 32-42. in Society Economic Paleontologists and Mineralogists, Carbonate Reservoir Rocks, Core Workshop No. 1, 183 p.
- Prouty, C.E., 1983. The tectonic development of the Michigan Basin intrastructures. p. 36-81 in Michigan Basin Geological Society, Tectonics, Structure, and Karst in Northern Lower Michigan, Field Conference, 139p.
- Sanford, B.V., Thompson, F.J., and McFall, G.H., 1985. Plate tectonics - A possible controlling mechanism in the development of hydrocarbon traps in southwestern Ontario. Canadian Petroleum Geology Bulletin, v. 33, p. 52-71.
- Sarg, J.F., 1982. Off-reef Salina deposition (Silurian), southern Michigan Basin-Implications for reef genesis. p. 354-384 in Society Economic Paleontologists and Mineralogists, Deposition and Diagenetic Spectra of Evaporites, Core Workshop No. 3, 395p.
- Sears, S.O., and Lucia, F.J., 1979. Reef growth model for Silurian pinnacle reefs, northern Michigan reef trend. Geology, v. 7, p. 299-302.
- Simo, A., and Lehmann, P., 1988. Deposition and diagenesis of a cratonic Silurian platform reef, Pipe Creek Jr., Indiana (Abs.). American Association Petroleum Geologists Bulletin, v. 72, p. 248-249.
- Smith, L., 1984. The Guelph-Lower Salina in southwestern Ontario: Subaerial exposure and episodic reef growth in a syn-erosional basin. Geological Association of Canada, Abstracts v. 9, p. 107.
- Smith, L., Grimes, D.J., and Charbonneau, S.L., 1988. Karst episodes and permeability development, Silurian reef reservoirs, Ontario. p. 124-132 in Geoscience Research Grant Program Summary of Research 1987-1988, edited by V.G. Milne, Ontario Geological Survey Miscellaneous Paper 140, 251p.

- Smith, L., and Charbonneau, S.L., 1990 . Karst episodes and permeability development, Silurian reef reservoirs, Ontario. in Geoscience Research Grant Program Summary of Research 1989-1990, edited by V.G. Milne, Ontario Geological Survey Miscellaneous Paper 150, p. 4-12.
- Trevail, R.A., and Smith, L., 1987. Cratonic tectonism as control of spatial distribution and form of Silurian pinnacle and platform reefs, southwestern Ontario. p. 61 in Reef Research Symposium, Canadian Society of Petroleum Geologists, Banff, Abstracts Volume, 111 p.

APPENDIX I

Plates showing Karst features
in Silurian reef bioherms,
Southwestern Ontario

PLATE 1

Large dissolution conduit, irregularly truncating both early porosity-fill cements and later conduit-lining isopachous marine cement. Nearly vertical for 2.7 m in core. Filled by gypsum, now blue anhydrite. Union Enniskillen 8-9-II A (Rosedale), Core No. 578, 627.3 m. White bar = 5 cm long.

PLATE 2

Examples from other pinnacle bioherms of karstic surfaces correlatable to that in Plate 1.

Left-Surface sculpted by differential karst dissolution during early stages of lithification. Sealed by layered fibrous calcite marine crust. Imperial 399, Warwick 4 - 12 - III SER, Core No. 526, 646.5 m.

Right-Irregular surface above paleosol breccia, where Lockport crinoidal dolostone changes abruptly to Guelph skeletal wackestone. Ram 5, Sombra 2 - 24 - IX (Terminus), Core No. 604, 585.2 m.

PLATE 3

The lowest portions of the Plate 1 conduit, showing two dissolution episodes. The earlier fill is of vadose silts and fragments, followed by isopachous marine cement (producing stromatactis features). The later conduit has vadose fragments below and anhydrite fill above.

PLATE 4

A sealed karst surface, overlain by a laminated, marine, dolostone crust, between the silt mound facies below and the reef complex above. Note enhanced porosity. Ram 5, Sombra 2 - 24 - IX (Terminus), Core No. 604, 581.9 m. White bar = 5 cm long.

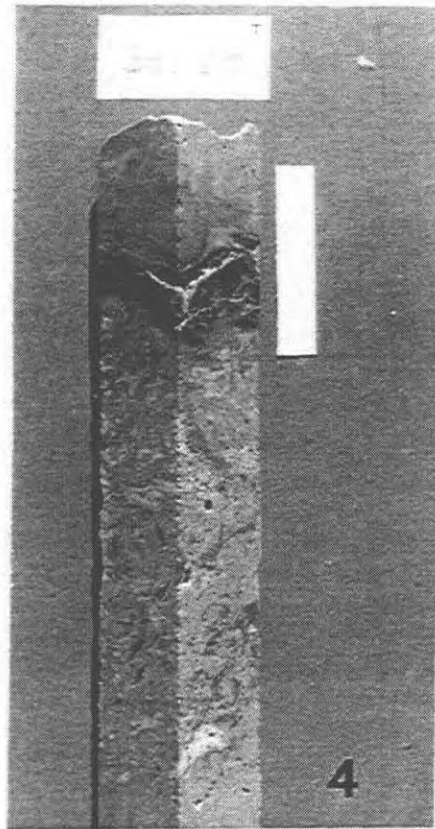
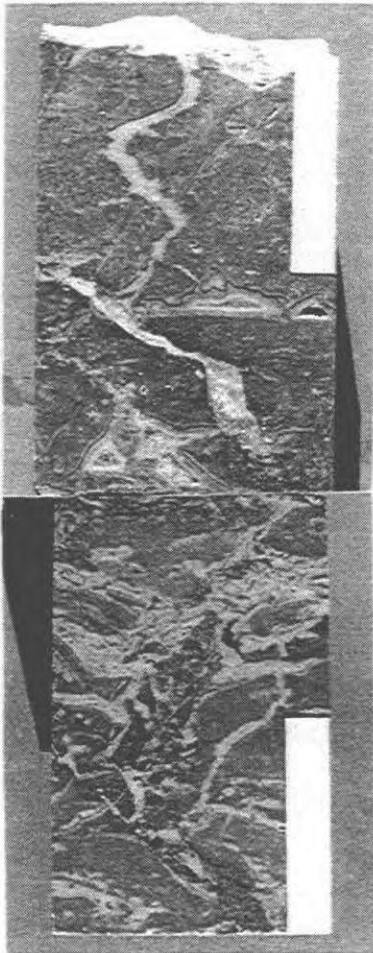
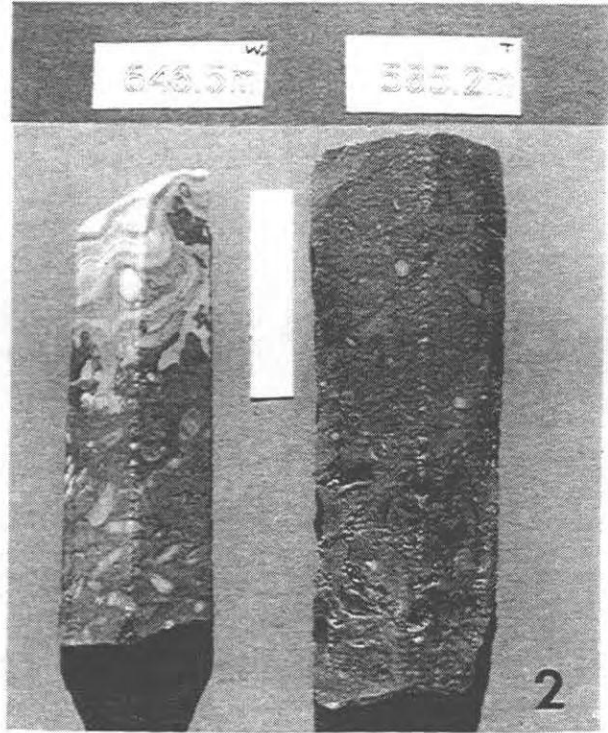
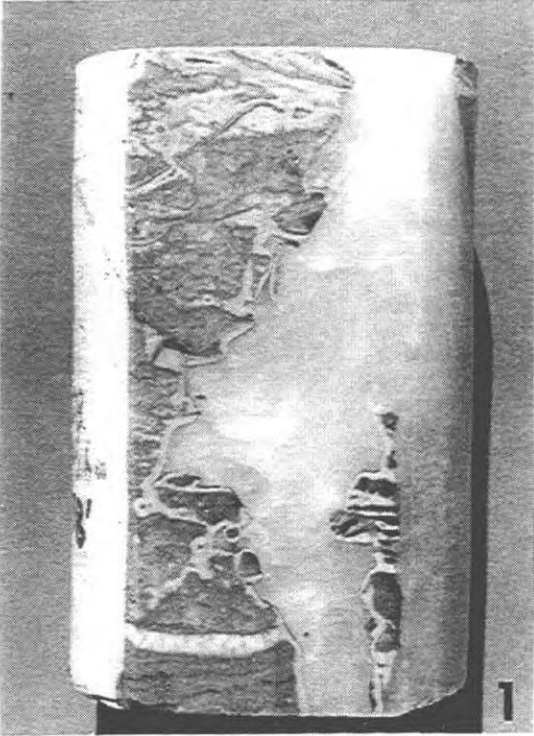


PLATE 5

Examples of laminated, vadose silt fills in irregular dissolution cavities, within the reef complex facies in Ram 5, Sombra 2 - 24 - IX (Terminus), Core No. 604.

Left-Conduit sealed by red-brown vadose crusts. Vertical length in core = 3 m. 541.3 m.

Right-Karstically-enhanced shelter porosity, mainly under stromatoporoids, nearly filled by brown vadose silts. 574.9 m.

PLATE 6

Well-developed dissolution pores and vugs in mid-to upper portions of reef complex in Union Enniskillen 8 - 9 - II A (Rosedale), Core No. 578. White bar = 5 cm long.

Left-Leached bioclastic wackestone, with halite filling larger vugs. 575.8 m.

Right-Cream-coloured, fibrous marine crust molded to irregular exposure surface above brown paleosol with residual fossil fragments. 551.4 m.

PLATE 7

Interconnected dissolution cavities in wackestone just below top of mound, nearly filled by fine, brown vadose silt. Note cross-laminations showing meteoric current direction. Remaining space filled by marine isopachous cement. Union Enniskillen 8 - 9 - II A (Rosedale), Core No. 578, 612 m.

PLATE 8

Karst dissolution vugs within stromatoporoids of the upper reef complex, partially infilled by isopachous marine cement. Union Enniskillen 8 - 9 - II A (Rosedale), Core No. 578, 547 m. See Plate 9. 5 cm white bar.

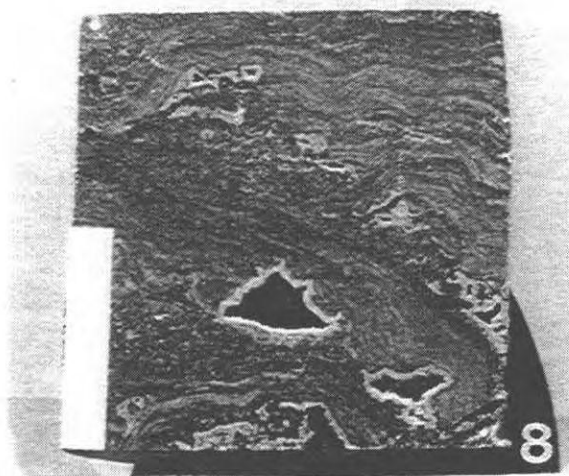
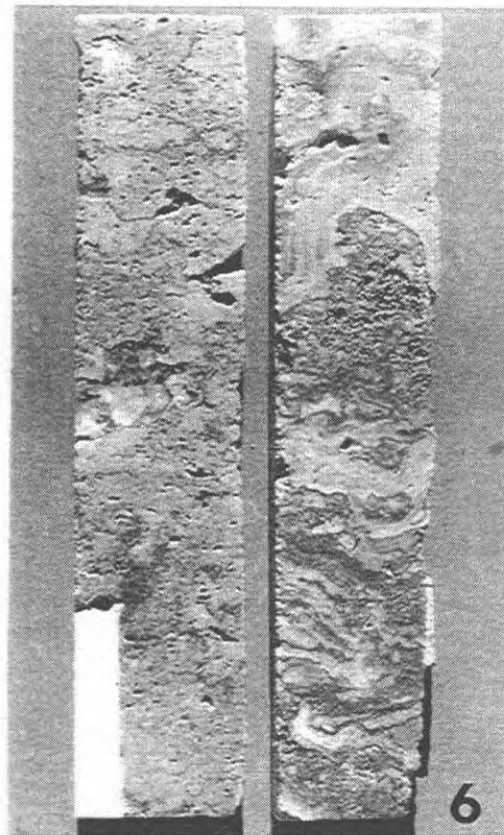
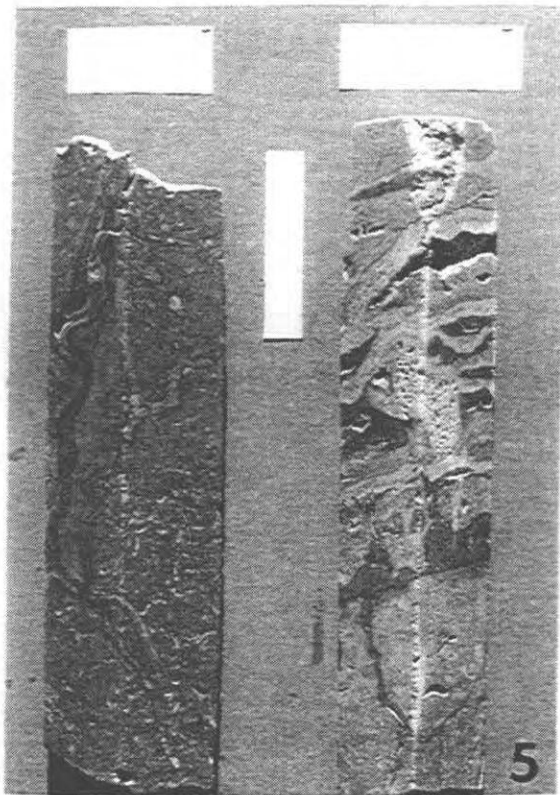


PLATE 9

Cyclic sealevel fall and rise shown by yellow-brown, slightly chalky paleosol, with fossil and lithic fragment rubble. Exposure surface, dipping to 35°, coated by marine, laminated algal mudstone with lower salinity packstone above. Union Enniskillen 8 - 9 - II A (Rosedale), Core No. 578, 545.6 m. 5 cm white bar.

PLATE 10

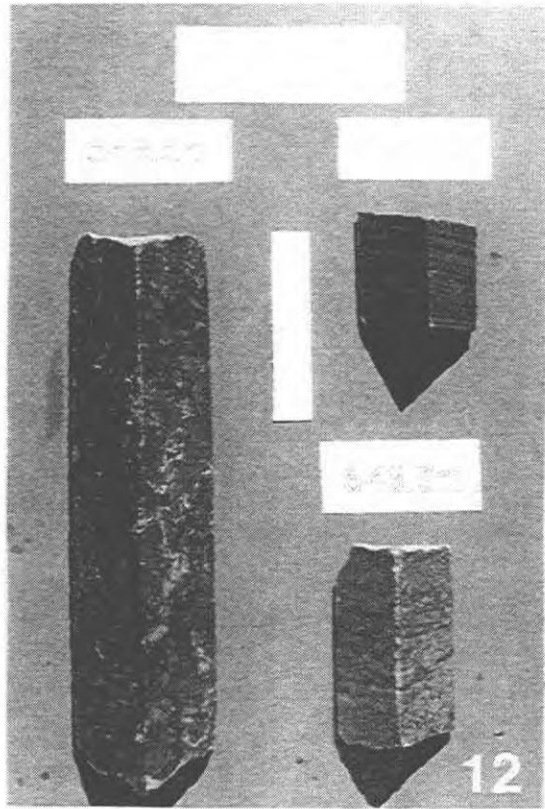
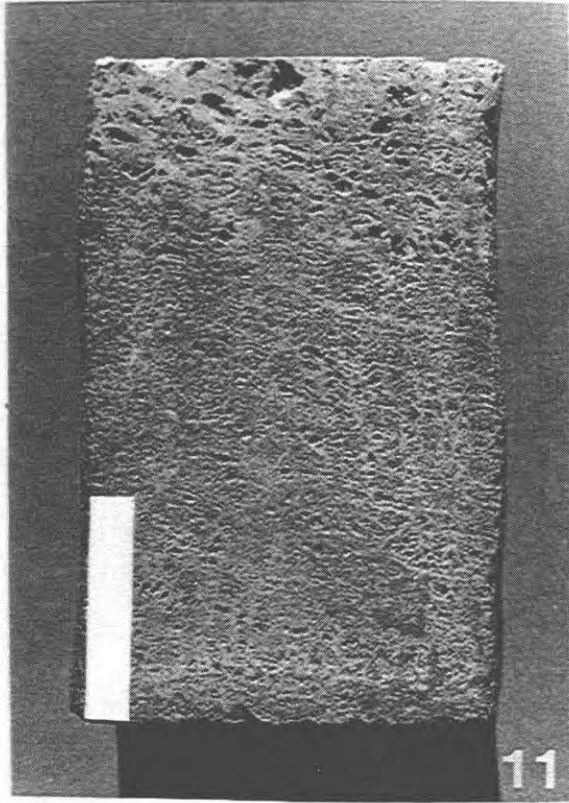
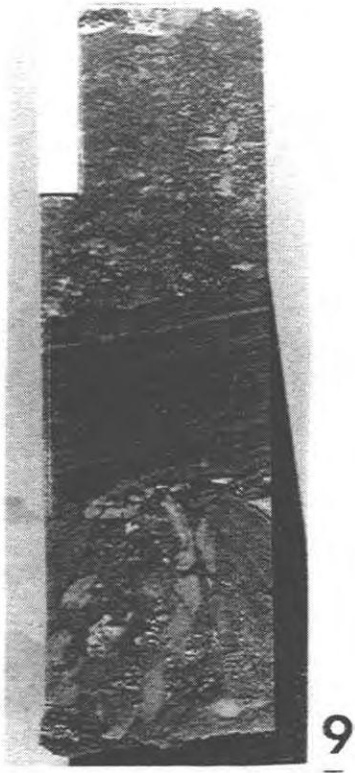
Exposure surface at top of green-shale-matrix major karst breccia. Very large fragments of algal stromatolite, some lower in breccia are crust-coated. Conduit extends for 6.3 m in core. Union Enniskillen 8 - 9 - II A (Rosedale), Core No. 578, 525.6 m. 5 cm white bar.

PLATE 11

Severe meteoric leaching of algal, travertine-like, stromatolitic boundstone of "A - 1 Carbonate". Some anhydrite (gypsum) pore-filling. Union Enniskillen 8 - 9 - II A (Rosedale), Core No. 578, 506.3 m. 5 cm white bar.

PLATE 12

Porous, yellow-brown, paleosol breccia at the top of the inter-reef Lockport Formation (648.5 m), overlain by Salina A - 0 algal - laminated marine carbonates (646.3 and 645 m)-an excellent source rock.



APPENDIX II

M. Sc. Thesis Report
of Steven L. Charbonneau

**Subaerial Exposure and Meteoric Diagenesis
in Middle Silurian Guelph Formation (Niagaran)
Pinnacle Reef Bioherms
of the Michigan Basin,
Southwestern Ontario**

by

Steven L. Charbonneau

A thesis submitted to the Department of Geological Sciences
in conformity with the requirements for
the degree of Master of Science

Queen's University
Kingston, Ontario, Canada
February, 1990

copyright © Steven L. Charbonneau, 1990

Abstract

Middle Silurian (Niagaran)pinnacle bioherms of the Guelph Formation developed in a near-concentric ring around the Michigan Basin. In southwestern Ontario, the Bayfield, Payne, Rosedale, Terminus, Warwick and Wilkesport pinnacle bioherms lie buried to depths of 500m to 600m modern subsea.

A vertical succession of facies is found in the pinnacles consisting of: a basal crinodal-skeletal facies; coral-stromatoporoid facies; algal-brachiopod facies; and, stromatolite facies. Capping the bioherm is a karstic facies.

Multiple episodes of subaerial exposure occurred during bioherm development. The number of exposure surfaces varies from a low of three in the Bayfield and Wilkesport pinnacles to seven in the Rosedale bioherm. Each surface is accompanied by differential dissolution and by meteoric cementation that reduced porosity and permeability. Previous workers had interpreted only a single erosional event during pinnacle development affecting the very top of the bioherm and terminating growth.

Only two karst surfaces can be correlated between all six pinnacles. One is the uppermost surface already identified basinwide. The other is found at the base of each pinnacle, and is interpreted herein as the contact between the Guelph and the underlying platform carbonates of the Lockport Formation. It suggests probable regional exposure of the platform prior to pinnacle initiation. Across this lowermost dissolution surface are: (1) changes from dolomite to limestone; (2) changes from characteristic Lockport rocks to those representative of the Guelph; and (3) appearance of reef-building organisms in number above the surface.

Near uniform thickness of the underlying Lockport Formation; the appearance of stromatoporoids at the same stratigraphic interval; the concentric nature of pinnacle distribution; and, the karst surface imply that fault block tectonics did not play a role in initiating the majority of pinnacle reefs. However, most karst surfaces cannot be correlated

indicating that not all bioherms experienced the same erosional episodes. Therefore, some mechanism, probably fault block movement, influenced their development after initiation. In addition, the lack of correlation suggests that each pinnacle reef studied has a unique growth history.

There is abundant evidence in all six pinnacles of diagenesis in seafloor, meteoric and burial environments. Seafloor diagenesis produced syngenic cementation, mainly by isopachous fibrous Mg-calcite and micrite, both containing random dolomite rhombs. In limestone pinnacles, almost all karst zones show abundant evidence of meteoric diagenesis in the form of: non-luminescent, pendant, stalactitic or meniscus vadose cements; and, meteoric epitaxial overgrowths and iron-poor, blocky calcite cements. Phreatic cements are zoned and brightly luminescent. Burial features include fracturing, stylotization, and saddle dolomite, dog-tooth calcite and iron-rich blocky calcite cements. Anhydrite and halite were the last minerals to be emplaced but are volumetrically most important.

Dolomite within the bioherms ranges from pervasive, anhedral crystals to cryptocrystalline patches associated with karst. In fully dolomitized pinnacles only major karst zones are detectable and evidence of meteoric cementation is lost.

Acknowledgments

A project of this size owes its existence to a number of helpful individuals. Dr. Leigh Smith suggested the topic and generously provided financial support throughout my stay at Queen's. Drs. Bob Dalrymple, Guy Narbonne, Noel James and Leigh Smith freely shared their vast knowledge of sedimentary geology with me, and consequently, I leave a much better geologist than when I arrived. My gratitude is extended to the members of my committee: Dr. J.M. Dixon; Dr. R. Gilbert; Dr. R.D. Gordon; Dr. N.P. James; and, Dr. L. Smith.

I especially thank Dr. Ted Sawford, Manager of Geology, and Charlie Bruce, Manager of Research, of Shell Canada Limited, for allowing me access to research equipment at the Calgary Research Centre in the summers of 1988 and 1989. Kathy Aulstead, Johannes Theissen and Dr. Christian Viau provided helpful insights into pinnacle reefs during my summer with Shell at the Calgary Research Centre in 1988. Special thanks are extended to Dr. Jeff Dravis who showed me the "ins" and "outs" of epifluorescence microscopy.

My stay at Queen's was heightened by a number of good friends including: Steve Aitken; Clint Cowan; Sarmistha Dey; Marc Dubord; Paul Fejer; Shane Pelechaty; Neil Robertson; Hamish Sandeman; and all the members past and present of Le Club du Hockey de Continental Drifters.

Ela Ruzak-Mazur and Chris Peck assisted with photography and Jerzy Adwent and Roger Innes prepared some outstanding polished thin sections. This thesis benefitted greatly from the helpful suggestions and constructive criticisms of Kathy Aulstead, Clint Cowan and Eric Gosselin of BP Canada Resources.

Lastly, I thank my parents, Leo and Sherie, and in-laws, Glenn and Ruth, but especially my wife Bonnie. For two years she has provided me with love and encouragement, always shown unwavering confidence in me, and made me realize that there is a wonderful life outside of geology.

Table of Contents

| | |
|---|-----|
| CHAPTER ONE..... | 1 |
| Introduction..... | 1 |
| 1.1 Overview and Purpose of this Thesis..... | 1 |
| 1.2 Historical Background..... | 2 |
| 1.3 Study Area..... | 3 |
| 1.4. Regional Stratigraphy..... | 6 |
| 1.5 Reef Inventory and Hydrocarbon Production..... | 8 |
| 1.5.1 Inventory of Reefs Studied..... | 8 |
| 1.5.2 Hydrocarbon Production in Southwestern Ontario..... | 14 |
| 1.6 Geologic Setting and Paleogeography..... | 17 |
| 1.7 Previous Work..... | 20 |
| 1.8 Analytical Techniques..... | 28 |
| 1.9 Summary..... | 31 |
| CHAPTER TWO..... | 33 |
| Lithofacies and Distribution Within Guelph Pinnacles..... | 33 |
| 2.1 Overview..... | 33 |
| 2.2 Rochester Formation..... | 33 |
| 2.3 Lockport Formation..... | 35 |
| 2.3.1 Gasport Member..... | 38 |
| 2.3.2 Goat Island Member..... | 41 |
| 2.3.3 Distribution of the Lockport Formation..... | 43 |
| 2.4 Guelph Formation..... | 44 |
| 2.4.1 Crinoidal-Skeletal Wackestone Facies..... | 44 |
| 2.4.2 Coral-Stromatoporoid Floatstone to Framestone Facies..... | 48 |
| 2.4.3 Algal-Brachiopod Wackestone to Mudstone Facies..... | 54 |
| 2.4.4 Stromatolite Boundstone Facies..... | 56 |
| 2.4.5 Subaerial Exposure Facies..... | 58 |
| 2.4.6 Facies Distribution in the Guelph Formation..... | 62 |
| 2.5 A-1 Evaporite Formation..... | 64 |
| 2.6 A-1 Carbonate Formation..... | 64 |
| 2.6.1 Algal Mudstone Facies..... | 65 |
| 2.6.2 Stromatolite Boundstone Facies..... | 65 |
| 2.6.3 Distribution of the A-1 Carbonate..... | 68 |
| 2.7 A-2 Evaporite Formation..... | 68 |
| 2.8 A-2 Carbonate Formation..... | 69 |
| 2.9 Summary..... | 69 |
| CHAPTER THREE..... | 71 |
| Karst Development Within Michigan Basin Silurian Pinnacle Reef Bioherms..... | 71 |
| 3.1 Overview..... | 71 |
| 3.2 Parameters Affecting Karst Development and Meteoric Diagenesis..... | 71 |
| 3.3 Solution and Precipitation in the Meteoric Environment..... | 72 |
| 3.4 Karst Development in Limestone Pinnacle Bioherms of the Michigan Basin..... | 81 |
| 3.4.1 Karst Surfaces Within the Warwick Pinnacle Bioherm..... | 81 |
| 3.4.1.1 Surfaces Observed in the Warwick Pinnacle Bioherm..... | 81 |
| 3.4.1.2 Discussion of Surfaces in the Warwick Bioherm..... | 90 |
| 3.4.2 Karst Surfaces Within the Rosedale Pinnacle Bioherm..... | 92 |
| 3.4.2.1 Surfaces Observed in the Rosedale Bioherm..... | 92 |
| 3.4.2.2 Discussion of Surfaces in the Rosedale Bioherm..... | 102 |
| 3.4.3 Karst Surfaces Within the Terminus Pinnacle Reef..... | 104 |
| 3.4.2.1 Surfaces Observed in the Terminus Bioherm..... | 104 |
| 3.4.3.2 Discussion of Surfaces in the Terminus Bioherm..... | 109 |

| | |
|---|-----|
| 3.5 Karst Development in Dolostone Pinnacle Bioherms in the Michigan Basin..... | 111 |
| 3.5.1 Karst Surfaces Within the Bayfield Pinnacle Bioherm..... | 111 |
| 3.5.1.1 Surfaces Observed in the Bayfield Bioherm..... | 111 |
| 3.5.1.2 Discussion of Surfaces in the Bayfield Bioherm..... | 113 |
| 3.5.2 Karst Surfaces Within the Wilkesport Pinnacle Bioherm..... | 114 |
| 3.5.2.1 Surfaces Observed in the Wilkesport Bioherm..... | 114 |
| 3.5.2.2 Discussion of Surfaces in the Wilkesport Bioherm..... | 117 |
| 3.5.3 Karst Surfaces within the Payne Pinnacle Bioherm..... | 117 |
| 3.5.3.1 Surfaces Observed in the Payne Bioherm..... | 117 |
| 3.5.3.2 Discussion of Surfaces in the Payne Bioherm..... | 118 |
| 3.6 Effects of Dolomitization on Meteoric Surfaces and Fabrics..... | 119 |
| 3.7 Correlation of Karst Surfaces in Guelph Pinnacle Reefs..... | 120 |
| 3.8 Summary..... | 120 |
| CHAPTER FOUR..... | 122 |
| Diagenesis of Guelph Formation Pinnacle Reefs..... | 122 |
| 4.1 Overview..... | 122 |
| 4.2 Seafloor Diagenesis in Guelph Formation Pinnacle Bioherms..... | 124 |
| 4.3 Meteoric Diagenesis in Guelph Formation Pinnacle Reefs..... | 128 |
| 4.4 Burial Diagenesis in Guelph Formation Pinnacle Bioherms..... | 131 |
| 4.5 Dolomitization in the Lockport, Guelph and A-1 Carbonate Formations..... | 135 |
| 4.6 Analysis of Stable Isotope Data..... | 139 |
| 4.7 Relative Timing of Diagenetic Events..... | 147 |
| 4.8 Summary..... | 148 |
| CHAPTER FIVE..... | 150 |
| Pinnacle Growth and Genesis..... | 150 |
| 5.1 Overview..... | 150 |
| 5.2 The Theory of Fault Control on Pinnacle Genesis..... | 150 |
| 5.3 Stages of Reef Growth..... | 151 |
| 5.4 Discussion of Fault Control on Reef Genesis..... | 161 |
| 5.5 Summary..... | 164 |
| CHAPTER SIX..... | 166 |
| Conclusions..... | 166 |
| References..... | 169 |
| APPENDIX A | |
| Core descriptions of studied wells..... | 179 |
| Warwick Reef | |
| Imperial #399..... | 179 |
| Imperial #619..... | 186 |
| Imperial #407..... | 188 |
| Rosedale Reef..... | 190 |
| Union Enniskillan 8-9-II A..... | 190 |
| Terminus Reef..... | 197 |
| Ram #2..... | 197 |
| Ram #4..... | 197 |
| Ram # 5..... | 199 |
| Ram #3..... | 201 |
| Wilkesport Reef..... | 204 |
| Imperial Sombra 14-XIII..... | 204 |
| Bayfield Reef..... | 206 |
| Bluewater Oil and Gas Porter #1..... | 206 |
| Payne Reef..... | 208 |
| Imperial Payne #4..... | 208 |

Appendix B

| | |
|---|-----|
| Carbon and Oxygen Isotope Results | 212 |
| VITA | 215 |

LIST OF FIGURES

| | | |
|--------------------|---|---------------|
| Figure 1: | Location map of the study area and reefs studied | 4 |
| Figure 2: | Stratigraphic nomenclature and relationships of Silurian units | 6 |
| Figure 3: | Map of the Bayfield bioherm contoured on the Guelph Fm. | 9 |
| Figure 4: | Map of the Warwick bioherm contoured on the Guelph Fm. | 11 |
| Figure 5: | Map of the Payne bioherm contoured on the Guelph Fm. | 12 |
| Figure 6: | Map of the Wilkesport bioherm contoured on the Guelph Fm. | 13 |
| Figure 7: | Map of the Terminus bioherm contoured on the Guelph Fm. | 15 |
| Figure 8: | Map of the Rosedale bioherm contoured on the Guelph Fm. | 16 |
| Figure 9: | Middle Silurian paleogeography showing two inlets | 18 |
| Figure 10: | Major reef belts that ring the Michigan Basin | 19 |
| Figure 11: | Pinnacle reef model southern Michigan Basin | 23 |
| Figure 12: | Pinnacle reef models northern Michigan Basin | 25 |
| Figure 13: | Different pinnacle reef models everyone has a favourite | 27 |
| Figure 13a: | Formations and relative thicknesses encountered in each core | 29 |
| Figure 14: | Diagram of gross facies and thickness variations | 34 |
| Figure 15: | Factors that influence the development of karst | 73 |
| Figure 16: | Zonations in the meteoric diagenetic environment | 74 |
| Figure 17: | Features of subaerial exposure caliche profiles and karst | 77 |
| Figure 18: | Cements from the meteoric environment | 79 |
| Figure 19: | Lithologic column for the Warwick Bioherm | pocket |
| Figure 19A | Legend for figures 19 to 24 inclusive | 82 |
| Figure 20: | Lithologic column for the Rosedale Bioherm | pocket |
| Figure 21: | Lithologic column for the Terminus bioherm | pocket |
| Figure 22: | Lithologic column for the Bayfield bioherm | pocket |

| | | |
|-------------------|---|--------|
| Figure 23: | Lithologic column for the Wilkesport bioherm | pocket |
| Figure 24: | Lithologic column for the Payne bioherm | pocket |
| Figure 25: | Correlation of karst surfaces among the six reefs studied | pocket |
| Figure 26: | The three diagenetic environments as used in this study | 123 |
| Figure 27: | $\delta^{13}\text{C}$ and $\delta^{18}\text{O}$ isotope plots for skeletal allochems | 141 |
| Figure 28: | $\delta^{13}\text{C}$ and $\delta^{18}\text{O}$ isotope plots for cements | 143 |
| Figure 29: | $\delta^{13}\text{C}$ and $\delta^{18}\text{O}$ isotope plots for paleosols and crusts | 145 |
| Figure 30: | Relative timing of diagenetic events | pocket |
| Figure 31: | Fault blocks and their influence on pinnacle growth | 152 |

LIST OF PLATES

| | | |
|-----------|--|----|
| Plate 1: | Rochester Formation rock types | 36 |
| Plate 2: | Rochester-Lockport contact | 37 |
| Plate 3: | Lockport lithologies | 39 |
| Plate 4: | Dolomite replacement in the Lockport | 40 |
| Plate 5: | Lockport stylolites and crinoid-skeletal wackestone facies | 45 |
| Plate 6: | Fractures and pore occluding cements | 47 |
| Plate 7: | Coral-stromatoporoid facies | 49 |
| Plate 8: | Halite emplacement and dolomite replacement | 50 |
| Plate 9: | Algae and fibrous marine cement | 52 |
| Plate 10: | Burial diagenetic features | 53 |
| Plate 11: | Algal-brachiopod facies | 55 |
| Plate 12: | Stromatolite boundstone facies | 57 |
| Plate 13: | Karst facies | 59 |
| Plate 14: | Karst facies and green clay | 61 |
| Plate 15: | A-1 Carbonate mudstone facies and porosity development | 66 |
| Plate 16: | A-1 Carbonate stromatolite facies and A-2 Evaporite | 67 |
| Plate 17: | Cockling and meteoric cements, Warwick bioherm | 84 |
| Plate 18: | Exposure and meteoric diagenesis, Warwick bioherm | 85 |
| Plate 19: | Breccia and strandline diagenesis, Warwick bioherm | 87 |
| Plate 20: | Vadose and meteoric phreatic cements, Warwick bioherm | 88 |
| Plate 21: | Exposure surfaces, Warwick bioherm | 89 |
| Plate 22: | Conduit formation, 627.0m, Rosedale bioherm | 93 |
| Plate 23: | Vadose and meteoric phreatic cementation, Rosedale bioherm | 94 |
| Plate 24: | Vadose silt and meteoric cementation, Rosedale bioherm | 96 |

| | | |
|------------------|--|------------|
| Plate 25: | Meteoric cementation, Rosedale bioherm | 97 |
| Plate 26: | Exposure surface, 556.9m, Rosedale bioherm | 99 |
| Plate 27: | Exposure surface, 545.6m, Rosedale bioherm | 100 |
| Plate 28: | Exposure surfaces, 540.1m and 527.3m, Rosedale bioherm | 101 |
| Plate 29: | Exposure surface and meteoric cements, Terminus bioherm | 106 |
| Plate 30: | Exposure surface, 578.8m, Terminus bioherm | 107 |
| Plate 31: | Meteoric cements and karst, Terminus bioherm | 108 |
| Plate 32: | Porosity occlusion and enhancement, Bayfield bioherm | 112 |
| Plate 33: | Dolomites and meteoric cements, Wilkesport bioherm | 115 |
| Plate 34: | Exposure surface and meteoric cements, Wilkesport bioherm | 116 |
| Plate 35: | Seafloor diagenesis | 125 |
| Plate 36: | Fibrous and prismatic cements | 127 |
| Plate 37: | Vadose and meteoric phreatic cements | 130 |
| Plate 38: | Burial diagenetic minerals | 133 |

LIST OF TABLES

| | | |
|-----------------|---|-----------|
| Table 1: | Previous work by various authors | 22 |
| Table 2: | The identified gross lithofacies and their thicknesses | 63 |

CHAPTER ONE

Introduction

1.1 Overview and Purpose of this Thesis

Previous depositional models of Middle Silurian, Guelph Formation pinnacle bioherms in the Michigan Basin allow for only one episode of subaerial exposure. This erosional event is interpreted to have occurred after the bioherms had developed fully and it resulted in the termination of their growth. Karsting is presumed to have affected the entire pinnacle, to the base, as the Michigan Basin drained and evaporite deposition began.

The purpose of this thesis is to document evidence that suggests that subaerial exposure occurred several times during pinnacle reef development and that it was not restricted to a single, catastrophic event. Three limestone pinnacle bioherms were selected to establish the presence of karst surfaces and to record the effects of meteoric diagenesis on the reefs. Since most pinnacles in the Michigan Basin have been dolomitized, three additional reefs were analyzed to observe whether or not the exposure surfaces could be detected through a dolomitic overprint. In addition, comparing the exposure surfaces between the six studied pinnacles tests the hypothesis that movement of small fault blocks initiated and governed the genesis of the reefs (Sanford *et al.*, 1985).

Dolomitization, as well as characteristics inherent to the reef itself, such as faunal content and distribution, have been documented from an observational perspective only. The causes of dolomitization, distribution of fauna within a given facies, and growth histories of the pinnacles do not constitute the main purpose of this study.

1.2 Historical Background

Middle Silurian, evaporite and mudstone-encased reefs of the Guelph Formation in the Michigan Basin have been of interest to geologists since the mid-Nineteenth Century. This interest was heightened when the first commercial quantity of oil in North America was discovered in these strata near Petrolia, Ontario in 1889. Although the subject of study for more than a century, many questions concerning stratigraphic relationships, depositional environments, diagenesis and the inferred ages of several of the formations remain.

Guelph Formation (Niagaran) pinnacle reefs occur in a nearly concentric ring within the Michigan Basin (Sanford, 1969). These pinnacles are separated from the basin centre by interpreted contemporaneous deep water carbonates of the Guelph Formation, and from the basin edge by an inner patch-reef belt and a rimming barrier reef-complex. Much of the recent work concerning genesis or the stratigraphic relationships of the pinnacle reefs has relied on the examination of individual pinnacles with extrapolation of the results basinwide (Gill, 1977; 1986; Huh *et al.*, 1977; Cercone, 1984; Cercone and Lohmann, 1986; Devaney *et al.*, 1986). Perhaps as a result of the limited scope of many studies, a number of diverse and conflicting theories exist to explain the growth histories and diagenesis of the pinnacle reefs. Lack of recognition of subaerial exposure features in the reefs has been noted as a major reason for the current conflicts (Kahle, 1988). Most workers interpret karsting of the pinnacles as a single event restricted to the final stages of reef development (Gill, 1973;1977;1979;1986; Cercone, 1984; Cercone and Lohmann, 1986; Huh *et al.*, 1977; Briggs *et al.*, 1980; Pearson, 1980; Sears and Lucia, 1980).

This study shows that the Middle Silurian Bayfield, Payne, Rosedale, Terminus, Warwick, and Wilkesport pinnacle reefs experienced multiple karst episodes throughout their growth histories. Meteoric diagenesis had a more significant influence on pinnacle reef genesis than has been previously documented. This study also shows that tectonism was the controlling mechanism of pinnacle reef development in the Michigan Basin (Sanford *et al.*, 1985), but only

after pinnacle growth had been initiated. Finally, a better understanding of how multiple exposure events affected vertical and lateral permeabilities, can be used in the development of pinnacle reef reservoirs, both in terms of production and their use as underground storage facilities.

1.3 Study Area

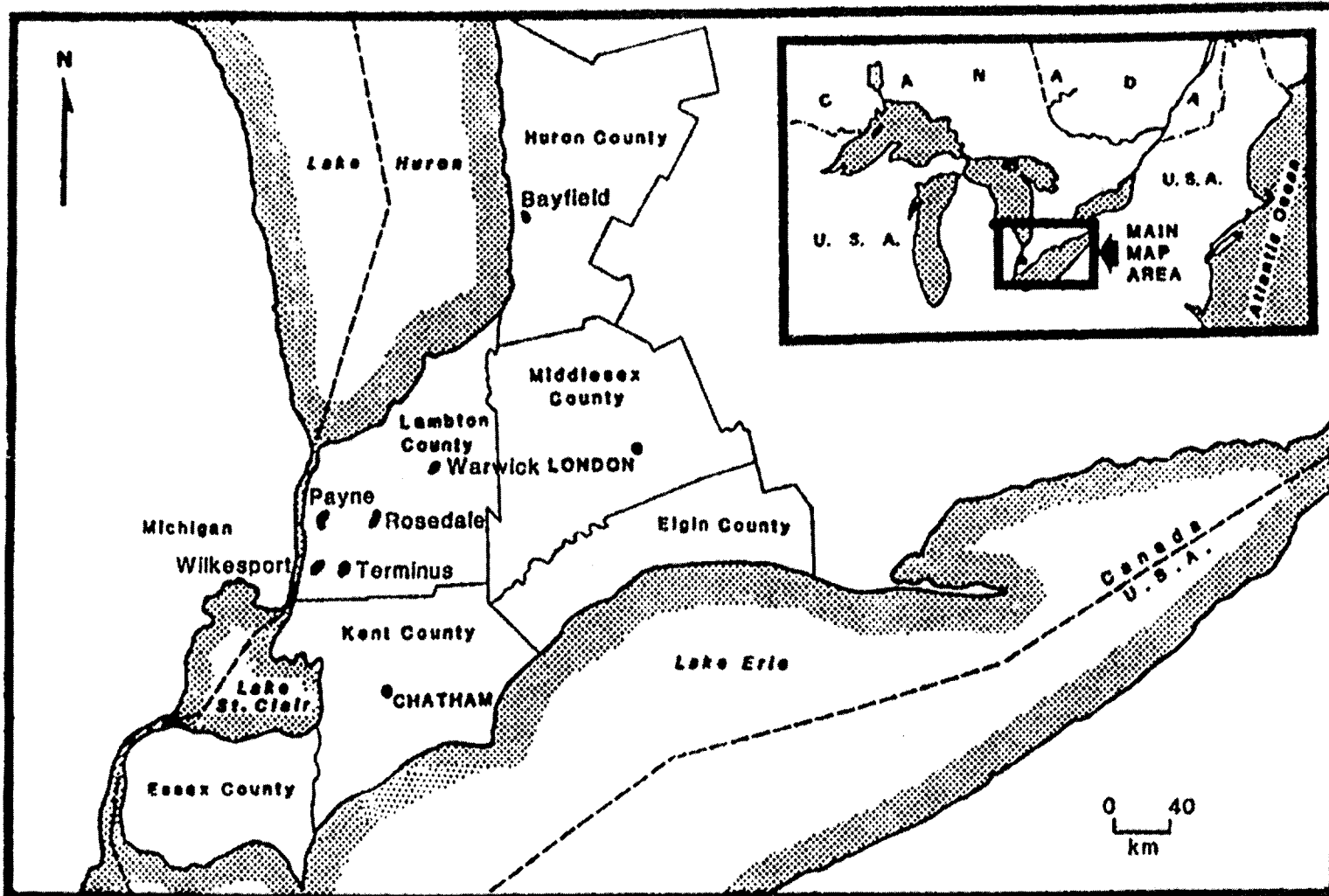
The area of study includes the Payne, Rosedale, Terminus, Warwick and Wilkesport reefs in Lambton County as well as the Bayfield pinnacle in Huron County (figure 1). Six pinnacle reefs were examined in the study over a distance of approximately 280 km (figure 1). The reefs were chosen for study based upon a number of factors, including: the number of cores available from each pinnacle; lithology; and, geographical separation.

As many pinnacles have but a single core taken, those with more than one were appropriate for study (Warwick, Terminus, Payne). Five reefs were cored throughout with their vertical extent from the Salina Group to the Lockport Formation (Warwick, Rosedale, Terminus, Payne, Wilkesport). The Rosedale, Payne and Warwick reefs have cores that penetrate to the Rochester Formation.

Some reefs were chosen because limestone is the dominant rock instead of dolostone (Warwick, Rosedale, Terminus) and because the preservation of subaerial dissolutional and depositional textures would be more readily observable in an undolomitized core. Dolomitized and partially dolomitized buildups were chosen to contrast with the limestone reefs. Also, these pinnacles represent dolomitized pinnacles that are uncharacteristically closer to the basin centre when compared to the limestone reefs.

Finally, examining reefs that are separated geographically from one another provides a means to evaluate the extent of karst events.

Figure 1: Location map showing the study area in southwestern Ontario and the geographical positions of the six pinnacle reef bioherms examined.



1.4. Regional Stratigraphy

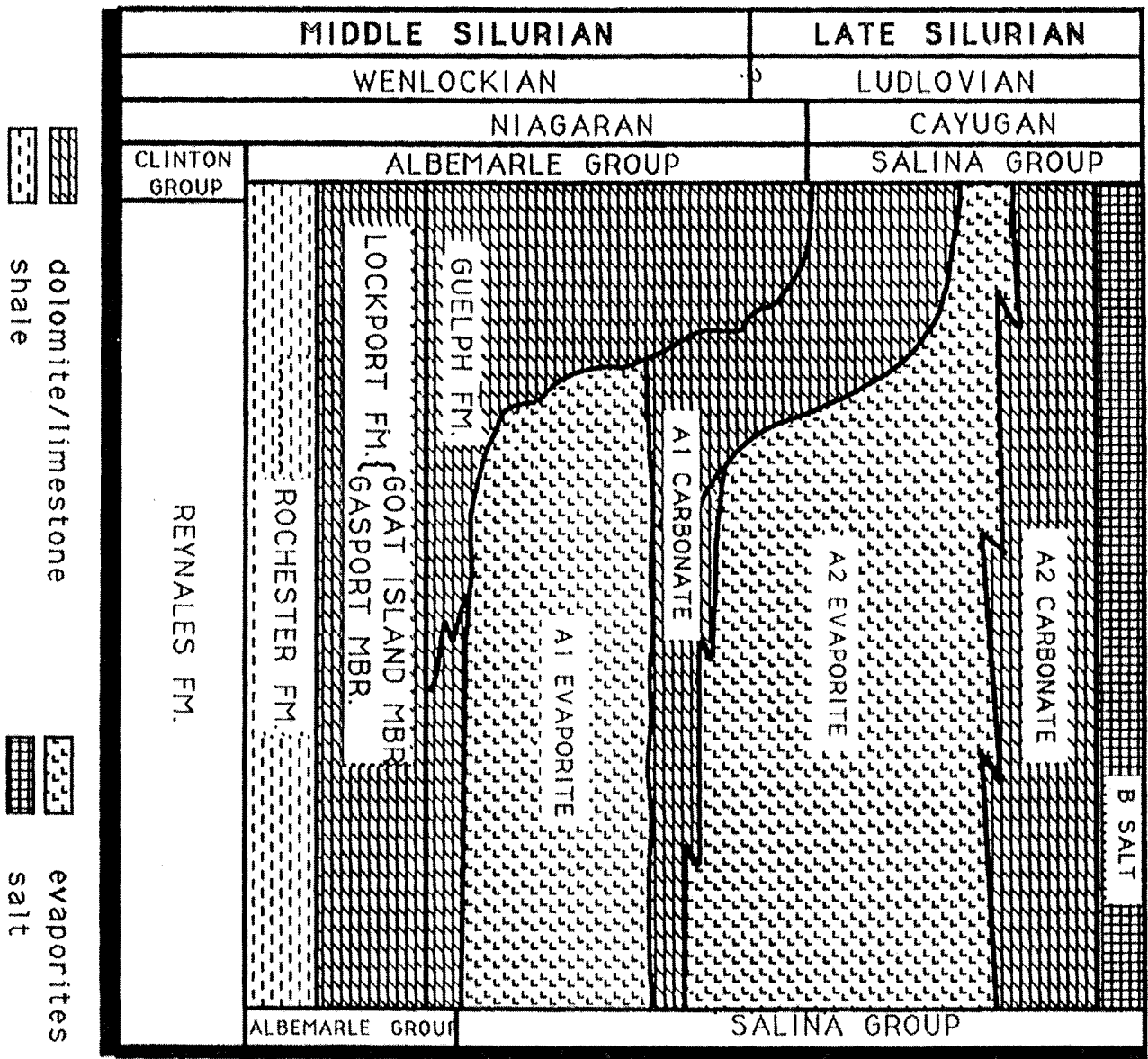
Regional stratigraphic relationships for the Middle and Upper Silurian rocks in the Michigan Basin are presented in figure 2. These rocks constitute part of the Paleozoic package of strata in southwestern Ontario that ranges from Late Cambrian to Late Devonian in age. Maximum known thickness of the Paleozoic cover is 1460 m, near Sarnia (Sanford, 1962). For the purposes of this study, only those Middle Silurian rocks from the Albemarle Group through to the A-2 Evaporite Formation of the Salina Group inclusive are considered. These formations are Wenlockian to Ludlovian in age (Niagaran to Cayugan) (Sanford and Brady, 1957; Sanford, 1962; Mesolella *et al.*, 1974).

The Rochester Formation, first studied by Hall (1839), is the lowermost unit of the Albemarle Group (terminology of Sanford and Brady, 1957) and unconformably overlies the limestones of the Reynales Formation (Sanford and Brady, 1957). It represents a regionally extensive, open marine, deep water shale that has been studied in various localities (Folk, 1962; Brett, 1983), but little has been documented about its occurrence in the Michigan Basin. This is due in part to a complete lack of outcrop and because only a few cores are taken through the entire formation.

In the Michigan Basin, the Rochester Formation is a dark grey to medium grey, fossiliferous, dolomitic to calcareous shale with thin, shaley dolomite interbeds (Sanford and Brady, 1957; Appendix A). It blankets the basin and varies in thickness from 3 m to 15 m (Sanford and Brady, 1957). Brett (1983), however, reports the Rochester Formation to be of more uniform thickness (12 m to 15 m) when traced from the Niagara Peninsula to Windsor. Only the upper portions of the formation were encountered by cores used in this study (Appendix A).

Overlying the Rochester Formation is the Lockport Formation. The Lockport Formation is a dolomitized, crinoidal wackestone with minor limestone and dolomitic limestone (Sanford and Brady, 1957; Sanford, 1962; Shukla and Friedman, 1983). It can be subdivided into two members: the lower Gasport Member, a light grey, fine to medium crystalline, porous,

Figure 2: Stratigraphic nomenclature and relationships of Silurian units in the Michigan Basin. Carbonate units are those encountered in the studied reefs. Modified from Gill (1986), Sanford and Brady (1957), Cercone (1988) and Bailey (1986).



EUROPEAN STAGES
NORTH AMERICAN STAGES

PINNACLE REEF

INTER REEF

carbonate; and the upper Goat Island Member, a more argillaceous, nodular and stylolitic carbonate that also shows a more diversified fossil assemblage (Appendix A). Shukla and Friedman, (1983) interpret the Lockport to be a shallowing-upward succession. As a platform limestone, the Lockport Formation thins dramatically towards the centre of the basin, taking on a hematitic red colour (Huh *et al.*, 1977) and has a regional dip of between 0.76° and 1.52° (Gill, 1979). In basin-margin areas the Lockport attains thicknesses of up to 90 m (Sanford, 1962).

The Guelph Formation completes the Albemarle Group (figure 2). Whereas the Rochester and Lockport Formations are primarily uniform in character over much of their extent, the Guelph Formation is quite diverse in depositional character (Appendix A). It includes facies of pinnacle, patch and barrier reef affinities, as well as inter-reef, basinal and slope settings (Sanford and Brady, 1957). Reef-complex facies show an upward transition from light brown, skeletal wackestones through coral and stromatoporoid reef facies to brown, algal wackestones and boundstones (Appendix A). Degree of dolomitization increases toward basin-margin areas (Sears and Lucia, 1980). Inter-reef Guelph strata consist of brown dolomite mudstone which thins to the centre of the Michigan Basin (Gill, 1977). Nurmi and Friedman (1977) report the Guelph-Lockport combined to be less than 3 m thick in the basin centre.

Like the Guelph Formation, rocks of the Upper Silurian Salina Group exhibit a variety of depositional facies (figure 2). In inter-reef areas, the Salina shows a cyclic stacking of evaporites and carbonates, beginning with the A-1 Evaporite overlying the Guelph Formation carbonates (Gill, 1977). It is nodular to felted anhydrite in the reef belt areas and grades to halite closer to the basin centre. Sylvite is also present near the centre of the basin (Nurmi and Friedman, 1977). The A-1 Evaporite abuts against the pinnacles but does not cover them (Huh *et al.*, 1977; Gill, 1977). Evaporite deposits are thickest in the centre of the basin (145 m, 475 ft.) and thin drastically toward the margins being only 6 m (20 ft.) near the pinnacles (Gill, 1977).

Unconformably overlying these evaporite deposits are the dolomitic algal mudstones and algal boundstones of the A-1 Carbonate of the Salina Group (Gill, 1977). A brown, microlaminated, dolomite mudstone with abundant carbonaceous material characterizes the A-1 Carbonate between the pinnacle reefs. In scattered inter-reef locations, the carbonate remains as limestone. Unconformably in contact with the Guelph Formation on top of the pinnacles (Gill, 1977; Cercone, 1984; Pearson, 1980; Grimes, 1988), the A-1 Carbonate is a brown, stromatolitic boundstone with minor burrowed mudstone. With the deposition of the A-1 Carbonate, the Salina Group begins a carbonate-evaporite pairing that repeats itself twice (figure 2). In contrast to the A-1 Evaporite, the A-1 carbonate thins toward the basin centre. It has a maximum known thickness of 40 m around the pinnacle reefs, thinning to 17 m at the centre of the basin (Gill,1977). The carbonate also thins as it drapes over the pinnacle reefs themselves.

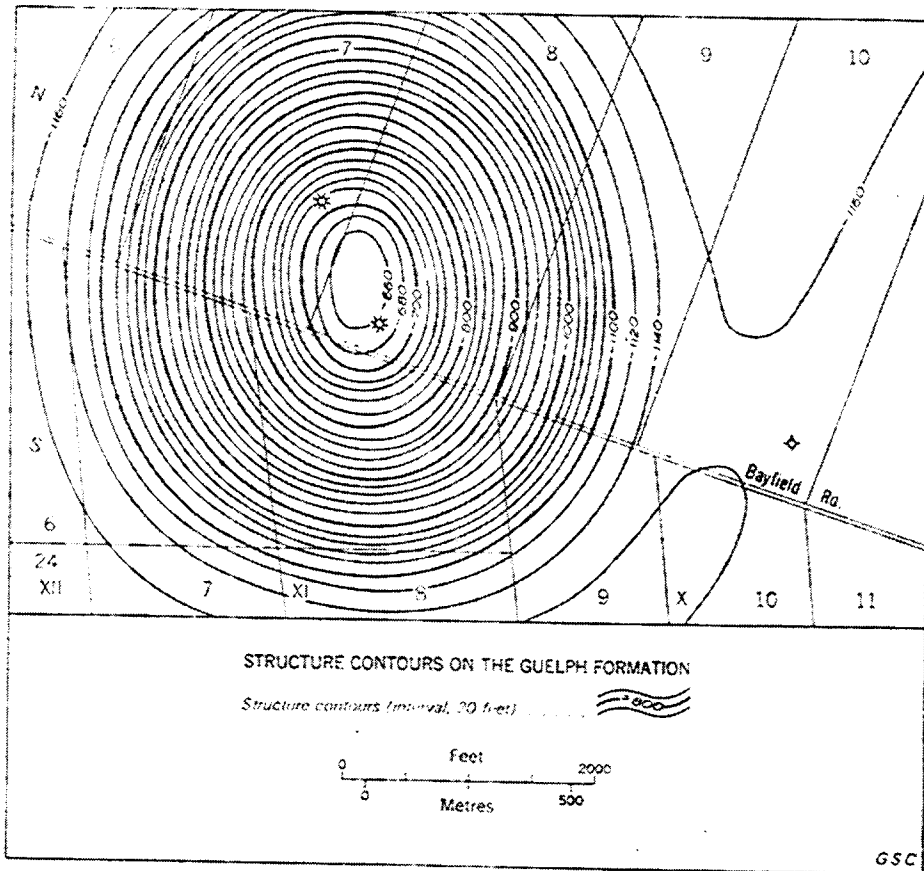
Completing the package of Silurian strata included in this study is the A-2 Evaporite. Like the A-1 Evaporite, the A-2 consists of nodular, felted and enterolithic anhydrite which changes to salt further toward the centre of the Michigan Basin. It also thickens substantially basinward. However, unlike the A-1, the A-2 Evaporite extends over the pinnacle reefs. This thin cap (usually less than 2 m) provides the evaporite encasement necessary to trap hydrocarbons in many pinnacle reefs.

1.5 Reef Inventory and Hydrocarbon Production

1.5.1 Inventory of Reefs Studied

Of the bioherms studied, only one exists outside of Lambton County (figure 1). The Bayfield reef is primarily situated in lots 7 and 8, Concession BRN, in Stanley Township, Huron County. It is a dolomitized pinnacle, approximately 97 ha in size (230 acres) and bulls-eye in shape (figure 3). Discovered in 1956, the field produced 1.52 million cubic metres (10^6 m^3) gas (53.6 million cubic ft.) from 2 wells (Koepke and Sanford, 1965) before being converted to a gas storage

Figure 3: Idealized map of the Bayfield pinnacle reef with structure contours on the Guelph Formation . Contour interval is 20 ft. Bayfield core studied is from well in lot 7, Bayfield Road North. See Figure 1 for location (From Koepke and Sanford, 1965).



facility in the 1970's. A single core 64 m long from the Guelph Formation was taken from a position close to the reef-crest.

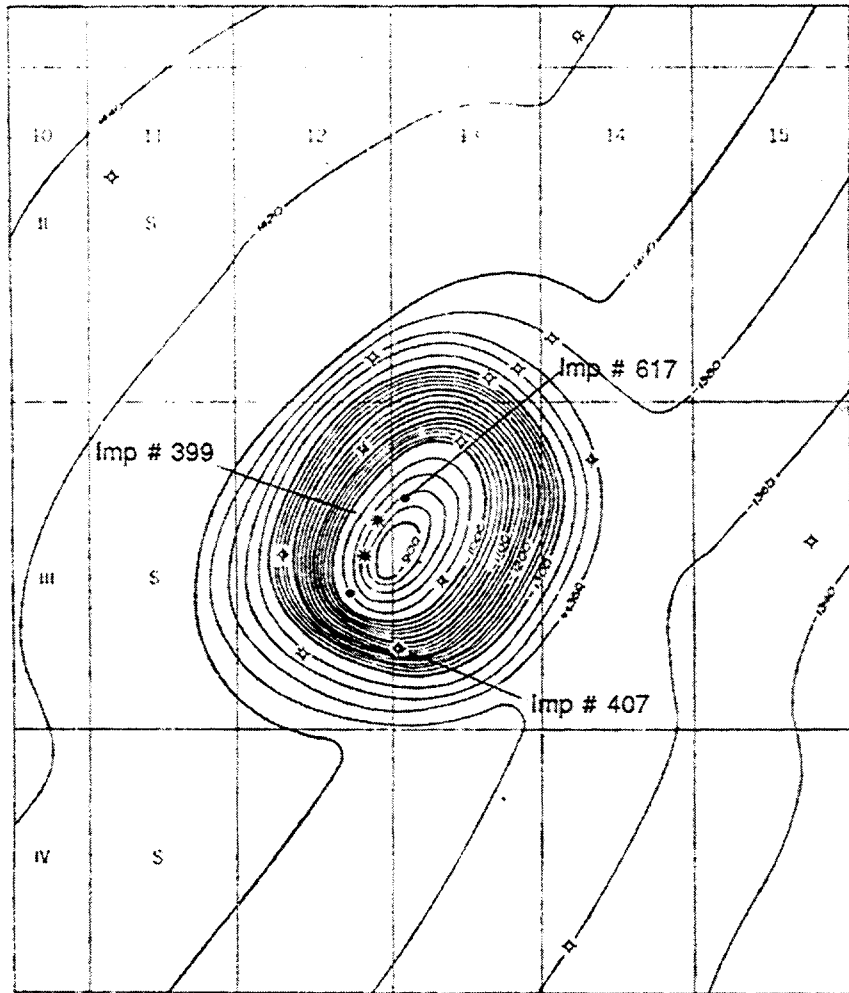
The Warwick reef (figure 1) produced oil from three wells from 1953 to the late 1970's. Peak production occurred in 1961 when $11\,419\text{ m}^3$ (71 937 barrels) of oil were produced (Pearson, 1980). By 1977, the field was pumping only $1\,427\text{ m}^3$ (8987 bbls) annually (Palonen and Booth-Horst, 1979). Since then the field, located in lots 12 and 13, concession III SER, Warwick Township, has been used for gas storage (figure 4). Total production was approximately $79\,365\text{ m}^3$ (500 000 bbls) from a pinnacle 32 ha (80 acres) in size (Palonen and Booth-Horst, 1979). Imperial Oil Enterprises cored three of the fifteen wells drilled into the structure, providing limestone cores of 190 m, 35 m and 87 m length. These cores penetrate from the A-2 Carbonate to the Rochester Formation; within the Guelph; and, from the A-2 Evaporite into the Guelph, respectively.

Further toward the centre of the Michigan Basin, the Payne bioherm has also been used for gas storage, since in 1957 (figure 1). Two cores of 69 m and 152 m were taken from the reef flank and reef-crest area by Imperial Oil in 1953 (figure 5). Both penetrate down to the Rochester Shale from the Guelph and A-1 Carbonate respectively. The Payne field is a partially dolomitized, kidney-bean-shaped build-up (Hill, 1966) situated mainly in lot 22, Concession VII of Moore Township, Lambton County (figure 5). Discovered in 1949, the pinnacle produced approximately 50 % of its estimated total reserves of $1.65\,10^9\text{ m}^3$ (58.3 bcf) from nine gas wells.


Closer to the Michigan Basin centre is the mainly dolostone Wilkesport reef, located in lot 4, Concession XIII, Sombra Township (figure 6). Imperial Oil pulled a single 111 m core, from a crest position (figure 6), that penetrates from the A-2 Evaporite through to the Lockport Formation. Discovered in 1966 and with initial tests of $623\,000\text{ m}^3$ (22 mcf) per day, the Wilkesport reef is now, like most other "old" pinnacles, a storage facility.

Two of the more newly discovered pinnacle bioherms, both limestone, are Terminus and Rosedale (figure 1). The Terminus reef, located in lots 23 and 24, concessions IX and X of Sombra Township, was drilled in 1968 by Ram Petroleum. Four cores from gas wells were recovered.

Figure 4: Map of the Warwick pinnacle reef with structure contours on the Guelph Formation. Contour interval is 20 ft. The positions of the studied cores, Imperial # 399, Imperial # 407 and Imperial # 619, are shown. See figure 1 for location (From Koepke and Sanford,1965).



STRUCTURE CONTOURS ON THE GUELPH FORMATION

Structure contours (interval 20 feet) 

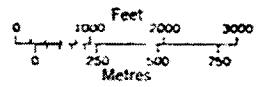


Figure 5: Map of the Payne pinnacle reef with structure contours on the Guelph Formation. Contour interval is 25 ft. Circles show the locations of the two wells, Payne # 4 and Payne # 8, that were cored. See Figure 1 for location (From Hill, 1966).

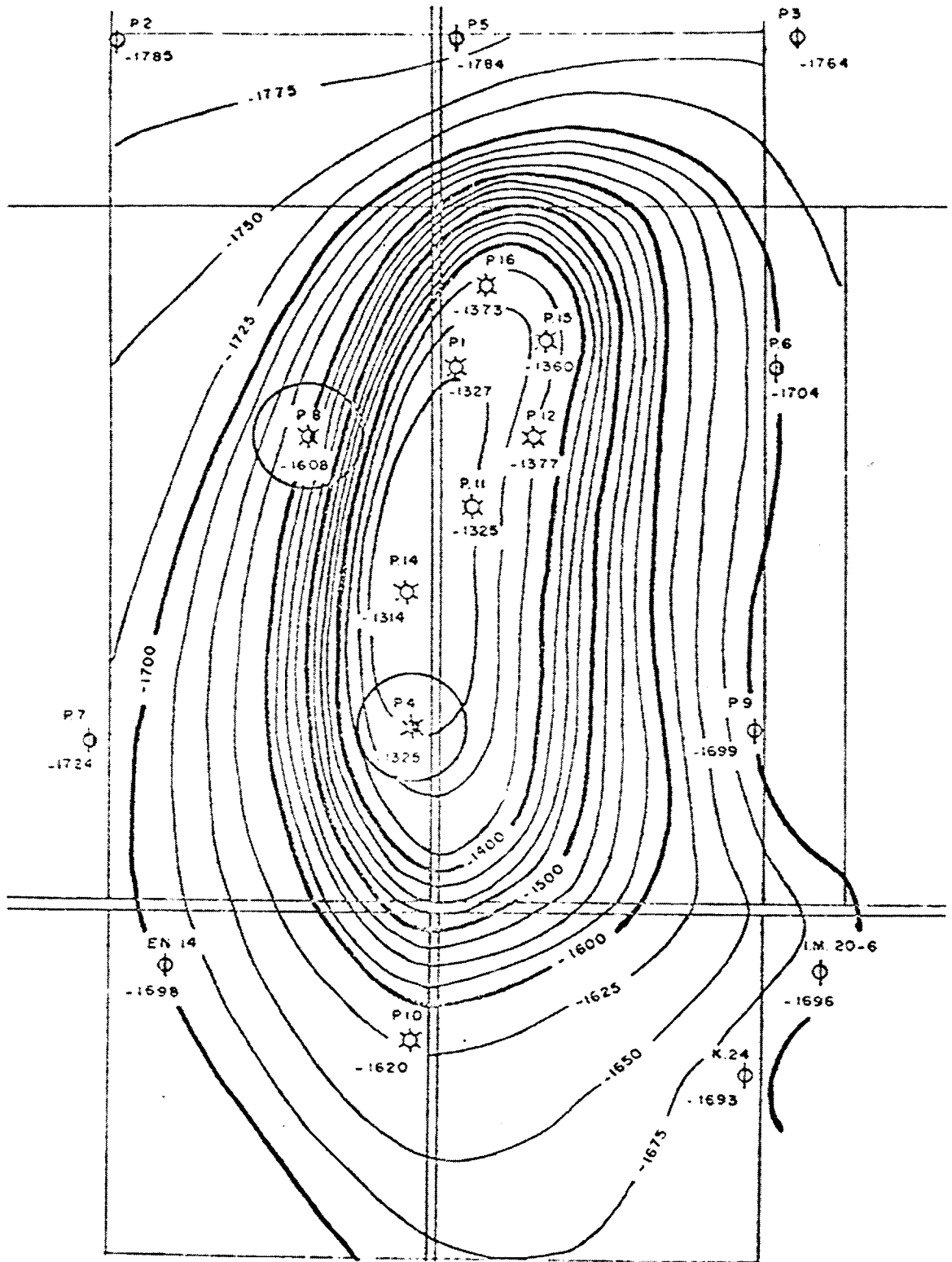
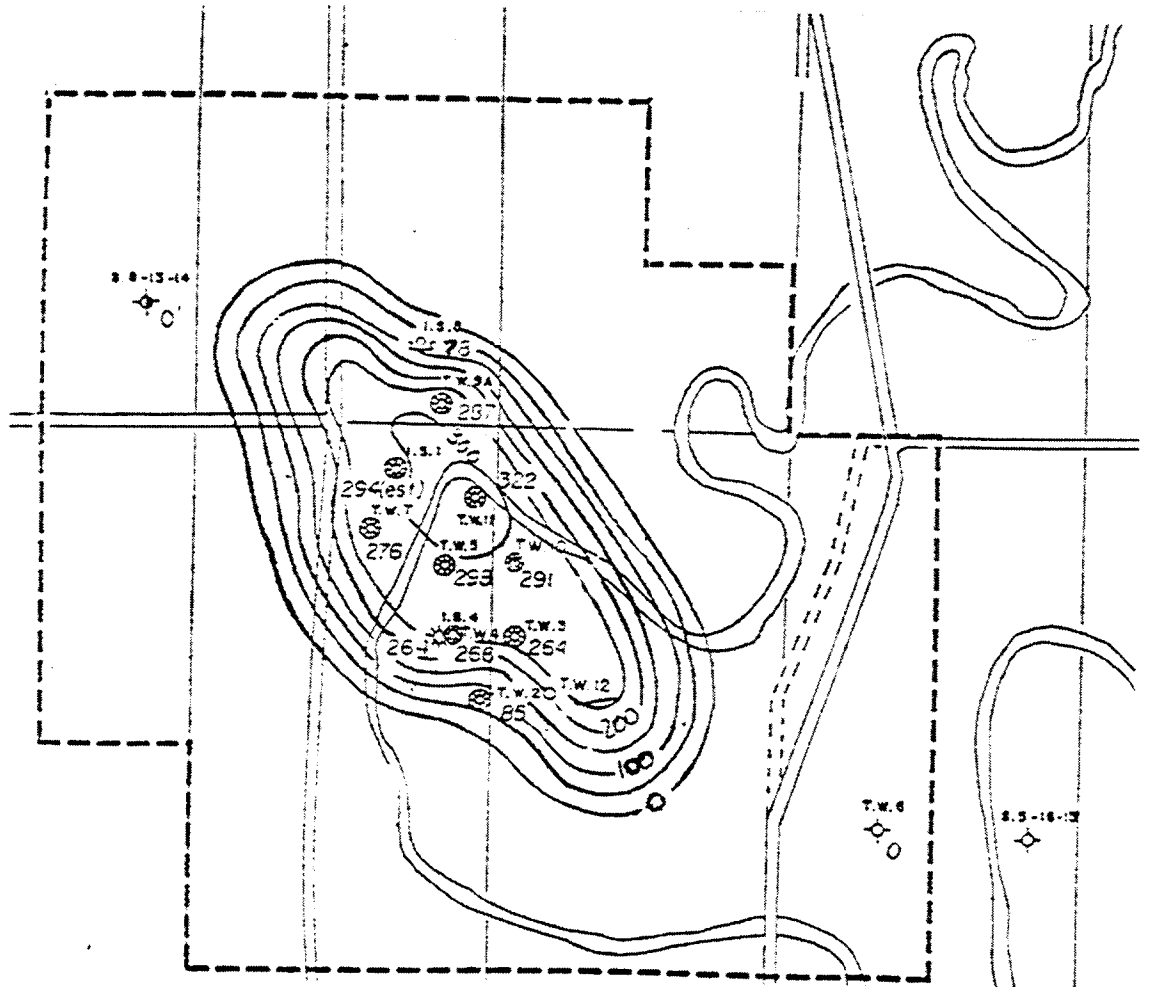


Figure 6: Map showing thickness of the Guelph and A-1 Carbonate Formations in the Wilkesport pinnacle reef. Contour interval is 50 ft. Reef shows the position of Imperial Sombra #14-XIII (I.S. 4). See Figure 1 for location (From Tecumseh Gas Storage Co., 1971).



Three of the cores were taken from a reef-crest location and are 101 m, 10 m, and 95 m in length (figure 7), and penetrate the A-1 Carbonate to Lockport, A-1 Carbonate, and A-2 Evaporite to Guelph respectively. The fourth core is a flank location, 54 m in length and covering the A-1 Carbonate to Lockport interval (figure 7).

The Rosedale pinnacle is the sixth bioherm studied (figure 8). It is located in Enniskillen Township, lots 8 and 9, Concessions I and II, close to North America's first wildcat well (near Oil Springs, 1857). Union Gas Ltd. cored the discovery well and most prolific producer of three gas wells, the 8-9-II (A). A 172 m core, penetrating from the A-2 carbonate to the Rochester Shale was obtained from a crest position in 1970. The well tested with a potential to produce 151 500 m³ (5.3 mcf) per day and had an estimated natural flow rate of 422 000 m³ (15 mcf) per day (Ontario Ministry of Natural Resources files). Since 1975 the Rosedale reservoir has been used as a gas storage facility.

1.5.2 Hydrocarbon Production in Southwestern Ontario

Oil and gas are extracted from the Cambrian, Ordovician, Silurian and Devonian sections; however, 36.7 % of all oil produced and a staggering 90% of all gas production is from Silurian strata (Palonen and Booth-Horst, 1979) . In the southern Michigan Basin about 300 productive reefs were discovered to the end of 1982. Of these, 190 are oil and 110 are gas producers (Gill, 1986). The percentage of successful drilling for some exploration companies is as high as 85% (Caughlin *et al.* , 1976).

In terms of the Silurian, most production is derived from the Niagaran aged, Guelph Formation of the Albemarle Group (Sanford and Brady, 1957) and from the Cayugan A-1 Carbonate of the Salina Group (figure 2). In the study area, the Guelph Formation consists of pinnacle reef bioherms and basinal carbonates which overlie the platform carbonates of the Lockport Formation (figure 2). Alternating evaporite and carbonate units of the Salina Group effectively encase the bioherms and provide a seal for hydrocarbon entrapment.

Figure 7: Map of the Terminus pinnacle bioherm with contours on the Guelph Formation. Locations of studied cores are shown. Contour interval is 10 m. See Figure 1 for location.

23

24

X

IX

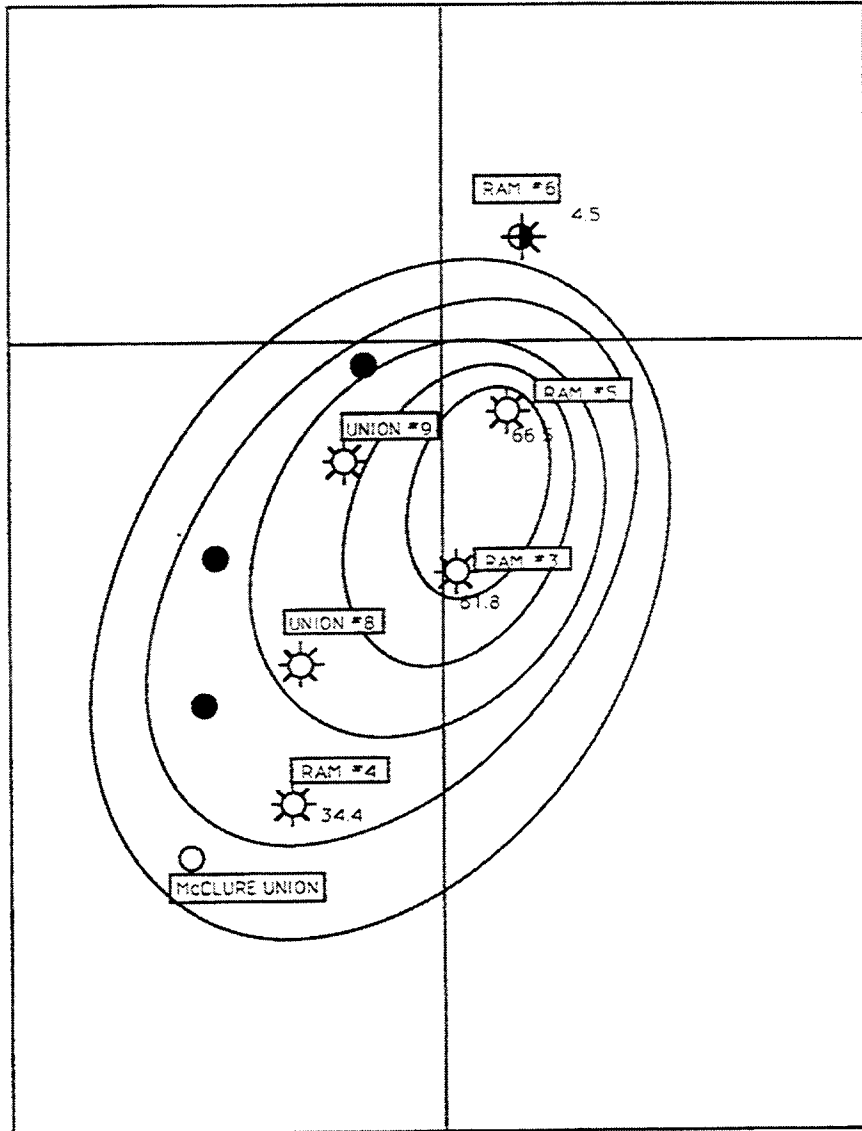
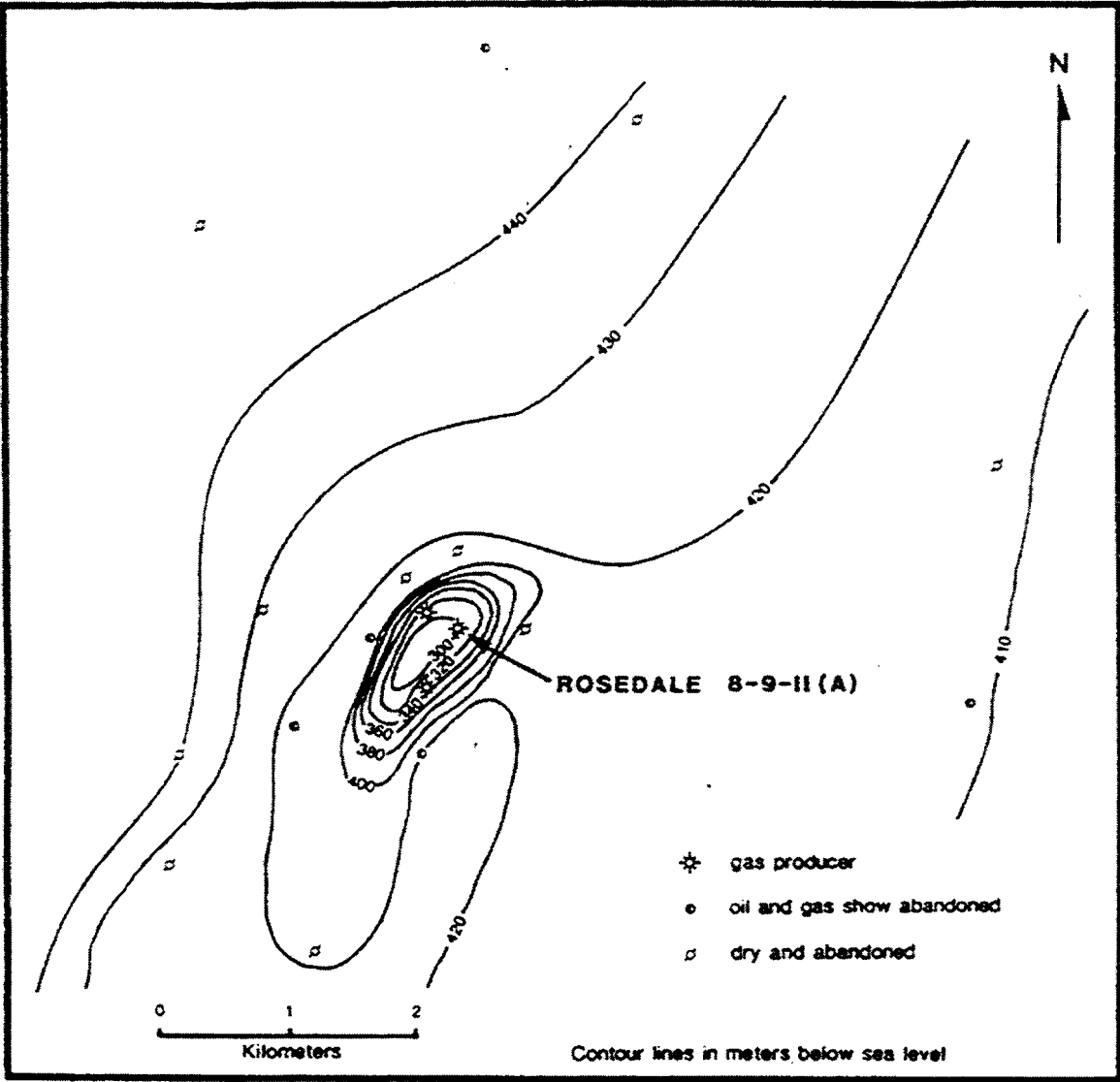


Figure 8: Map of the Rosedale pinnacle reef with structure contours on the Guelph Formation. Contour interval is 20 m. Map shows the location of the Union Rosedale 8-9-II (A) well. See Figure 1 for location. (From Grimes, 1988).



In Elgin, Kent and Essex counties as well as the majority of Middlesex County (figure 1), hydrocarbons are produced from patch-reef bioherms. Huron and Lambton counties (figure 1) show Silurian hydrocarbon production primarily from pinnacle reefs, with Lambton County accounting for slightly greater than 50% of the province's entire annual production (Palonen and Booth-Horst, 1979). Annual cumulative production from all stratigraphic levels in Ontario approximately equates to the daily production of the Western Canada Sedimentary Basin (Pearson, 1980).

1.6 Geologic Setting and Paleogeography

The present-day Michigan Basin, in plan view, is roughly circular in shape and underlies the Great Lakes regions of both Canada and the United States (figure 9). This area, roughly 300 000 km² in size, is bounded in Ontario by two positive structural elements: to the north by the Canadian Shield; and to the east by the Algonquin Arch (Bolton, 1957). Locally, the Arch is a positive structural feature trending northeast-southwest through southwestern Ontario. Its axis shifted back and forth, during the Paleozoic, toward the Michigan Basin to the west and Appalachian Basin to the southeast as the Bruce megablock to the north of the arch, and Niagara megablock to the south, subsided differentially (Sanford *et al.*, 1985). Most sediments thicken toward the paleo-centre of the Basin located in southern Michigan (Gill, 1977). However, the reefal carbonates of the Middle Silurian, show the opposite trend in thicknesses (Gill, 1977).

Several workers (Sanford, 1969; Caughlin *et al.*, 1976; Huh *et al.*, 1977; Briggs *et al.*, 1980) have shown that during deposition of the Guelph Formation, the Michigan Basin developed three near-concentric reef belts that ring the basin (figure 10). Outermost, there exists a fringing, barrier reef-complex. Basinward, the barrier reef is replaced, in a slope setting, by a patch-reef belt. The patch-reef belt is in turn succeeded by a belt of pinnacle reefs. Following the pinnacle reefs, basinal sediments continue to the centre of the basin. Sanford

Figure 9: Middle Silurian paleogeographic map showing two inlets or channels that connected the basin with the open sea. (From Briggs *et al.* 1980).

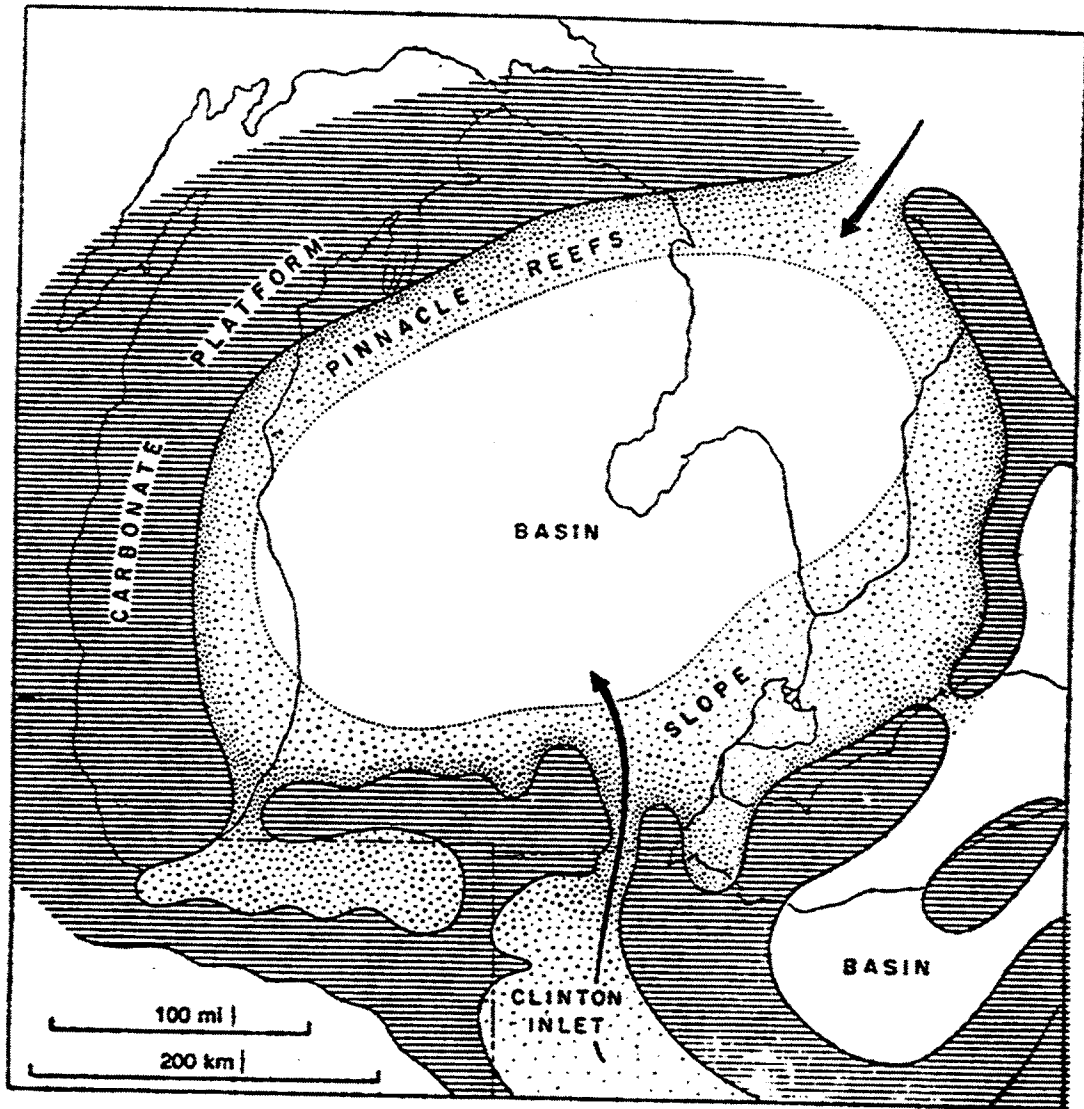
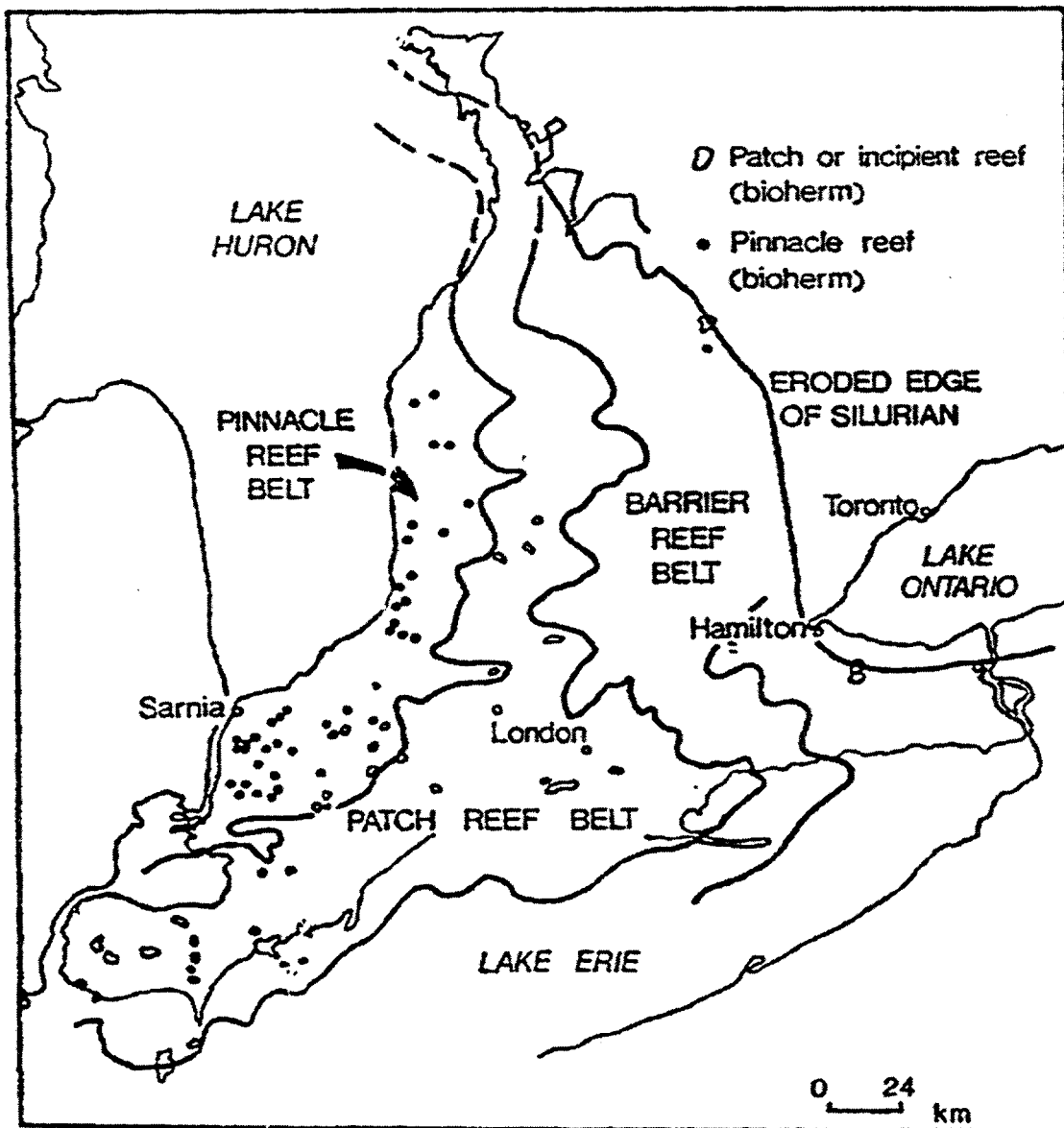


Figure 10: The major reef belts that ring the Ontario side of the Michigan Basin.
(From Pearson, 1980; after Sanford, 1969).



also recognized a belt of lagoonal sediments that lay to the south east of the barrier complex, toward the Appalachian Basin.

Pinnacle reefs in the Michigan Basin are characterized by limited areal extent (12 to 344 ha, 30 to 850 acres range; 32 ha, 80 acres average). The bioherms are also thick, being an average of 90 m high in the southern part of the basin and 180 m high in the northern Michigan pinnacle reef trend (Gill, 1979). Steep reef flanks with interpreted dips of 30 to 45 degrees are common (Gill, 1979). Up to 95.2 million m³ of oil (600 million barrels) and 2.3 to 3.8 trillion m³ (3 to 5 tcf) of gas is estimated to exist in these small structures (Caughlin *et al.* , 1976) which have a distribution density of approximately one pinnacle per 4 km² (Sears and Lucia, 1980). Gill (1979) found that reefs show increasing dolomitization and oil gravity toward the margin, whereas height, pay thickness, burial depth, reservoir pressure, hydrogen sulphide content and salt plugging increase basinward.

Only two slim inlets through the barrier reef-complex (figure 9) are thought to have existed in Niagaran time (Briggs *et al.*, 1980; Droste and Shaver, 1983). One, to the south, connected the basin with epicontinental seas and the more southerly Illinois and Appalachian Basins. The second passageway is placed in the area of present-day Georgian Bay, south of Manitoulin Island, and connected the Michigan Basin with the Hudson Bay Basin to the north.

Sanford *et al.* , (1985) concluded that the Michigan Basin was influenced by several Early Paleozoic events. However, movement could not have been significantly differential relative to the basin sides given the present-day near-concentric configuration of the basin.

1.7 Previous Work

Previous work detailing the Middle Silurian in the Michigan Basin is extensive and dates back to the mid-Nineteenth Century (eg. Hall, 1862; Chamberlain, 1877). The vast majority of research has been carried out by American geologists concentrating on reef build-ups

in Michigan, Indiana, Ohio and Illinois. Investigations of reefal carbonates on the Canadian side of the Michigan Basin have not been as plentiful.

Recent research has focused on several topics: (1) developing models for pinnacle growth; (2) determining the mechanism causing cyclicity of the Salina Group carbonates and evaporites, and their relationship to Guelph pinnacles; and (3) the dolomitization processes within the pinnacles. This section highlights some of this recent work and the models that have resulted. By doing so, the various models are both compared and contrasted to one another. In addition, this section serves to contrast with the ideas and results presented in future chapters of this study.

The most widely accepted model for pinnacle reef growth in the Michigan Basin proposes shallow- water reef genesis concluding with an enormous and catastrophic draining of the basin at the end of the Wenlockian (Huh *et al.* , 1977; Gill, 1977, 1979, 1986; Cercone, 1984; Cercone and Lohmann, 1985, 1986; Pearson, 1980; Sears and Lucia, 1980; Mesolella *et al.* 1974; Briggs and Briggs, 1974; Briggs *et al.* 1980; Bailey and Cochrane, 1990). To some of these workers, the resultant subaerial event effectively killed bioherm growth, and the overlying algal facies in the A-1 Carbonate are a genetically separate entity from the pinnacle bioherms. Others see the A-1 Carbonate as an extension of the reefs separated only by a time gap (Mesolella *et al.*, 1974; Bailey and Cochrane, 1990). Further still, other workers do not believe the A-1 Carbonate to cap the pinnacles at all (Hill, 1966; Bailey, 1986). Regardless, most authors agree that sea-level in the Michigan Basin fell about 100 m to 180 m (Gill, 1973, 1977) over a short period of time, exposing the pinnacle reefs. This single exposure episode is believed to have karsted the entire reef section.

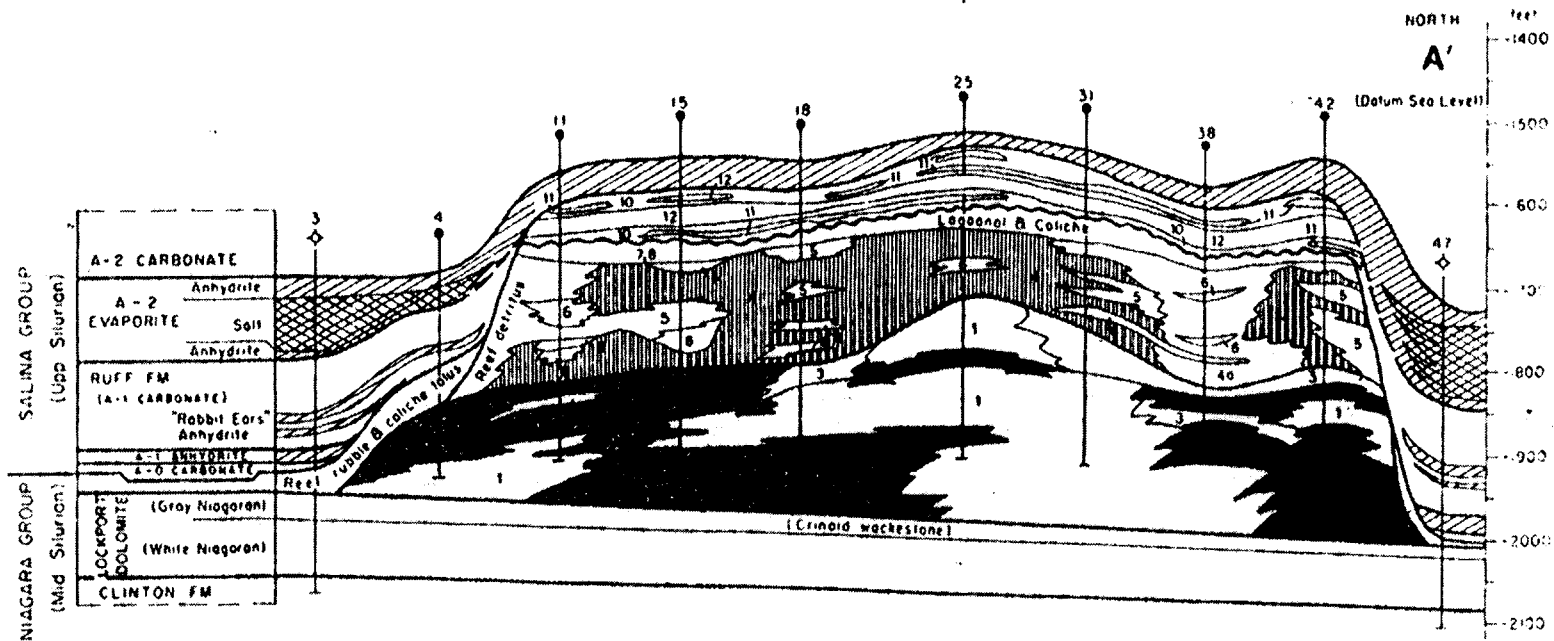
Many authors have examined individual pinnacle bioherms, separating the Guelph Formation reef from the A-1 Carbonate with the massive exposure episode. Most delineate a number of shallow-water reef-growth stages and facies (Table 1; figure 11) and identify the A-1 Carbonate as draping the pinnacle bioherm (Huh *et al.* ,1974; Cercone,1984; Pearson,1980;

Table 1: Previous work by various authors showing the number of interpreted reef growth stages, correlation of A-1 Carbonate, and the number of recognized karst episodes.

| AUTHOR | STUDY AREA | NUMBER OF STAGES OF REEF GROWTH | A1 CARBONATE ABOVE PINNACLES | NUMBER OF KARST EPISODES |
|---|----------------------------|---------------------------------|------------------------------|--------------------------|
| TEXTORIS AND CAROZZI, 1964 | INDIANA | 6 | NOT ADDRESSED | NOT ADDRESSED |
| HILL, 1966 | PAYNE PINNACLE | 5 | NO | 1 |
| MESOLELLA ET AL., 1974 | NORTHERN MICHIGAN | 4 | YES, PART OF REEF | 1 |
| HUH ET AL., 1977 | NORTHERN MICHIGAN | 4 | YES | 1 |
| GILL, 1977 1979 | NORTHERN MICHIGAN | 4 | NO | 1 |
| SEARS AND LUCIA, 1979 | NORTHERN MICHIGAN | 3 | YES | 0 |
| PEARSON, 1980 | WARWICK PINNACLE | 5 | YES | 1 |
| SEARS AND LUCIA, 1980 | NORTHERN MICHIGAN | 3 | YES | 1 |
| CERCONE, 1984; CERCONE AND LOHMANN, 1986 | UNION 8 PINNACLE | 4 | YES | 1 |
| SANFORD ET AL., 1985 | SOUTHWEST ONTARIO | NOT ADDRESSED | YES, ALSO A1 EVAPORITE | NOT ADDRESSED |
| BAILEY, 1986 | SOUTHWEST ONTARIO | NOT ADDRESSED | NO | NOT ADDRESSED |
| GILL, 1986 | BELLE RIVER MILLS PINNACLE | 4 | YES | 1 |
| GRIMES, 1988 | ROSEDALE-FLETCHER REEFS | 3 | YES | MULTIPLE |

Figure 11: Previous Silurian pinnacle reef modeling:

Reef growth in four phases with associated facies. Facies 1 to 3 represent biohermal stage. Facies 4 to 7 are the organic reef stage. Facies 8 and 9 belong to the subaerial stage. Facies 10 to 12 represent the Maumee Algal Stromatolite Cap stage considered to represent a possible equivalent of the A-1 Carbonate (From Gill, 1986).



Grimes, 1988; Gill, 1986; Cercone and Lohmann, 1985,1986). Others, however, show the A-1 to abut against the side of the reef (Bailey, 1986; Gill, 1973, 1977, 1979).

Sears and Lucia (1979) proposed a reef growth model based upon their observations of pinnacles located in northern Michigan (figure 12). Their model consists of three stages of reef growth, with the absence of subaerial exposure. Observed pisoliths and caliche crusts on the top of the pinnacles were thought to reflect rising salinity levels. Sarg (1982) also proposed pinnacle growth without exposure.

Three models for reef growth, with two based on a rapid sea-level lowering, were developed by Mesolella *et al.*, (1974). Model 1 proposed that the reef pinnacles were fully developed, showing a biotic succession prior to sea-level lowering, karsting, and the deposition of off-reef Salina evaporites and carbonates. This model was rejected by the authors based on their own biostratigraphic evidence. They found the brachiopod *Howellella aff. corallinensis* Grabau in a pinnacle core suggesting that the pinnacle was possibly Pridolian in age and therefore it postdated the off-reef Salina. Of note, however, is that only a single core contained the brachiopod out of about 60 cores studied.

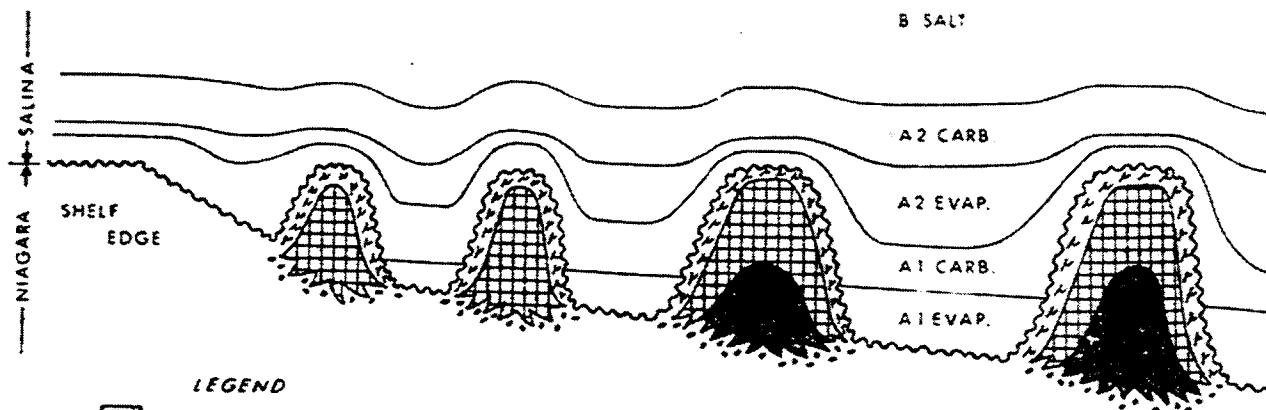
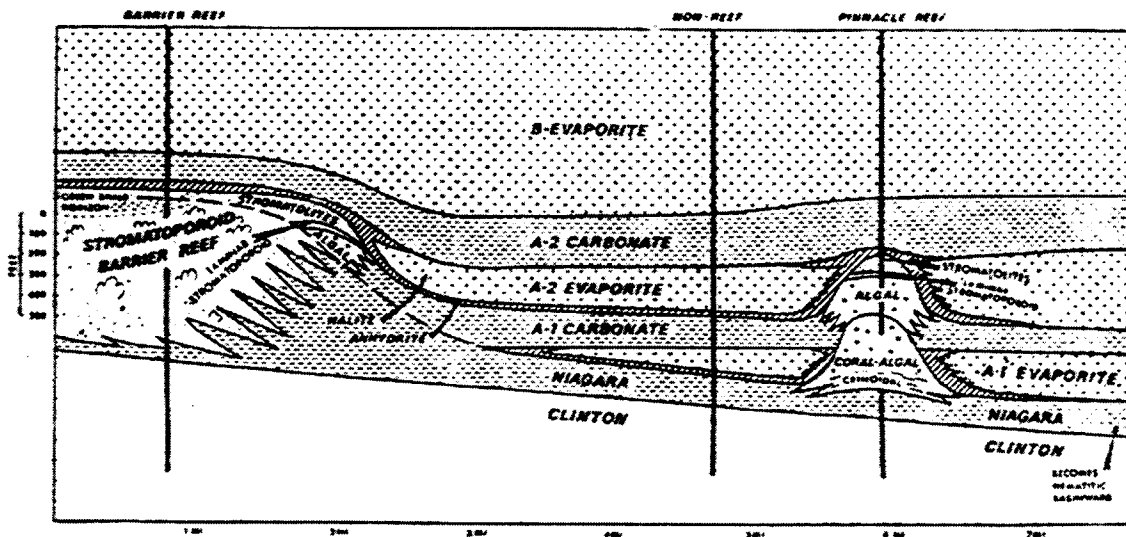
The second model proposed that the Guelph pinnacles and the inter-reef Salina units were contemporaneous in their deposition. In effect, the reef organisms in the pinnacles lived while evaporites were deposited directly adjacent to them. This model was also rejected as it required depositional conditions necessary for reef growth and depositional conditions necessary for evaporite deposition simultaneously.

Model 3 (figure 12) proposed that the carbonate units contained in the Michigan Basin resulted from high relative sea levels. Conversely, the evaporite units resulted from very low sea levels. This model infers that the algal facies of the A-1 Carbonate (a high sea-level deposit) are an extension of the pinnacle reefs (a high sea-level deposit) separated by an episode of subaerial exposure. Crinoids and corals exist in the lower stage (pinnacle) while laminar stromatoporoids, encrusting algae and stromatolites are found in the top stage (A-1 Carbonate). It appears however, (Sears and Lucia, 1979; this study) that laminar





Figure 12: Previous Silurian pinnacle reef modeling:

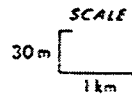
A) Stage 1, crinoidal mound material, is succeeded by coral-algal reef mound of stage 2. Growth is terminated during A-1 Evaporite deposition, with an exposure episode and rejuvenated during A-1 Carbonate deposition (stage 3). Reef growth is permanently halted by A-2 Evaporite deposition (stage 4) (From Mesolella et al., 1974).

B) Three phases of reef growth as developed across the Michigan Basin. A carbonate mud mound is replaced by a coral-stromatoporoid reef which is in turn replaced by a restricted algal cap. No subaerial exposure episodes and succession is interpreted to represent response to increasing sea levels and salinities (From Sears and Lucia, 1979).



LEGEND

-  RESTRICTED MARINE
-  CORAL-STROMATOPOROID REEF
-  CARBONATE MUD MOUND
-  FLANKING CRINOIDAL



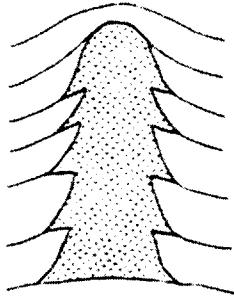
stromatoporoids are not found in the A-1 Carbonate overlying the reef, and the unit is more a restricted carbonate facies. This, coupled with the massive karst episode that terminated coral and stromatoporoid growth, suggests that while the A-1 Carbonate is part of the overall pinnacle reservoir, it is not part of the reef *sensu stricto*. Droste and Shaver (1977) determined that the paleontological data used by Mesolella *et al.*, (1974) to refute models one and two, and support model three, were erroneous.

Devaney *et al.*, (1986) proposed that the Pipe Creek Jr. patch-reef bioherm in Indiana is in fact a carbonate clinothem as detailed by Wilson (1975). Their work contends that the bioherm is made up of allochthonously-derived skeletal material from a prograding wedge along the shelf-basin transition in the Michigan Basin. As such, there is no reef core made up of organisms from the baffler or frame builder guilds (Fagerstrom, 1988). While this new idea is interesting, a number of workers have documented the presence of a reef core in Michigan Basin pinnacles and reef-building organisms in large numbers (Textoris and Carozzi, 1964; Cercone, 1984; Sears and Lucia, 1979; Gill, 1986; Mesolella *et al.*, 1974; Pearson, 1980; Grimes, 1988; this study). Other authors have also reported vertically-zoned cores in other Silurian reefs (Narbonne and Dixon, 1984; Bourque and Gignac, 1983; Bourque *et al.*, 1986). Consequently, it appears that the clinothem theory is perhaps more applicable to the reefs of the U.S. Midwest (Wilson, 1975).

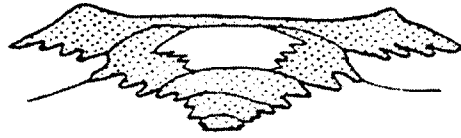
A final theory on reef genesis involves reef growth in water depths of hundreds of feet (McGovney *et al.*, 1982), a model that was originally proposed in the 1930's. The abundance of shallow-water organisms in the bioherms tends to preclude such an environment of deposition.

It is clear that a number of Silurian pinnacle reef models exist, and a collection of interpretive sketches of the bioherms is displayed in figure 13. Few workers, however, discuss karsting as an important diagenetic process (Kahle, 1988; Grimes, 1988). Virtually all others invoke a single, subaerial exposure event which ended bioherm growth.

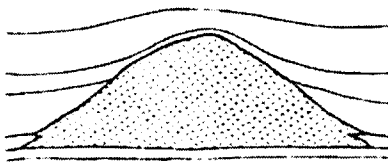
Figure 13: The different Silurian reef models result in everyone having a favourite (From Shaver, 1977).



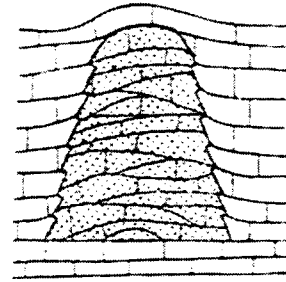
BLUE SPRUCE



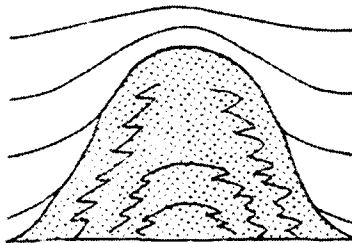
SPREADEAGLE



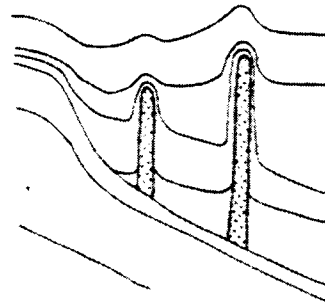
MAMMARY GLAND



LIME KILN



HAYSTACK



TELEPHONE POLES

1.8 Analytical Techniques

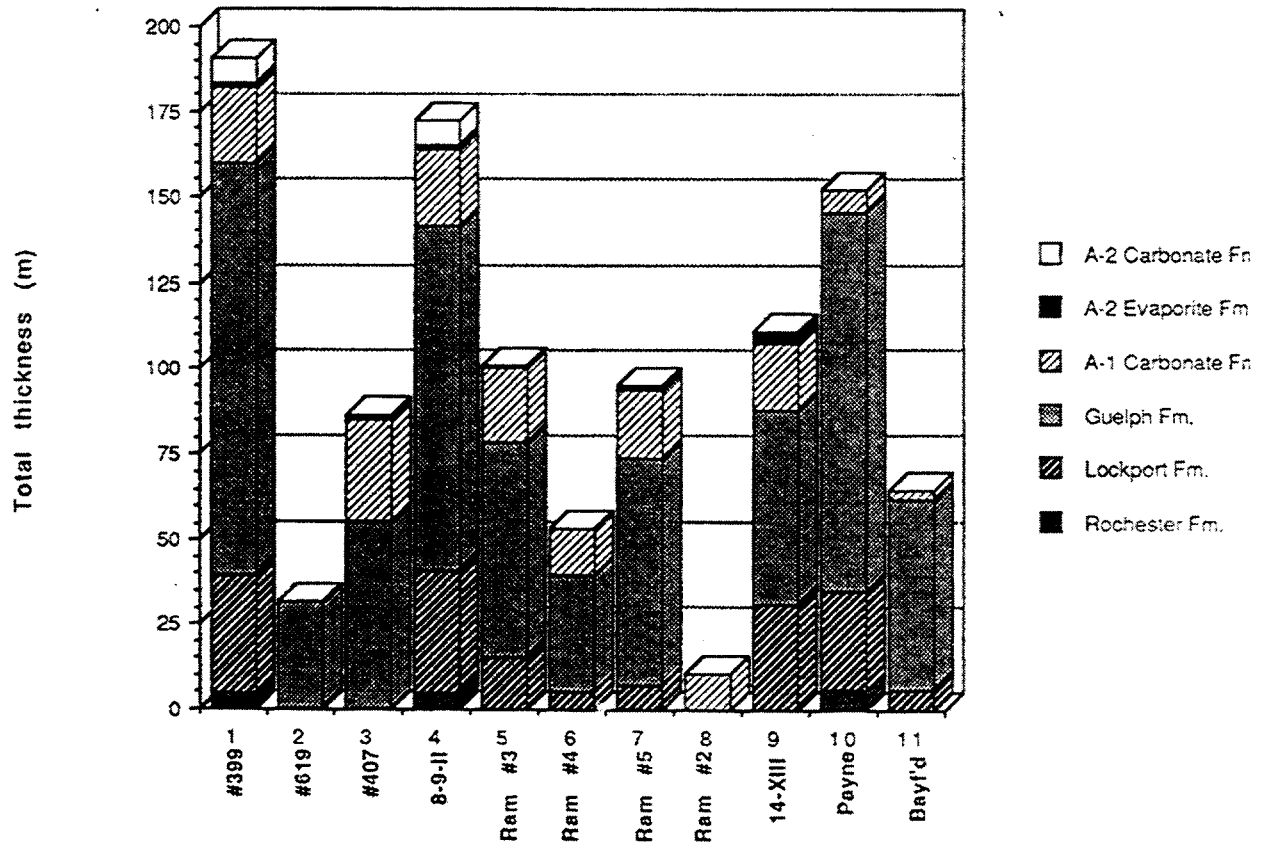
A number of analytical techniques were used to obtain the data needed for this study including: core analysis; wireline log analysis; thin section staining and petrography; epifluorescence microscopy; petrographic image analysis; cathodoluminescence; and stable isotope analysis.

The six reefs yielded a number of cores, varying in length and in the number per reef (Figure 13A). All the cores except Ram # 3 from the Terminus reef and the Union 8-9-II-A Rosedale core, are only available as a one-eighth piece of the original 15 cm diameter core. Both a three-quarters and a one-eighth slab are available from the Rosedale core, and the Ram #3 core was of one-third size. Core from the Payne bioherm has been sampled by previous workers and little remained of selected areas. Consequently, thin sections were not made of this core. All of the cores are stored at the Ontario Ministry of Natural Resources Subsurface Core Laboratory in London, Ontario.

The Bayfield pinnacle provided a single, 64 m (211 ft.) core while the Wilkesport reef core is 111 m (364 ft.) long. The Payne bioherm has two cores of 152 m and 69 m (499 ft. and 226 ft.) in length. All are dolomitized, with fair to good recovery, but the cores are not of the best quality. The Rosedale 8-9 well was cored for 172 m (564 ft.). Core recovery and core quality are good and the core is limestone. Three cores were studied from the Warwick bioherm, 190 m, 87 m and 35 m (623 ft., 285 ft., 115 ft.) in length respectively, and are mainly limestone, also with good recovery and quality of core. Four cores were studied from the Terminus reef; 101 m, 95 m, 54 m, 10 m (331 ft., 312 ft., 177 ft., 33 ft.) in length. These cores are also mainly limestone and of fair to good quality. However, the quality and recovery of the Ram #3 core are substandard.

The cores were described in detail using the classification scheme of Dunham (1962) and the subsequent modifications of Embry and Klovan (1971). Porosity was described using the system of Choquette and Pray (1970), and grain and crystal sizes were described using the terminology

Figure 13A: Stacked bar graph showing the formations and relative thicknesses encountered by each core.



of the Canadian Stratigraphic Services Ltd. Gamma ray, sonic, neutron and density logs were used to adjust core depths and for signature comparisons.

From the cores, 140 thin sections were analyzed. Most were polished and uncovered to allow for further cathodoluminescence, epifluorescence and image analysis. All were later stained, following the techniques of Dickson (1965), with Alizarin Red S to differentiate between calcite and dolomite, and Potassium Ferricyanide for iron detection. Thin sections were examined and photographed using a Zeiss microscope and internally contained Leica camera at Shell Canada Ltd.'s Calgary Research Centre (CRC) during the summers of 1988 and 1989.

Image analysis to quantify pore geometries was also attempted at CRC using a Cambridge scanning electron microscope and an attached Joyce Loebel image analyzer. It was hoped that the analyzer could document preferential horizontal orientation of the long axes of pores in karsted areas, signifying horizontal movement of meteoric phreatic water. However, a number of factors could cause the creation of pores with horizontal axes. As such, it was felt that use of the image analyser would not significantly add to the data base (J.H. Theissen, pers. comm., 1988).

Ultraviolet fluorescence (epifluorescence) was performed at CRC in the summer of 1988 and at Esso Resources Canada Ltd in Calgary in the summer of 1989. Epifluorescence can be used to detect the presence of hydrocarbons trapped in fluid inclusions, thereby aiding in understanding diagenetic timing, or, it may show delicate crystal growth structures by detecting the presence of organic material. The analysis involved using a Zeiss microscope (CRC) or a Leitz microscope (Esso) and ultraviolet light with a wave length of 366 nm . In both cases Zeiss neofluor lenses of 2.5x, 6.3x and 10x were used to enhance the resultant images (Jeff Dravis, pers. comm., 1989). Photomicrographs were taken with attached Leica cameras. Coloured paper or white recipe cards were placed under the thin section to enhance the fluorescence of the slide (Jeff Dravis, pers. comm., 1989).

Cathodoluminescence work was performed at CRC in the summer of 1989 using a gas assisted, Technosyn Model 2000 cold cathode analyzer, and at Queen's University, also with

Technosyn equipment. Photomicrographs were taken with Leica and Nikon cameras, respectively. A voltage of approximately 20 000 KV and gun current of 420 micro-amperes was maintained within a vacuum to allow trace element excitation. Certain trace elements contained within the crystal lattice enhance (Mn^{2+} , Pb^{2+} , rare earths) or inhibit (Fe^{2+} , Ni^{2+} , Co^{2+}) luminescence within carbonates. This can be used as a useful tool in recognizing diagenetic environments and crystal growth patterns.

Finally, stable isotope analysis was performed on a total of 56 samples collected from the cores of the six reefs. The samples were selected from various allochems, cement layers, and crystals to analyze calcite and dolomite for enrichment/depletion of C^{13} and O^{18} . A minimum of 8.0 mg of powder was extracted from the sample using a dentist's drill. Samples were shipped, in separate, sealed vials, to Shell Canada Ltd. and then were processed at the University of Calgary in the laboratory of Dr. Roy Krouse. The samples were placed in separate vessels, roasted in a vacuum to purge them of contaminants and bathed in phosphoric acid. The resultant gas was trapped in a separate container to stop further reaction and then each was analyzed with a mass spectrometer. A laboratory gas, standardized to PDB (Hudson, 1977) was used to compare the resultant carbon 13 and oxygen 18 measurements. The results were then compared to published work to interpret depositional and environmental conditions in the Michigan Basin during Guelph pinnacle formation.

1.9 Summary

Middle Silurian (Niagaran) Guelph Formation pinnacle bioherms of the Albemarle Group ring the Michigan Basin in a near-concentric belt, attaining heights of over 90 m in Ontario. Areal sizes range up to 344 ha in Ontario, and there are upwards of 300 actively producing bioherms in the state of Michigan and in Ontario. The Guelph Formation pinnacles sit atop platform carbonates of the Lockport Formation and are, in turn, shrouded by an apron of evaporites. The A-1 Carbonate of the Salina Group caps the reefs and rests unconformably on

both the pinnacles and the evaporites. A number of models exist to explain pinnacle reef genesis but none invoke more than one subaerial exposure event.

Six pinnacles were selected for study of which three are predominantly limestone and three are predominantly dolomite. Eleven cores totalling 1064 m were analyzed by way of core description, log analysis, thin section petrography, epifluorescent and cathodoluminescent microscopy, image analysis, and stable carbon and oxygen isotopes. From this evidence will be presented that suggests that a number of subaerial exposure events affected the Guelph pinnacles during their life-span. Each karst episode caused porosity and permeability enhancement in the reefs.

CHAPTER TWO

Lithofacies and Distribution Within Guelph Pinnacles

2.1 Overview

Although the main focus of this thesis is to establish that subaerial exposure events occurred throughout the growth history of Guelph Formation pinnacle bioherms, to do so it is necessary to outline the facies found within the reefs. This chapter examines only the gross overall lithofacies associated with the pinnacles (figure 14) and their distribution in the bioherms from observations made from core analysis (Appendix A). Each of these gross lithofacies can be subdivided into smaller, more refined facies; however, the purpose of this study is not to examine the facies within the pinnacle bioherms in detail. Interested readers are instead referred to Gill (1986), Huh *et al.*, (1977) Pearson (1980) and Grimes (1988) for facies descriptions.

While the Rochester Formation has identifiable members and facies (Brett, 1983), it is not subdivided as it is well below the pinnacles and is largely uncored. Both the A-2 Evaporite and A-2 Carbonate of the Salina Group are also each treated as single entities as these formations overlie the bioherms. The Lockport Formation is subdivided in accordance with its established two members, the Gasport and the Goat Island. Only the Guelph Formation pinnacles and the overlying algal units of the A-1 Carbonate are examined in terms of facies.

2.2 Rochester Formation

Shale from the Rochester Formation represents only the basal few metres of three cores. Both the Imperial Warwick # 399 core and the Union Rosedale 8-9-II core penetrated the Rochester for 4.9 m. The Imperial Payne #4 core shows 5.8 m of Rochester Formation shale.

Figure 14: Diagram showing gross lithofacies, thickness variations and formations present in the pinnacle bioherms of this study. Guelph Formation lithologies vary from limestone to dolostone.

FACIES

FORMATION

| | | |
|--|--|---------------|
| | nodular anhydrite | A-2 EVAPORITE |
| | stromatolite boundstone good fenestral porosity, minor breccia 9.0m to 14.3m | A-1 CARBONATE |
| | algal wackestone and algal mudstone very good inter-crystalline porosity and small vugs 6.0m to 17.5m, | |
| | stromatolite boundstone, 2.1m to 4.3m karst surfaces with clay | GUELPH |
| | algal wackestone some skeletal allochems vuggy porosity 12.3m to 47.8m | |
| | coral-stromatoporoid floatstone to framestone abundant skeletal allochems good porosity in places 25.0m to 61.4m | |
| | crinoid-skeletal wackestone with stromatactis 2.4m to 12.8m | |
| | crinoidal wackestone inter-crystalline porosity 29.9m to 34.4m | LOCKPORT |
| | dolomitic shale pyritic 5.8m + | ROCHESTER |

- | | | | | | | | |
|--|-----------|--|---------------|--|----------------|--|------------|
| | shale | | Coenites | | stromatolites | | vugs |
| | dolomite | | Favosites | | stromatactis | | crinoid |
| | limestone | | Halysites | | stromatoporoid | | bryozoan |
| | anhydrite | | rugose corals | | styolites | | brachiopod |

In the study area, the Rochester Formation is a regionally extensive medium grey to dark grey, dolomitic and calcareous shale (plate 1). The Rochester Formation varies from being fossil poor and possessing only tiny crinoid fragments to having sections showing thin, fossiliferous beds or lenses up to 3.0 cm thick. These local, fossil-rich accumulations are made up of crinoid pieces with a maximum diameter of 3.0 mm, and very thin shelled brachiopods, trilobites and indeterminate fossil debris. Brett (1983) interpreted these fossil-rich beds to result from the transport of lag deposits from more shallow environments due to storm action. Such storm deposits smothered bottom fossil assemblages (Brett, 1983). Pyrite is common within the Rochester Shale, occurring mainly as disseminated grains. However, pyrite can be found in patches, lining or clogging burrows, and replacing allochems, brachiopods in particular.

In the three cores that penetrate the Rochester Formation, the shale is laminated in part, and fissile. It becomes more competent and lightens to an olive colour locally, as the contact with the Lockport is approached (plate 2). An irregular, undulatory and sharp surface separates the Rochester Formation from the overlying Lockport Formation. Abundant pyrite is found below the contact and minor amounts above. Dolomitization is pervasive above the contact and the core further lightens in colour to light grey. The surface lacks any brecciation and there is no evidence of shallowing conditions as the surface is approached. This, together with the profuse amounts of pyrite suggests that the contact is a submarine hardground surface (James and Choquette, 1983). Borings into the surface were not detected, but any present may be obscured by the copious amounts of pyrite present.

2.3 Lockport Formation

The Lockport Formation overlies the Rochester Shale and is also a widespread unit. Two regionally extensive members, the lower Gasport Member and the upper Goat Island Member, both open marine, platform carbonates, can be identified in the study area (Gill, 1986; Pearson,

Plate 1: Rochester Formation rock types

Plate 1A: Sample from the Rochester Formation revealing dark grey, dolomitic shale. A thin layer of crinoid debris (a) can be found near the top of the sample and thin shelled brachiopod fragments are scattered throughout. Middle of the core shows concentration of pyrite (w). Union Rosedale 8-9-II-A.

Plate 1B: Thin section photomicrograph under crossed polars of Rochester Formation taken from the core piece in Plate 1A. Brachiopod (q) and crinoid (c) fragments are present. Scattered anhedral to euhedral dolomite crystals (d) can be found mostly in the fine grained matrix, but some are present in allochems. Bar scale represents 1mm. Union Rosedale 8-9- II-A, 663.6m subsea.

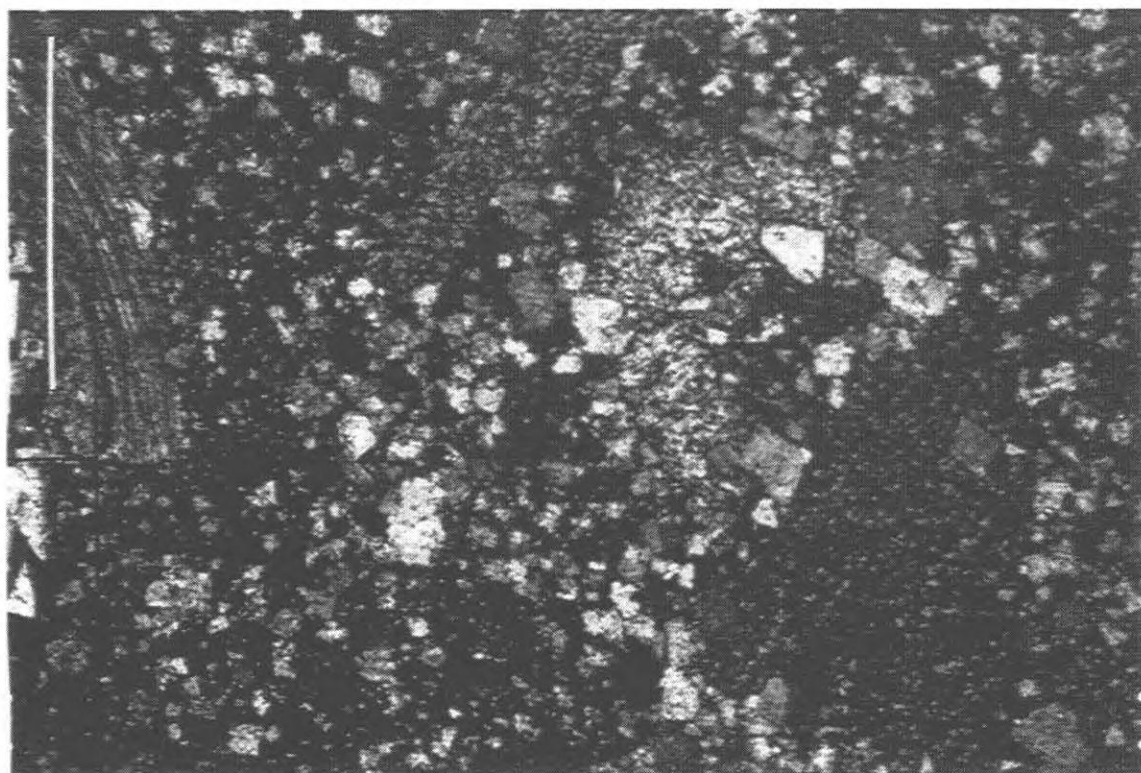
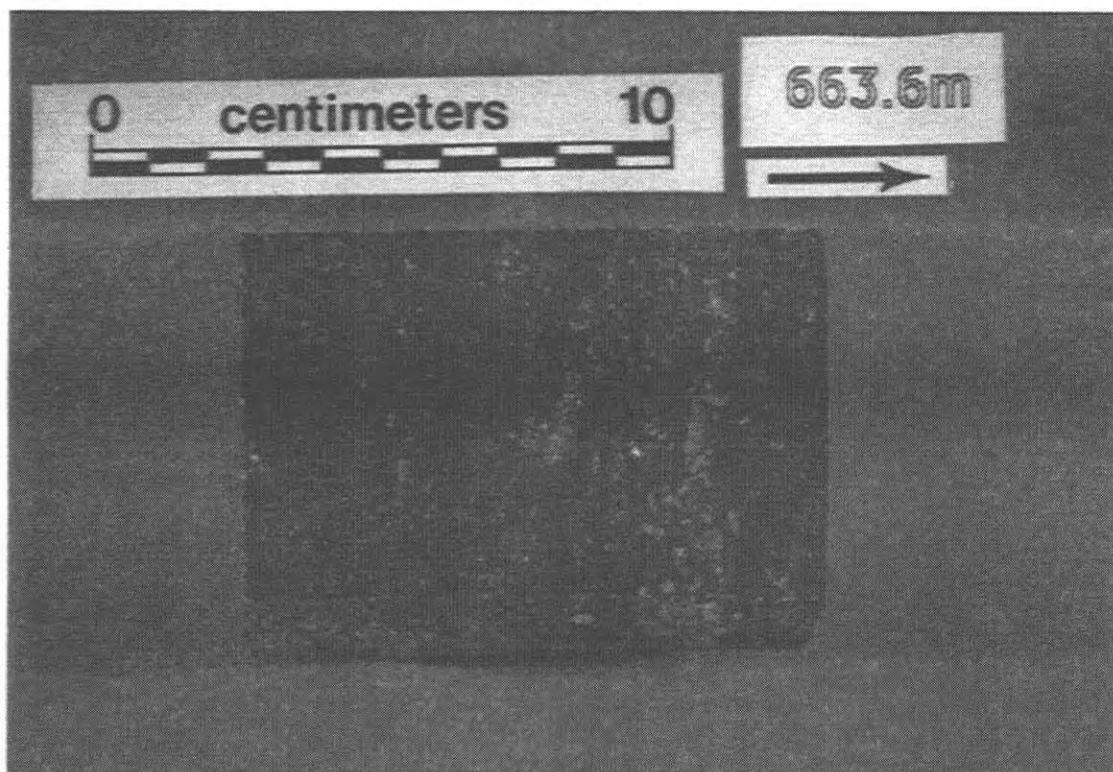
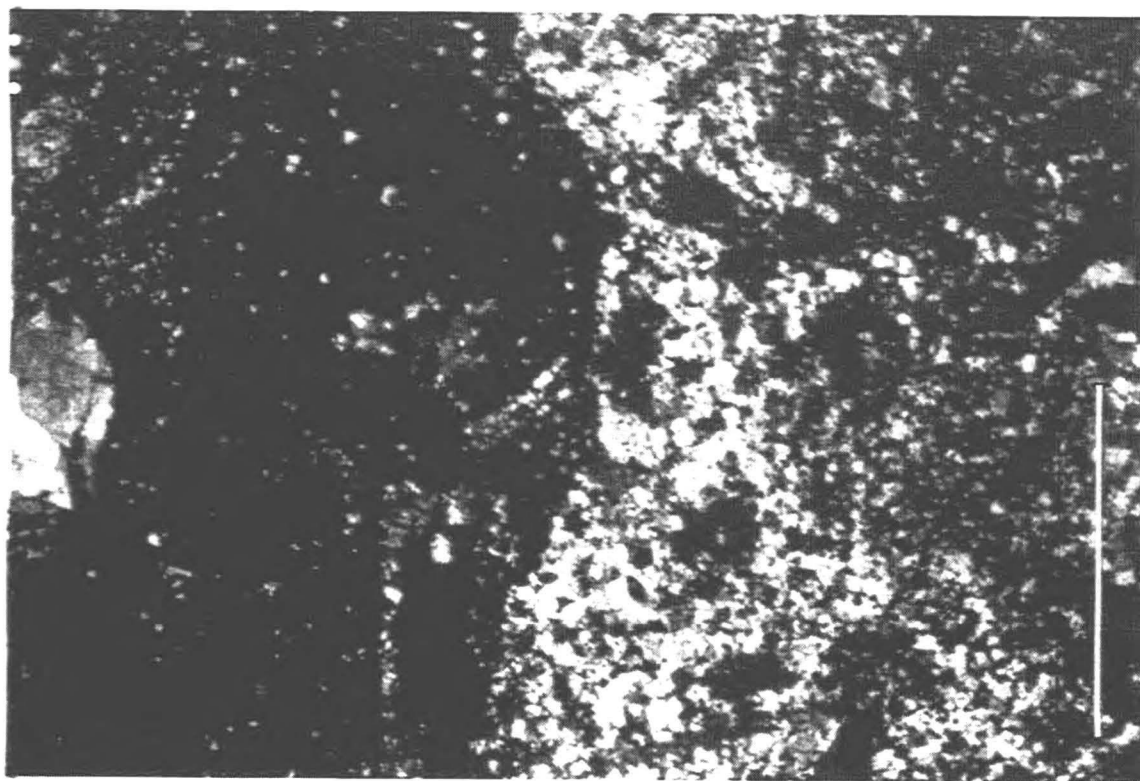
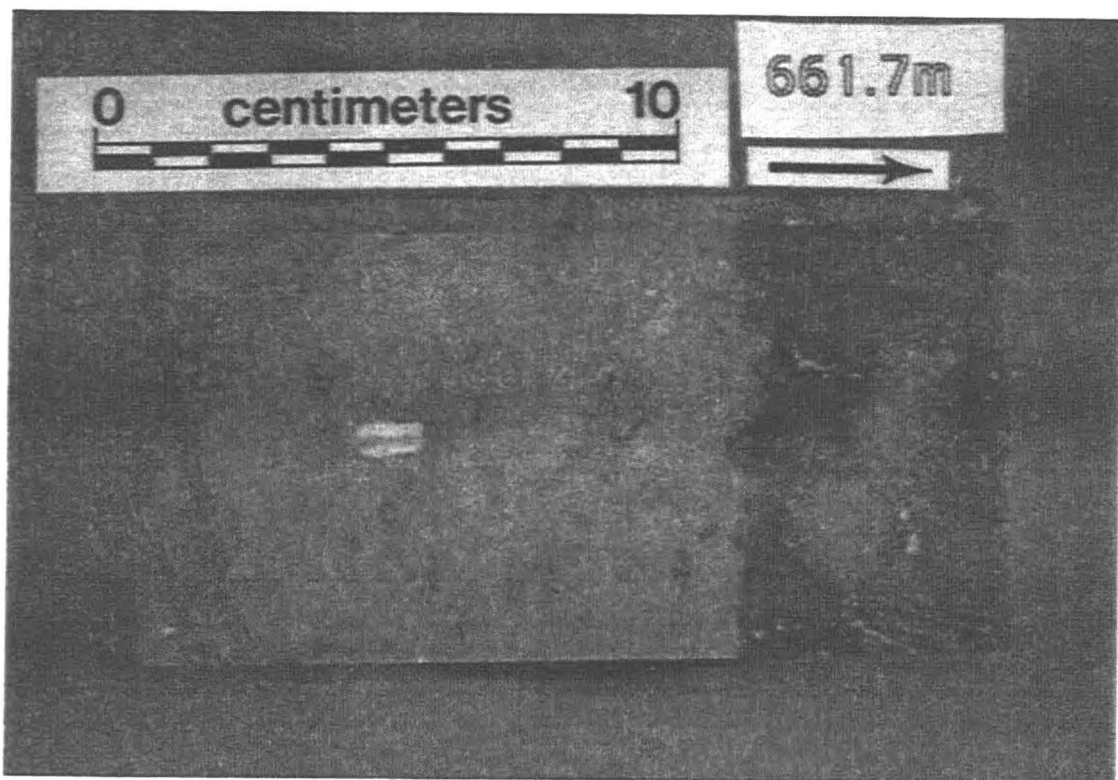


Plate 2: Rochester-Lockport contact

Plate 2A: Contact between the Rochester and Lockport Formations. The Rochester has lightened to olive-grey and is sharply overlain by the medium grey Lockport at what is interpreted as a submarine hardground (H). Abundant pyrite (P) can be found both above and below the contact. Large crinoid fragment (C) rests a few centimetres below the contact. Union Rosedale 8-9-II-A.

Plate 2B: Thin section photomicrograph under crossed polars of the Rochester-Lockport contact showing profusion of pyrite (dark) and dolomite (light) both above and below. Bar scale represents 1 mm. Union Rosedale 8-9-II-A, 661.7m subsea.



1980; Grimes, 1988). In New York State, the Lockport has been subdivided into five members in ascending order; the Decew, Gasport, Goat Island, Eramosa, and Oak Orchard (Shukla and Friedman, 1983). However in Ontario, both the Eramosa and the equivalents of the Oak Orchard are deemed to be stratigraphically higher than the Lockport. The Decew Member is present in the Niagara Escarpment area and along Lake Erie, underlying or interfingering with the Gasport (Bailey, 1986), but it is not found in the pinnacle reef belt. Lockport carbonates are thickest near the Michigan Basin-margin (Sanford, 1962) and are thinnest at the basin centre (Huh *et al.*, 1977).

2.3.1 Gasport Member

The stratigraphically lower Gasport Member consists of a light grey, crinoidal, dolomitic wackestone (plate 3). Small, thin sheets of crinoid packstone up to 4.0 cm thick are randomly found throughout. Crinoids and accessory allochems such as brachiopods, trilobites and bryozoans are small in size. Above the Rochester Formation contact, the crinoids are 2.0 mm in diameter but attain sizes of 4.0 mm by the top of the Gasport Member. Brachiopods are thin shelled and up to 4.0 mm long. Bryozoan fragments are horizontal in orientation and are a maximum to 15.0 mm long by 2.0 mm wide.

Dolomitization is pervasive within the Gasport. Two different textures of dolomite were observed with additional later, saddle dolomite crystals. Much of the matrix of the Gasport is made up of anhedral, finely crystalline dolomite estimated to average 50 μm in size. Euhedral, dolomite crystals, up to an estimated 300 μm in size, were also observed replacing allochems locally (plate 4). There is good inter-crystalline porosity throughout and vuggy porosity is found in places. Late, coarse, euhedral, saddle dolomite crystals occur sporadically in larger vugs but are very minor in terms of percentage of total dolomite. Some large, bladed crystals of celestite (?) also occur with the saddle dolomite.

Plate 3: Lockport Formation lithologies

Plate 3A: Sample from the Wilkesport bioherm showing crinoid wackestone of the Gasport Member of the Lockport Formation with swarms of wispy stylolites. Dolomitization is pervasive. Imperial Sombra 4-14-XIII.

Plate 3B: Nodular, argillaceous and stylolitic skeletal wackestone from the Goat Island Member of the Lockport Formation. A thin tabular stromatoporoid (s) with sediment infill is at the top of sample 596.5m. Sample 592.4m shows thin grainstone (g) layer of crinoid debris. Large crinoid ossicle is also visible (o). Ram # 3, Terminus.

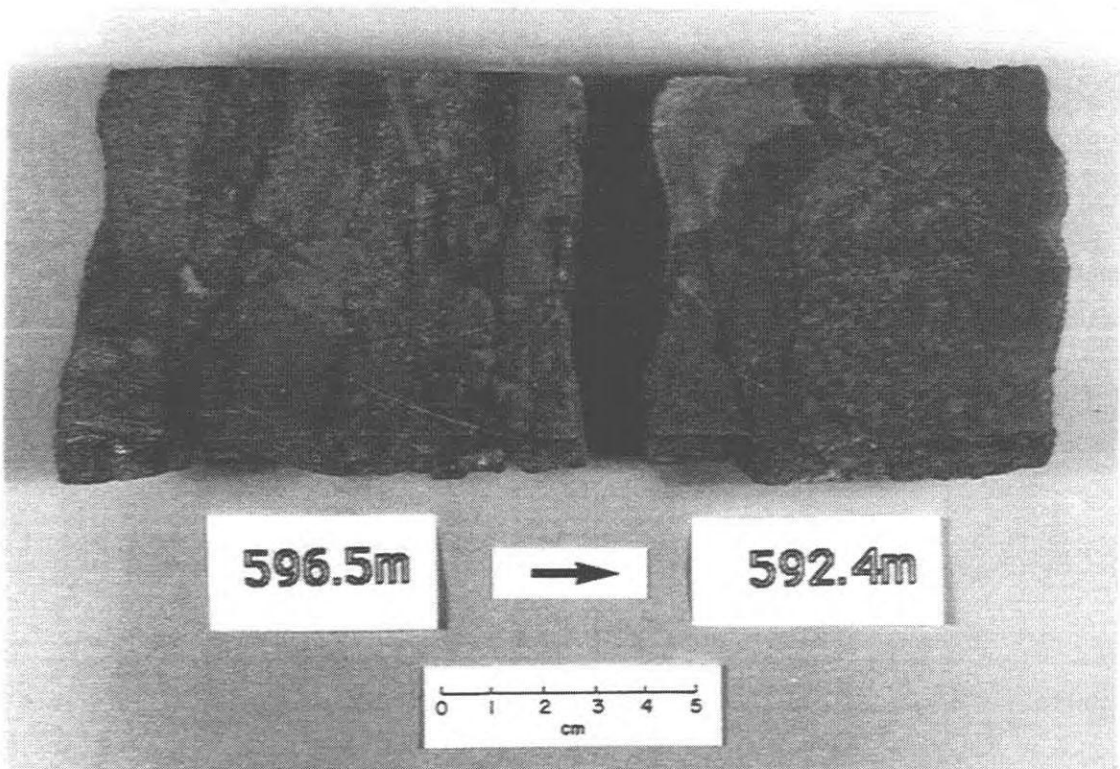
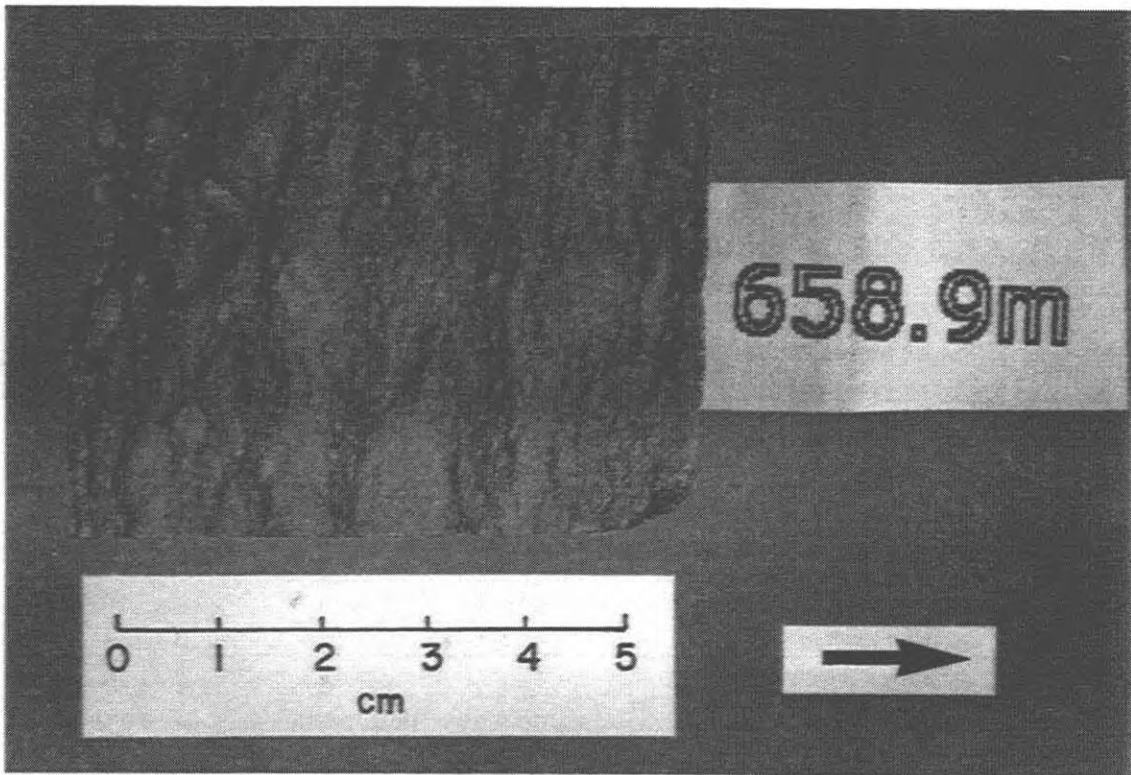
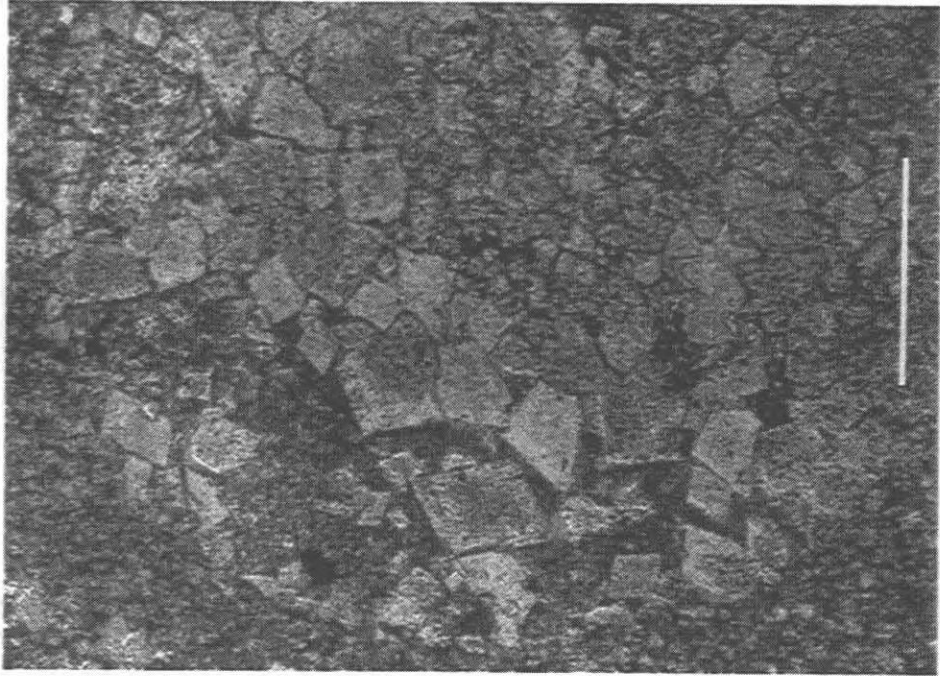


Plate 4: Dolomite replacement in the Lockport Formation

Plate 4A: Thin section photomicrograph in plane light showing anhedral and euhedral dolomite crystals in the Lockport Formation. Crinoid ossicle (C) occupies much of the photo and occurs as a partially obscured sphere. Bar scale approximates 1mm. Union Rosedale 8-9-II-A, 633.9 m subsea.

Plate 4B: Same photomicrograph as in 4A now shown under cathodoluminescence. Dull red luminescent, anhedral dolomite crystals are replacing fine grained matrix of the Lockport. Euhedral dolomite crystals replacing crinoid (orange luminescent), show dull red luminescence, but are also zoned. Non-luminescent growth zones appear in the core of some crystals (n) but most often occur as the final growth phase. Bar scale approximates 1mm. Union Rosedale 8-9-II-A, 633.4m subsea.



The Gasport has a mottled texture, possibly due in part to bioturbation or to the effects of dolomitization. Disseminated pyrite grains are scattered throughout and are also associated with stylolites in places.

2.3.2 Goat Island Member

The Goat Island Member of the Lockport Formation gradationally overlies the Gasport Member. Like the Gasport Member, the Goat Island is a light grey, crinoidal, dolomite wackestone (plate 3). However, it displays an increase in skeletal content and diversity towards the upper contact. In addition, the Goat Island is much more argillaceous than the Gasport and much more stylolitic. A nodular texture often results.

In lower parts crinoids, brachiopods and bryozoans have sizes similar to those in the underlying Gasport Member, but by the top of the Goat Island Member interval, crinoids may be up to 2.0 cm in diameter. Colonial corals *Halysites*, *Coenites* and *Favosites*, as well as solitary rugose corals, make their first appearance approximately three-quarters of the way up the Goat Island section. Stromatoporoids, tabular to bulbous, and encrusting are locally plentiful, but by the top few metres of the Lockport, the number of organisms has decreased. Not all cores however, contain abundant numbers of coral and stromatoporoids. Those cores drilled in reef-flank locations show fewer organisms. Where present, the allochems are held within a finely crystalline dolomite. The Goat Island Member changes to limestone below the Guelph Formation-Lockport Formation contact in the Rosedale, Warwick and Terminus reefs.

Like the Gasport, two textures of dolomite can be found in the Goat Island. The anhedral dolomite is matrix confined, while the euhedral dolomite rhombs partially replace allochems (plate 4). Despite the dolomite, porosity is low, possibly due to the increase in argillaceous content. Saddle dolomite crystals are not as plentiful as in the Gasport.

Shukla and Friedman (1983) observed three different types of dolomites within the Lockport Formation in upper New York State. Their type-1 dolomite involved dolomitization

of the matrix only. Type 2 dolomite includes matrix and allochems while type 3 is a crystal mosaic with no precursor features or fabrics. This study has found petrographic evidence that the Lockport underlying the pinnacle bioherms has two dolomite textures similar to type 1 and type 2 (plate 4). However, the type 3 dolomite of Shukla and Friedman (1983) was not observed. Rather, saddle dolomite crystals were found to have grown in selected vugs. Shukla and Friedman (1983) do not report the presence of saddle dolomites in their work. Under epifluorescence, Lockport dolomites from this study revealed three families of dolomite (Jeff Dravis, pers. comm., 1989), the third dolomite fabric appearing as dark hazy crystals less than 100 μm in size and detectable only with the use of fluorescence microscopy. Whispy swarms of stylolites are plentiful and have little residual matter associated with them (plate 5). Sutured seams are subordinate in number to the whispy stylolites. The maximum observed thickness of residium found along stylolites was approximately 1.0 mm.

Placement of the boundary between the Lockport Formation-Guelph Formation has been problematic in the past. Under the pinnacle bioherms, the contact is reportedly undetectable from both chip samples (Bailey, 1986) and core (Mesolella *et al.*, 1974; Gill, 1979). Several authors have avoided the problem completely by grouping the Lockport and Guelph together for studies undertaken in Canada (Pearson, 1980; Bailey, 1986). Others (Grimes, 1988) have set the Lockport-Guelph contact at that point where dolomite changes to limestone. Use of this method, however, can fail, as many of the overlying pinnacles are themselves dolomite. Also, areas under some pinnacle reefs show limestone to still be prevalent within the Lockport Formation (Pearson, 1980; this study).

Similarly, authors working in the United States commonly group the Lockport Formation and Guelph Formation together and: 1) assign the time stratigraphic label "Niagaran" to the whole package (Mesolella *et al.*, 1974; Cercone, 1984; Cercone and Lohmann, 1985; Sears and Lucia, 1980); 2) use the informal industry nomenclature "Grey Niagaran" for the Lockport and "Brown Niagaran" for the Guelph (Cercone and Lohmann, 1986); or, 3) interpret the Guelph

Formation as a reefal facies of the Lockport Formation and, as such, having no precise stratigraphic position (Huh *et al.*, 1977; Gill, 1979).

However, each of the six pinnacles examined in this study showed an irregular surface in the area of the Lockport-Guelph contact. This surface appears to vary from pinnacle to pinnacle and includes such features as: a massive cavity filled with anhydrite (Rosedale); an irregular, razor-sharp surface (Warwick); and a single, undulating, highly irregular surface (Wilkesport). Some of the changes observed across the surface are: lithologic changes from dolomite to limestone, abrupt facies changes, and biologic changes in fauna types. Existence of such a surface has been previously unreported. Chapter 3, documenting karst within the pinnacles, and Chapter 5, detailing the growth of the reefs, examines this surface more closely.

2.3.3 Distribution of the Lockport Formation

Many authors have reported the Lockport to underlie the pinnacle reefs (Mesoella *et al.*, 1974; Huh *et al.*, 1977; Gill, 1979 and 1986; Briggs *et al.*, 1980; Pearson, 1980; Cercone, 1984; Grimes, 1988;). Both the Gasport Member and the Goat Island Member underlie the pinnacle bioherms across the study area and individually show minor variations in thickness. Collectively, however, the members show a much more consistent thickness that follows recognized trends in the Michigan Basin. This overall total thickness varies from 35.9 m and 34.4 m in the Rosedale and Warwick cores to 29.5 m and 31.1 m in the Payne and Wilkesport cores respectively. The thinner Lockport section under the bioherms that are closer to the centre of the basin confirms the work of Gill (1979), who found the Lockport to thin basinward as it dipped between 0.76° and 1.52° .

2.4 Guelph Formation

Overlying the platform carbonates of the Lockport Formation, pinnacle reefs of the Niagaran-aged Guelph Formation attain depositional heights of over 90 m in southwestern Ontario (Sanford and Brady, 1957). Studies conducted across the southern portion of the Michigan Basin document that the pinnacles have steep sides, with dips of 30° to 40°, and that some have flat tops (Mantek, 1976). The number of reef growth stages reported by different authors varies from three to six (Table 1). In this study, the six pinnacle reefs examined reveal four gross facies that change vertically and are characteristic of the growth of the evolving reef. Individual pinnacles show slight facies variations, and dolomitization makes some facies difficult to interpret.

In the pinnacle reefs, the Guelph Formation has an overall vertical facies progression from a lowermost crinoidal-skeletal wackestone, through a reef core of coral-stromatoporoid floatstones and rudstones, to algal-dominated mudstones and wackestones. Algal units grade further into algal-stromatolite boundstones. Uppermost in the Formation, a massive subaerial exposure episode overprints the boundstones and, in some instances, the algal wackestones. Additional subaerial events occurred throughout the growth of an individual pinnacle, imparting a variety of karst fabrics overtop of the existing facies, and are examined in Chapter 3.

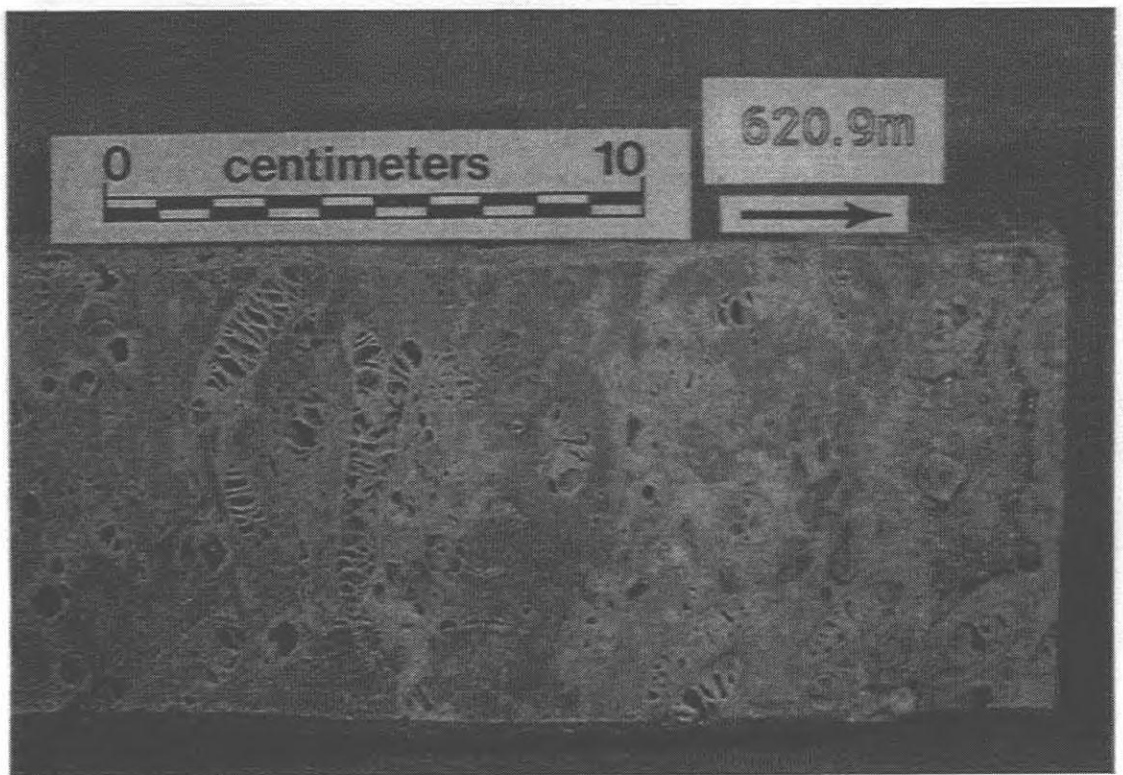
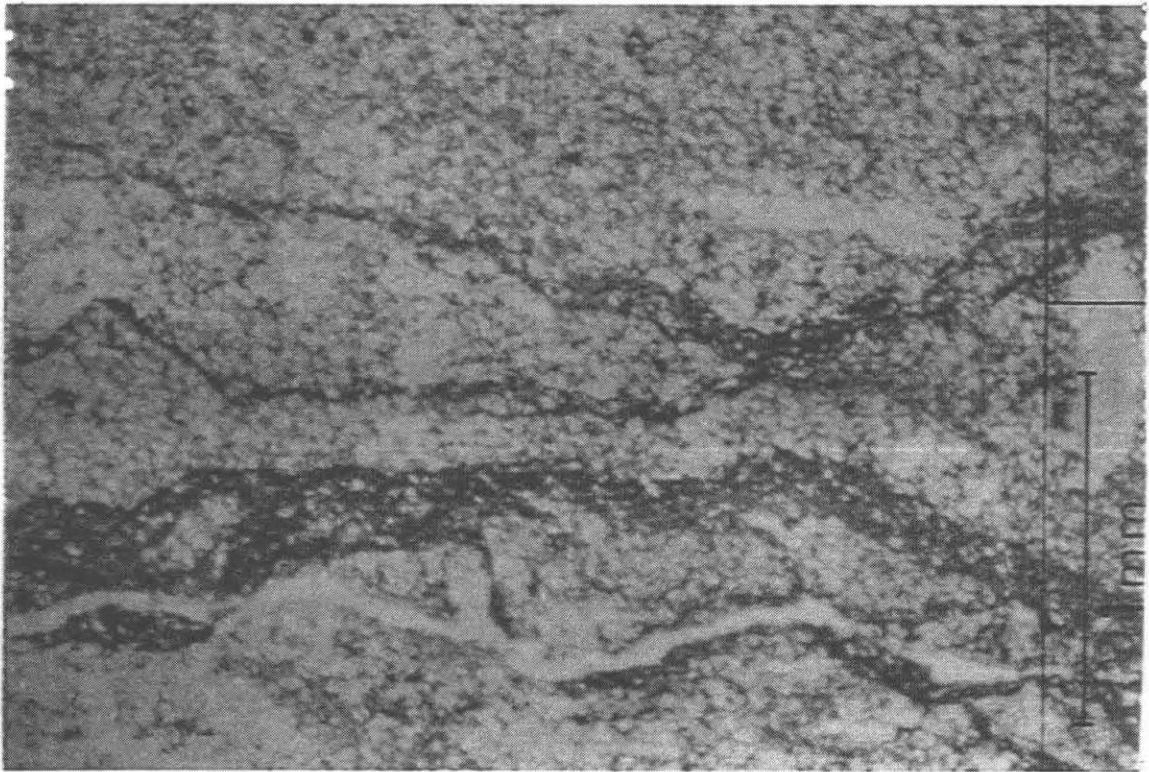
2.4.1 Crinoidal-Skeletal Wackestone Facies

Basal Guelph pinnacle sections are composed of a light brown to buff, crinoidal to skeletal wackestone (plate 5). Brachiopods, bryozoans, trilobites, cephalopods, molluscs, small corals and thin, tabular, encrusting stromatoporoids constitute debris in the wackestone. In the lower portions of the facies, the allochems are small sized. Crinoids and brachiopods average approximately 5.0 mm in diameter and length. Often the shells are concentrated into thin

Plate 5: Lockport stylolite and crinoid-skeletal wackestone facies

Plate 5A: Thin section photomicrograph in plane light showing Lockport dolomite cross cut by stylolites. Little residual material (r) accompanies the seam. Union Rosedale 8-9-II-A, 633.4m subsea.

Plate 5B: Sample from the skeletal wackestone facies showing local concentration of rugose corals. Fibrous marine cement (m) isopachously coats some of the corals and infills (i), and gypsum (g) has occluded large void. Union Rosedale 8-9-II-A.



layers up to four to five centimetres thick. Bryozoans are thin (2.0 mm to 4.0 mm thick), horizontally oriented and provide shelter porosity. These three faunal types on average make up the bulk of the wackestone allochems and are held in a muddy matrix.

Rugose corals locally are plentiful (plate 5), attaining sizes up to 1.0 cm in diameter and 3.5 cm long. Minor occurrences of small *Favosites*, *Coenites* and *Halysites* complete the corals present. Stromatoporoids are usually less than 1.0 cm thick.

Crinoid-skeletal wackestone facies reveals abundant stromatactis fabric (Bathurst, 1959;1982). Former shelter cavities contain a sediment veneer causing a flat to near-flat floor. This is in turn followed by fibrous calcite cement, which grows perpendicular to the remaining cavity walls and closes off the void with a well-defined suture line. Fibrous cement was also observed to radiate outward in all directions from nuclei of bryozoans, *Coenites* and rugose corals. In places, the marine cement consists of several isopachous zones.

Because of the abundance of pore-occluding marine cement there is little remaining porosity (plate 6). Small vugs caused by incomplete cementation or the possible dissolution of shells, and intra-fossil porosity in corals represent most of the porosity present. Minor amounts of salt are found in this facies in the Rosedale, Wilkesport and Terminus reefs while in the Bayfield reef pores are extensively salt plugged.

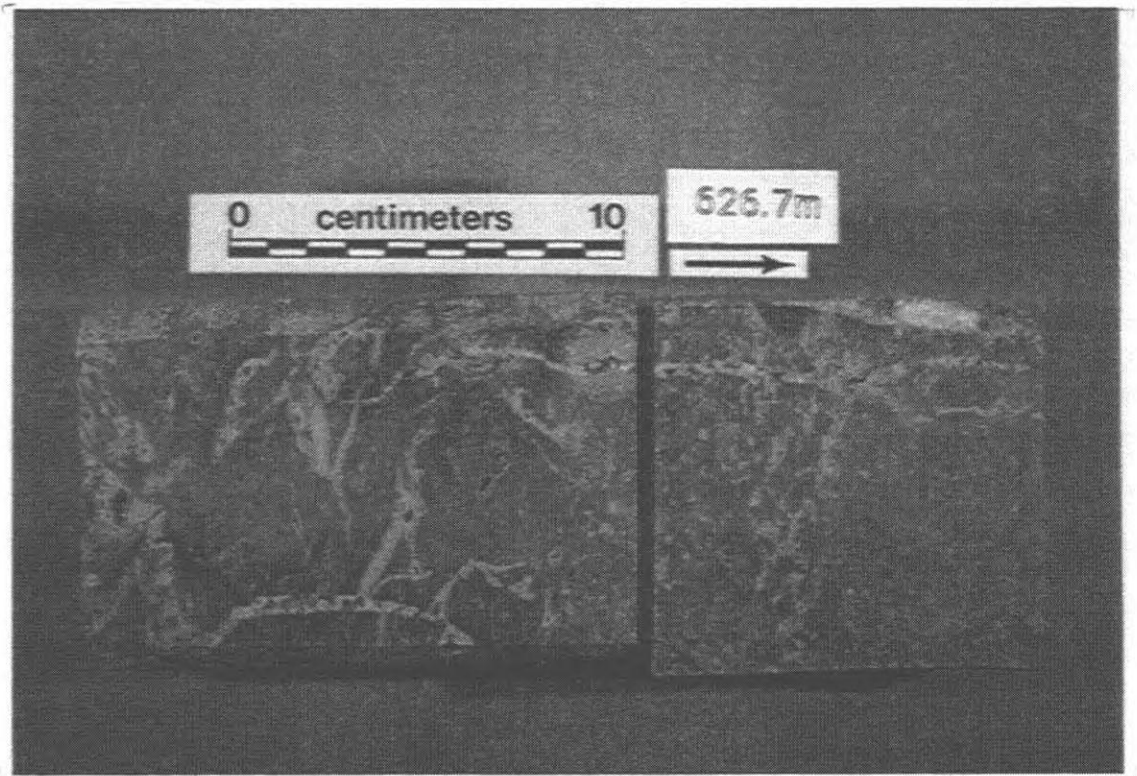
Degree of dolomitization varies within this facies. Some of the reefs (Bayfield, Wilkesport and Payne) are dolomitized throughout with anhedral to subhedral, interlocked crystals. Others (Rosedale, Warwick, Terminus), display little to no dolomite. In the Rosedale reef, the only dolomite observed was late, saddle dolomite crystals found in small fractures (plate 6).

Previous authors have reported a similar facies making up the lower part of the Gueiph section in pinnacle bioherms in several areas of the Michigan Basin (Cercone, 1984; Pearson, 1980; Sears and Lucia, 1979, 1980; Mesoella *et al.* , 1974; Huh *et al.* , 1977; Gill, 1986; Grimes, 1988). It is interpreted that this facies represents initial stabilization and colonization

Plate 6: Fractures and pore-occluding cements

Plate 6A: Thin section photomicrograph under crossed polars showing large wedges of fibrous marine calcite cement (F) infilling shelter cavity under a bryozoan (B). Cement grows perpendicular to the walls of the cavity and very little porosity remains. Blocky ferroan calcite (R) completes the pore fill. Union Rosedale 8-9-II-A, 627.6m subsea.

Plate 6B: Sample from crinoid-skeletal wackestone facies showing a later fracture cross cutting allochems and cements. Feathery bryozoans are truncated by the fracture (T). Coarse euhedral saddle dolomite crystals (D) line the fracture. Union Rosedale 8-9-II-A.



(Walker and Alberstadt, 1975; James, 1983) of the sea floor by pelmatozoans and shelly organisms.

2.4.2 Coral-Stromatoporoid Floatstone to Framestone Facies

A coral-stromatoporoid floatstone to framestone facies gradationally overlies the wackestone facies. This facies is light brown to buff in colour and contains abundant tabular or bulbous stromatoporoids, *Favosites*, *Coenites*, *Halysites*, *Heliolites* and rugose corals. Bulbous stromatoporoids may attain sizes up to 15.0 cm thick while Favositid corals were observed to be up to 12.0 cm thick. Corals and stromatoporoids encrust and are in turn encrusted by one another. In addition these organisms may be *in situ* or overturned with evidence of abrasion.

Accompanying the reef builders are various skeletal allochems. Crinoids are plentiful but have been supplanted as the main accessory allochem by brachiopods whose shells are up to 1.0 cm long. Bryozoans are less plentiful than in the underlying crinoidal-skeletal wackestone facies, but still common, and create shelter porosity. Skeletal allochems are concentrated into layers up to 1.0 m thick (average 10.0 cm) that are found throughout the coral-stromatoporoid facies. The beds are packstones but in some areas grade into grainstones. A muddy matrix is associated with the shells. Algae also occur near the top of the coral-stromatoporoid facies section.

Fibrous marine cements infill shelter cavities and vugs within this facies. Some reefs such as Warwick show extensive, multi-generation, marine cement (plate 7) with up to 6 separate growth zones of cavity fill. Others such as Terminus or Rosedale have little marine cement and an abundance of open vugs and molds (plate 7).

Salt emplacement is variable (plate 8). The Bayfield reef has vugs with extensive plugging by halite while the Warwick reef has little salt associated with it. In some vugs, the halite is predated either by isopachous marine cement or by coarse, scalenohedral, burial calcites. Other vugs have only halite occluding their spaces. Despite the filling of pores by

Plate 7: Coral-stromatoporoid facies

Plate 7A: Sample from the coral-stromatoporoid facies showing fibrous marine cement with multiple growth zones (Z) filling cavity under Favosites (E). Coral is cut by sutured seam (S). Imperial # 399 Warwick.

Plate 7B: Example of the large, open dissolution voids that occur locally in the coral-stromatoporoid facies. Union Rosedale 8-9-II-A.

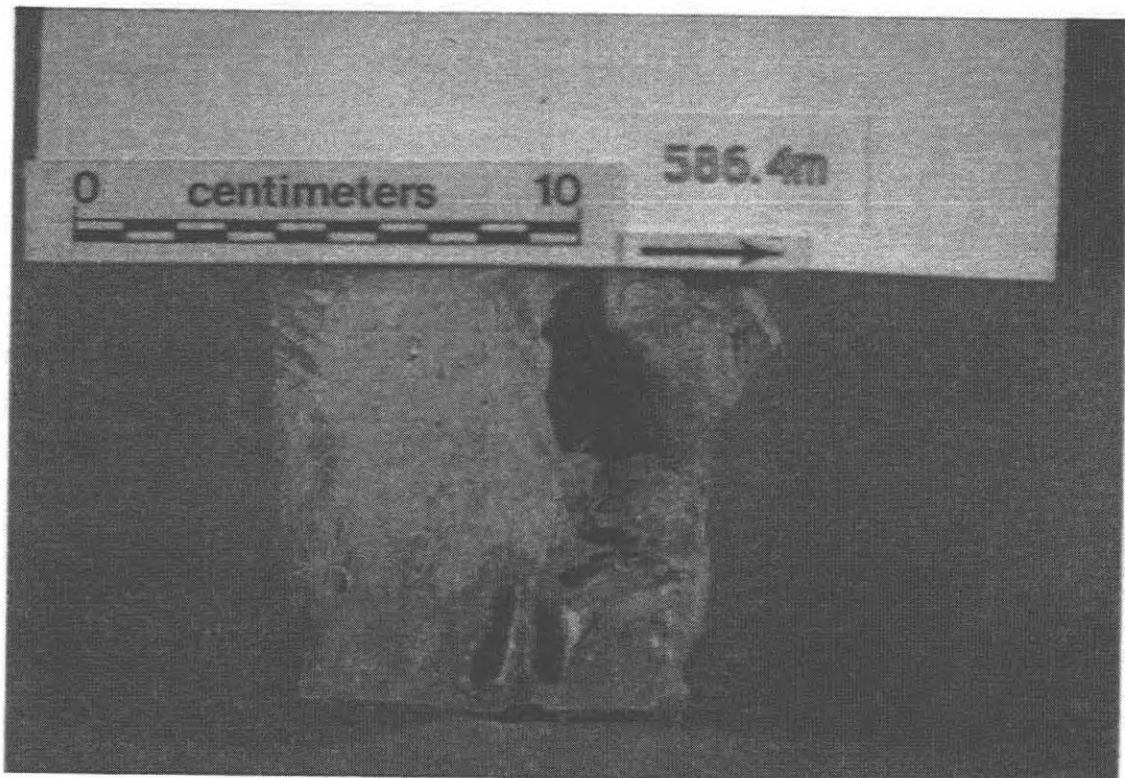
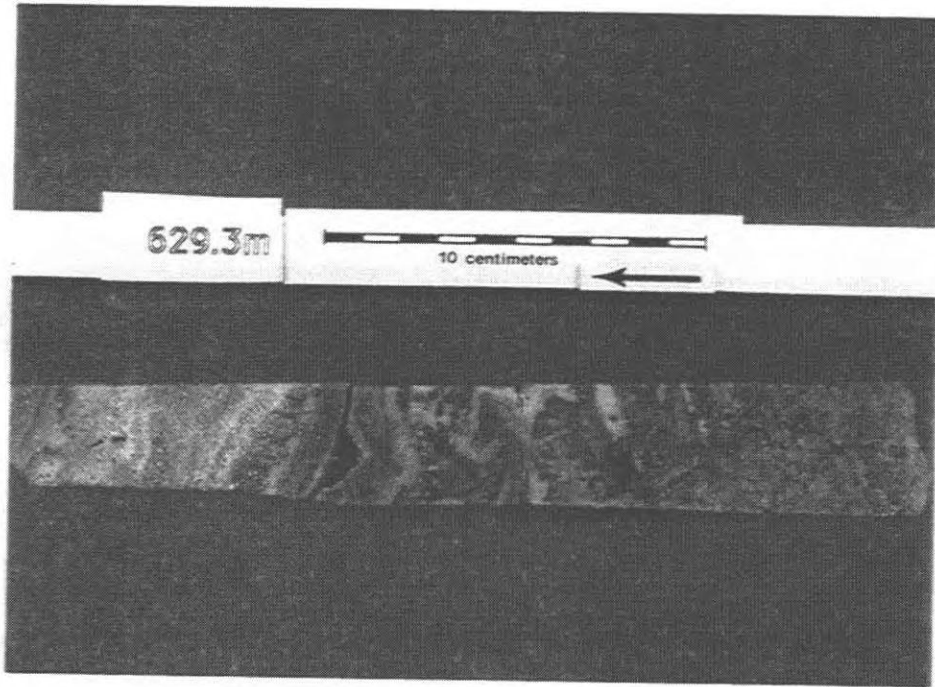
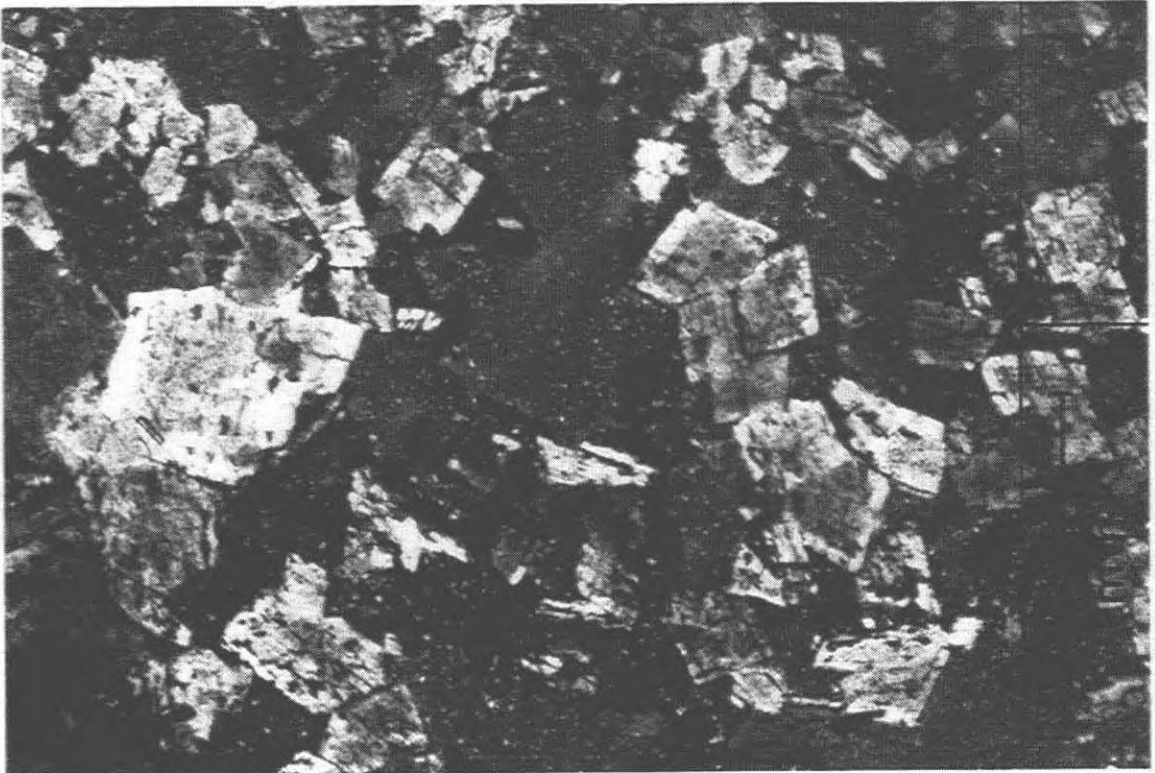
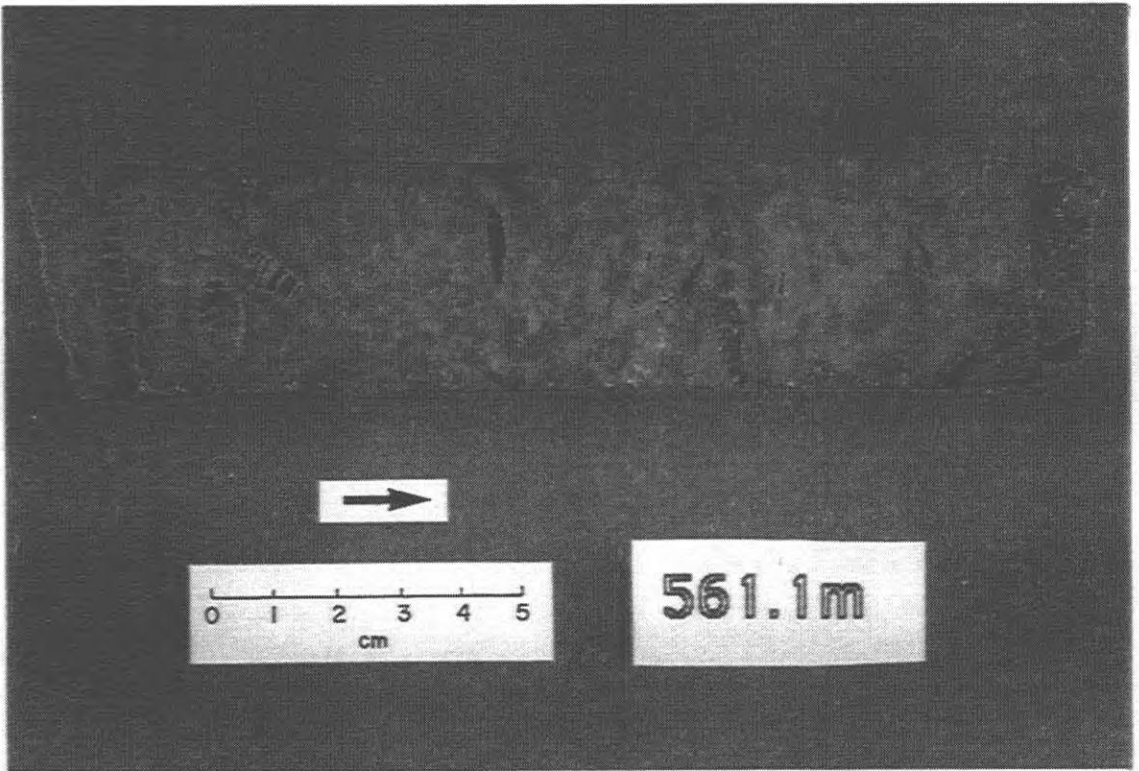


Plate 8: **Halite emplacement and dolomite replacement**

Plate 8A: Two rugose corals showing selective emplacement by halite. One coral reveals good intra-fossil porosity (A) while the one beside (E) it is halite plugged. Porter #1, Bayfield.

Plate 8B: Thin section photomicrograph in plane light illustrating pervasive dolomitization by anhedral and euhedral dolomite crystals. Inter-crystalline porosity is present. Imperial Sombra 4-14-XIII, Wilkesport, 612.6m subsea.



marine cement, dolomite, scalenohedral calcite, anhydrite and lastly halite, overall there is porosity associated with the coral-stromatoporoid facies.

Dolomitization in the coral-stromatoporoid facies is highly variable. It is pervasive in the Wilkesport and Bayfield bioherms and consists of anhedral to subhedral crystals averaging an estimated 200 μm in size (plate 8). In the Warwick reef, dolomite exists mainly as crypto-crystalline patches that are found in muddy areas and are associated with subaerial exposure surfaces. Dolomite is also found, in the Rosedale, Terminus and Warwick bioherms, as scattered euhedral rhombs in recrystallized, fibrous calcite cements (plate 9) and in fine-grained matrix material. Late, saddle dolomite crystals occur in pores and fractures areas of all pinnacles.

Burial features are present in the form of small, short fractures and stylolites. The fractures are rarely more than 5.0 mm wide and less than 40.0 cm long. Saddle dolomite and scalenohedral calcite crystals are the most common residents of the fractures, but anhydrite occurs in places (plate 9). Rarely, salt is found as the final fracture filler. Single, sutured stylolite seams have amplitudes of less than 2.0 cm. Swarms of wispy stylolites are found in more muddy areas. In all cases, the stylolites rarely cross-cut allochems (plate 10). The sutured seams were observed on occasion to cross-cut the wispy stylolites. Allochems rarely show compaction features (plate 10).

The presence of a core of reef-building organisms has been recognized by several authors in studies of Silurian bioherms of the Michigan Basin (Textoris and Carozzi, 1964; Sears and Lucia, 1979; Crowley, 1973; Kahle, 1978, 1988; Archer and Friedman, 1986; Shaver *et al.*, 1983). In smaller Silurian reefs, this core may be mainly mudstone (Shaver, 1989). In the six pinnacle bioherms studied, similar cores of reef-building corals and stromatoporoids are present. These organisms are held together by themselves, encrusting organisms or mud. This facies is believed to represent diversification (Walker and Alberstadt, 1975; James, 1983) of the reef community.

Plate 9: Algae and fibrous marine cement

Plate 9A: Thin section photomicrograph in plane light showing euhedral dolomite rhombs (Y) scattered within recrystallized fibrous marine calcite cement. Numbers on the bar scale partially obscured read 250 μm . Imperial # 399, Warwick, 657.5m subsea.

Plate 9B: Thin-section photomicrograph under crossed polars showing daesycladacean algae cross-cut by two fractures. One fracture (U) crosses almost normal to the algae, the other is anhydrite filled (K) and truncates the end of the algae. Bar scale equals 1 mm. Union Rosedale 8-9-II-A, 627.6 subsea.

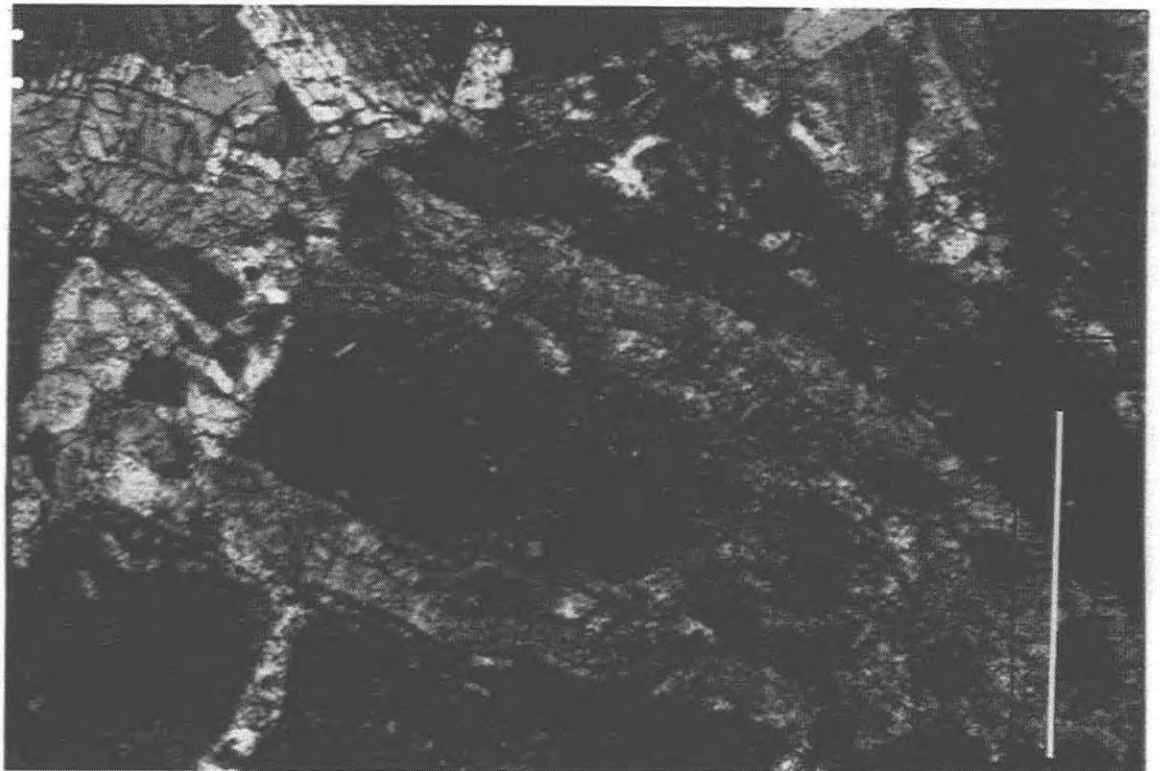
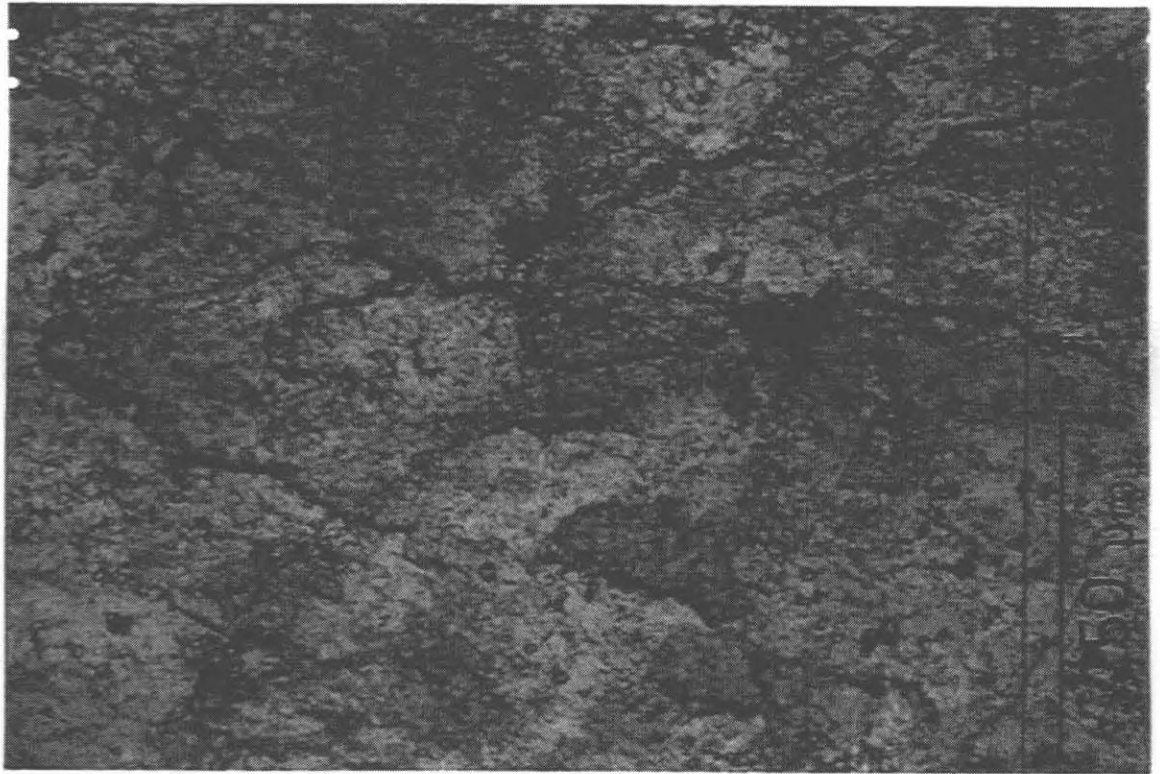
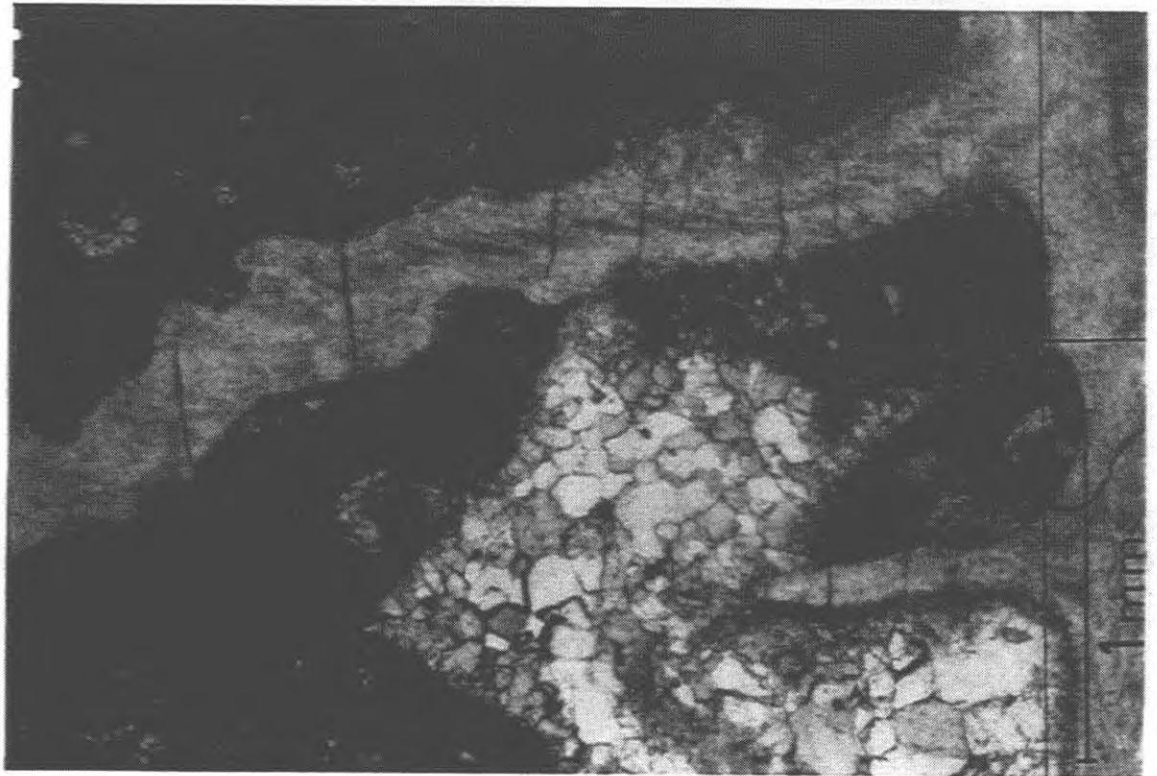


Plate 10: Burial diagenetic features

Plate 10A: Thin section photomicrograph using cathodoluminescence of stylolite cross cutting crinoid fragment. Such examples are rare. Tiny, dull red luminescent dolomite rhombs (s) close to the crinoid are also cross cut. Blue spots represent tiny holes in the thin section. Bar scale approximates 1mm. Union Rosedale 8-9-II-A, 627.8m.

Plate 10B: Rugose coral with small fractures resulting from compaction. Micrite (m), prismatic calcite crystals (i) and blocky calcite cement (J) fill coral internally. Imperial # 399 Warwick, 639.9m subsea.



2.4.3 Algal-Brachiopod Wackestone to Mudstone Facies

Dominance by algae results in a medium brown to chocolate brown coloured, algal-brachiopod wackestone to mudstone facies that overlies the coral-stromatoporoid facies (plate 11). Major organism remains are algae with biconvex, rounded brachiopods up to 1.0 cm long, small ostracods (?), bryozoans and gastropods. Thin, dark brown mudstone layers occur in places. Mesolella *et al.*, (1974) and Pearson (1980) identify the algae as *Girvanella* and *Sphaerocodium*. Thin, tabular or bulbous, encrusting stromatoporoids, as well as solitary favositid corals are randomly scattered throughout. Many occur *in situ*. Pellets are a common allochem in the upper part of section, are elliptical in shape and are less than 1.0 mm in size.

Porosity is variable within this facies. Mudstones have little porosity; however, vugs and molds up to 1.5 cm in size are common in the wackestone, with most of the molds resembling brachiopods. Dissolution of stromatoporoids created larger voids, up to 5.0 cm in size. In places the dissolution was incomplete and portions of the stromatoporoid remain.

Noticeable in the algal-brachiopod facies is the reoccurrence of stromatactis. Small vugs are lined by a white to cream-coloured, isopachous fibrous cement (plate 11). Internal floor sediment was not noticed and cement completely occludes any pore space in the stromatactis cavity. Rarely, part of the void remains and, here, the cement has a botryoidal morphology as it juts out into the cavity. The isopachous cement is followed in some areas by coarse, scalenohedral calcite crystals (plate 11).

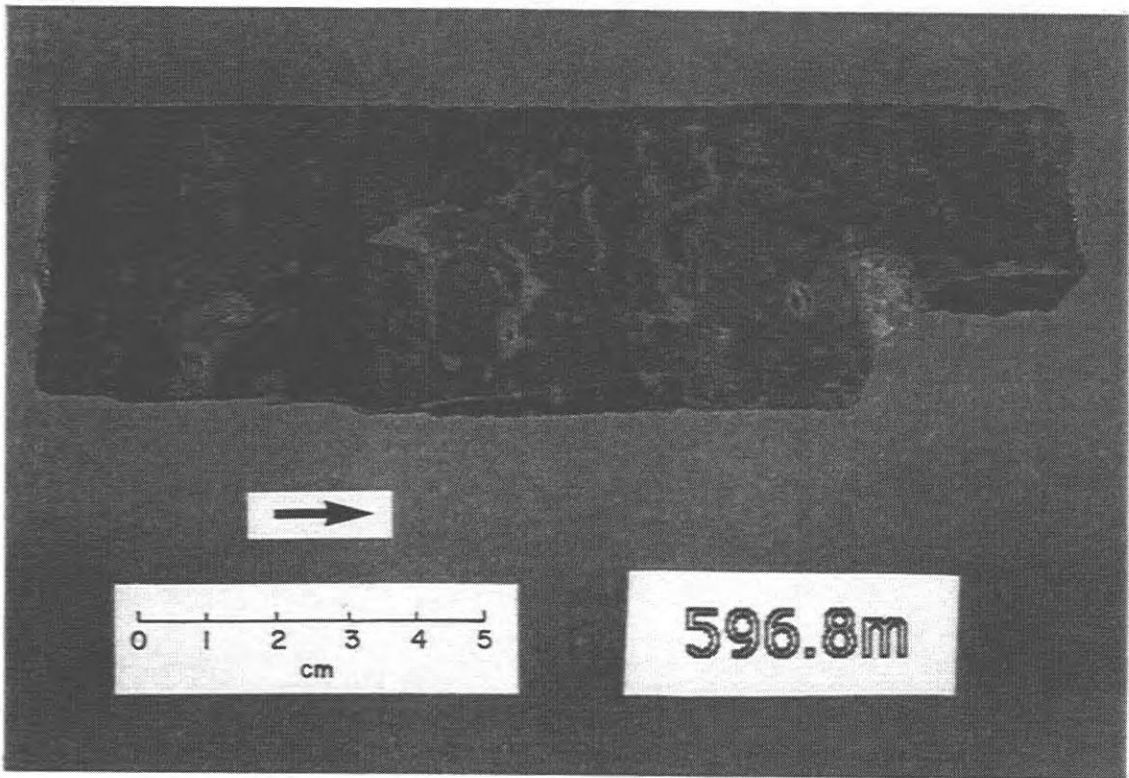
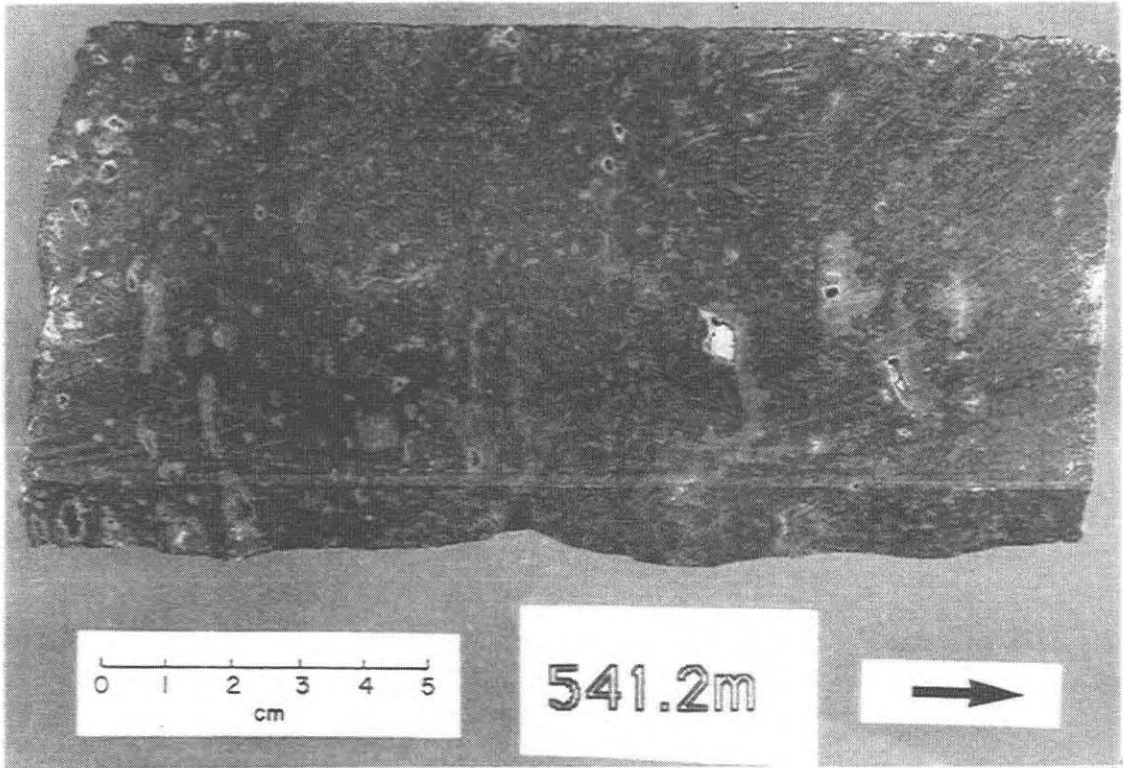
Existing porosity is further reduced by halite emplacement. Stromatactis-like cavities are observed in places to contain salt with no precursor calcite cement. Overall, salt is confined to pores larger than 2.0 cm, although it does clog some brachiopod molds and fills individual corallites.

Dolomitization varies from being pervasive in the Bayfield and Wilkesport bioherms to patchy in the Terminus and Payne pinnacles and to nearly absent in the Warwick and Rosedale reefs. Where it is present, the finely-crystalline, anhedral to subhedral dolomite is found in

Plate 11: Algal-brachiopod facies

Plate 11A: Sample from the algal-brachiopod facies showing algae (v), muddy characteristics of this facies and marine calcite cement that occludes pores. Ram # 3, Terminus.

Plate 11B: Similar muddy sample as above but with abundant brachiopods, some with geopetal fill (y) and coarse, blocky calcite cement (z). Imperial Sombra 4-14-XIII, Wilkesport.



the matrix mud and has inter-crystalline porosity associated with it. No saddle dolomite crystals were observed in this facies.

Thin, wispy stylolites occur in swarms throughout this facies. Sutured seams are not as numerous. Neither the wispy stylolites nor the sutured seams have large amounts of residue material associated with them. Rather stylolites occur as thin lines cross-cutting the core. The largest observed thickness of insoluble residue occurring along a stylolite was approximately 2.0 mm.

Sears and Lucia (1979) and Mesolella *et al.*, (1974) recognize the presence of an algal-dominated facies in pinnacles studied in the northern portion of the Michigan Basin. Pearson (1980) and Gill (1986) substantiate the same for reefs in the southern Michigan Basin. Other authors (Grimes, 1988; Cercone, 1984) describe a mudstone facies that caps the pinnacle reefs in the southern and northern portions respectively. This facies is interpreted to represent the first occurrence of a dominant organism in the evolution of the reef community (Walker and Alberstadt, 1975; James, 1983).

2.4.4 Stromatolite Boundstone Facies

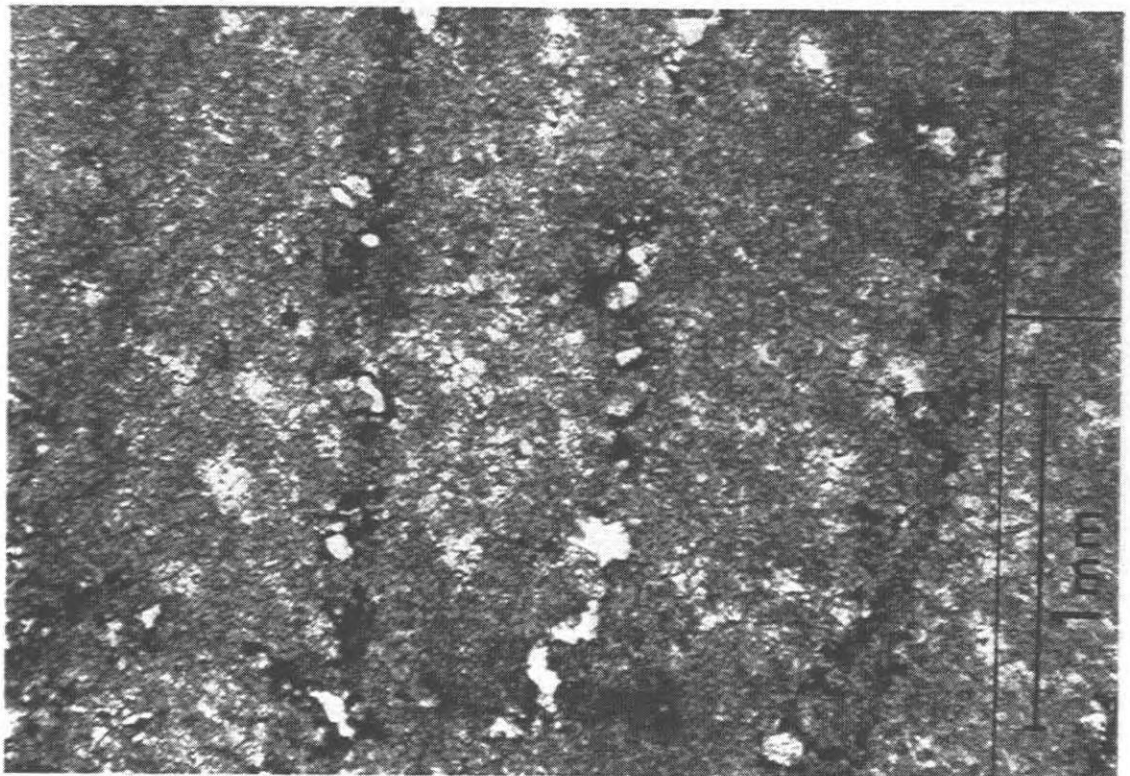
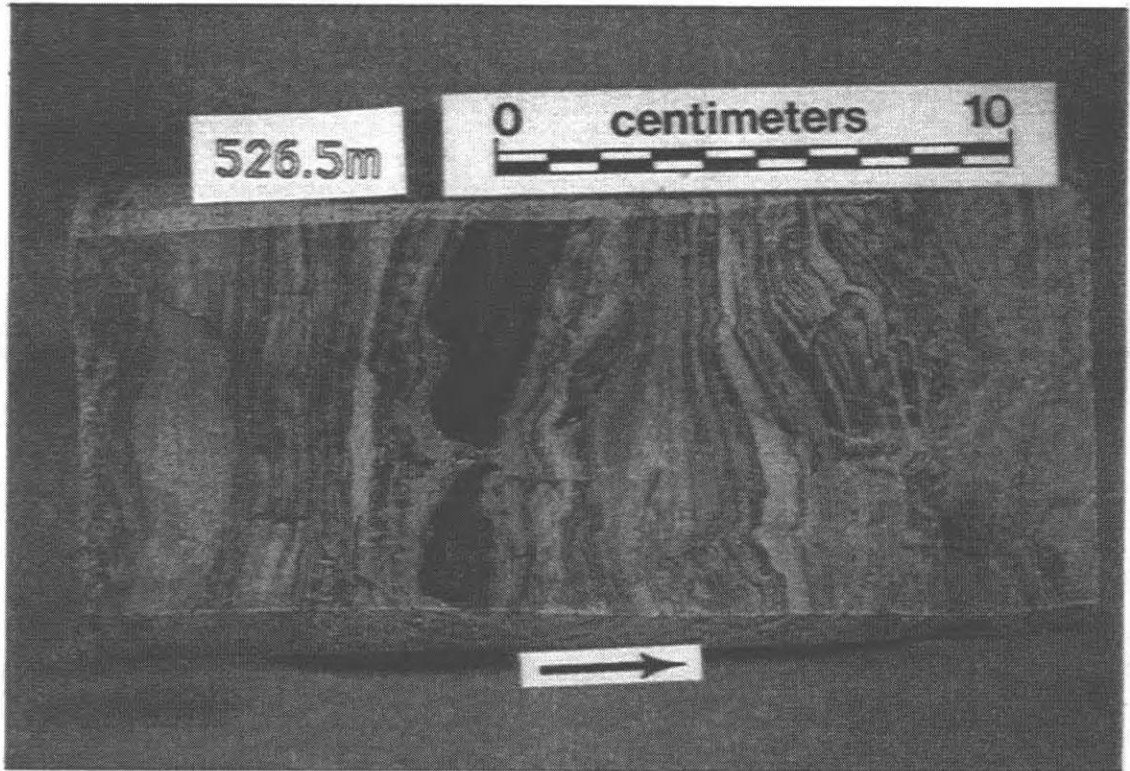
A stromatolite boundstone gradationally overlies the algal-brachiopod facies at the top of the pinnacle bioherms (plate 12). This medium brown boundstone represents the last observable facies that reflects growth on the bioherm. The stromatolites show alternating light and dark laminae that vary between approximately 0.1 mm and 1.1 mm in thickness. In general, the lighter coloured laminae are thicker than the dark ones. Laminations are crinkly, wavy or near-horizontal. Huh and Briggs (1981) document them as being laterally-linked hemispheroids (Logan *et al.*, 1964).

Dolomitization is variable, ranging from pervasive to having little significance. Complete dolomitization makes the recognition of the laminations difficult. Stylolites are plentiful

Plate 12: Stromatolite boundstone facies

Plate 12A: Example of the stromatolite boundstone facies showing alternating light and dark coloured laminations. Laminations mimic one another and topographic irregularities are reproduced through several generations of laminations. Stylolites are common. Union Rosedale 8-9-II-A.

Plate 12B: Thin-section photomicrograph in plane light illustrating fenestral porosity (blue-white holes) that is found in the boundstone facies. Porosity is locally occluded by bitumen and dead hydrocarbons (black). Little dolomitization is present. Union Rosedale 8-9-II-A, 527.2m subsea.



with single, low-amplitude seams tracing a path along laminae boundaries. Little residue material is associated with the stylolites.

Porosity is mainly inter-crystalline and fenestral (plate 13), and when compared to other facies in the pinnacles, is minor. Small vugs are also present, averaging approximately 5.0 mm in size. In places, larger vugs (to 7.5 mm), show a fine-grained silt flooring as well as tiny scalenohedral calcite crystals jutting into the remaining void space.

Strong overprinting by subaerial exposure is evidenced in the stromatolite boundstone facies with laminations interrupted by breccias, conduits and mudstone fills. Stromatolite growth continued in some instances with the return to near-horizontal laminations followed by further brecciation. At the top of the pinnacle bioherm, the stromatolites are thoroughly pulverized and bioherm growth apparently terminated. The Bayfield pinnacle does not contain *in situ* stromatolites; however, stromatolites occur as breccia clasts contained within the underlying algal wackestone facies, suggesting that the organisms were present.

2.4.5 Subaerial Exposure Facies

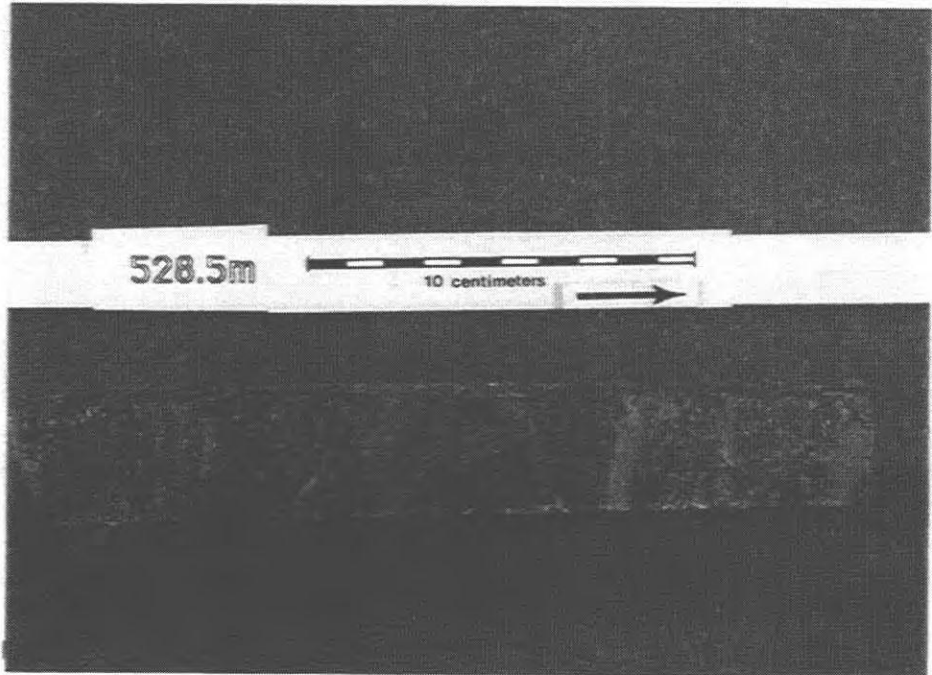
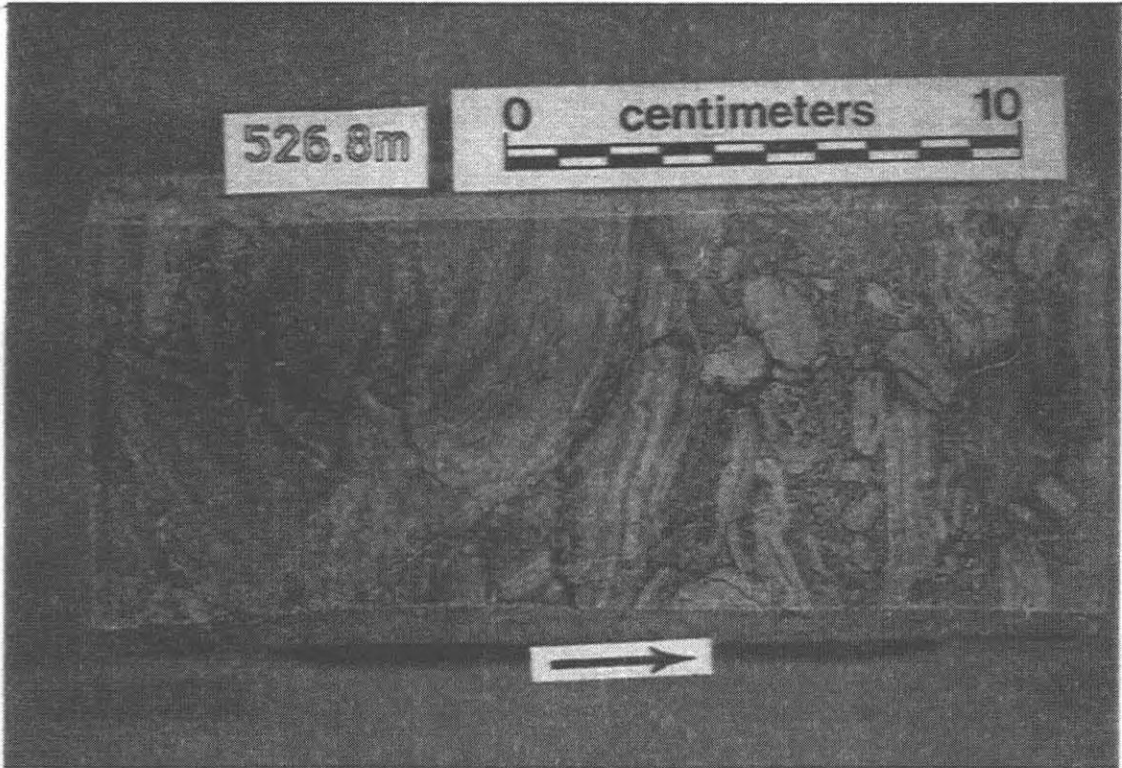
Abruptly overlying the stromatolite facies and superimposed on it, the karst facies terminated bioherm growth. Although several other subaerial exposure events occurred during the growth of the pinnacle reefs, this final event left a very visible, karst breccia.

Large solution cavities can be found in the underlying stromatolite facies, in places down to the algal wackestone facies. These cavities trace irregular routes through the reef and are filled with a combination of breccia clasts and mudstone (plate 13). Breccia clasts are composed of stromatolite, mudstone, pisolith and laminated crust pieces and are to a maximum of 8.0 cm long. Smaller clasts are found lower down in the solution conduits with larger ones higher up. This results in either a matrix-supported breccia or a clast-supported one, however, the breccia does not exhibit any grading. Evaporite minerals are present only as individual laths and are

Plate 13: Karst facies

Plate 13A: Karst facies showing broken stromatolites in a variety of sizes contained in a dark mudstone matrix. Facies varies locally from clast supported (E) to matrix supported (A). Union Rosedale 8-9-II-A.

Plate 13B: Example of the karst facies but with higher mud content. Imperial # 399, Warwick



not common. In places, both the walls of the cavity and the clasts are coated with a cream to dark brown to black isopachous rind. Stylolites are common and rim breccia clasts.

Dolomitization is patchy and not fabric selective. Fine-grained material as well as clasts may be dolomitized. Porosity also occurs in patches, with some areas showing small molds and vugs, fenestral and inter-crystalline porosity. Overall, porosity is poor as areas directly adjacent can be completely sealed with silt, sediment and cement. Later salt emplacement has occluded much of the remaining pore space.

Overlying the karst facies, a green clay is found. Up to 1.0 m of the solution cavity may be filled with green clay and it contains breccia clasts similar to those in the conduit below. It forms a very sharp surface with the overlying A-1 Carbonate (plate 14). Churcher and Dusseault (1981) and Meadows *et al.*, (1986) determined the clay found on top of the Wilkesport pinnacle and the Fletcher patch-reef, respectively, was illite. Churcher and Dusseault (1985) interpret the green clay to result from pressure solution at the top of the pinnacles.

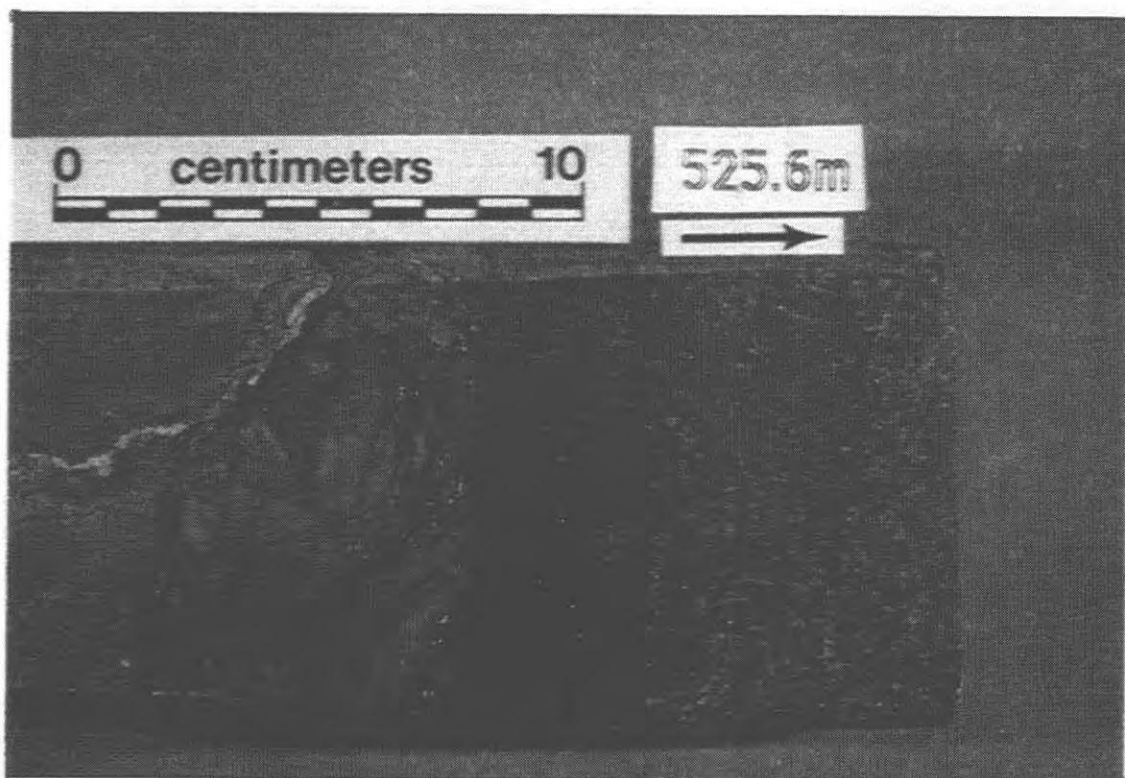
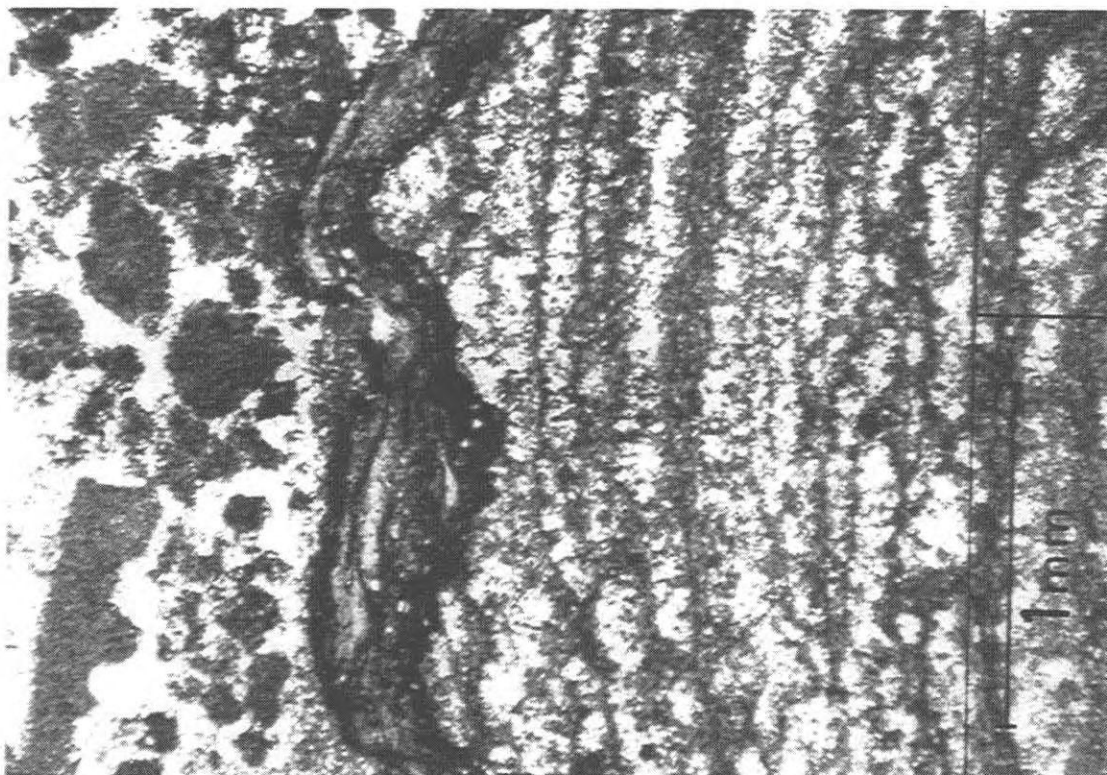
A karstic interpretation is favoured over other interpretations, such as evaporite solution collapse, due to the presence of pisoliths and stromatolites, and the lack of grading in the breccia. In addition, micro-laminations found in the isopachous rinds may be algal in origin. Other than stylolites, there is a paucity of burial evidence to support a deep, late-stage dissolution origin.

The karst facies results from the only subaerial exposure event that most previous workers recognize to have occurred (Gill, 1973, 1977, 1979, 1986; Cercone, 1984; Cercone and Lohmann, 1985, 1986; Huh *et al.*, 1977; Bailey, 1986; Briggs *et al.*, 1980; Mesolella *et al.*, 1974; Shaver *et al.*, 1983; Sears and Lucia, 1980). Others (Sears and Lucia, 1979; McGovney *et al.* 1982) do not acknowledge subaerial exposure.

Plate 14: Karst facies and green clay

Plate 14A: Thin-section photomicrograph from the karst facies in plane light. Large stromatolite clast is separated from smaller breccia clasts and finely crystalline matrix material by residue from a stylolite. Union Rosedale 8-9-II-A.

Plate 14B: Contact between the severely karsted top of the Guelph Formation and the unconformably overlying chocolate brown mudstone of the A-1 Carbonate Formation. A stylolitic green clay (h) is present at the top of the bioherm contacting the A-1 Carbonate and contains breccia clasts (p). Union Rosedale 8-9-II-A.



2.4.6 Facies Distribution in the Guelph Formation

Five gross facies, identified in the Guelph Formation, constitute pinnacle reef growth as the bioherms responded to the physical and chemical environment around them. Derivations of these facies can be found in each reef. The Warwick reef contains 127 m of Guelph section making it the tallest pinnacle studied in terms of vertical extent.

The lowermost crinoid-skeletal wackestone facies shows a large variation in thickness between individual pinnacles (Table 2). It is thickest at 12.8 m in the Rosedale reef and thinnest in the Bayfield reef at 2.4 m. Pinnacles more proximal to the basin centre show a smaller crinoid wackestone facies. This facies is responsible on average for 5% to 8% of the reef mass.

Coral-stromatoporoid facies represent the bulk of the bioherm mass (Table 2). Up to 61.4 m of vertical section (Warwick) is formed by this facies. The Wilkesport reef shows only 25 m of coral-stromatoporoid facies section, however it is a much smaller pinnacle than the others studied and the core was taken from a flank position. On average 50% to 55% of the total pinnacle reef is composed of a coral and stromatoporoid dominated section. Algal-brachiopod facies constitutes the most of the remainder of the Guelph section (Table 2). With the algal-brachiopod facies and the coral-stromatoporoid facies combined, 85% to 90% of the pinnacle bioherm is accounted for. A maximum of 52 m of algal wackestone facies was observed in the Warwick reef. In terms of the total Guelph section, the stromatolite boundstone facies is the smallest. However, because this facies has been overprinted and eroded by the karst facies, it may have been previously responsible for a greater percentage of the reef interval. This facies makes up 2% to 5% of the total reef with a maximum observed thickness of 5 m occurring in the Warwick bioherm.

Influencing the upper portions of the bioherm, the karst facies overprints both of the algal facies. Karst breccia and the effects of solutioning can be detected for thicknesses up to 6.3 m (Table 2).

Table 2: The identified gross lithofacies and their thicknesses in each well.
Percentages shown are a percentage of the total vertical thickness of the bioherm.

**GUELPH
FACIES**

**A-1
CARBONATE
FACIES**

| REEF | CRINOID SKELETAL WACKESTONE m | CORAL STROM FLOATSTONE m | ALGAL WACKESTONE m | STROMATOLITE BOUNDSTONE m | KARST m | ALGAL MUDSTONE m | STROMATOLITE BOUNDSTONE m |
|--------------------|--|---|-----------------------------------|--|--------------------|---------------------------------|--|
| Warwick #399 | 7.0 | 61.4 | 52.0 | 4.3 | 6.0 | 11.7 | 14.1 |
| Warwick #407 | not cored | 21.3+ | 28.7 | 2.1 | 3.1 | 17.5 | 12.3 |
| Rosedale | 12.8 | 41.8 | 36.3 | 3.0 | 6.3 | 12.0 | 11.4 |
| Terminus Ram #3 | 3.6 | 35.1 | 17.0 | 3.4 | 4.4 | 7.2 | 14.3 |
| Terminus Ram #5 | 5.1 | 45.6 | 12.3 | 2.4 | 1.1 | 6.0 | 9.0 |
| Wilkesport | 3.1 | 25.0 | 19.5 | 3.0 | 5.8 | 7.7 | 12.7 |
| Bayfield | 2.4 | 50.9 | not observed | not observed | 0.9 | not cored | not cored |
| Payne | 3.2 | 53.2 | 47.8 | 4.0 | 2.0 | not cored | not cored |

2.5 A-1 Evaporite Formation

Anhydrite deposits of the A-1 Evaporite unconformably overlie inter-pinnacle facies of the Guelph Formation (Gill, 1977), and although depicted in figure 2, the A-1 Evaporite of the Cayugan-aged Salina Group was not encountered in any of the reefs studied. Adjacent to the pinnacles, the anhydrite attains thicknesses of approximately 6.0 m (Gill, 1977) as it abuts against them. This light blue, nodular anhydrite has felted, enterolithic and chicken-wire textures in places and thickens to 145 m in the centre of the Michigan Basin (Gill, 1979). Gill (1977) and Cercone (1984) describe an additional carbonate unit, the A-0, that lies between the Guelph and the A-1 Evaporite. This unit is not known to be present everywhere and little documentation has been made of it in the subsurface of southwestern Ontario.

2.6 A-1 Carbonate Formation

Unconformably draping the pinnacle reefs and following the subaerial exposure event that terminated bioherm growth, is the A-1 Carbonate Formation. Medium to chocolate brown coloured, mudstones and boundstones overlie the pinnacles with a maximum thickness of 23.4 m observed in a reef-crest core (Rosedale reef) and 29.8 m observed in a reef flank core (Imperial Warwick # 407). The A-1 Carbonate contributes to the reservoir of the pinnacle bioherm (Mesolella *et al.*, 1974).

Two gross facies are recognized within the A-1 Carbonate (Table 2), although Gill (1977) has recognized several facies on a more detailed level. Directly and unconformably overlying the pinnacle reefs, a coralline algal mudstone is found in thicknesses up to 12.0 m. The mudstone is then succeeded by an algal-stromatolite boundstone facies which makes up the remainder of the interval and this formation.

Separated from the pinnacle bioherm by the massive karst horizon that underlies it, together with a low abundance and diversity of organisms, and a lack of reef builders, the A-1

Carbonate is not considered part of the reef proper in this study. Most other authors agree that reef growth was terminated prior to the deposition of the A-1 Carbonate (Sears and Lucia, 1979; Gill, 1986; Huh et al, 1977; Briggs *et al.* , 1980). Only Mesolella et al.(1974), Pearson (1980) and Bailey and Cochrane (1990) group the A-1 Carbonate as part of the pinnacles.

2.6.1 Algal Mudstone Facies

Algal mudstones of the Cayugan-aged A-1 Carbonate unconformably overlie the karsted, stromatolite boundstones and algal wackestones of the Niagaran-aged Guelph Formation (Mesolella *et al.* , 1974; Gill, 1986; Cercone, 1984; Pearson, 1980; Grimes, 1988). This mudstone represents the first deposits of the Salina Group to cover the pinnacle bioherms. It is light brown to chocolate brown in colour with a mottled texture (plate 15).

Dolomitization is pervasive with only the Rosedale reef remaining limestone. Inter-crystalline porosity occurs throughout (plate 15) as do small vugs and molds. Limestone in the Rosedale reef contains little porosity. Areas with very high porosity have, in places, small anhydrite laths associated with the inter-crystalline porosity, and salt plugging associated with vugs. Some saddle dolomite crystals are also found in vugs, pre-dating both the anhydrite and the halite. Very wispy stylolites were the only compaction feature noticed.

2.6.2 Stromatolite Boundstone Facies

Stromatolite boundstones are separated from the underlying algal mudstone facies by a gradational contact. Similar to the boundstone facies in the Guelph Formation, light brown to tan coloured and darker, medium brown laminations alternate, with the lighter coloured laminations being thicker. Individual laminae attain maximum thicknesses of 1.1 mm, but average 0.2 mm to 0.5 mm in thickness. Laminae mimic each other, and dips, curves and irregularities are preserved through several laminations (plate 16). Wavy, crinkly and near-

Plate 15: A-1 Carbonate mudstone facies and porosity development

Plate 15A: Sample showing chocolate brown and light brown rocks of the algal mudstone facies of the A-1 Carbonate Formation which drape the pinnacle bioherms. Numerous vugs present throughout. Union Rosedale 8-9-II-A.

Plate 15B: Thin-section photomicrograph in plane light showing anhedral and euhedral dolomite crystals (D) and large pores within the A-1 Carbonate. Locally, the A-1 Carbonate is tight, but on average has porosity. Imperial # 399 Warwick, 509.4m subsea.

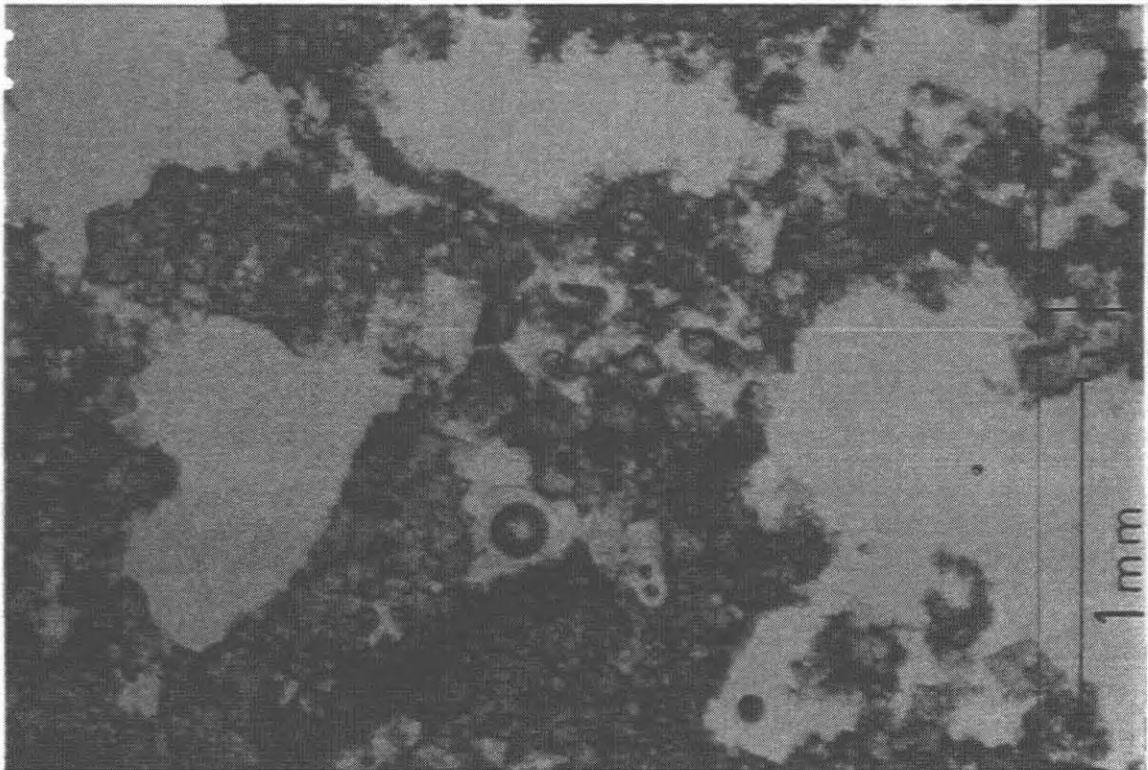
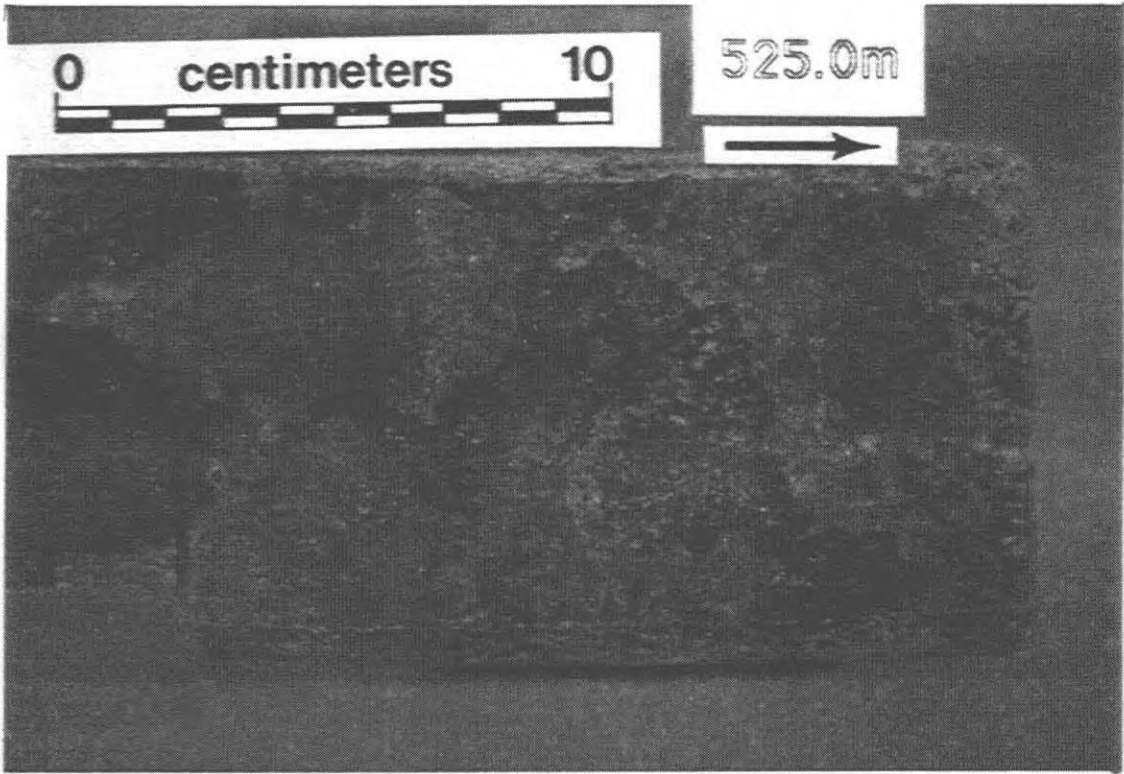
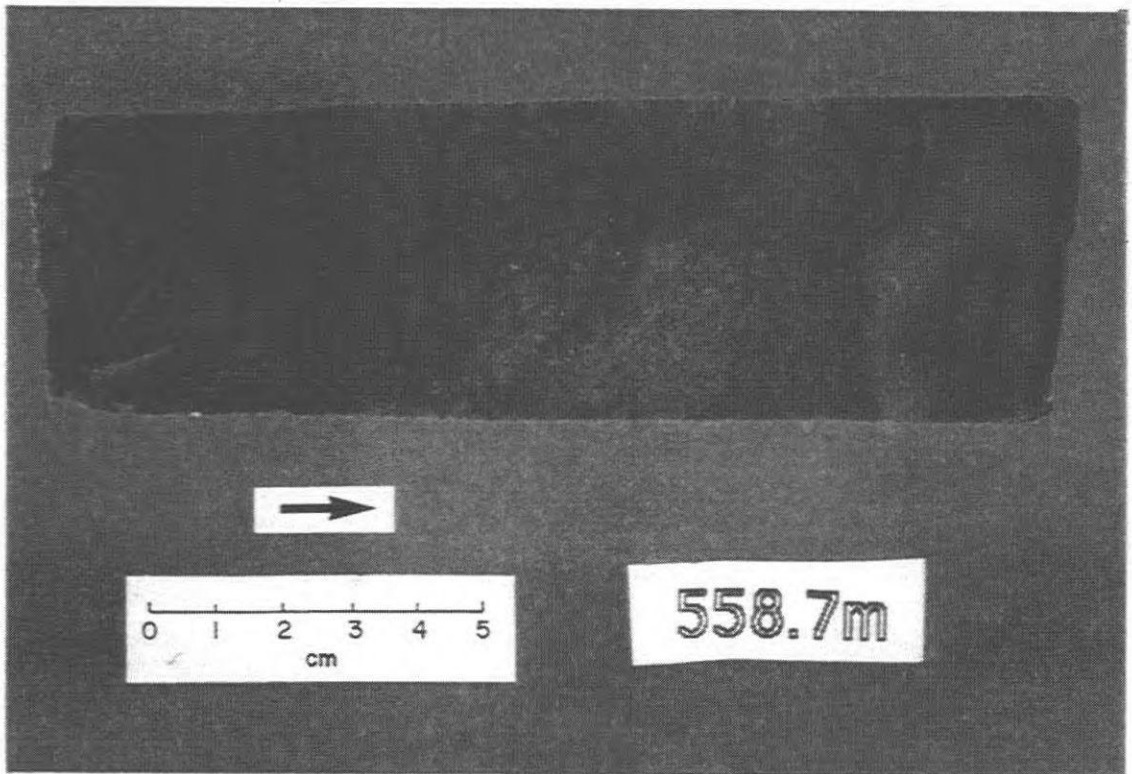
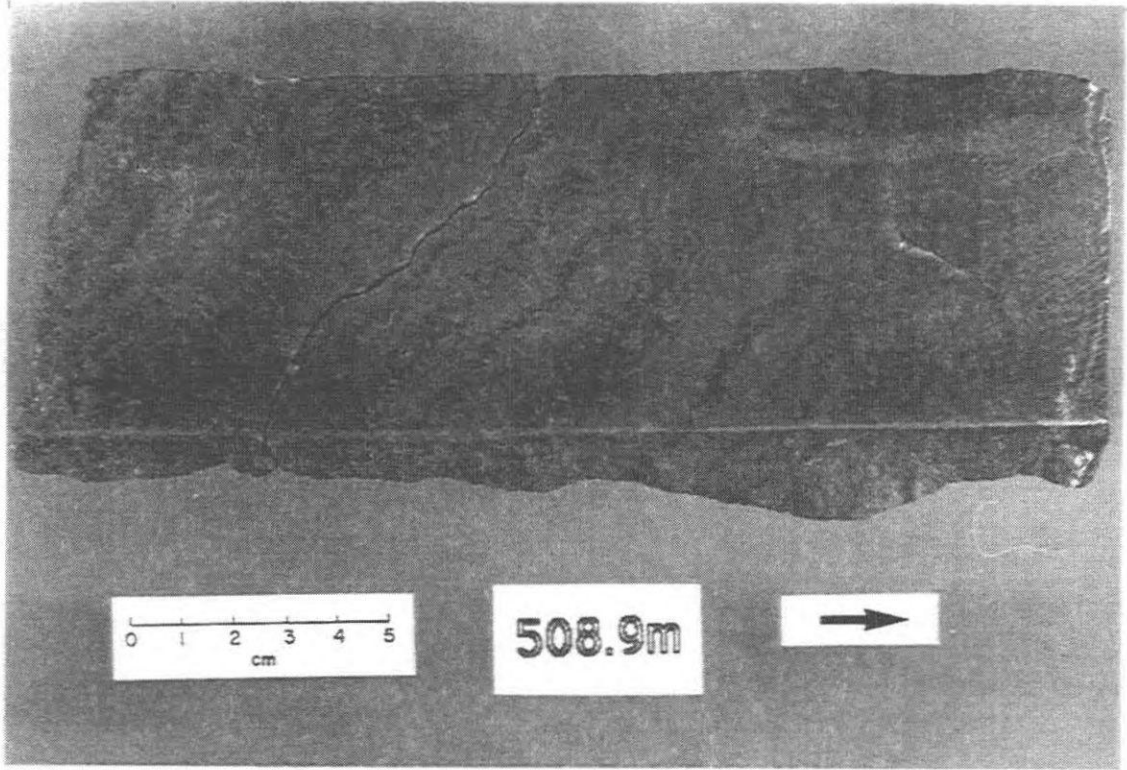


Plate 16: A-1 Carbonate stromatolite boundstone facies and A-2 Evaporite

Plate 16A: Example of stromatolitic boundstone from the A-1 Carbonate Formation. As with the boundstone of the Guelph Formation, laminae mimic underlying laminae and irregularities in growth are often seen through several generations of growth. Ram # 3, Terminus.

Plate 16B: Anhydrite of the A-2 Evaporite. Locally, chicken-wire textures exist but anhydrite is usually nodular (N). Light brown to gold-brown dolo-micrite (E) is present throughout as wisps. Imperial Sombra 4-14-XIII, Wilkesport.



horizontal laminations were observed. Several breccia zones containing small clasts were encountered in this facies and may be the result of exposure and dessication.

This facies is highly dolomitized and porosity is primarily inter-crystalline although fenestral porosity and small vugs are abundant. Pores are variably plugged with salt; some cores showing partial emplacement of salt in cavities while others are free of salt. Stylolites are common with thin, wispy seams tracing routes along lamination boundaries. In places, the upper few metres of the facies contain very large, acicular anhydrite laths up to 1.5 cm long and randomly oriented within the boundstone.

2.6.3 Distribution of the A-1 Carbonate

Although not detected by some authors (Hill, 1966; Gill, 1977, 1979; Bailey, 1986), the A-1 Carbonate was observed in this study to consistently overlie the pinnacle bioherms. In most instances, the algal mudstone facies are of greater thicknesses than the overlying stromatolite boundstone facies. However, the reverse is true for pinnacles closer to the basin centre. Reef-crest wells show an A-1 Carbonate thickness of up to 22.4 m (Rosedale). Reef-flank wells have greater thicknesses with an observed maximum of 29.8 m found in cores of the Warwick reef.

2.7 A-2 Evaporite Formation

Anhydrite of the A-2 Evaporite Formation is the first evaporite unit to cap the pinnacle reefs. This not only encases the pinnacles in anhydrites and mudstones and seals them, but also acts as a seismic reflector. Over the tops of the pinnacles, the A-2 Evaporite thins dramatically (Gill, 1977) and it is less than 2.0 m in thickness over any of the studied bioherms. The amount of anhydrite above the pinnacles varies considerably from being almost absent to having thicknesses of over 3.0 m (Terry Carter, pers. comm., 1989).

Similar to the A-1 Evaporite, the A-2 is blue and nodular (plate 16). Thin wisps of tan to gold coloured, crypto-crystalline, micritic dolomite are contained in the anhydrite.

2.8 A-2 Carbonate Formation

The A-2 Carbonate represents the highest unit, stratigraphically, examined in any of the studied cores. It is a light grey, argillaceous, crypto-crystalline to very finely crystalline dolomite mudstone that has shaley interbeds. Minor amounts of stromatolite boundstone are also present. Porosity is low as most available pores are occluded by salt.

2.9 Summary

In the study area, dolomitic basinal shales of the Rochester Formation are overlain by the carbonate platform deposits of the Lockport Formation. The Gasport Member, a stratigraphically lower, crinoidal dolomite member of the Lockport Formation, is overlain by a crinoidal and skeletal dolomite unit, the Goat Island Member. Corals and stromatoporoids first occur in the Goat Island near the top of the section but decrease in number in most cores as the contact with the overlying Guelph Formation is approached. The carbonates of the Lockport are separated from the pinnacle reef facies of the Guelph Formation by a previously unreported, irregular surface.

Examination of the pinnacle reefs reveals a number of gross facies to be present in the Guelph Formation. Vertically these facies include: crinoid-skeletal wackestones; coral-stromatoporoid floatstones to framestones; algal-brachiopod wackestones and mudstones; and, algal-stromatolite boundstones. Both of the algal facies are overprinted by the karst facies, resulting from a massive subaerial exposure episode that is interpreted by most authors to have terminated bioherm growth. The largest pinnacle reef studied, the Warwick reef, has a Guelph section 127 m thick.

Approximately one-half of the Guelph section is a reef core consisting of corals and stromatoporoids. When coupled with the overlying algal-brachiopod facies, up to 90% of the Guelph section may be accounted for. The crinoid-skeletal wackestone at the base and the algal boundstone facies at the top account for the remainder of the bioherm section.

In off-reef areas, the Salina Group represents a repetitive, cyclic succession of evaporites and carbonates. The lowermost unit, the A-1 Evaporite, is not present over the pinnacles and is believed to have been deposited in inter-pinnacle areas. The overlying A-1 Carbonate does unconformably drape the pinnacles and a maximum thickness of 22.4 m was observed in a reef-crest well. Capping the pinnacles with anhydrite, the A-2 Evaporite effectively encases the reefs in a combination of evaporites and mudstones.

CHAPTER THREE

Karst Development Within Michigan Basin Silurian Pinnacle Reef

Bioherms

3.1 Overview

After first reviewing the parameters necessary for karst development, this chapter documents multiple subaerial exposure events that occurred during the genesis of the pinnacle reefs. Most of these exposure events are found in the coral-stromatoporoid and algal-brachiopod facies. A previously unreported karst surface near the Lockport-Guelph contact was observed in all six of the pinnacles studied, and may in fact represent the Lockport-Guelph contact regionally. That an exposure episode, potentially regional in scope, occurred before pinnacle reef development began is addressed in Chapter 5.

Additionally, examination of the degree of correlation of the exposure surfaces between the pinnacles provides insight into whether fault block movements exerted influence on the pinnacle reefs during their growth.

3.2 Parameters Affecting Karst Development and Meteoric Diagenesis

"Karst is a diagenetic facies, an overprint in subaerially exposed carbonate bodies, produced and controlled by dissolution and migration of calcium carbonate in meteoric waters, occurring in a wide variety of climatic and tectonic settings and generating a recognizable landscape" (Esteban and Klappa, 1983). An appreciation of the extensive role of subaerial exposure in ancient carbonates is at the forefront of carbonate sedimentology and diagenesis, largely due to recent documentation of paleokarst (eg. Read and Grover, 1977; Cherns, 1982;

Kahle, 1978, 1988) as well as work synthesizing processes and features that occur in the meteoric environment (Longman, 1980; Esteban and Klappa, 1983; James and Choquette, 1984).

When subjected to subaerial exposure, a number of intrinsic and extrinsic factors (figure 15) work to influence the resulting carbonate (James and Choquette, 1984; 1988). Two diagenetic end members of surface exposure exist: the karst facies; and the soil or caliche facies (Esteban and Klappa, 1983). These facies may overprint or truncate one another.

Initial mineralogy is the most important of the intrinsic factors (James and Choquette, 1984). In meteoric water, limestone is several orders of magnitude more soluble than dolomite and hence dissolves more readily (Choquette and James, 1988). In addition, the various other carbonate mineral species dissolve at different rates. In general, aragonite is the most unstable followed by magnesium rich calcite (Mg-calcite) and then low Mg-calcite (Walter, 1983). Grain size helps to control the rate at which carbonate dissolution takes place while permeability and porosity regulate flow rates (James and Choquette, 1984). Other intrinsic factors such as stratal thickness and attitude, the presence of fractures and available structural conduits have been cited by Choquette and James (1988) as influencing karst development.

Climate is the most important extrinsic factor such that a wet, warm climate promotes karst development and a cold, dry environment inhibits development (James and Choquette, 1984; 1988). Each dictates specific characteristics of the resultant karst. Warm wet environments produce terra rosa, well-developed soils, sinkholes, karren and collapse breccia, while cold, dry climates may produce local karsting at slow rates (Choquette and James, 1988). Vegetation contributing CO₂ to aid in dissolution and time to allow all processes to operate are also important.

3.3 Solution and Precipitation in the Meteoric Environment

Longman (1980) subdivided the shallow subsurface environment into four major diagenetic zones (figure 16 A). James and Choquette (1984) identified three of these zones in the

Figure 15: The factors that influence the development of karst (After James and Choquette, 1984; 1988).

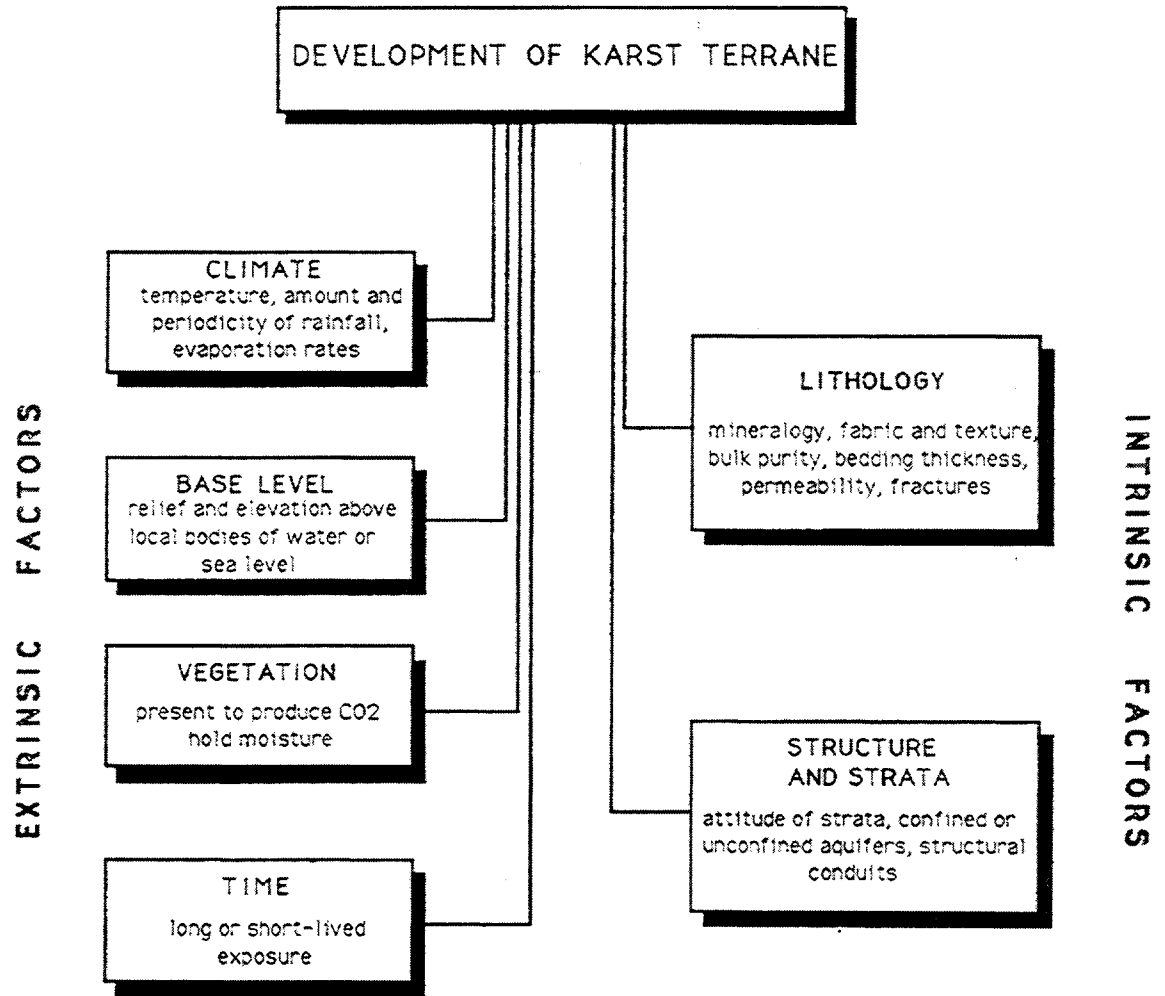
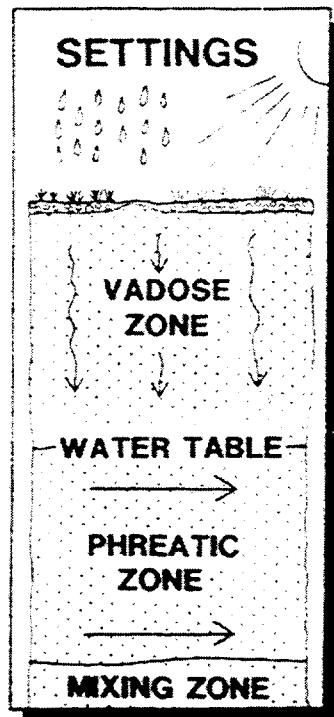
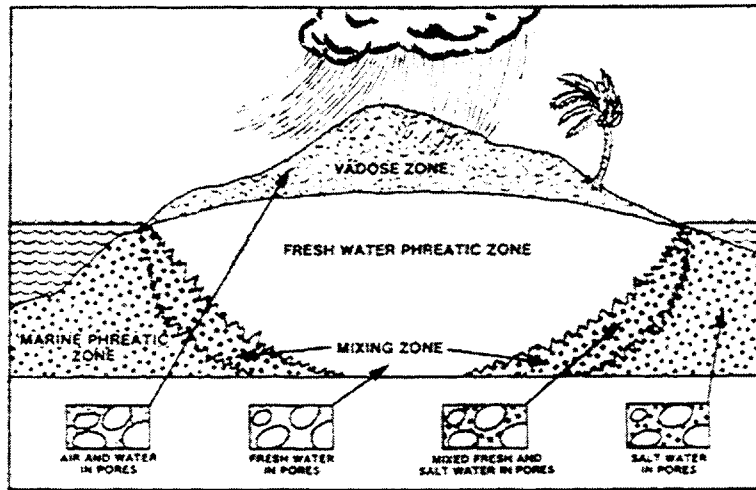


Figure 16: A) Idealized schematic diagram showing an island and the four diagenetic zones as occurring in the shallow subsurface (From Longman, 1980.) B) The three zones in the meteoric diagenetic environment (From James and Choquette, 1984).



meteoric diagenetic environment (figure 16 B). The meteoric vadose zone is the site of a complex array of water-rock interaction as fresh water is introduced into the carbonate rock system. Complexity of the vadose setting is heightened by the presence of vegetation, soils, and evaporation at the top of the zone. Pores are only intermittently filled with water and most often contain differing amounts of water, air and biogenic gas (James and Choquette, 1984).

Below the water table, the phreatic zone has pore spaces filled with meteoric water with varying amounts of dissolved carbonate (Longman, 1980). Within this zone, water is moving in a horizontal to sub-horizontal direction. The depth to which this zone extends below sea-level is governed by the height of the water table above sea-level. Longman (1980) cites a phreatic zone thirty two meters below sea-level for every metre above whereas James and Choquette (1984) suggest a ratio of forty to one.

At the base of the phreatic zone, the mixing zone is the site of physical and diffuse mixing of meteoric and marine waters (Longman, 1980). Described by Longman (1980) as a thin zone, James and Choquette (1984) maintain that the zone has the potential to be thick. This zone has been proposed as a site for early dolomitization (Badiozamani, 1973), but work by Hardie (1987) disputes this.

A host of complicated principles and processes governs the dissolution and precipitation of carbonate in the various zones, some better understood than others (James and Choquette, 1984). Reversible reactions in all zones, occur between minerals of different solubilities, and are influenced by factors such as partial pressure of carbon dioxide dissolved in water, temperature, and the degree of carbonate saturation, . Rather than outline these processes here, the interested reader is directed to Bögli (1980), Bathurst (1975) or James and Choquette (1984).

James and Choquette (1984) recognized that meteoric diagenesis is governed by two factors; water-controlled alteration between water and carbonates, and mineral-controlled alteration between water and the different carbonate mineral species. From this, a legion of solution and precipitation features result.

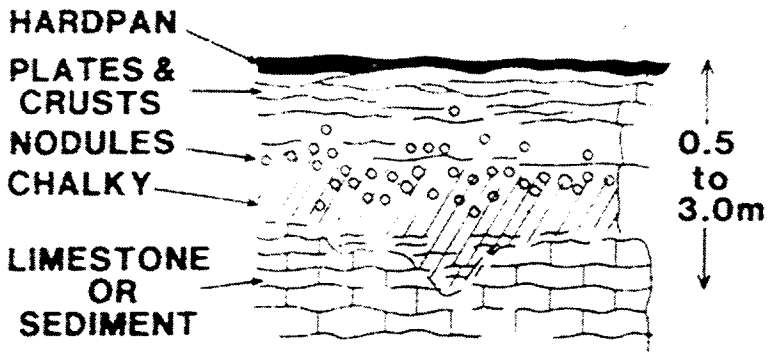
At the rock-air interface, extensive alteration can take place, and the karst or soil/caliche end-members of Esteban and Klappa (1983) may be found. Caliche horizons represent lithified soils and form in semi-arid climate. Characterized by laminated crusts, pisoids, breccia, chalky carbonate and iron oxides, caliche deposits may accumulate to metres in thickness (James and Choquette, 1984). Esteban and Klappa (1983) describe four rock types in a typical caliche profile (figure 17), progressing upwards from a massive, chalky carbonate to a nodular carbonate to a series of subhorizontal carbonate plates. Immediately above the platey carbonate is a micro-crystalline to crypto-crystalline hardpan crust. A transition zone of altered carbonates may underlie the entire sequence.

On bare rock or under soil cover, the karst facies may develop and dissolution features may range from centimetres to metres in areal and vertical in extent (figure 17). Corrosion is a very active process under soil cover while dissolution on bare rock leaves various forms of karren (James and Choquette, 1984). These authors emphasize that surface karst is difficult to recognize in the rock record and often is represented by irregular bedding contacts.

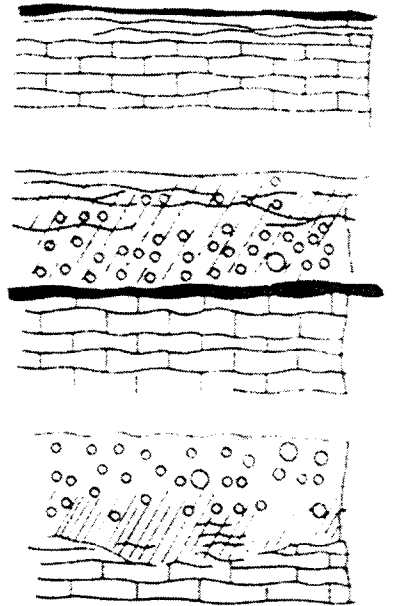
Just as solution can take place on bare rock, it also can occur in the zones identified within the meteoric diagenetic environment and pre-existing porosity and permeability may be greatly enhanced. Extensive precipitation of carbonates may also occur. The vadose zone is subdivided by Longman (1980) into an upper zone of solution and an underlying zone of precipitation. Dissolution occurs as fresh water, undersaturated with respect to calcium carbonate and containing dissolved carbon dioxide possibly from a soil zone, contacts the rock in the vadose zone. Until the water is saturated with respect to calcium carbonate, dissolution will continue. Saturation is dependent on: the composition of the carbonate (aragonite versus Mg-calcite versus low Mg-calcite); the amount of water present and its rate of movement; the partial pressure of carbon dioxide; and the presence and thickness of any soil zone (Longman, 1980). Once saturated, the water stops dissolution (if dealing with a single composition carbonate) often within decimetres of the surface (James and Choquette, 1984). Vertically

Figure 17: A) Schematic diagram showing an idealized caliche profile and possible variations (From James and Choquette, 1984). B) Schematic diagrams showing surface features that can result from karsting (From James and Choquette, 1984).

CALICHE PROFILE

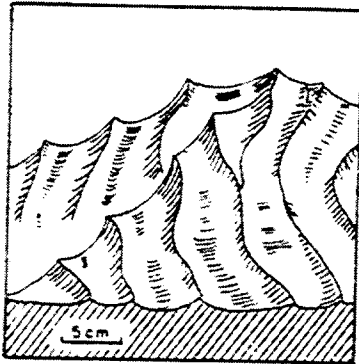


VARIATIONS

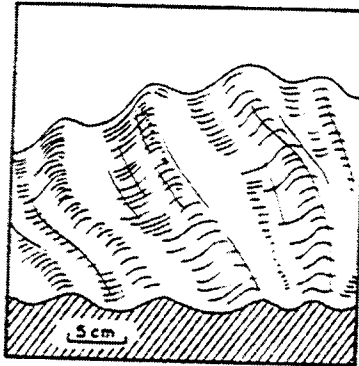


SURFACE SOLUTION SCULPTURE (KARREN)

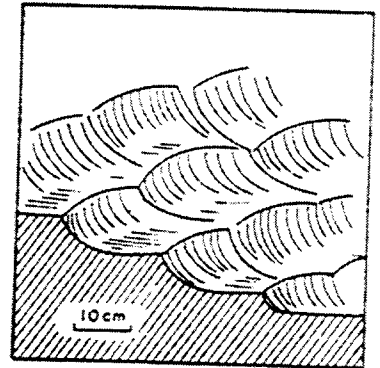
FLUTES



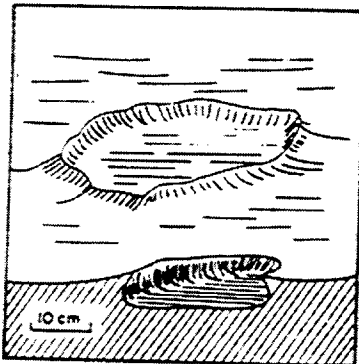
GROOVES



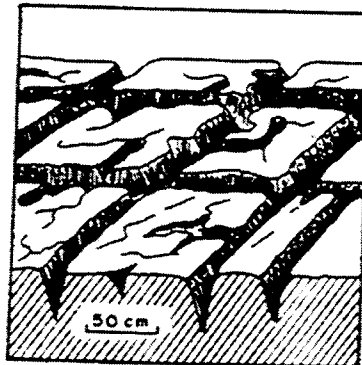
HEEL-PRINTS



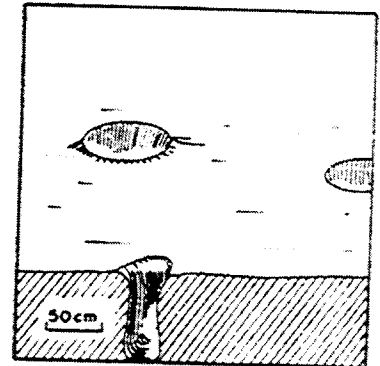
BASINS OR PANS



CLINTS & GRIKES



ROOTS



elongated caves may result. Prezbindowski and Tapp (1989) cite asymmetrical dissolution textures as evidence of vadose diagenesis.

Once saturated, slight changes caused by evaporation, decreases in the partial pressure of carbon dioxide or increases in temperature, may result in precipitation. Overall, the volume of cementation in the vadose zone is minor (Longman, 1980). Figure 18 illustrates the different cement types commonly found in this environment. Because the water system is saturated with calcium carbonate and percolation through the zone is not uniform, most cements are calcite and irregularly distributed (Longman, 1980; James and Choquette, 1984). Meniscus and gravitational cements are common and James and Choquette (1984) also report the growth of epitaxial overgrowths on echinoid fragments.

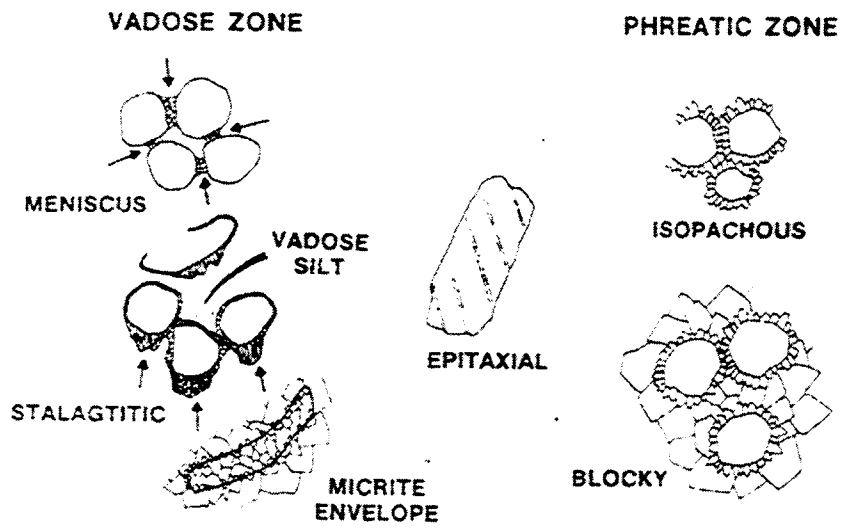
The water table, where vadose and phreatic waters mix, is a site of severe corrosion in subterranean systems closed to outside air and is the site of many laterally-extensive caves (James and Choquette, 1984). They document a wide variety of precipitation features that form as vadose water with high partial pressures of CO_2 , degasses as it enters cave systems filled with air of lower partial pressures of CO_2 . Deposits include speleothems, moonmilk, sinter, stalactites and stalagmites.

Most dissolution occurs below the water table in the phreatic zone where Longman (1980), in an idealized sequence, identified five characteristic areas based on saturation of calcium carbonate. Water entering the phreatic zone, may initially be undersaturated with respect to calcium carbonate. Once in the phreatic zone, however, it becomes progressively more saturated.

Uppermost, there is a zone where both aragonite and calcite are dissolved. Below this is a zone where only aragonite dissolves followed by an area of simultaneous aragonite dissolution and calcite precipitation. Lower still is a zone of calcite cementation where no dissolution occurs, underlain by a zone of little water movement. Mg-calcite with its variable solubility may precede aragonite dissolution or follow it. Zones may be small or missing and the mixing of waters may cause the zones to be out of sequence (Longman, 1980). Dissolution in the phreatic

Figure 18: Various cement morphologies that can form in the vadose and meteoric phreatic zones (From James and Choquette, 1984).

METEORIC CEMENTS



zone by undersaturated waters often results in vuggy or moldic porosity and the possible neomorphism of unstable grains (Longman, 1980).

Cements precipitated in the phreatic zone are mainly calcite (figure 18). Because water fills all available pore space, cements are equally distributed around most grains. Isopachous, bladed crystal morphologies are often the first cement encountered on grains or lining pores (Longman, 1980). Equant, blocky calcite crystals follow, coarsening toward the pore centre and forming an interlocking network. Syntaxial overgrowths commonly form on echinoderm fragments (James and Choquette, 1984; Longman, 1980).

Because the vadose zone is an oxidizing environment, neither the Mn^{2+} or Fe^{2+} ions can exist. Consequently, cements formed in the vadose environment do not have these ions within their crystal structure and are non-luminescent to poorly luminescent when viewed with cathodoluminescence microscopy (James and Choquette, 1984). In the phreatic zone, a reducing environment exists however, and both of these ions, as well others cited in section 1.8, are present and can be incorporated into the calcite crystal structure. Therefore, cements from the phreatic zone can be highly luminescent, reflecting the Mn^{2+} present, and often zoned. Pierson (1981) suggests that 100 parts per million (ppm) of Mn^{2+} yields luminescence whereas Machel (1985) places the figure as low as 20 to 40 ppm. Recent work by Have and Heijnen (1985) suggests that when iron concentrations are less than 200 ppm, as little as 15 -30 ppm of manganese is sufficient to activate luminescence in calcites and 30-35 ppm in dolomites. These authors also suggest that the intensity of luminescence is a function of the absolute amount of manganese and is not dependent on the Fe^{2+}/Mn^{2+} ratio. Zonations in crystals reflect differential amounts of manganese during growth caused by either changes in the Mn^{2+} concentration in the precipitating fluid, or by changes in the growth rate of the crystal independent of manganese concentrations (Have and Heijnen, 1985). Luminescence is fully quenched by greater than 15,000 ppm of Fe^{2+} (Pierson, 1981).

Water in the mixing zone is not interpreted to contribute greatly toward cementation, although James and Choquette (1984) recognize the possibility that Mg-rich cements and

dolomites may be found lower down in the zone . Rather, non-fabric selective dissolution appears to be important in the upper reaches of the zone (Back *et al.* , 1978), where mixed water is more dilute with respect to fresh water.

3.4 Karst Development in Limestone Pinnacle Bioherms of the Michigan Basin

Three limestone pinnacle bioherms, Rosedale, Warwick and Terminus, were selected for study to establish the presence of subaerial exposure surfaces within the pinnacles and to record the effects of meteoric diagenesis on the reefs. With these surfaces identified and the effects of meteoric diagenesis demonstrated, the three dolostone pinnacles, Bayfield, Wilkesport and Payne, are then critically assessed to document the effects of later dolomitization on meteoric diagenetic fabrics and exposure surfaces.

Finally, the degree of correlatability of the karst surfaces among all six pinnacles studied provides insight into whether or not fault block tectonism was the mechanism governing reef initiation and development.

3.4.1 Karst Surfaces Within the Warwick Pinnacle Bioherm

3.4.1.1 Surfaces Observed in the Warwick Pinnacle Bioherm

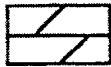
Pearson (1980) observed only one subaerial exposure event in the Warwick bioherm, occurring at the top of the reef. This study, however, has identified several irregular, sharp, undulatory and cross-cutting surfaces that are found throughout the pinnacle (figure 19, in pocket).

Surface one is at the base of the Guelph Formation at 646.5 m (figure 19). Lower in the section, stromatoporoids are first encountered at 657.7 m with corals at 654.3 m (figure 19).

Figure 19A: Legend for figures 19 to 24inclusive

LEGEND

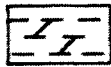
LITHOLOGY



DOLOMITE



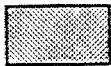
LIMESTONE



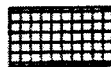
DOLOMITIC SHALE



NODULAR ANHYDRITE



GREEN CLAY



HALITE

ALLOCHEM



STROMATOLITE



BRACHIOPOD



COENITES



FAVOSITES



HALYSITES



RUGOSE CORALS



STROMATOPOROIDS



BRYOZOAN



CRINOID

DIAGENETIC FEATURES



STROMATACTIS



STYLOLITE



KARST SURFACE



PYRITIC CRUST



CALICHE HORIZON



LAMINATED RINDS



ANHYDRITE FILL



MUDSTONE FILL



PYRITE NODULE



BRECCIA

These organisms increase in size and abundance upward, but the stromatoporoids then decrease in number as the surface is approached.

At 646.5 m, a cockling-like surface is abruptly overlain by multiple generations of fibrous marine calcite cement which tend to have grown perpendicular to the substrate surface. Razor-sharp edges characterize the surface in places, while other areas are very delicate and knarled with contorted prominences jutting forward only to be enveloped by the cement (plate 17). Some of the projections have gastropods, brachiopods or other organisms perched on top. Numerous, irregularly shaped grooves cut into the surface, with relief of approximately 2 cm, enhance the topographic aberration (plate 17). Minor amounts of disseminated pyrite can be detected below the surface as well as slight porosity enhancement. Cathodoluminescence of samples taken from just below the surface reveals dark, prismatic non-luminescent cement crystals up to 200 μm in size, followed by zoned, brightly luminescent blocky cements up to 2 mm in size (plate 17). These cements are in evidence for approximately 4 m below the surface. Staining of the thin sections studied revealed little iron in any of the calcite or dolomite cements found in any of the pinnacles. Iron was detected to accompany the cements associated with interpreted karst surfaces in only a few selected locals, and in all instances it was affiliated with a later pore-filling cement.

Surface two is located from 597.0 m to 598.6 m (figure 19). Here, a void, filled with buff coloured, crinoid-rich packstone and a later iron-rich blocky cement, is carved into the original, light grey, crinoidal limestone (plate 18). A thin, dark rind locally rims the void. Crinoid fragments in the cavity have very irregular, ragged edges, in places are asymmetrical in shape, and are followed by syntaxial overgrowths. Under cathodoluminescence (plate 18), the overgrowths have a small, pendant, non-luminescent growth phase followed by a highly zoned, dull to bright yellow and orange luminescent cement. In rare instances, the non-luminescent phase and the zonation selectively occurs on the downward side of the crinoid ossicle only. Rind material has dull luminescence to a blotchy luminescence. Staining shows the blocky calcite cement to have iron present and to show some inclusion rich crystals. It occurs

Plate 17: Cockling and meteoric cements, Warwick bioherm

Plate 17A: Contorted and knarled cockling surface with features that appear sharp and abrupt yet finely sculpted through dissolution (S). All sides of the core reveal similar pinnacle-like projections jutting upward and grooves cut into the limestone. Gastropod (G) sits on top of one limestone finger while a brachiopod (B) is suspended within marine cement showing multiple growth zones. This surface at the base of the bioherm correlates with other irregular erosion surfaces at the base of each pinnacle studied. Imperial # 399, Warwick.

Plate 17B: Thin section photomicrograph under cathodoluminescence revealing interpreted meteoric cementation near karst surface in 17A. Small, non-luminescent, prismatic crystals of vadose origin (U) are 20 μm to 100 μm in size and project from pore walls. Brightly luminescent, zoned blocky crystals of meteoric phreatic origin (T) follow. Bar scale approximates 500 μm . Imperial # 399, Warwick, 649.7m subsea.

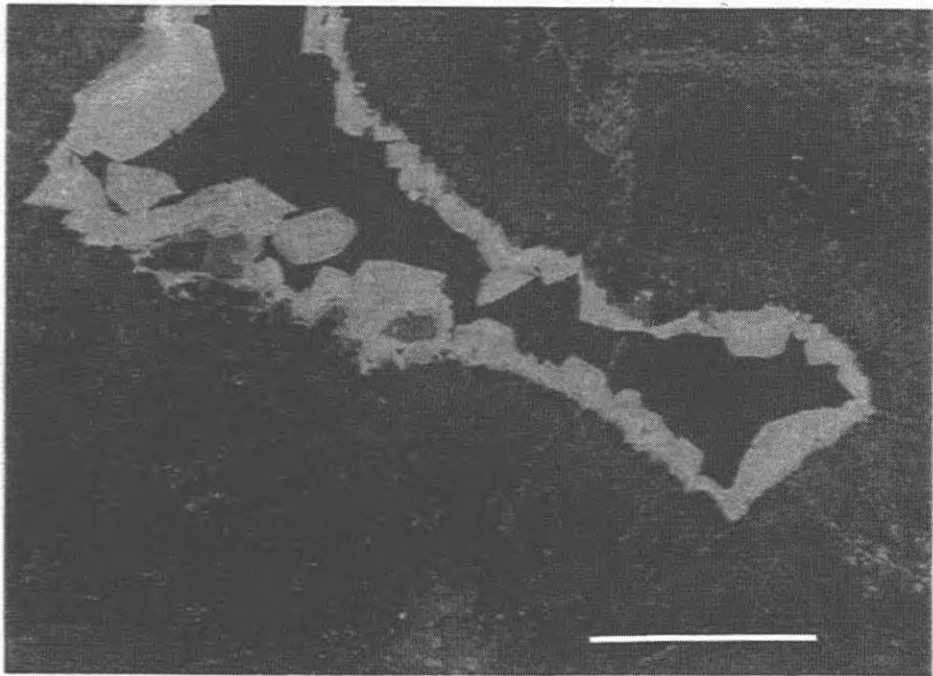
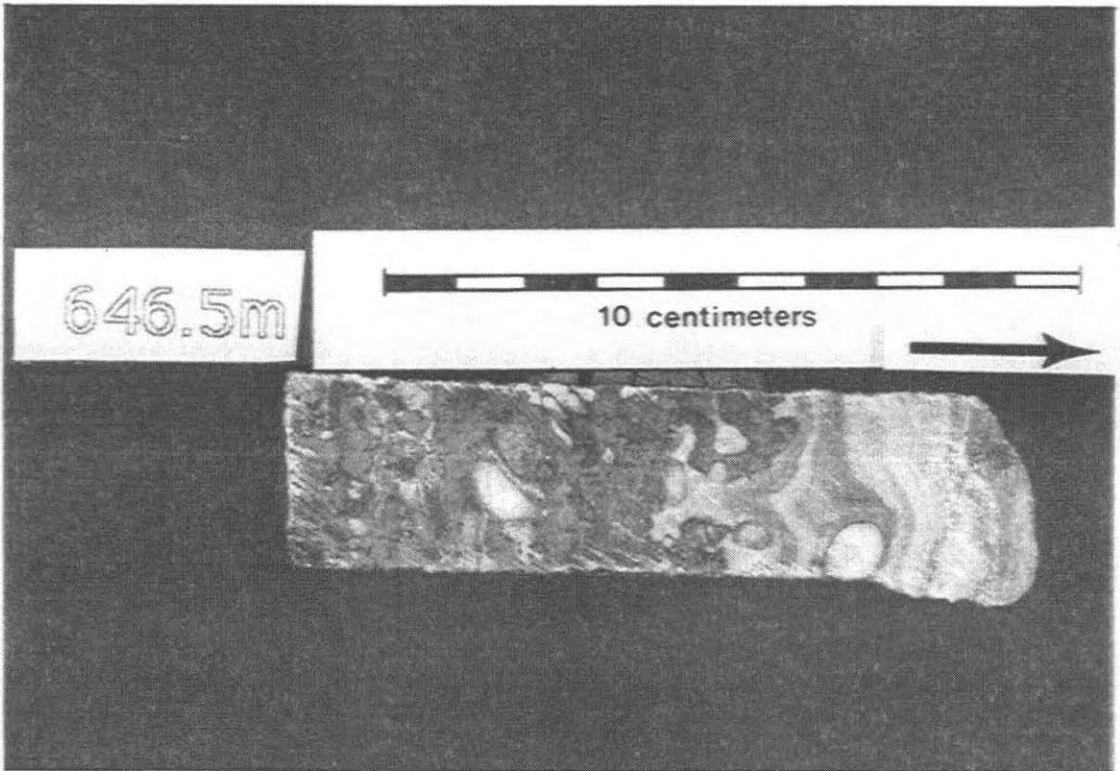
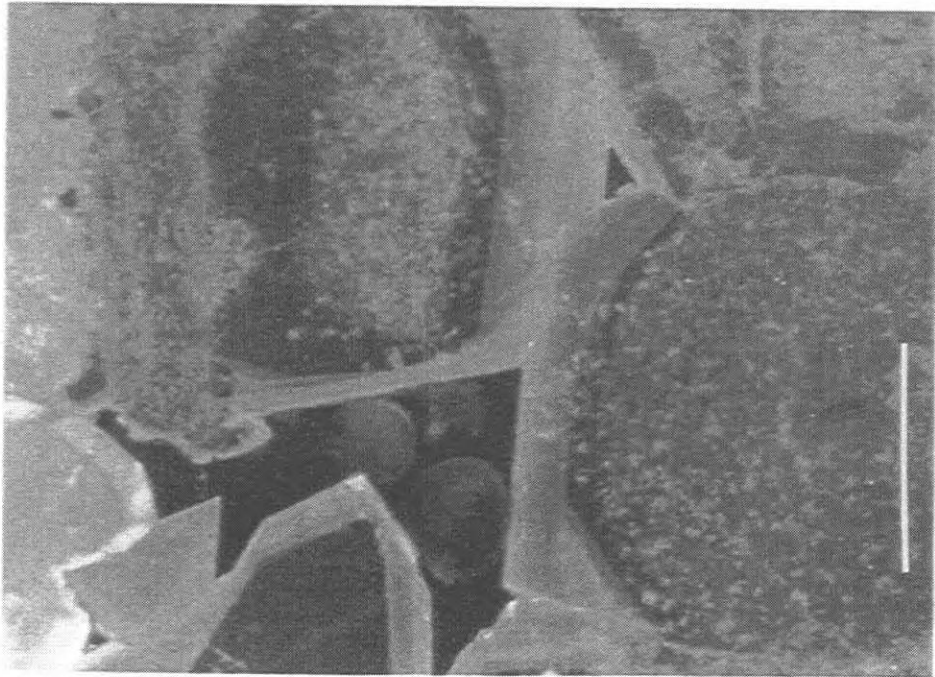
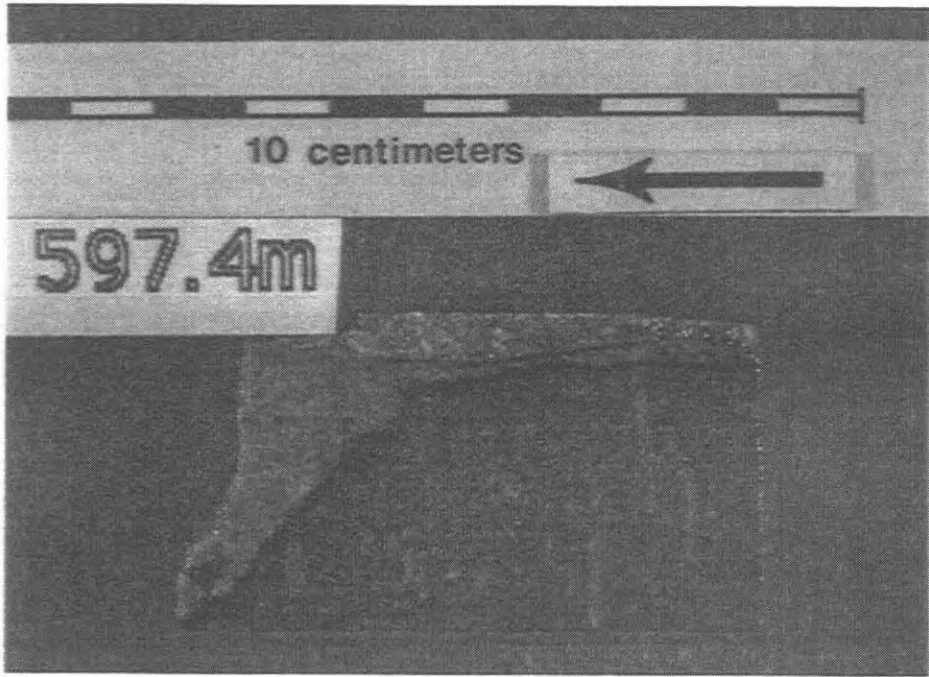


Plate 18: Exposure and meteoric diagenesis, Warwick bioherm

Plate 18A: Subaerial exposure surface diagonally and sub-vertically cross cutting original wackestone. Thin dark rind locally lines the cavity wall and a buff coloured packstone, rich with crinoid debris fills cavity. Imperial # 399, Warwick.

Plate 18B: Thin section photomicrograph under cathodoluminescence showing overgrowth on crinoid fragments from karsted area. Edges of the crinoids are corroded and a thin growth of non-luminescent, pendant (n) from the vadose zone is followed by zoned, brightly luminescent overgrowths of meteoric phreatic origin (r). Bar scale approximates 500 μm . Imperial # 399, Warwick, 597.0m subsea.



in the centre of the void feature and consists of blocky, equant crystals that coarsen outwards toward the centre of the pore. This cement is zoned and luminescent.

Stratigraphically higher in the reef, surface three occurs from 571.0 m to 571.9 m., and a small cavity is filled with angular breccia clasts (figure 19). The clasts are made up of abraded skeletal fragments and includes several rounded clasts that have semi-concentric rings. The maximum observed skeletal clast size was 3 cm long by 2 cm wide. A dark finely crystalline mud matrix surrounds the clasts (plate 19). When viewed with cathodoluminescence, the breccia area features dark, non-luminescent cements with prismatic morphologies and with well-defined terminations. The crystals occur normal to growth surfaces, hang downwards and are an estimated 200 μm to 300 μm in size.

Crinoids observed in between the surfaces at 597.0 m and 571.0 m, and associated with irregular surface features at 589.4 m, show no evidence of overgrowths. Rather, there is a light brown, fibrous, marine calcite cement, growing in wedges, normal from their surface (plate 19). This cement is then abruptly overlain by equant, blocky calcite cement. However, when viewed with epifluorescence, the fibrous cement has thin, faint, pendant growth bands within it and cathodoluminescence reveals a tiny growth of non-luminescent cement (plate 20).

From 544.7 m to 545.0 m evidence of another irregular, abrupt surface (surface four) is found (figure 19). In this interval, rocks of the algal-brachiopod facies are diagonally crosscut by a light brown dolomite mudstone. A thin, laminated rind, less than 1 mm in thickness separates the overlying algal-brachiopod wackestone from the mudstone and is noticeable in thin section. Thin section analysis also reveals pre-existing fabrics truncated by the dolomite. The mudstone can be traced downward for 0.3 m and it darkens in colour with depth. It truncates horizontally against a light grey, bleached limestone (plate 21). The lower contact which has irregular topographic relief of up to 0.5 cm anhydrite is associated with it.

Lastly, from 525.8 m to 531.8 m, the surface observed by Pearson (1980) occurs (figure 19). This surface (surface five) represents the most extensive and pronounced feature observed in the Warwick reef. A large conduit is filled with broken breccia clasts consisting of stromatolite,

Plate 19: Breccia and strandline diagenesis, Warwick bioherm

Plate 19A: Sample from karst zone showing small breccia clasts (C) averaging 1 cm in size surrounded by a dark brown mudstone matrix (s). Imperial # 399, Warwick.

Plate 19B: Thin-section photomicrograph in plane light with a brown, isopachous fringe of marine calcite (S) growing normal on a crinoid fragment (U). Blocky calcite follows (R). Note the tiny white deposit of cement locally on the fragment. Bar scale approximates 500 μm . Imperial # 399, Warwick, 589.0m subsea.

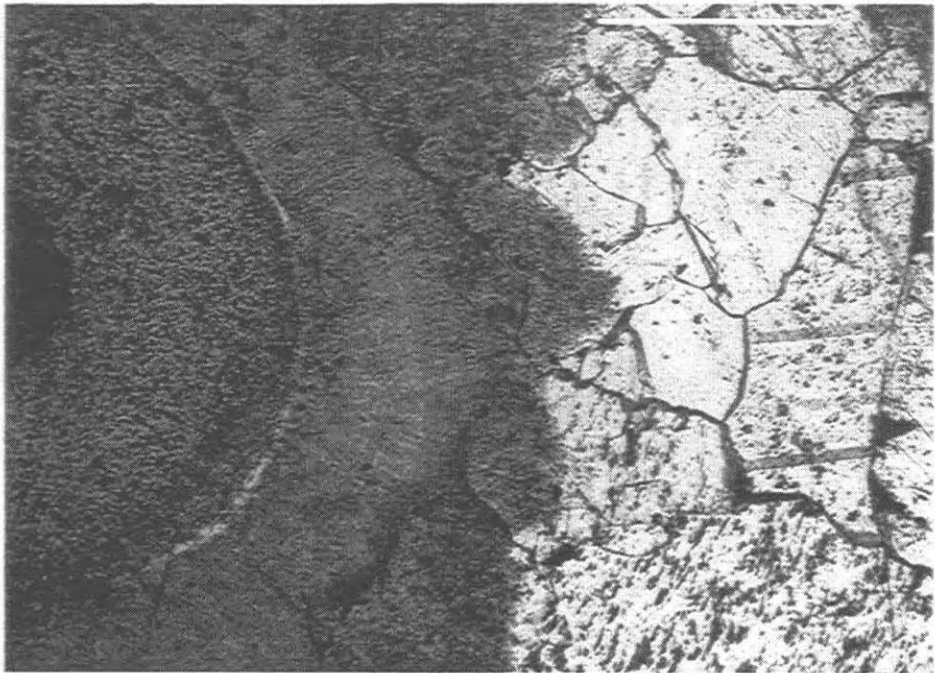
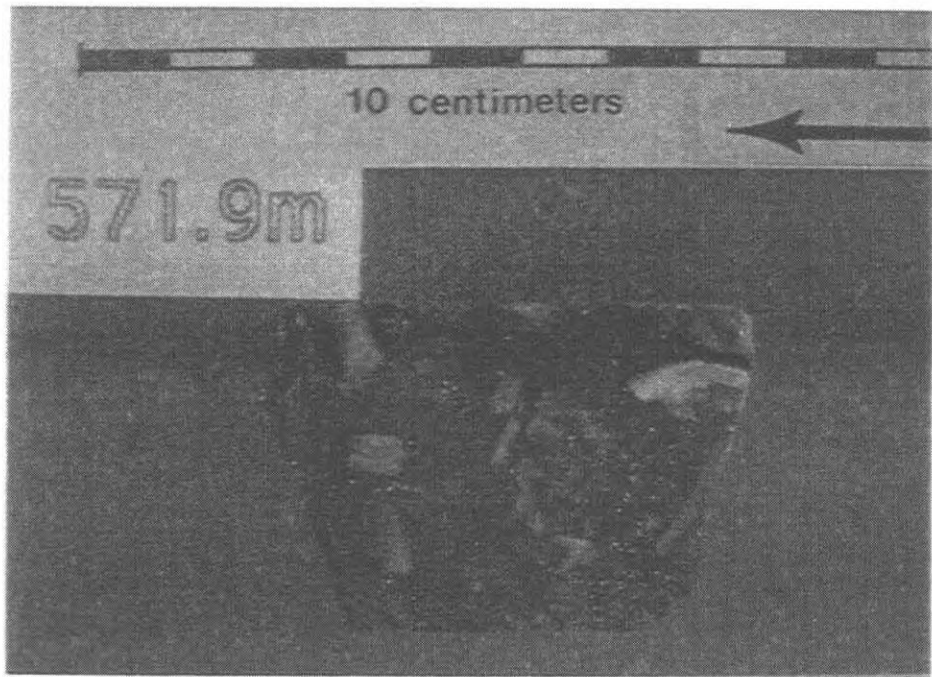


Plate 20: Vadose and meteoric phreatic cementation, Warwick bioherm

Plate 20A: Same photomicrograph as in Plate 19B but under cathodoluminescence. Crinoid is dully luminescent but thin white cement is non-luminescent (E) and pendant suggesting vadose origin. Fibrous marine calcite (M) has dull red luminescence similar to centre of the crinoid (Z). Vadose and marine cementation on the crinoid is interpreted to have formed in a beach environment. Blocky calcite cement (T) in centre of the void shows zonation. Bar scale approximates 500 μm . Imperial # 399, Warwick, 589.0m subsea.

Plate 20B: Thin section photomicrograph using epifluorescence of the same crinoid (C) in Plate 19B and Plate 20A. Non-luminescent pendant vadose cement (V) clings to fragment but very thin pendant-shaped growth bands (O) are now visible within the marine cement (H). Bar scale approximates 250 μm . Imperial # 399, Warwick, 589.0m subsea.

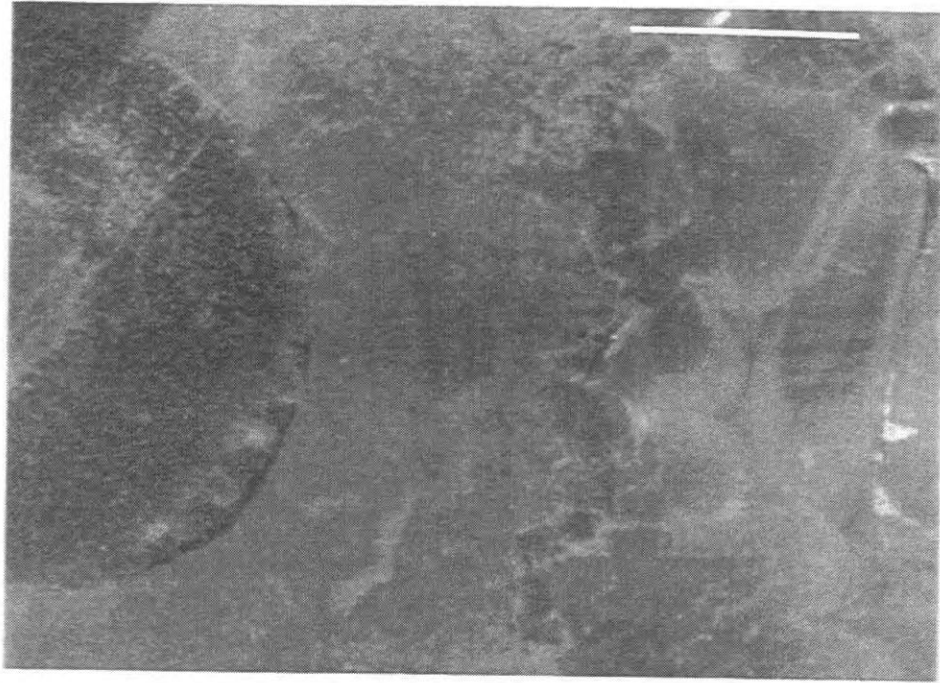
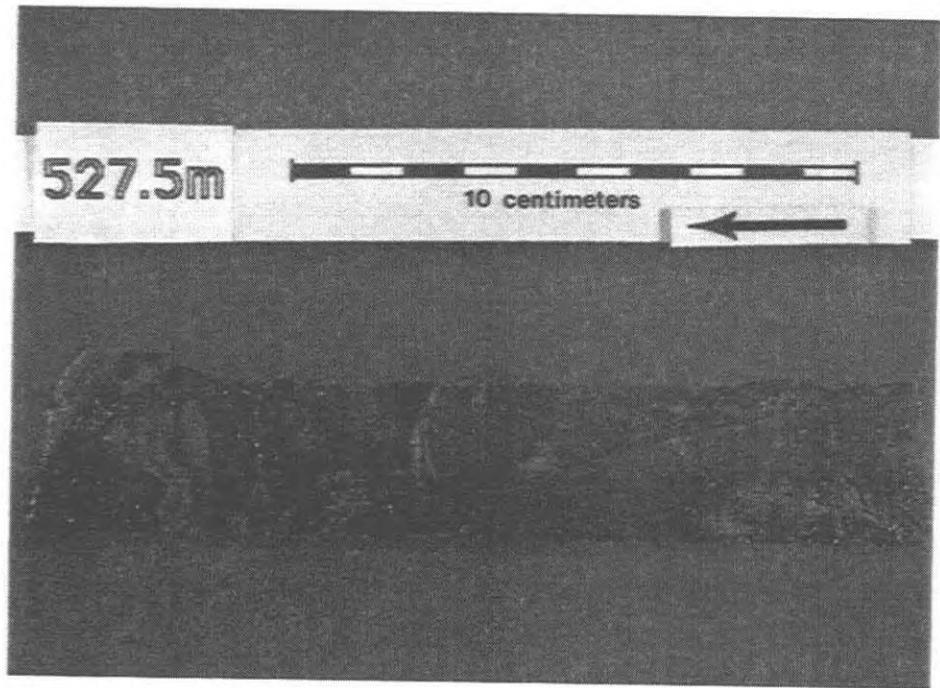
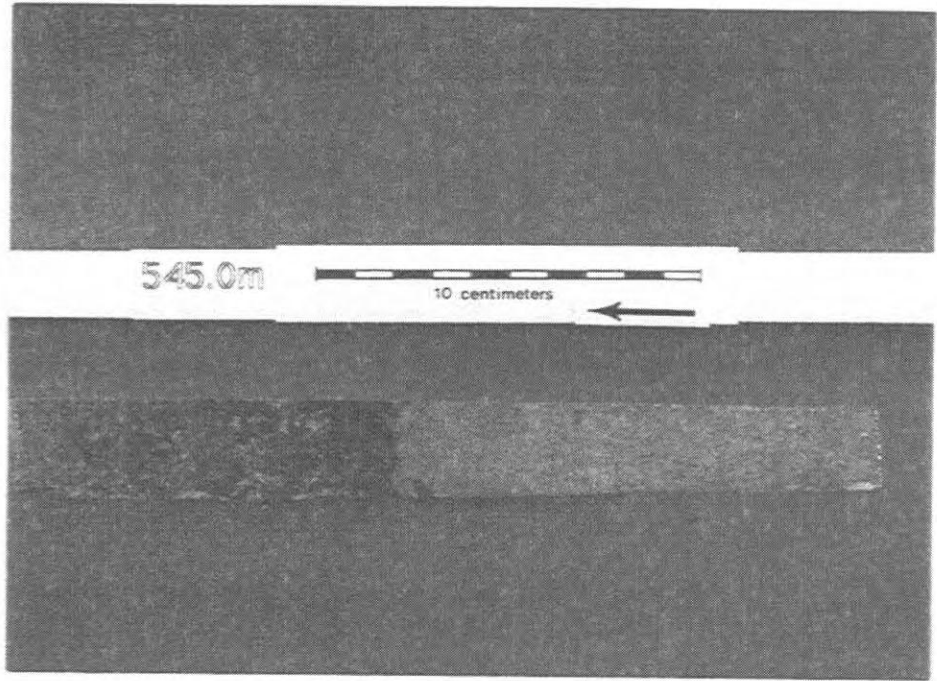


Plate 21: Exposure surfaces, Warwick bioherm

Plate 21A: Karst surface where light brown dolomite terminates with an irregular horizontal contact against light grey-brown wackestone. Dolomite can be followed downward, diagonally cross cutting the core for 0.3m, before it abruptly forms the horizontal contact. Contact surface is pyritized. Imperial # 399, Warwick.

Plate 21B: Subaerial exposure surface at the top of the bioherm featuring broken stromatolite clasts (E), dark brown mudstone fragments and mudstone filled fractures (t). Original stromatolite boundstone (O) is also present. Imperial # 399, Warwick.



mudstone and thin, laminated crust fragments (plate 21). The clasts are randomly oriented, have a maximum observed long axis of 7.0 cm, and are surrounded by a dark brown mudstone matrix. Dolomitization is patchy and fractures are present. Porosity is low and halite plugging occurs. Traces of a green clay capping the breccia fill in the cavity are seen in thin section.

3.4.1.2 Discussion of Surfaces in the Warwick Bioherm

Irregular surfaces identified within the Warwick reef (figure 19) have several features associated with them that suggest diagenesis in a meteoric setting. The first surface encountered, the cockling-like surface at 646.5 m, has non-luminescent prismatic and brightly luminescent blocky cements associated with it. That the cement is non-luminescent, suggests that either a sufficient amount of Fe^{2+} ions is present to quench any luminescence that may exist, or there is insufficient amounts of Mn^{2+} ions within the cement to cause luminescence. Staining of these cements revealed a lack of iron associated with them. Therefore, the non-luminescence observed must be caused by a lack of Mn^{2+} ions. This can be explained if the cements formed in the vadose environment where oxidizing conditions preclude the existence of Mn^{2+} ions and their incorporation into the cement crystal structure.

Zoned, brightly luminescent cements suggest an abundance of manganese ions in the crystal structure, a reducing environment, and possibly a changing pore water chemistry as the cement precipitated. This coupled with the timing of the cements, post-dating the vadose cements, is interpreted to indicate a meteoric phreatic origin.

Surface two at 597.0 m, features crinoids with zoned overgrowths. Although overgrowths are known to form in the vadose, meteoric phreatic, as well as the burial diagenetic zone (James and Choquette, 1984), the non-luminescent pendant cement followed by the luminescent zoned overgrowth suggests formation in a vadose environment followed by a meteoric phreatic

setting. This is further indicated when combined with a lack of petrographic evidence of burial features such as fractured grains, healing of fractures by cement and few stylolites.

Brecciation found with surface three at 571.0 m, is interpreted to represent collapse breccia due to subaerial exposure. Non-luminescent cements with stalagtitic morphologies support a genesis in the vadose zone. At 589.0 m, the light brown, wedge-shaped bundles of fibrous marine calcite found growing on crinoid fragments, and the pendant growth forms within the cement detected by epifluorescence and cathodoluminescence, are interpreted to represent origin in a strandline setting. Combined evidence from vadose and marine environments is a very rare occurrence in any of the pinnacles. This combination likely formed in a beach type environment. Under these circumstances, vadose cements can be found co-existing with marine cements. It is uncertain if these features result from the karst event at 571.0 m or the one at 597.0 m. These cements may also indicate a separate exposure surface independent of the other two. This example does, however, illustrate the potential to have fluctuating sea levels and changing environments as the pinnacles developed.

The two remaining surfaces are also interpreted to have resulted from exposure. At 545.0 m, (surface four) evidence of pyrite, dissolution of pre-existing facies and the truncation of fabrics is used to argue for a meteoric origin. Also, the lack of burial features associated with the surface supports a subaerial genesis rather than a hydrothermal or tectonic origin. At the top of the bioherm (surface five), abundant breccia, laminated crusts and stromatolite clasts are interpreted as evidence of a subaerial event. Pearson (1980) also recognized pisoliths in this area.

In the Warwick pinnacle reef, the Guelph Formation contains five separate exposure events, resulting in karst formation in the coral-stromatoporoid facies. The first occurs at the Guelph-Lockport contact, and an additional three subaerial exposure surfaces can be detected within the Guelph. A final major karst episode caps the Guelph section. Unconformably overlying this final karst surface is the chocolate brown dolomite of the A-1 Carbonate.

3.4.2 Karst Surfaces Within the Rosedale Pinnacle Bioherm

3.4.2.1 Surfaces Observed in the Rosedale Bioherm

While Grimes (1988) documented six karst episodes in the Rosedale pinnacle, this study has detected seven irregular surfaces (figure 20, in pocket) within the pinnacle bioherm.

Surface one is found at the base of the pinnacle near the Lockport-Guelph contact, from 628.5 m to 625.8 m (figure 20). Here, a massive cavity has been carved into the crinoid-skeletal wackestone (plate 22). Pre-existing fabrics and allochems are truncated where contacted by the cavity and walls show scalloping and the effects of dissolution. Fingers of limestone, connected to the walls, jut outward into the void and occur as breccia clasts. It is difficult to determine the top of the cavity, however, the bottom is abruptly terminated by a stylolite.

Locally, a thin rind of calcite cement lines the walls of the void. It is fibrous and composed of long, wedge-shaped crystals, up to an estimated 700 μm in size, that grow normal to the wall. This cement does not coat the walls isopachously as it is not evidenced on the other side of the cavity (plate 22). Following the cement, turquoise anhydrite completely plugs the conduit (plate 22). Lower reaches of the cavity contain a fine angular breccia, fibrous calcite cement, equant blocky cement and minor anhydrite. Porosity is poor, being filled with the cement and anhydrite.

Across the feature there is a change in rock type from a light grey, crinoid dominated facies typical of the Goat Island Member, to a buff coloured skeletal wackestone that is more representative of the Guelph Formation. Rugose corals and stromatoporoids begin to occur in abundance above the surface. When viewed with cathodoluminescence, pore spaces proximal to the surface reveal non-luminescent prismatic cements up to 500 μm in length with well-developed terminations. These cements are followed by equant, blocky, zoned, brightly luminescent cements (plate 23). Or, the prismatic crystals are followed by dull luminescent

Plate 22: Conduit formation, 627.0m, Rosedale bioherm

Plate 22A: Karst feature found at the base of the Rosedale pinnacle bioherm. Large dissolution conduit cross cuts downward for approximately 3 m. Clasts of wackestone (i) float in turquoise anhydrite or are protrusions from the cavity wall. Walls show scalloping and allochems and cements are truncated (W). Marine fibrous calcite cement locally lines the cavity walls (n). Union Rosedale 8-9- II-A.

Plate 22B: Photo showing the localized nature of thin isopachous rinds of marine calcite cement. Note the clast composed of wackestone and coated with fibrous calcite suspended in the anhydrite. Union Rosedale 8-9-II-A.

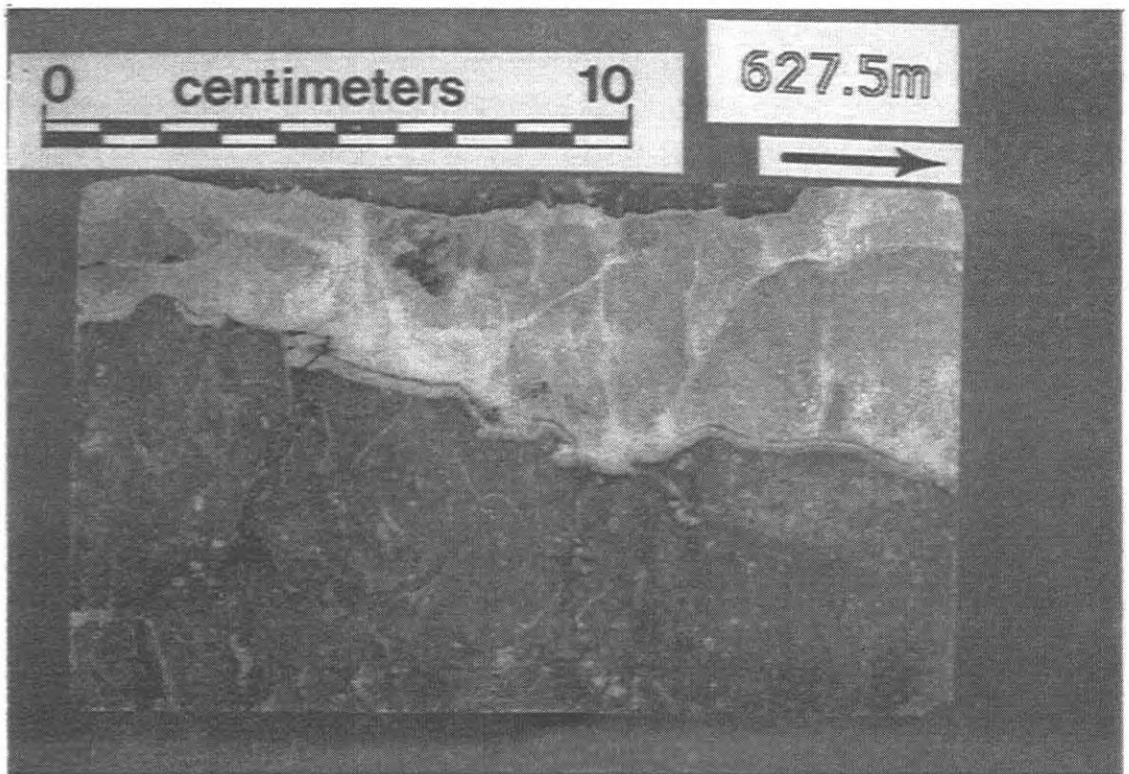
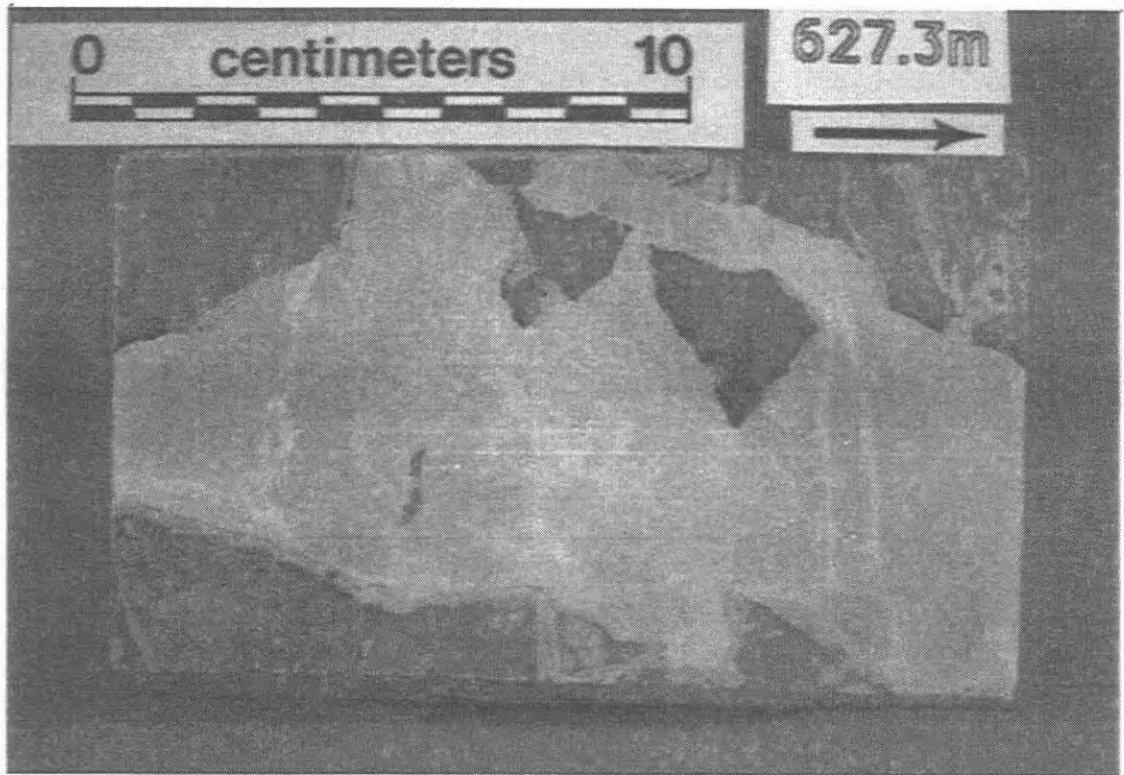
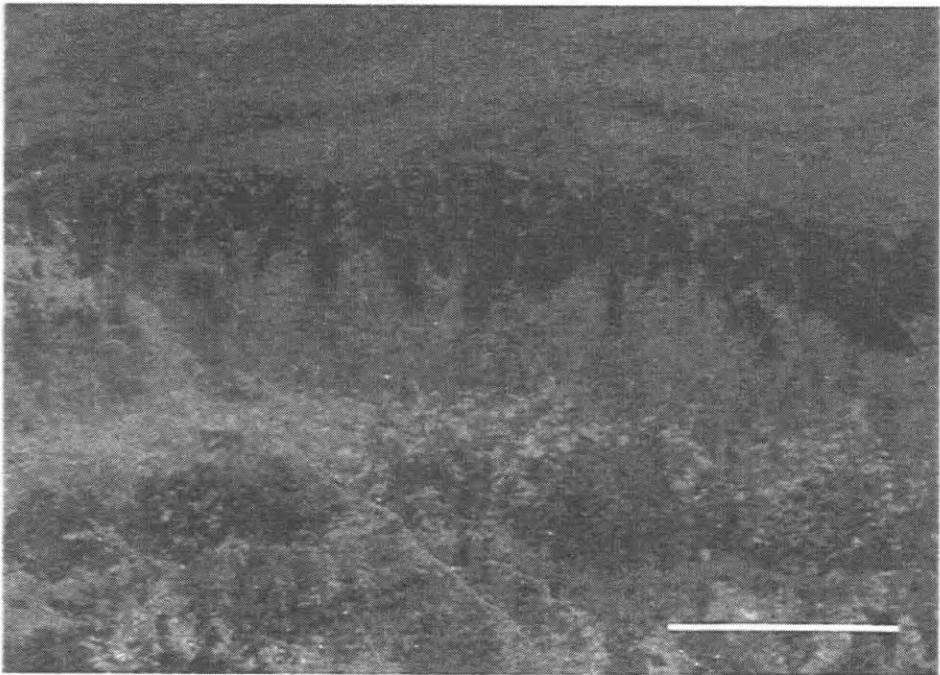


Plate 23: Vadose and meteoric phreatic cementation, Rosedale bioherm

Plate 23A: Thin section photomicrograph using cathodoluminescence showing non-luminescent prismatic calcite cement of vadose origin (a) followed by zoned, brightly luminescent, blocky meteoric phreatic cements (T). Cementation sequence can be viewed in small pores (e) in bryozoan (?). Two zoned dolomite crystals (h) are at the top of the photo. Bar scale approximates 1mm. Union Rosedale 8-9-II-A, 627.0m subsea.

Plate 23B: Thin section photomicrograph showing non-luminescent, prismatic calcite crystals from a vadose environment growing normal to bryozoan fragment (E). In this example, marine calcite cement follows the prismatic vadose cements. Marine carbonate shows blotchy luminescence. Bar scale approximates 1mm. Union Rosedale 8-9-II-A, 627.4m subsea.



fibrous calcite cements (plate 23). Non-luminescent and luminescent cements can be detected for at least 5.8 m below the surface.

Another irregular feature (surface two) can be detected from 612.2 m to 604.8 m (figure 20). At 612.2 m, a fine-grained, brown silt plugs former voids and when viewed in thin section, the silt has very thin, faint laminations. Overlying the silt, a fine, angular breccia is found in a narrow cavity. Irregularly shaped clasts, derived from the local rock, are up to 1.0 cm in size and are circumscribed by numerous, single seam stylolites. A white blocky calcite cement fills smaller areas of the cavity not occupied by the clasts. A later, blue-white, blocky, calcite cement, that stained for iron, occludes the remaining space in the cavity. Silt is present up to 604.8 m (plate 24). Pyrite is common in places and is associated primarily with the silt. Non-luminescent cements line pore walls and are followed by zoned, brightly luminescent blocky crystals (plate 24). Iron-rich calcite crystals occur brightly luminescent and unzoned. Very coarse white calcite, saddle dolomite and halite are also found associated with the feature. Non-luminescent cements occur for 3.9 m below the detected bottom of the feature.

At 571.2m, (surface three) a zone of abraded and partially removed corals is found (figure 20). This section of the core also represents the change from a coral and stromatoporoid dominated facies to facies that are more algal-dominated. The core features corals and stromatoporoids, that are partially to completely leached, over a 0.3m interval. Porosity is enhanced below 575.5 m, with large, irregularly shaped vugs several centimetres in size. A later salt plugs many voids. There is no calcite lining pores which pre-date the salt. The top of the zone is characterized an elaborately sculpted, open, void 5.0 cm wide.

Cathodoluminescence of samples from below the surface reveals small, non-luminescent, prismatic crystals estimated to be 100 μm to 200 μm in size, followed by brightly luminescent blocky crystals (plate 25). These cements can still be found 3.7 m below surface three. Staining shows these cements to be iron-poor.

Within the algal-brachiopod facies three laminated, brecciated and chalky surfaces were observed. Surface four occurs at 556.6 m (figure 20). At this interval, each of the two slabbed

Plate 24: Vadose silt and meteoric cementation, Rosedale bioherm

Plate 24A: Very finely laminated medium brown silt (dark brown) fills irregularly shaped labyrinth of cavities cut into wackestone. Breccia is found lower in core at 610.2m. Union Rosedale 8-9-II-A.

Plate 24B: Thin section photomicrograph showing pore in dull red and blotchy luminescent marine calcite (e). Non-luminescent, prismatic vadose calcite cements with well chiselled and well defined terminations (i) are followed by blocky, locally zoned, brightly luminescent cements (o) of meteoric phreatic origin. Bar scale approximates 1mm. Union Rosedale 8-9-II-A, 616.1m subsea.

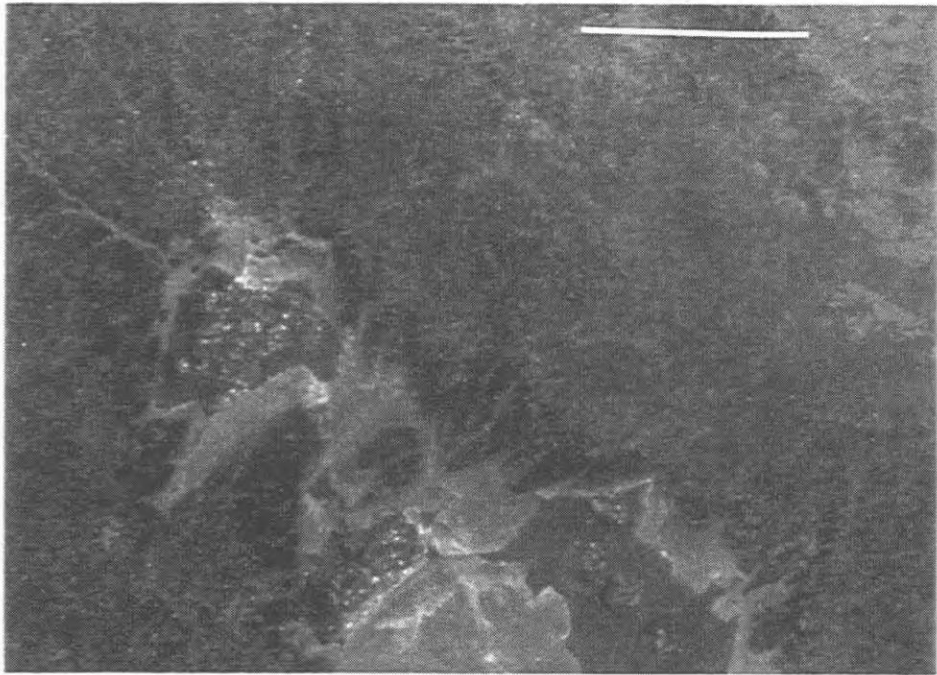
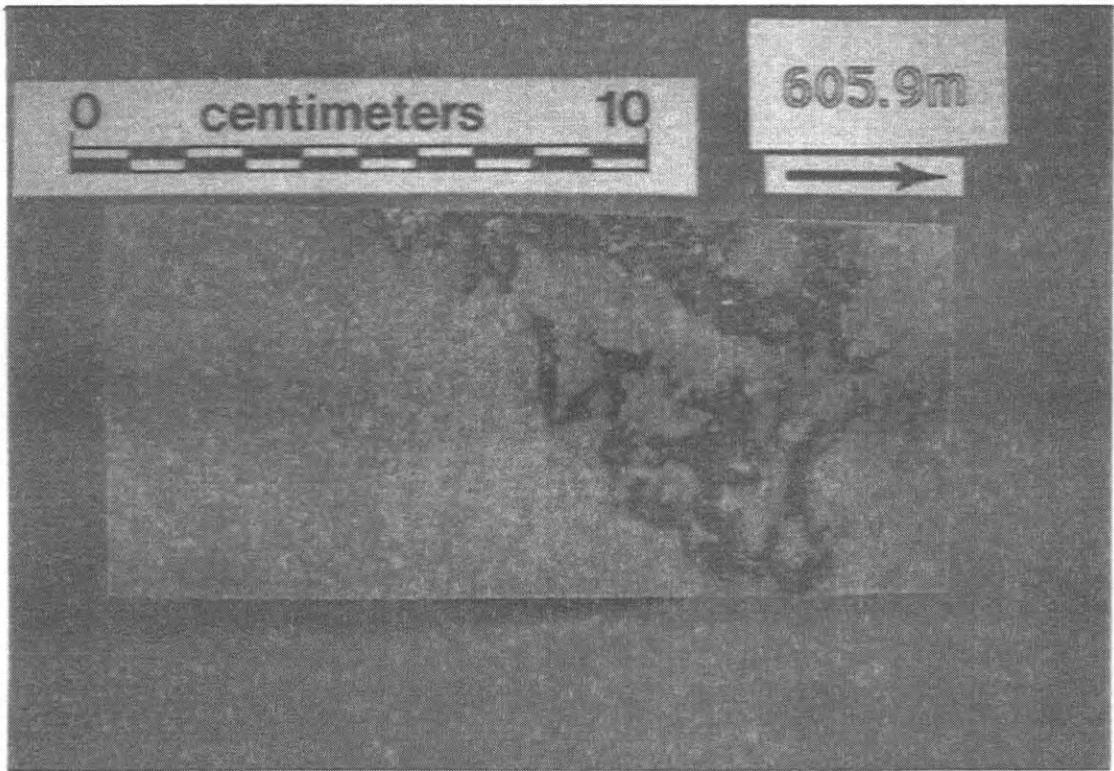
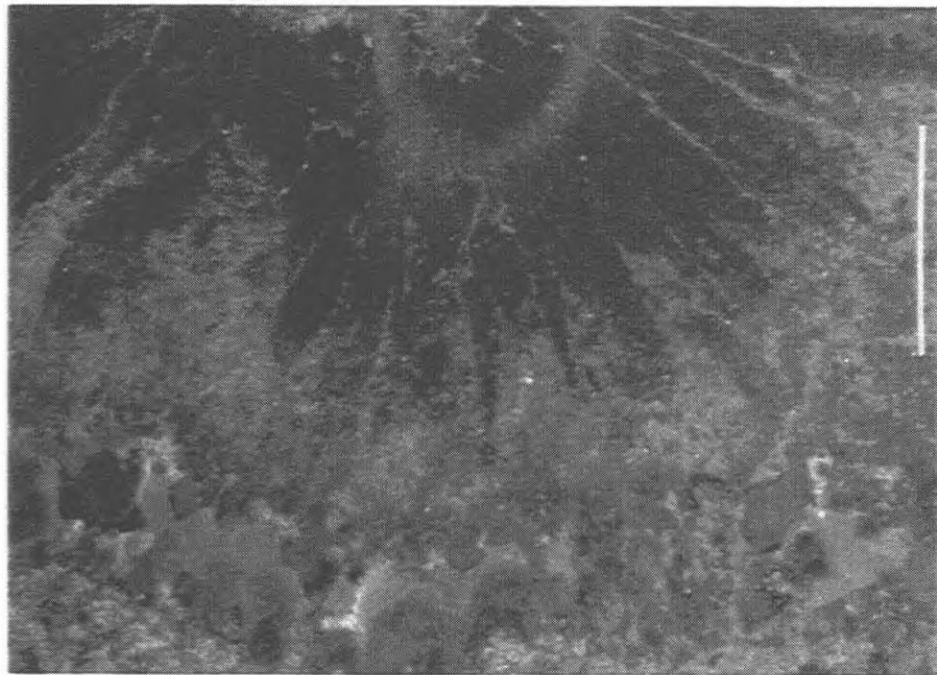


Plate 25: Meteoric cementation, Rosedale bioherm

Plate 25A: Thin section photomicrograph using cathodoluminescence of a rugose coral that is dark red, dully luminescent (r) with lighter red, dully luminescent sediment fill in chamber (U). Sediment is followed by tiny prismatic non-luminescent vadose cements and blocky, zoned brightly luminescent meteoric phreatic cements. Bar scale approximates 500 μm . Sample is from well below exposure zone at 571.2m. Union Rosedale 8-9-II-A, 599.2m subsea.

Plate 25B: Thin section photomicrograph using cathodoluminescence showing unknown allochem with dull purple luminescence and with non-luminescent cements growing prismaticly. Partial replacement of the vadose cements as well as the zoned brightly luminescent meteoric phreatic cements by finely crystalline anhedral and euhedral dolomite rhombs (E) has occurred. Locally, the euhedral dolomite rhombs have a non-luminescent growth zone. Bar scale approximates 500 μm . Sample is closer to exposure zone at 571.2m. Union Rosedale 8-9- II-A, 575.2m subsea.



sides of the Rosedale core shows a different progression upwards (plate 26). One side of the core reveals a 7.5 cm, near-horizontally laminated, brown mudstone overlying algal-brachiopod wackestone. The mudstone is overlain by a lithified, cream-coloured crust 3.0 mm to 4.0 mm in thickness. This crust is then overlain by a porous, chalky, poorly lithified layer that has a high gypsum content.

The other side of the core also contains the brown mudstone and overlying thin crust. However, here the crust is brecciated and is mixed with the mudstone. The chalky layer has also been disrupted, mixed with the lower units, and left as a series of contorted swirls (plate 26).

Surface five is an irregular feature within the algal wackestone facies occurring at 545.6 m (figure 20). Laminated, brown mudstone rests on top of the wackestone and shows a dip of approximately 35° (plate 27). The mudstone is capped by a cream-coloured crust. This is overlain by an 8 cm thick layer of breccia consisting of angular pieces of mudstone, crust and allochem fragments. The breccia is overlain by a thin 1.0 mm to 3.0 mm black crust and the whole sequence is topped by another laminated mudstone layer. This mudstone is similar to the first, 6 cm in thickness, but it has laminations that are more horizontal in orientation. In thin section, the lower laminated mudstone appears fibrous and displays allochems that have been sharply truncated and overlain by the breccia layer (plate 27). In addition, the deposit lacks any grading. Breccia clasts, while elongated and showing a preferential orientation, are not sorted.

The final surface within the algal-brachiopod facies (surface six) is found at 540.0 m (figure 20). Similar to the preceding feature in composition, this portion of the core also begins with a laminated mudstone. The mudstone is 5.0 cm thick and is first capped by a thin, cream-coloured crust and then by a poorly lithified, chalky lens of breccia clasts and gypsum laths (plate 28). Clasts are very similar lithologically to the underlying crust and may have been derived from it. A laminated mudstone tops of the succession and fills in topographic irregularities.

Plate 26: Exposure surface, 556.9m, Rosedale bioherm

Plate 26A: Interpreted exposure zone showing very finely laminated mudstone (from arrowhead upward) capped by chalky, calcareous layer with high gypsum content (G). Union Rosedale 8-9-II-A.

Plate 26B: Same core piece but showing opposite side. The chalky, gypsum rich layer (G) has been left as a series of contorted swirls within the underlying mudstone. Fine breccia clasts up to 5 mm in size are present in the swirls. Union Rosedale 8-9-II- A.

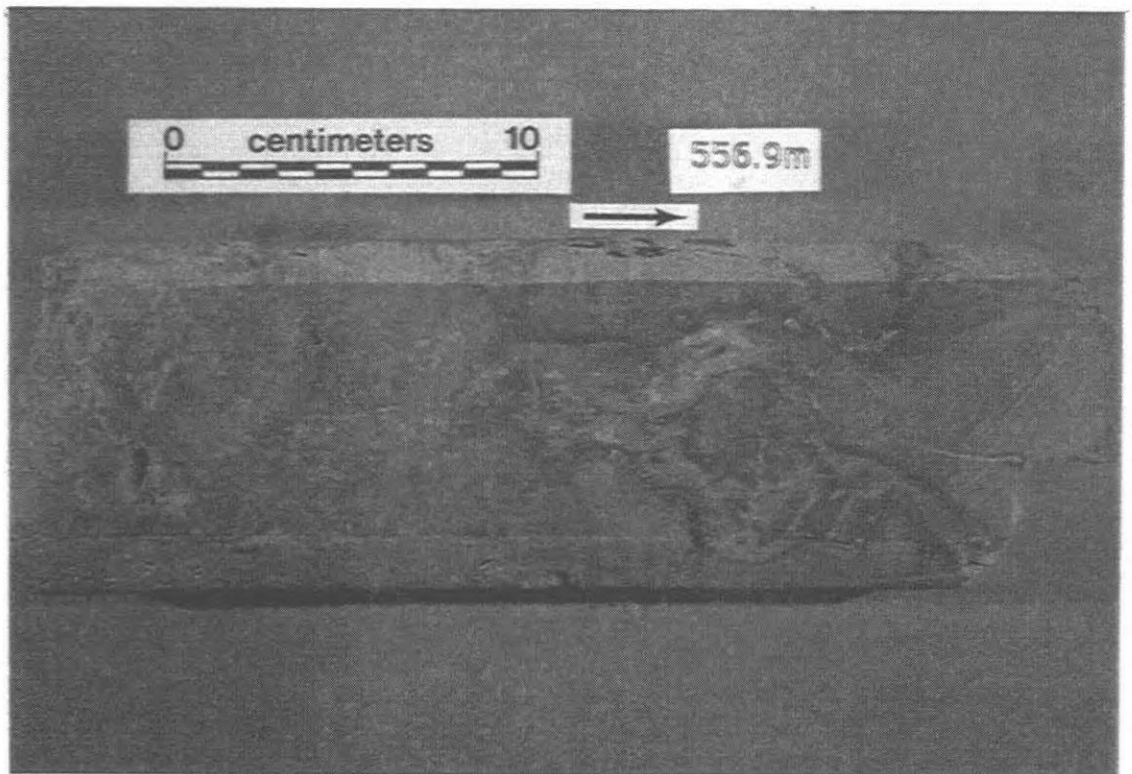
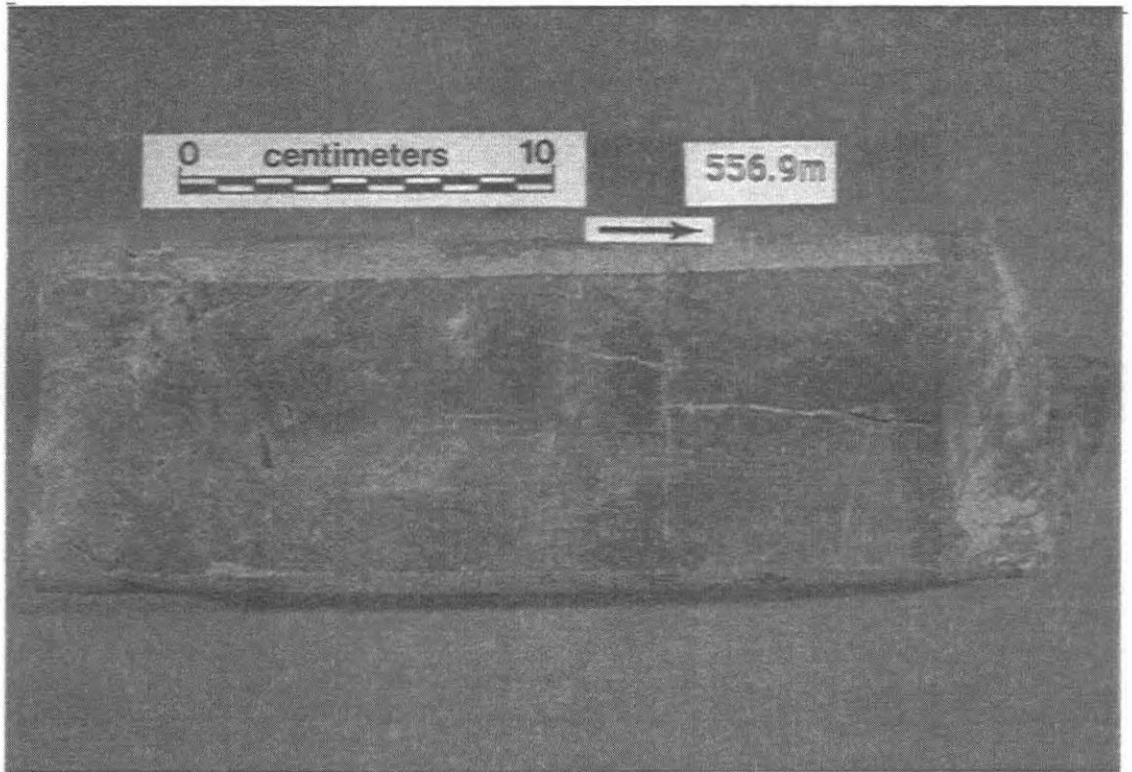


Plate 27: Exposure surface, 545.6m, Rosedale bioherm

Plate 27A: Subaerial exposure surface with interpreted development of caliche profile. Laminate mudstones are well lithified and breccia layer is calcareous and poorly lithified, locally chalky. Union Rosedale 8-9-II-A.

Plate 27B: Thin section photomicrograph in plane light showing favositid coral fragment truncated by finely crystalline mudstone. Sample occurs at the base of the lower mudstone layer in 27A. Union Rosedale 8-9-II-A, 545.9m subsea.

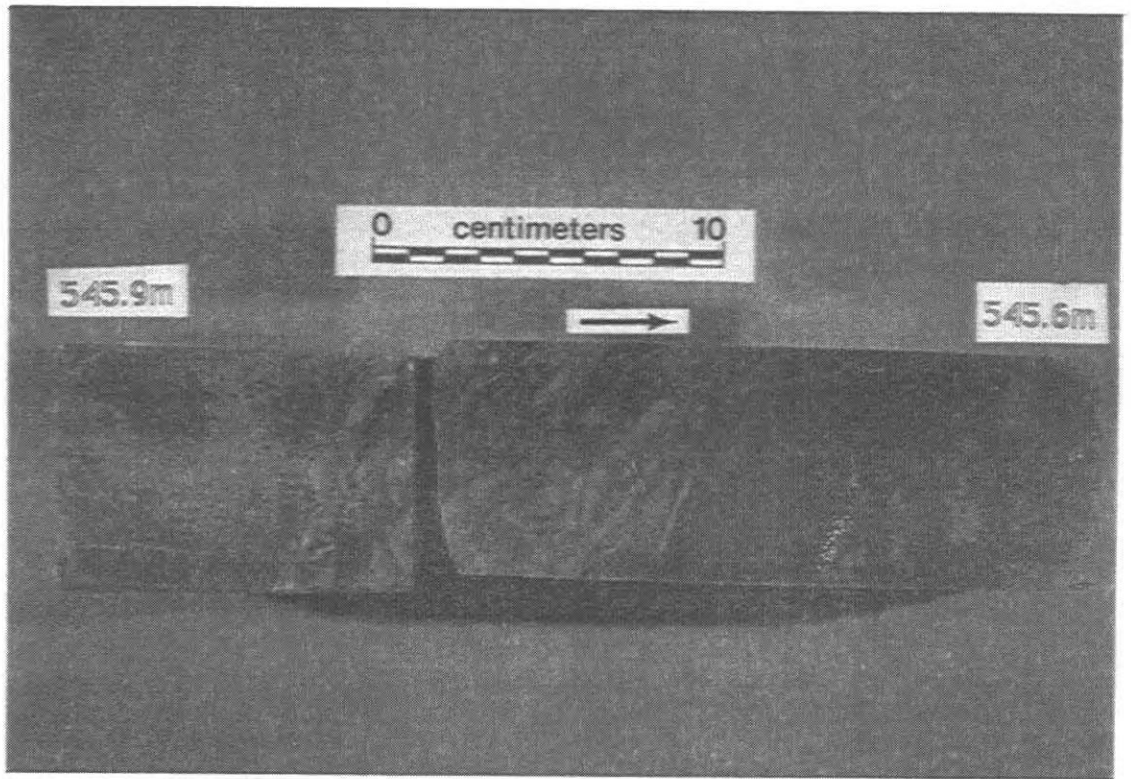
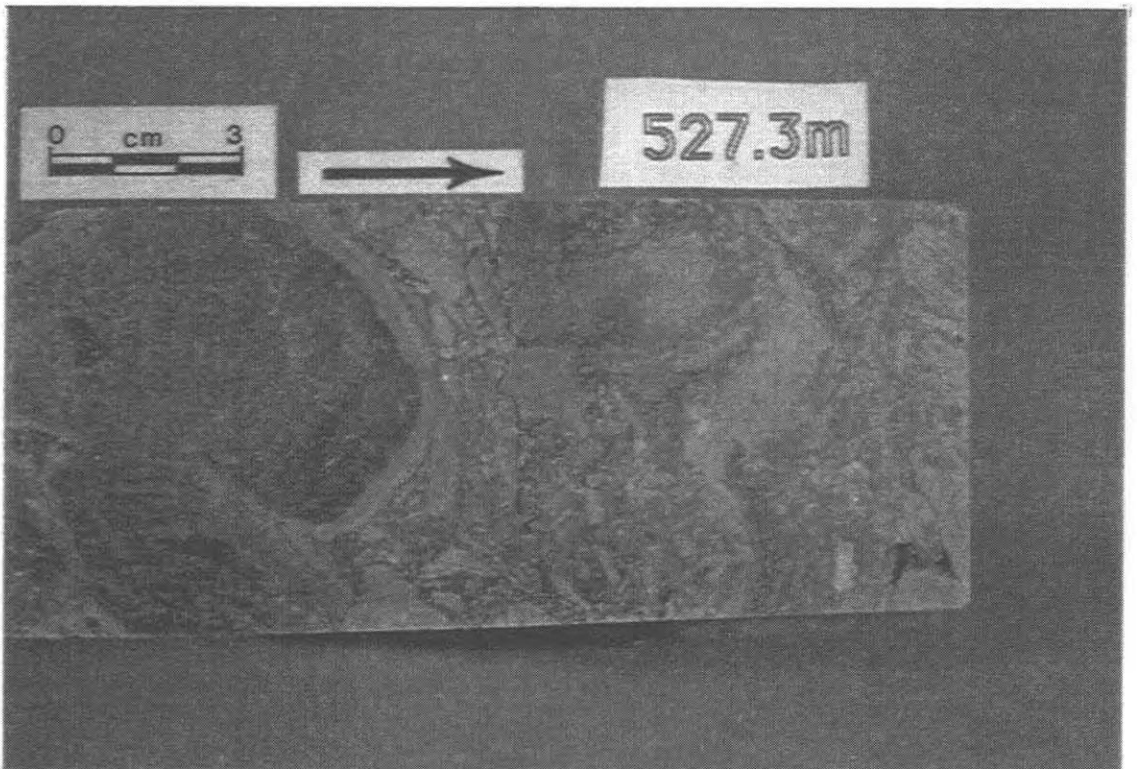
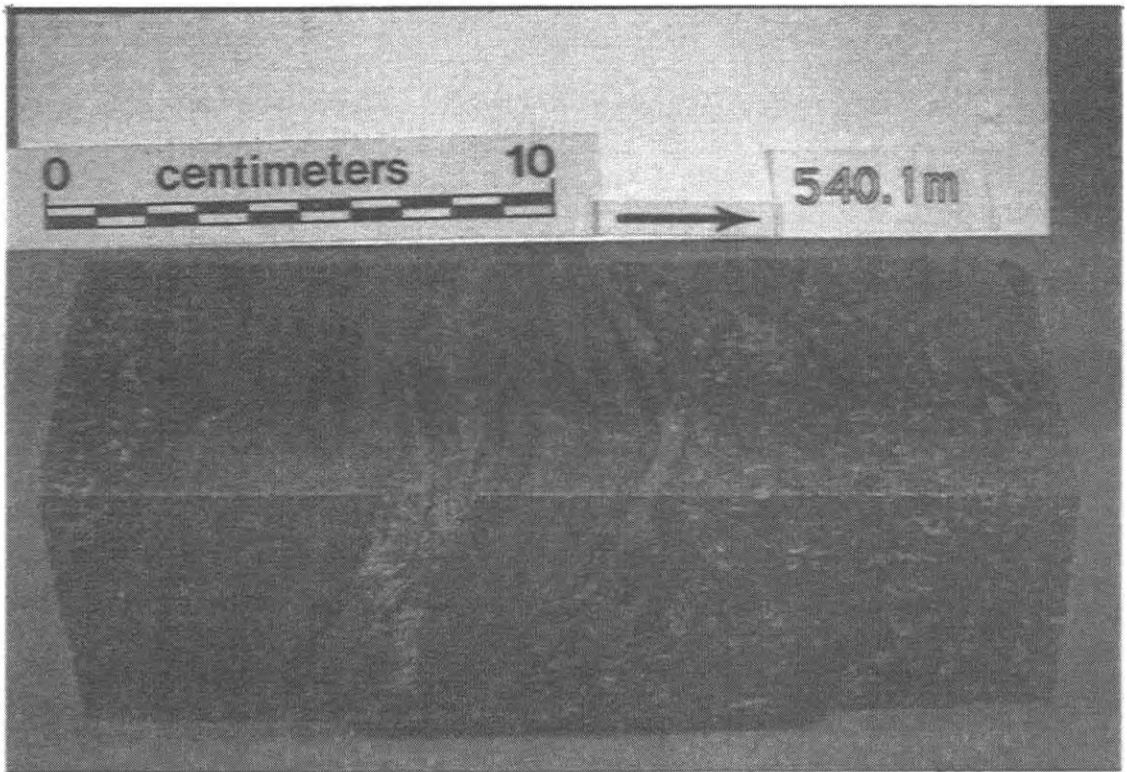


Plate 28: Exposure surfaces, 540.1m and 527.3m, Rosedale bioherm

Plate 28A: Irregular upper and lower contacts of laminated mudstone and chalky lens interpreted to be the result of subaerial exposure. Planar laminated mudstone drapes the existing algal mudstone and is overlain by mudstone with undulatory laminations, some showing displacement. Chalky lens is poorly lithified and has gypsum. Union Rosedale 8-9-II-A.

Plate 28B: Subaerial exposure found at the top of the Rosedale bioherm. Clasts are coated with laminated crusts (L) and appear randomly oriented. Fragments of stromatolite, crust and mudstone fill topographic irregularities. Union Rosedale 8-9-II-A.



Surface seven in the Rosedale reef is situated at the top of the bioherm at 527.0 m (figure 20). For 6.3 m, the stromatolitic boundstone is cross-cut by a massive cavity that contains angular breccia clasts of stromatolites, mudstone, and laminated crusts. The clasts are up to 8 cm long near the top of the cavity with smaller pieces found lower in the void (plate 28). A dark brown mudstone also fills in the pipe which sharply truncates all pre-existing fabrics. Stromatolite growth locally intersects the crevice and re-establishes well-developed horizontal laminations. This growth however is overlain by additional brecciation. A distinct, green clay fills in the uppermost reaches of the cavity and is overlain unconformably by the chocolate brown algal mudstones of the A-1 Carbonate (see back to plate 14). Stylolites are common throughout.

3.4.2.2 Discussion of Surfaces in the Rosedale Bioherm

The irregular surfaces observed in the Rosedale pinnacle have features associated with them suggesting genesis under meteoric conditions. Like the Warwick reef, Rosedale is characterized by cavity and conduit formation in the coral-stromatoporoid facies, and mudstones in the algal-brachiopod facies.

At the base of the Rosedale bioherm, the large conduit filled with anhydrite (surface one) reveals non-luminescent prismatic cements and zoned, brightly luminescent blocky cements. As argued for the Warwick reef cements, non-luminescent cements are interpreted to be of vadose origin while the zoned, brightly luminescent cements are interpreted to have formed in a meteoric phreatic environment. Scalloping and dissolution is evident with this feature and there is lack of symmetry between opposite walls of the cavity.

It may be argued that this feature is characteristic of a neptunian dyke, however, the luminescence revealed by the cements argues against this interpretation. In addition, this cavity is found at the base of the bioherm, a position stratigraphically similar to the lowermost karst surface in the Warwick bioherm.

Similar non-luminescent and brightly luminescent cements are associated with the surfaces at 612.2 m (surface two) and 571.2 m (surface three). Both of these surfaces are interpreted to be karstic in origin, with the cements reflecting origin in the vadose and meteoric phreatic zones. Laminated silt associated with the surface at 612.2 m is concluded to be vadose in origin and the breccia the result of collapse. Saddle dolomites, halite and iron-rich calcite cement are interpreted to have formed during later events.

Irregular surfaces in the algal-brachiopod facies (surfaces four, five and six) are interpreted to be the result of subaerial exposure. In Rosedale, exposure of this facies does not result in the formation of large scale cavities or conduits. Rather, mudstones with clasts, chalky layers and thin well lithified crusts are the norm and each of the three surfaces in the algal-brachiopod facies contain these features. In addition, the mudstones are homogeneous in thin section, consisting of fibrous calcites. Surface four at 556.6 m, reveals contorted, disrupted layers left as swirls infilling topographic irregularities. Intermediate, surface five at 545.6 m, shows eroded allochems. While it may be argued that this is perhaps a storm deposit, the feature lacks any grading. Uppermost, surface six at 540.0 m contains clasts derived from underlying layers.

All of the surfaces in the algal-brachiopod facies reveal macroscopic features similar to modern caliche profiles. As such, these three features are interpreted to represent poorly developed paleosols and caliche horizons resulting from exposure. This supports the findings of Grimes (1988). However, it is important to note that when viewed in thin section, little microfabric is present in each of the features. Consequently, alternative interpretations are possible. The surfaces may represent deposits formed by microbial bacteria as warm, marine waters flooded across an exposure surface (N.P. James, pers. comm., 1990). This however, does not change their overall interpretation as resulting from exposure.

Lastly, surface seven at the top of the bioherm features breccia and collapse fragments, mud infilling solution features, truncated fabrics, and a green clay. This surface is interpreted to

represent the final exposure event that terminated bioherm growth and it correlates with a similar surface found at the top of other pinnacle bioherms.

In all, seven exposure events are interpreted to have occurred in the Rosedale pinnacle. These range from large solution features, to the development of caliche and paleosol profiles. As documented previously, caliche surfaces are indicative of a semi-arid, subaerial environment (Esteban and Klappa, 1983). Caliche was not observed in any facies other than the algal-dominated facies. While karst can form in a variety of settings, the lack of caliche lower down in the reef suggests to an environment that was not semi-arid. Instead perhaps there was an environment more favourable to dissolution and with a greater amount of rainfall. Thus it is possible that as the algal facies of the pinnacle reefs were being deposited, the environment for the Michigan Basin was changing, or had changed, from one with greater amounts of rainfall to one with semi-arid conditions. Alternatively, the caliche may represent the response of the algal-dominated facies to weathering. These rocks, because of their more muddy content, may simply produce a different product when subaerially exposed than do the rocks of the facies dominated by corals, stromatoporoids and skeletal debris.

3.4.3 Karst Surfaces Within the Terminus Pinnacle Reef

3.4.2.1 Surfaces Observed in the Terminus Bioherm

Many irregular and abrupt surfaces were detected in the Ram # 5 and Ram # 3 cores (figure 21, in pocket). However, several additional surfaces that were found in either well could not be correlated between the two. Only surfaces at 585.2 m, 574.2 m and at the top of the reef are seen in both cores. Additionally, three poorly to well lithified mudstone crusts within the algal-brachiopod facies seem to correlate between the cores.

Surface one in the Terminus reef occurs at the base of the bioherm itself (figure 21). In the Ram # 3 core, the surface reveals a small conduit, starting at 587.2 m, cross-cutting a fine-

grained, medium brown mudstone for 0.5 m . Core recovery through this interval is very poor with most of the core broken. However, breccia clasts of the same medium brown mudstone are found to infill the cavity, surrounded by white, very coarse, iron-poor, poikilotopic calcite cement.

In the Ram # 5 core, an irregular surface occurs at 585.2 m. Here, light grey dolomite gradationally changes to a medium brown colour, and then across an undulatory surface, to a light brown coloured limestone (plate 29). Crinoids are present, and stromatoporoids and corals are abundant above the contact, with the limestone becoming buff coloured. When differences in the elevation of the Kelly Bushing are accounted for, this surface is within 0.3 m of being stratigraphically equal to the Ram # 3 surface at 587.2 m described above. Cathodoluminescence of thin sections from just below the surface reveals prismatic, non-luminescent cements followed by zoned, dull-luminescent to brightly luminescent cements (plate 29). Traces of these cements are still in evidence at 600.3 m.

Evidence for surface two is found from 574.9 m to 578.8 m (figure 21). It begins with a light brown, faintly laminated silt which floors cavities. At 578.8 m, a similar silt, but medium brown in colour, overlies an irregular scalloped surface. Relief across the surface is as much as 4.0 cm (plate 30) which is substantial given that the core is only a one-eighth sliver of the original. Porosity in the area is enhanced with vugs and molds averaging 1.0 cm in size. Cathodoluminescence of thin sections from the area revealed only rare instances of non-luminescent cements, mostly prismatic in morphology, and post-dating, more brightly luminescent, blocky cements showed little zonation (plate 31).

Higher in the algal-brachiopod facies, the development of three thin crusts (figure 20) is evidenced in both cores. Crust thicknesses range from 4.5 cm to 5.0 cm. In the Ram # 5 core, each of the crusts has a finely laminated, often poorly lithified mudstone overlain by a well lithified, cream-coloured hardpan-like crust. The Ram # 3 core also shows the crusts to be finely laminated but these mudstones are not capped by cream-coloured crusts. Crusts cross-cut the core at varying angles. In thin section the crusts are composed of fibrous calcite similar to

Plate 29: Exposure surface and meteoric cements, Terminus bioherm

Plate 29A: Interpreted karst surface at the base of the Terminus bioherm. Light grey crinoid dolomite wackestone changes colour to medium brown near the surface. Across the contact there is a change to light brown crinoidal wackestone that becomes buff coloured decimetres above the surface. Irregularities in the surface (e) are infilled with material from above. The backside of the core piece shows the surface to rise up 2 cm to 3 cm in an undulatory manner. Ram # 5, Terminus.

Plate 29B: Thin section photomicrograph using cathodoluminescence with non-luminescent, prismatic calcite cements growing prismatically from dull red luminescent brachiopod fragment. A thin non-luminescent envelope rims selected allochems. Bar scale approximates 1 mm. Ram # 3, Terminus.

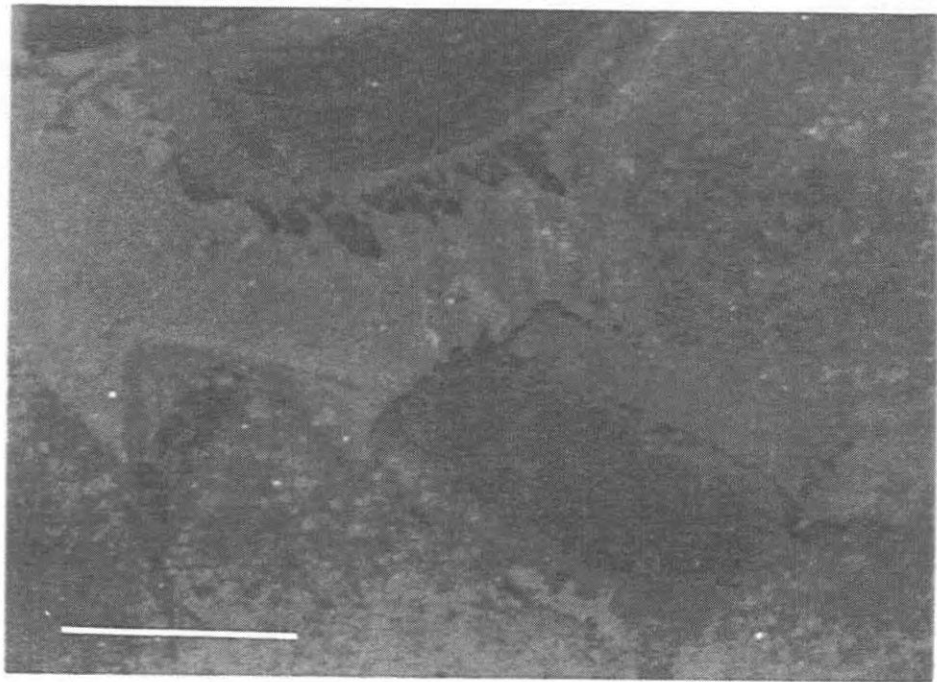
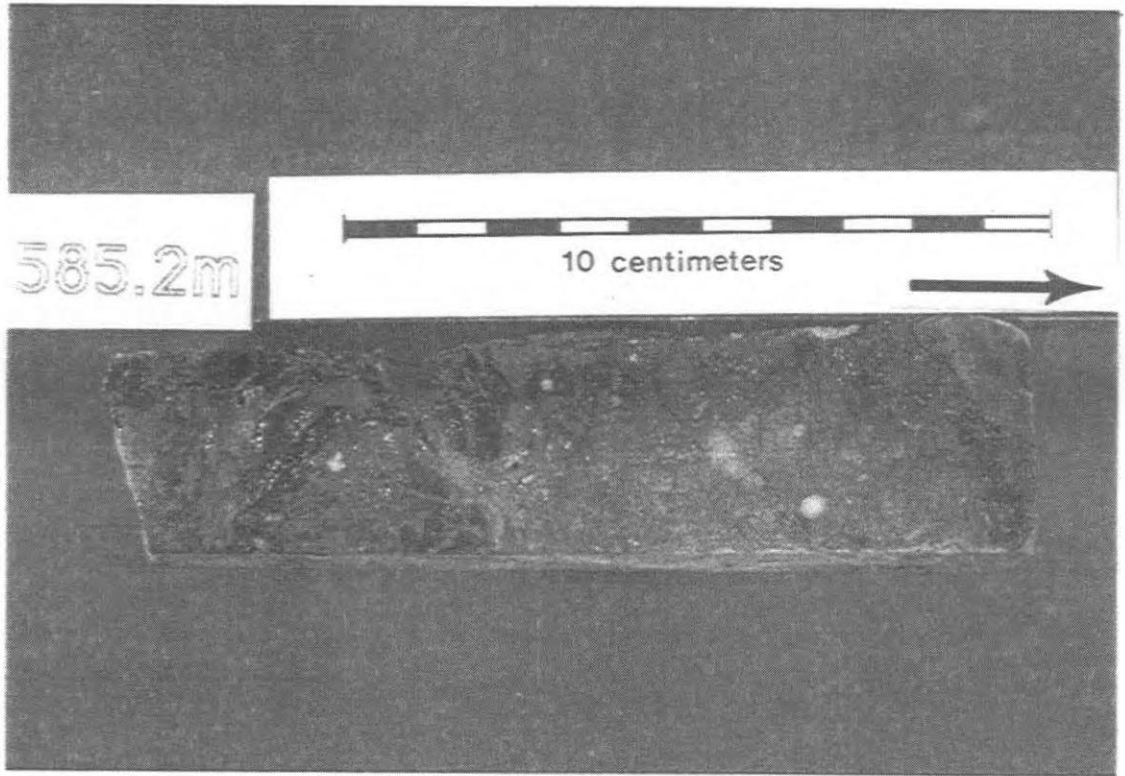


Plate 30 Exposure surface with relief of up to 4 cm separates medium brown mudstone from buff coloured wackestone. Other sides of the core also show the surface to be highly irregular and undulatory. Ram # 5, Terminus.

578.8m

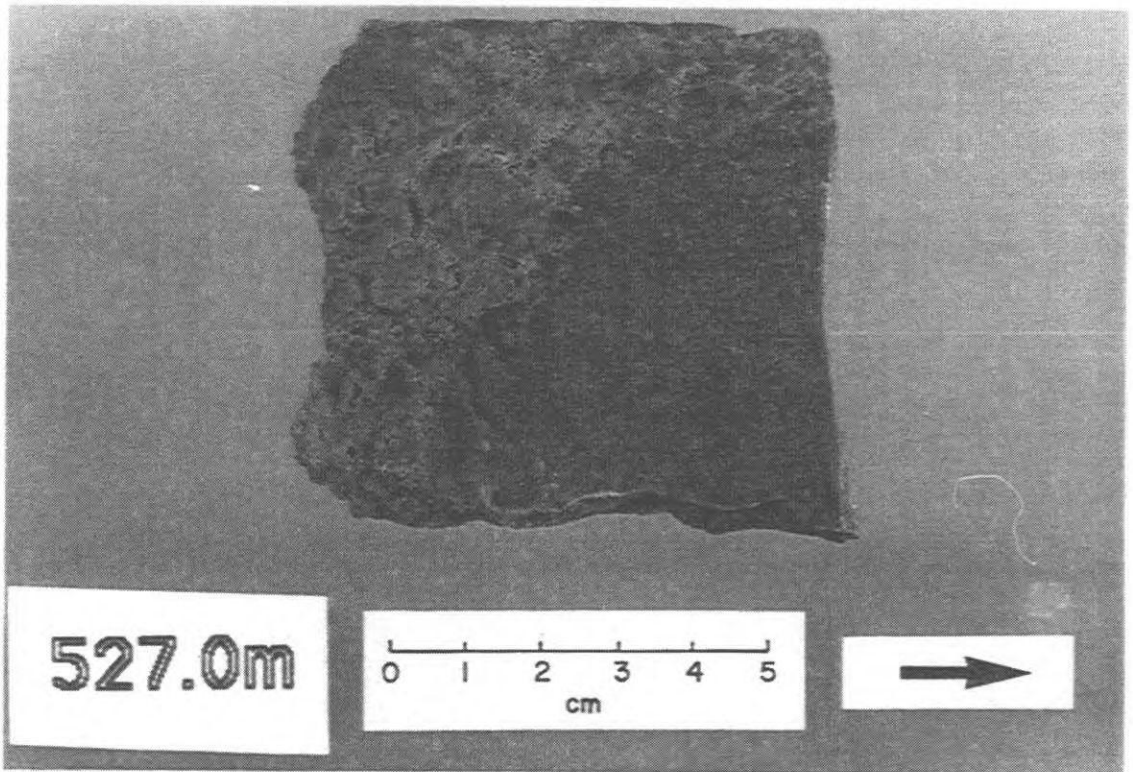
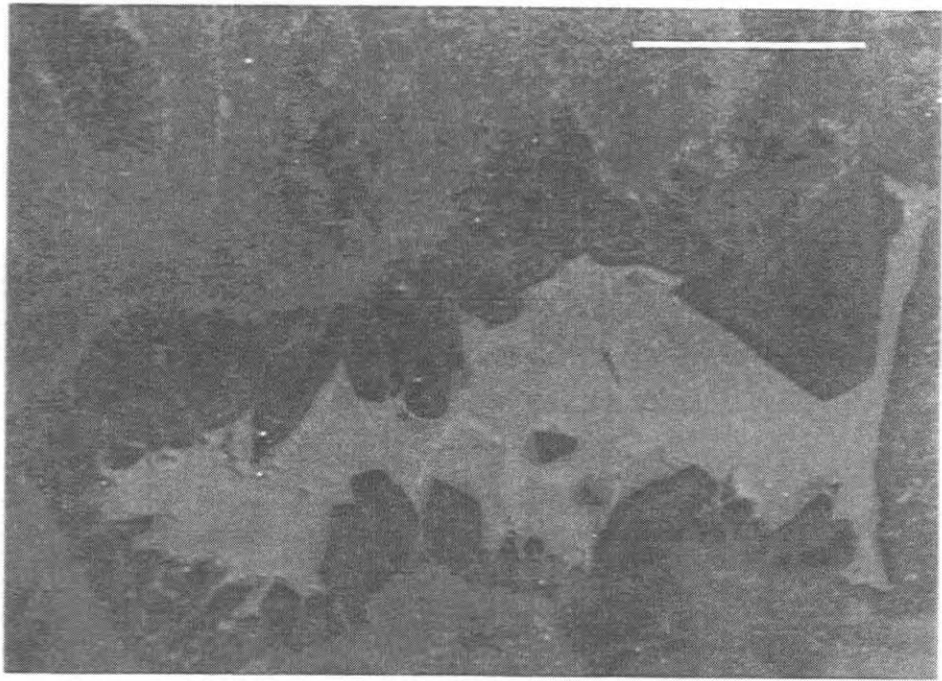
10 centimeters



Plate 31: Meteoric cements and karst, Terminus bioherm

Plate 31A: Thin section photomicrograph using cathodoluminescence showing meteoric cements in pore space. Dull red luminescent favositid coral (L) shows dull luminescent sediment infill of chambers (e). Large pore is lined by dully luminescent zoned to non-luminescent, prismatic calcite cements (R) that are followed by more brightly luminescent blocky cements (E). Pore fill is interpreted to represent cementation from the meteoric phreatic setting. Bar scale approximates 500 μm . Ram #3 Terminus, 579.7m subsea.

Plate 31B: Lower portion of the subaerial exposure surface at the top of the Terminus bioherm. Irregular surface separates medium brown algal-mudstone from light brown, breccia laden dolomite. Clasts average less than 5 mm in size. Ram # 3, Terminus.



that observed in the Rosedale core and interpreted by Grimes (1988) to be caliche. Cathodoluminescence revealed brightly luminescent, blocky cements in pores that did not stain positive for iron.

The final irregular surface (surface three) extends from 518.5 m to 523.9 m in the Ram # 3 core and from 518.5 m to 519.6 m in the Ram #5 core. As with all other pinnacles, a large, well-developed cavity cross cuts the core truncating fabrics (figure 20). Breccia made up of stromatolites, crusts and mudstone fragments, up to 5.0 cm in size, fill the conduit with a dark brown mudstone matrix. Dolomitization of the mudstone is patchy and stylolites skirt around the individual clasts (plate 31). Traces of the green clay, that is associated with this surface in the Warwick and Rosedale bioherms, were observed in the Ram # 5 core but not the Ram # 3 core.

3.4.3.2 Discussion of Surfaces in the Terminus Bioherm

Only those surfaces that correlate between the Ram # 3 and Ram #5 cores, have been cited in this study. Additional, irregular surfaces are present in each core, but these cannot be correlated between wells. There are a number of possible explanations as to why the surfaces cannot be correlated. Different relative positions of the two wells, with Ram # 5 being a crest location and Ram # 3 being a crest-flank location, may account for the discrepancies. But, some surfaces that seem to correlate are off-set by as much as 20 m vertically. This suggests that a fault within the pinnacle may explain the lack of correlation. However, electric logs for the two wells reveal no evidence of a fault and individual formations are of near uniform thickness and signature. Also, a fault through the reef would cause all karst surfaces to be off-set, not just a few. Nevertheless, the surfaces that cannot be correlated probably represent exposure surfaces as well. Correlation of the surfaces is not crucial for in modern situations, surfaces are extremely variable (N.P. James, pers. comm., 1990).

When viewed with cathodoluminescence, surface one at 585.2 m revealed non-luminescent cements followed by brightly luminescent cement. Similar luminescence was observed near the surface at 574.2 m (surface two), but less often. Based on luminescence, these cements are interpreted to have formed in vadose and meteoric phreatic environments using arguments presented in previous sections. The lowermost exposure surface, at the base of the bioherm appears to be contemporaneous with the karst surfaces found at the base of the Warwick and Rosedale reefs.

In the algal-brachiopod facies, the three mudstone crusts represent a more difficult subaerial interpretation. Similar to exposure surfaces in the Warwick and Rosedale pinnacles, cathodoluminescence provides little convincing evidence of meteoric cementation. Some brightly luminescent, blocky cements were noted, possibly of meteoric phreatic origin, but these had little zonation and were not associated with any cements that could be interpreted as vadose. In thin section the crusts are made up of fibrous calcite similar to that found in interpreted caliche horizons in the Rosedale pinnacle (Grimes, 1988; this study). Crust morphology and appearance differ between the two cores and it is uncertain whether or not these deposits represent caliche or paleosol development due to subaerial exposure. It is possible that because of its crest-flank position, formation of any caliche or paleosol profiles in the Ram # 3 core, would appear different to those created in the Ram # 5.

Uppermost in the bioherm, the cavity containing breccia and mudstone is interpreted to be an exposure surface (surface three). This karst event, correlatable with similar event and surfaces in the Rosedale and Warwick bioherms, resulted in termination of the pinnacle and it is overlain unconformably by the A-1 Carbonate.

In all, three karst surfaces can be correlated between the two cores that penetrate the Terminus reef into the Lockport Formation. A number of additional surfaces are found throughout the Ram # 5 core (figure 20) but these surfaces do not correlate with the Ram # 3 core. Three more exposure events may be present, as the thin laminated mudstone crusts found in the algal-brachiopod facies are similar in thin section to caliche surfaces in the Rosedale

bioherm. It is uncertain if cements associated with these crusts formed contemporaneously with the laminated mudstones or result from a later overlying karst event.

3.5 Karst Development in Dolostone Pinnacle Bioherms in the Michigan Basin

Numerous subaerial exposure events have been documented to have occurred during the growth history of the limestone Warwick, Rosedale and Terminus pinnacle bioherms. Three dolostone pinnacles, Bayfield, Wilkesport and Payne are examined to observe and contrast the effects of dolomitization on the exposure surfaces and on meteoric fabrics.

3.5.1 Karst Surfaces Within the Bayfield Pinnacle Bioherm

3.5.1.1 Surfaces Observed in the Bayfield Bioherm

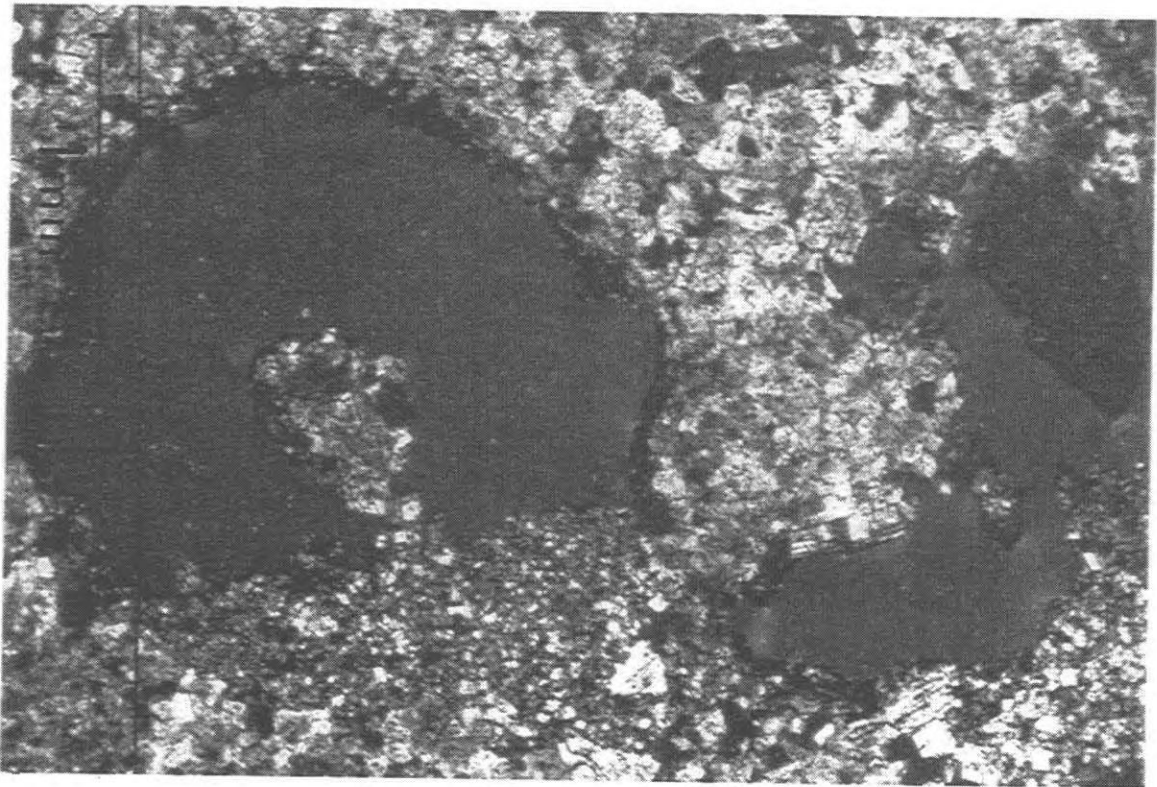
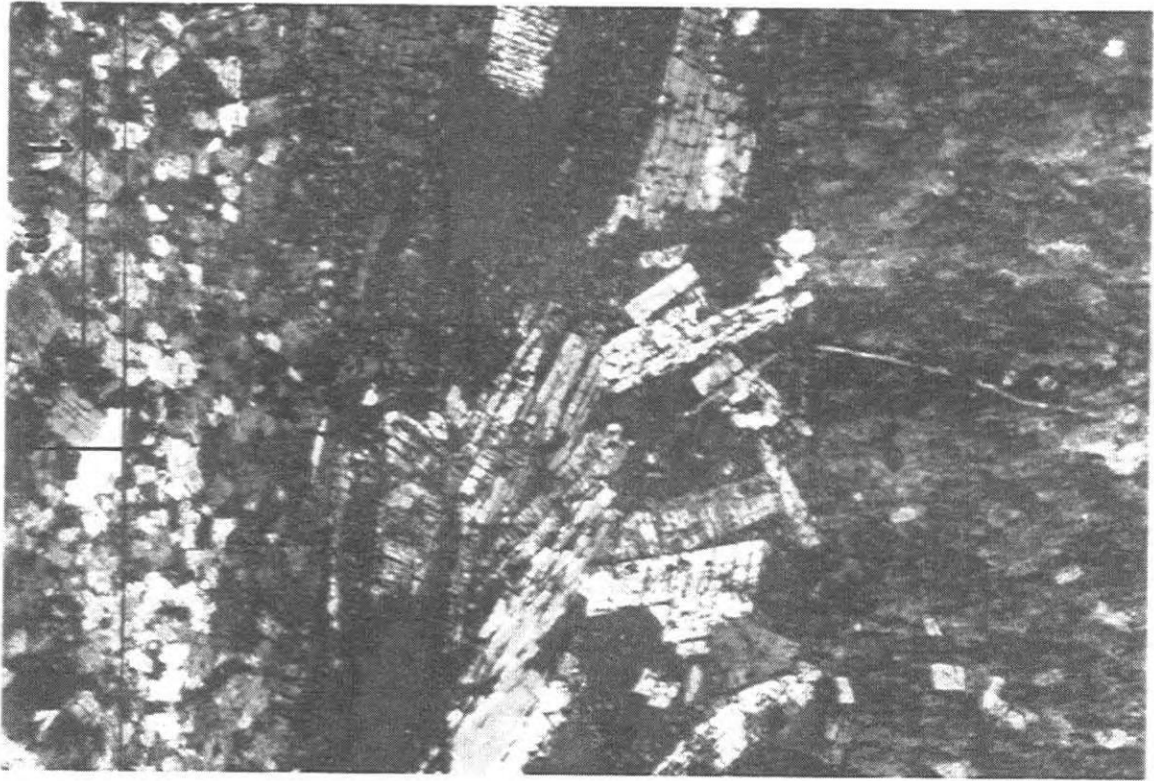
Three irregular surfaces were detected in the short Bayfield reef core with the first at the base of the pinnacle (figure 22, in pocket). A sharp, undulatory surface (surface one) at 586.4m separates light grey, stylolitic, crinoidal dolomite wackestone from an olive-brown skeletal dolomite wackestone. The lower unit initially shows thin, encrusting stromatoporoids and *Halysites* but these are absent as the surface is approached. Solitary rugose corals, *Favosites* and *Coenites* occur a short distance above the surface. This surface lacks the breccia, conduit formation or cockling surface found under the other pinnacles at the same stratigraphic level. It has an irregular abrupt face similar to that observed in the Ram # 5 core but with less relief. Cathodoluminescence revealed only zoned dolomite rhombs.

At 559.9 m (surface two), the Bayfield core is diagonally cross-cut by a 4 cm wide, anhydrite plugged cavity (figure 22) that truncates allochems and fabrics (plate 32). Breccia clasts up to 3.0 cm in size are contained within the anhydrite and the clasts are coated with an

Plate 32: Porosity occlusion and enhancement, Bayfield bioherm

Plate 32B: Thin section photomicrograph in plane light of a narrow fracture filled with anhydrite and associated with interpreted karst surface at 559.9m. Dolomitization is pervasive on one side of the fracture, but appears to be only scattered on the other side. Bayfield Porter # 1, 560.1m subsea.

Plate 32A: Thin section photomicrograph under crossed polars showing moldic and vuggy porosity found near interpreted karst surface. Finely crystalline dolomite at top of the photo may represent one-time geopetal fill in gastropod shell. Bayfield Porter #1, 560.1m subsea.



isopachous dark rind. In places, the cavity walls are also rind coated. Below the surface porosity may be enhanced, due to the removal of allochems and creation of vugs, or relatively tight for short distances (plate 32). Dolomitization is pervasive and cathodoluminescence revealed zoned dolomite crystals.

Surface three in the Bayfield pinnacle is found capping the bioherm at 530.0 m (figure 22). For 3.1 m, the core is cross-cut by a breccia consisting of stromatolite and mudstone clasts. Mud also fills the conduit. Dolomite and stylolites are pervasive and porosity was not observed.

3.5.1.2 Discussion of Surfaces in the Bayfield Bioherm

Fewer irregular surfaces were observed in the dolostone Bayfield pinnacle than in the limestone pinnacles studied. Additionally, cathodoluminescence of the pervasively dolomitized bioherm revealed zoned dolomite rhombs only. Dolomitization appears to have affected any meteoric cements that may have been present, and may act to mask exposure surfaces.

Although, the surface at 586.4 m lacks most of the features found in the limestone pinnacles, such as brecciation or conduit formation, it is irregular and abrupt. Colour changes are noted but most importantly, this surface occurs at a similar stratigraphic position as the lowest karst surface in each of the three limestone bioherms. On this basis, this surface is interpreted to be karstic in origin.

Both the irregular cavity at 559.9 m (surface two) and the conduit found at the top of the reef (surface three) are interpreted to be karstic also. Breccia clasts are contained within the cavities and the feature at 559.9 m has moldic and vuggy porosity associated with it. The uppermost conduit correlates with karst surfaces occurring at the top of each limestone pinnacle. Original rock appears to be from the algal-brachiopod facies and if the stromatolite facies found capping most reefs is present, it is poorly developed, obscured by the effects of dolomitization, or removed by karsting.

3.5.2 Karst Surfaces Within the Wilkesport Pinnacle Bioherm

3.5.2.1 Surfaces Observed in the Wilkesport Bioherm

Similar to the Bayfield pinnacle, the mainly dolostone Wilkesport reef also exhibits three irregular, abrupt surfaces or cavities (figure 23, in pocket). While the upper and lower karst surfaces can be correlated between the two reefs, the middle surface cannot.

At the base of the Wilkesport core, surface one is sharp and undulatory and it separates light grey, crinoidal dolomite wackestone from a buff coloured skeletal wackestone at 634.0 m (figure 23). In addition to the lithologic change from dolomite to limestone and the colour change, minor amounts of pyrite as disseminated grains and small nodules, are found scattered below the contact. Porosity is enhanced in the underlying dolomite wackestone. Cathodoluminescence discloses only zoned anhedral to subhedral dolomite crystals (plate 33).

At 593.4 m the core is cross-cut by a small cavity (surface two) that has scalloped walls and an anhydrite fill. Like a similar feature in the Bayfield bioherm, a thin dark rind locally lines the cavity walls and separates the anhydrite from the original reef rock. Cathodoluminescence of samples taken from positions stratigraphically below the cavity shows non-luminescent cements followed by zoned, brightly luminescent blocky, pore-filling cements. Non-luminescent cements are blocky, or prismatic with zoned tips (plate 33). Staining revealed that iron is not associated with these cements.

The third feature in the Wilkesport reef is situated at the top of the pinnacle (figure 23). From 577.6 m to 583.4 m, surface three is a breccia consisting of stromatolites, crustal fragments and mudstone randomly oriented in a large, conduit (plate 34). Other features include stylolites, salt plugging, and low porosity. Thin sections reveal extensive dolomitization near the surface, but limestone areas exist. Cathodoluminescence reveals zoned dolomite crystals, or

Plate 33: Dolomites and meteoric cements, Wilkesport bioherm

Plate 33A: Thin section photomicrograph using cathodoluminescence showing dull red luminescent, zoned anhedral to subhedral dolomite crystals. Sample taken from below lower karst surface in the Wilkesport bioherm and illustrates the lack of meteoric phenomenon where dolomite is pervasive. Bar scale approximates 500 μm . Imperial Sombra 4-14-XIII, Wilkesport, 637.7m subsea.

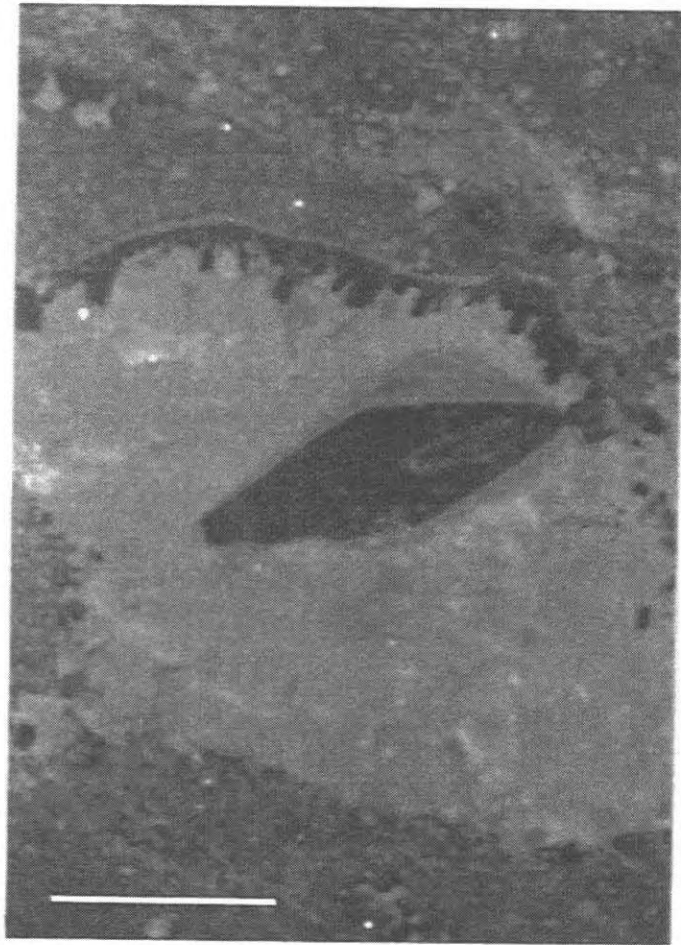
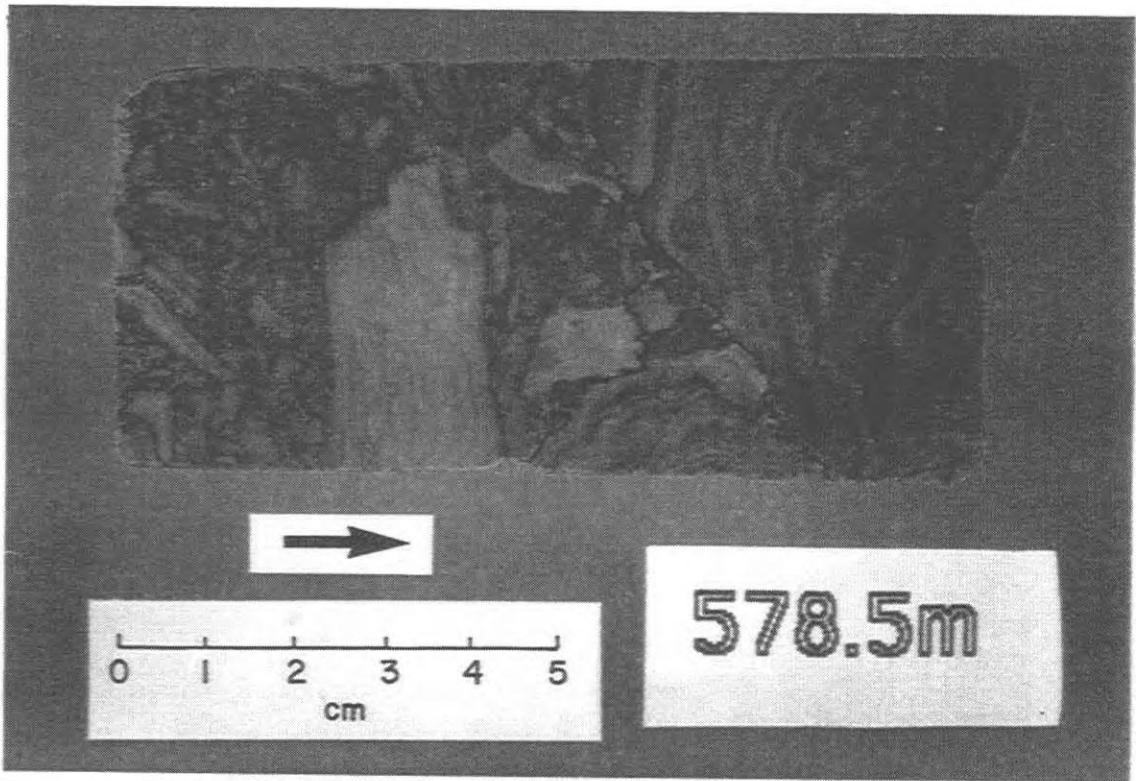
Plate 33B: Thin section photomicrograph using cathodoluminescence of prismatic calcite cements with zoned tips followed by zoned brightly luminescent blocky calcite cements. All cements are interpreted to have formed in the meteoric phreatic zone with zonation reflecting either fluctuating concentrations of Mn^{2+} ions or accelerated crystal growth independent of manganese concentrations. Bar scale approximates 500 μm . Imperial Sombra 4-14-XIII, Wilkesport, 609.3m subsea.



Plate 34: Exposure surface and meteoric cements, Wilkesport bioherm

Plate 34A: Brecciation found at the top of the Wilkesport pinnacle bioherm showing large and small stromatolite and mudstone clasts accompanied by mudstone matrix. Breccia is locally clast supported or matrix supported. Arrow points down in this photo. Imperial Sombra 4-14-XIII, Wilkesport.

Plate 34B: Thin section photomicrograph using cathodoluminescence of non-luminescent prismatic calcite cements growing normal from pore roof. Brightly luminescent blocky calcite cements follow. Sequence is interpreted to represent vadose followed by meteoric phreatic cementation. Bar scale approximates 500 μm . Imperial Sombra 4-14-XIII, Wilkesport, 580.0m subsea.



in limestone areas, non-luminescent cements along pore walls followed by zoned, brightly luminescent pore-filling cements (plate 34).

3.5.2.2 Discussion of Surfaces in the Wilkesport Bioherm

Dolomitization in the Wilkesport bioherm leaves an overprint on potential subaerial exposure surfaces. Where limestone is proximal to interpreted karst surfaces, some non-luminescent and brightly luminescent cements are visible with cathodoluminescence. Areas that have been pervasively dolomitized reveal zoned, dull luminescent crystals. This is consistent with a trend noticed in the Bayfield pinnacle.

At the base of the bioherm, the sharp undulatory surface at 634.0 m is interpreted to be the result of subaerial exposure. It features the afore mentioned changes in colour and lithology as well as pyrite association. Additionally, this surface is stratigraphically correlatable with the karst surface found at the base of each limestone bioherm and the Bayfield pinnacle.

The two remaining surfaces are also interpreted as being karstic in origin. These surfaces feature non-luminescent and luminescent cements concluded to reflect residence in the vadose and meteoric zones respectively, following the reasoning used with the other pinnacles in this study. Brecciation and conduit formation at the top of the bioherm correlates with the upper karst surface in each of the other pinnacles studied.

3.5.3 Karst Surfaces within the Payne Pinnacle Bioherm

3.5.3.1 Surfaces Observed in the Payne Bioherm

Within the Payne pinnacle bioherm, five irregular surfaces have been detected (figure 24, in pocket). As with all other reefs studied, the first surface is encountered at the base of the pinnacle and the final surface is found at the top of the reef.

At 727.6 m an abrupt surface separates underlying light grey, skeletal dolomite wackestone from buff coloured crinoidal dolomite wackestone. Disseminated grains of pyrite and tiny nodules of pyrite occur below the contact. Similar to some the Rosedale and Warwick pinnacles, stromatoporoids occur below the surface. Near the surface, the stromatoporoids are not apparent. A few metres above the feature, corals and stromatoporoids reoccur.

Surface two is found 56.4 m above the base of the pinnacle, at 671.2 m (figure 24). This cavity feature is similar in appearance to the middle exposure event in both the Bayfield and Wilkesport reefs. However, instead of breccia-laden anhydrite filling a small solution cavity in dolomite, in the Payne bioherm, breccia-laden mudstone fills a cavity in limestone. Walls of the cavity are coated in places with a thin crust that has wavy laminations. Small patches of very finely crystalline dolomite are found near the void. Porosity is enhanced and, locally below the feature, the core has a popcorn appearance. This surface also marks the change from the coral-stromatoporoid facies to that of the algal-brachiopod facies.

At surface three, conduit is found from 651.9 m to 653.0 m, comparable to that just described (figure 24). This area lacks only the thin, crustal coatings on the scalloped cavity walls. As with the underlying surface, medium and light brown mudstone breccia clasts and dark brown mudstone fill the void.

From 627.1 m to 629.9 m, blue-green anhydrite containing randomly oriented, rind-coated clasts fills a cavity (surface four). Walls of the cavity are irregular, scalloped and undulatory. From 617.5 m to 619.5 m (surface five), mudstone and stromatolite breccia, and anhydrite clog a conduit. Cavity walls are sharp and truncate stromatolite boundstone laminations.

3.5.3.2 Discussion of Surfaces in the Payne Bioherm

The partially dolomitized Payne bioherm has five features that are interpreted as karstic in origin. At the base of the pinnacle, the surface at 727.6 m, is correlatable with exposure

surfaces in all other pinnacle reefs studied. It is abrupt, irregular and pyritic, and across the surface, there is a colour change.

Lack of available thin sections for the Payne pinnacle makes interpretations of the three irregular surfaces at 671.2 m, 651.9 m and 627.1 m difficult. With a lack of cathodoluminescence and petrographic evidence available, these surfaces are interpreted as karstic based on their physical appearances only. Each shows cavity or conduit development truncating allochems and fabrics, with breccia, and fills of anhydrite or mudstone. Cavity walls are scalloped and, locally, rind-coated.

At the top of the bioherm, the conduit containing breccia and mudstone can be correlated with the exposure episode that appears in each pinnacle of this study. As such it is interpreted as being a karst phenomenon.

3.6 Effects of Dolomitization on Meteoric Surfaces and Fabrics

Dolomitization has resulted in a severe overprint of most meteoric diagenetic fabrics in the pinnacle reefs studied. This is especially evident when comparing the limestone bioherms, (Rosedale, Warwick and Terminus), to the pinnacles that are dolostone (Bayfield) or partially dolomitized (Wilkesport).

It appears that only major erosional surfaces survive the processes of dolomitization well enough to texturally show evidence of karsting. Few of the surfaces detected are sharp and undulatory. Instead most are cavities, filled with anhydrite or mudstone, or have breccia associated with them. In the partially dolomitized Wilkesport build-up, meteoric cements survive, but only in those areas that remain limestone. Dolomitized areas and all areas of the Bayfield reef show zoned dolomite crystals under cathodoluminescence.

This may help explain why previous workers have not identified subaerial exposure surfaces in the pinnacle bioherms they studied.

3.7 Correlation of Karst Surfaces in Guelph Pinnacle Reefs

Correlation and comparison of the karst surfaces identified in the six pinnacles studied is presented in figure 25 (in pocket). Only two subaerial surfaces, the first and the last, can be correlated between all six reefs (figure 25). The first exposure episode occurs at the base of the pinnacles and represents karsting prior to reef initiation. That this surface can be correlated among all six pinnacles suggests that exposure was widespread, with probable regional implications for the Michigan Basin.

The last subaerial incident represents a regional lowering of sea-level that resulted in all of the pinnacles being exposed basin-wide. This event has been recognized by most authors (Table 1) and caused the termination of bioherm growth.

Other exposure surfaces within the pinnacles correlate among two or three reefs, but these surfaces do not correlate among all of the reefs studied. As such, it appears that only certain pinnacles were affected by any one given episode of exposure. This suggests that either the pinnacles were at different stages of bioherm development during the various karst events or an extrinsic factor, such as tectonic movement, influenced their relief from the basin floor.

3.8 Summary

All of the pinnacle reefs studied exhibit multiple surfaces indicative of subaerial exposure. The Bayfield and Wilkesport reefs were karsted three times and the Payne reef possibly five times. Terminus was exposed three times, however possible development of caliche horizons near the top of the reef suggests additional exposure events may have occurred. The Warwick pinnacle shows evidence of five individual karstic events and the Rosedale reef experienced the most subaerial exposure with seven separate occurrences.

Only two of the exposure episodes can be correlated among all six pinnacles studied. The first is found at the base of each pinnacle and records an erosional event prior to reef initiation.

This karst surface may be regional in its extent. The second common exposure feature is a karst breccia and large solution cavity situated at the top of each pinnacle. Bioherm development and growth was terminated at this time.

That the other exposure surfaces cannot be correlated among all pinnacles suggests that exposure did not affect all pinnacles concurrently. This may be due to differential development of the pinnacles themselves or to the influence of an extrinsic factor such as tectonism.

Dolomitization has had a destructive effect on the karst surfaces masking all but the more pronounced erosion surfaces. Additionally, dolomitization appears to obliterate meteoric cements, leaving only zoned dolomite crystals.

CHAPTER FOUR

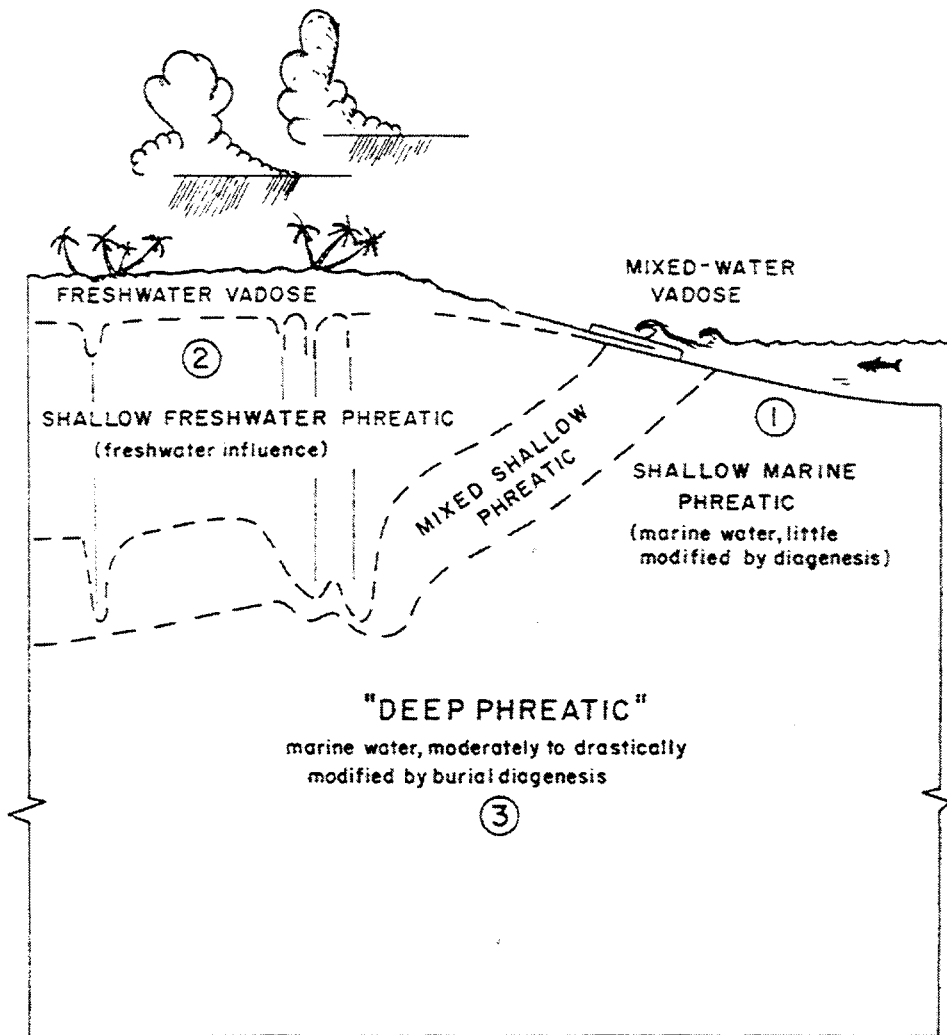
Diagenesis of Guelph Formation Pinnacle Reefs

4.1 Overview

Guelph Formation pinnacle reefs of the Michigan Basin show evidence of diagenesis from three diagenetic settings, the seafloor environment, the meteoric environment and the burial environment. This chapter provides additional data, from petrographic and geochemical sources, to compliment data already introduced, to demonstrate that diagenesis occurred in these three environments. In addition, dolomitization and its effects on the pinnacles is discussed and the results of analyses of carbon and oxygen isotopes analyzed.

The seafloor diagenetic environment (figure 26) is characterized by marine waters that have undergone little modification by diagenesis. This includes areas such as the seafloor, the underlying shallow marine phreatic zone, and areas of marine and fresh water mixing such as beaches (James and Choquette, 1983). Meteoric diagenetic conditions encompass fresh water settings, both in the vadose zone above the water table and the phreatic zone below the water table (figure 26). As well, the mixing zone of shallow phreatic fresh and marine waters is included in the meteoric environment (James and Choquette, 1984). The deep burial environment (figure 26) is described by James and Choquette (1983) as typified by "waters that were once marine, but that have been moderately to drastically modified by burial diagenesis". It is found below the area of near-surface diagenesis but above the field of low grade metamorphism (Choquette and James, 1986).

Figure 26: Sketch showing the three diagenetic environments as discussed in this study. Shallow marine phreatic zone is the seafloor environment, freshwater vadose and shallow freshwater phreatic zones make up the meteoric environment, and deep phreatic is the burial environment. (From James and Choquette, 1983).



4.2 Seafloor Diagenesis in Guelph Formation Pinnacle Bioherms

Seafloor diagenesis in the pinnacle reefs of the Michigan Basin is commonly manifest by syngedimentary cementation. The most pervasive cement type is fibrous, isopachous marine cement, although a botryoidal morphology was observed locally in the Warwick and Rosedale bioherms. These cement morphologies are confined mainly to the skeletal and coral-stromatoporoid facies. More muddy facies are dominated by micritic lime mud.

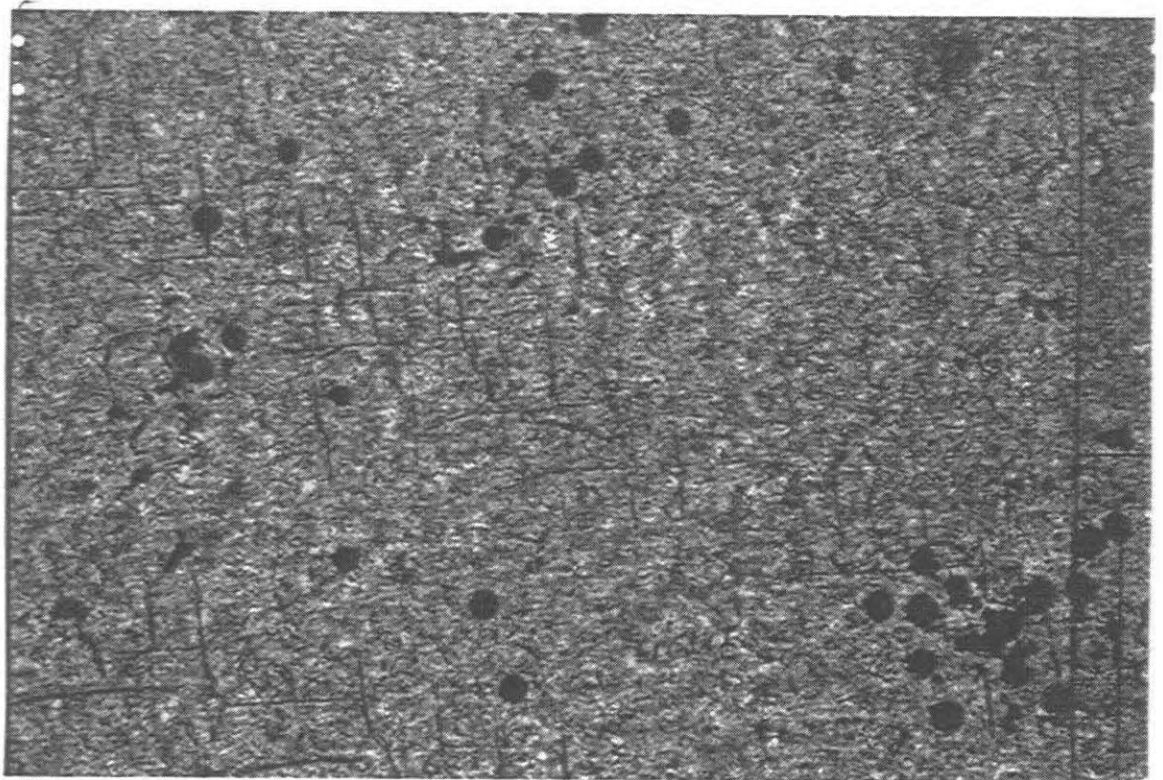
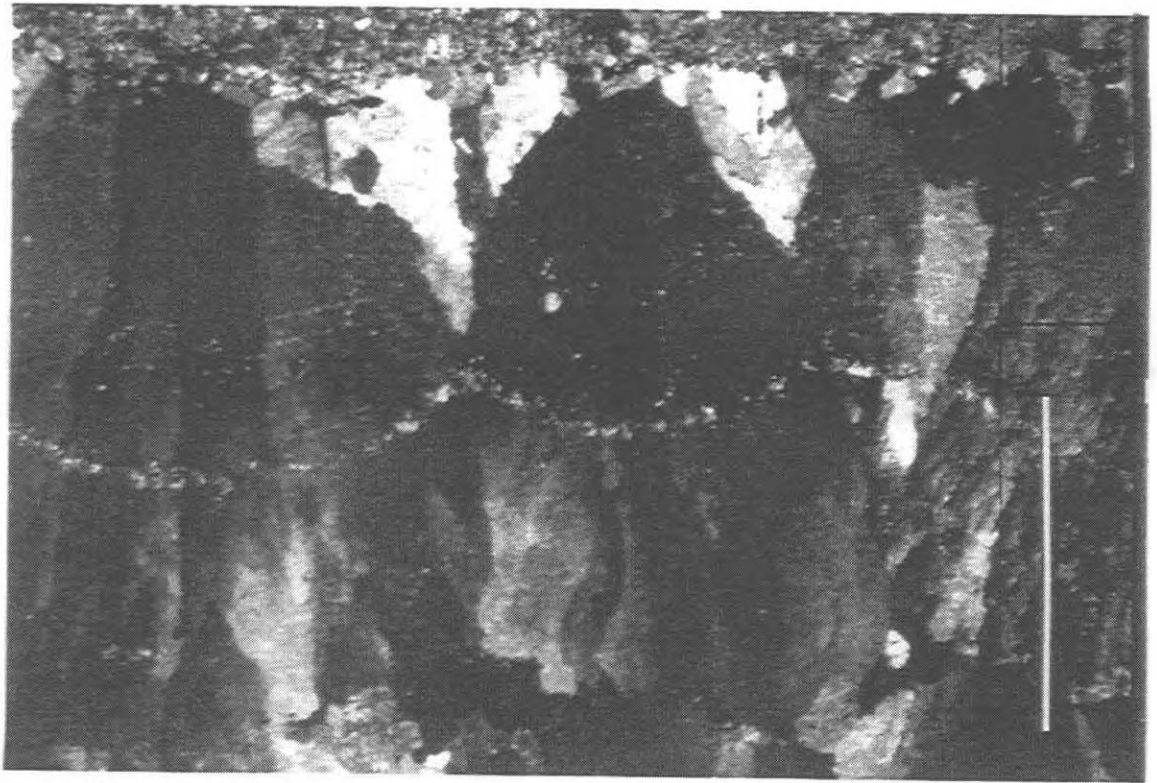
Fibrous cements occur as isopachous, multi-generation fringes that line irregularly shaped pores and fill moldic porosity (plate 35). In thin section, the cements are seen to have grown perpendicular to the substrate surface, in spindly bundles or nested cones and represent the first cementation event found along pore walls or skeletal allochems. Crystals are iron free and vary between inclusion rich and inclusion poor. Where growing crystals contact one another, a distinct well-developed suture line results. The cements often internally fill skeletal allochems in conjunction with geopetal fills but sediment was rarely found inter-layered with the cement. Borings by marine organisms were not observed in the pinnacle reefs, but were noticed in the Rochester Formation (plate 35). Absence of any vadose cement characteristics and the dull to blotchy luminescence of the cements offers further support of a marine origin. Isotope data show slight enrichment of $\delta^{13}\text{C}$, and depletion of $\delta^{18}\text{O}$ (see section 4.6) and are reasonably consistent with data of Wilkinson (1982), Davies (1977) and graphs of James and Choquette (1983) for the Silurian.

Most of the fibrous cements show characteristics similar to "fascicular-optic" cements described by Kendall (1977). These cements are interpreted to be the replacement product of a marine, acicular cement precursor. Blotchy and weak luminescence has been reported for cements interpreted to be neomorphosed Mg-calcites by Lohmann and Meyers (1977) and James and Klappa (1983). Davies (1977) documented that cements of this type are a neomorphic replacement of an original fibrous or acicular Mg-calcite cement. Although a relict acicular microfabric was not observed in the cements of the pinnacle reefs, tiny micro-crystals of

Plate 35: Seafloor diagenesis

Plate 35A: Thin section photomicrograph with crossed polars showing fibrous isopachous marine calcite cements occluding pore space. Cement grows in wedges or bundles. Tiny dolomite crystals appear within cement and mimic the overall fan shape of the cement. Bar scale equals 1mm. Union Rosedale 8-9-II-A, 627.6m subsea.

Plate 35B: Thin section photomicrograph with crossed polars showing crinoid fragment with numerous borings. Pyrite infills the borings. Numbers have been truncated off the bar scale which is 100 μm long. Union Rosedale 8-9-II-A, 663.6m subsea.



dolomite are found within fibrous calcite crystals (plate 36). These have been described by Macqueen and Ghent (1970) and Lohmann and Meyers (1977) as being the result of exsolution of Mg-calcite during early diagenesis. Microprobe analysis of these cements to determine Mg content would be beneficial for comparative purposes. The neomorphic characteristics of the observed cements agrees with precipitation originally as some form of meta-stable carbonate.

In stromatactis cavities, fibrous cement also occurs, however here it may be radial fibrous calcite cement (Bathurst 1959;1975). Cement grows perpendicular to the substrate, consisting of elongated crystals with numerous subcrystals that do not extinguish uniformly and diverge away from the pore wall. It also features convergent optic axes in the overall crystal. Curved twins amid the crystals with concave surfaces facing away from the cavity wall are diagnostic of radial fibrous cements, but these twins were not observed. Rarely, in other pores where suture lines have not formed, an equant cement follows this cements.

Rarely, botryoidal cement was locally found in the Warwick and Rosedale reefs postdating fibrous calcite cement. It consists of small hemispheroids ranging in size from approximately 5 mm to 7 mm. Botryoids grew outward from the underlying fibrous cement layers, often coalesce but never completely fill a given pore. Similar botryoidal calcites were interpreted by Davies (1977), James and Klappa (1983) and Sandberg (1983) as originally aragonite subsequently dissolved and immediately replaced by calcite. The similar morphology and characteristics of these cements to those observed in the pinnacle bioherms suggests that a similar origin is possible. However, Wilkinson (1982) suggests that during the Silurian cements were precipitated as calcite and not aragonite.

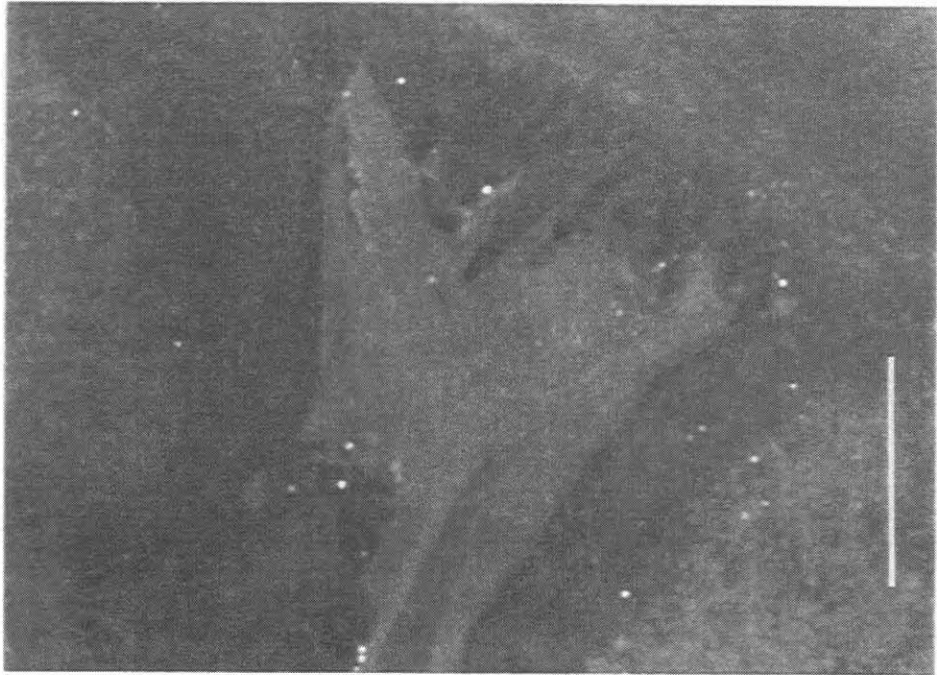
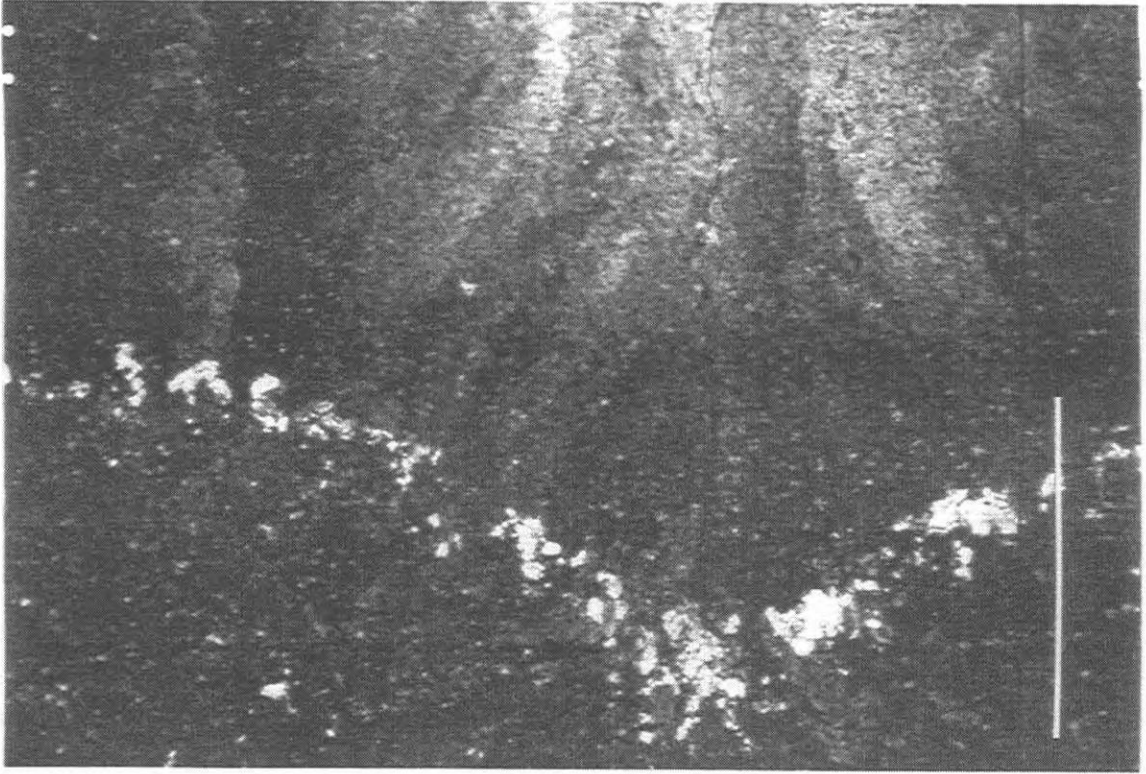
Finally, areas are dominated by lime mud. Tiny rhombs of dolomite, estimated to be less than 20 μm in size, are found scattered randomly throughout. Just as fibrous calcite cements have tiny residual rhombs of dolomite resulting from neomorphism of high Mg-calcite, it is possible that the mud was Mg-calcite originally but has since neomorphosed also.

Overall, marine cement is the dominant cement by volume in most all facies in the bioherm. The amount of marine cement varies but may account for an estimated 90% of the cement in a

Plate 36: Fibrous and prismatic calcite cements

Plate 36A: Thin section photomicrograph with crossed polars of tiny microcrystals of dolomite contained within fibrous marine calcite cement wedges. Well developed suture line can be noticed between wedges. See Plate 35A for larger view. Bar scale equals 250 μm . Union Rosedale 8-9-II-A, 627.6m subsea.

Plate 36B: Thin section photomicrograph using cathodoluminescence and showing vadose and meteoric phreatic cementation. Dark, non-luminescent to dull luminescent prismatic calcite crystals grow normal from brachiopod fragment and are overgrown by more brightly luminescent blocky cement. Bar scale approximates 500 μm . Ram # 3, Terminus, 592.4m subsea.



given part of the reef. Only the karst facies at the top of the reef and individual karst surfaces show dominance by non-marine cements.

4.3 Meteoric Diagenesis in Guelph Formation Pinnacle Reefs

Evidence of diagenesis from both the vadose and phreatic zones attests to the extensive influence of meteoric diagenesis in the pinnacle bioherms. In addition to the neomorphism of cements, the dissolution of allochems and the removal of carbonate, a diverse record of meteoric cement fabrics results. This includes: prismatic calcite cement; equant, blocky calcite cement; and epitaxial overgrowths on crinoids.

Understandably, meteoric cements are closely associated with interpreted karsted areas. Here, significant volumes of fresh water not only seeped and percolated through the exposed reef top, eroding and forming vadose cements, but also temporarily established a water table, below which meteoric phreatic cements precipitated. That meteoric cements are not found pervasively throughout the pinnacle bioherms, suggests that the final karst event that terminated bioherm growth did not karst the pinnacles to their bases, as has been theorized by previous authors (eg. Gill 1977, Cercone and Lohmann, 1986). Had such karsting occurred, meteoric and vadose cements should be evidenced everywhere in the bioherms. The association of meteoric cements near interpreted exposure surfaces only, suggests that exposure episodes were multiple.

Diagenesis in the vadose zone results in many of the numerous erosional features described in Chapter 3. Prismatic calcite cement is also a product of residence within this setting. Individual cement crystals are approximately 200 μm to 300 μm in length and have well chiselled, scalenohedral terminations (plate 36). Commonly these cements grow from skeletal allochems and very often exhibit non-luminescent properties.

Other forms of gravitational cements can also be found within the the pinnacle reefs. Prior to the formation of overgrowths, many crinoid fragments have a tiny zone of pendant, non-

luminescent cement. The thickness of the vadose cement is in the order of 100 μm to 200 μm , but in places it exceeds 300 μm thickness. Meyers and Lohmann (1978) observed a similar cement stratigraphy on crinoid overgrowths and attributed it to evolution in a meteoric phreatic environment. Their cements contained Mn^{2+} and Fe^{2+} .

Staining reveals the overgrowths to be iron-poor. In addition, because the vadose cements have been incorporated into the ensuing epitaxial overgrowth, recognition of individual growth bands is not possible through cathodoluminescence. The use of epifluorescence however allows the bands to be highlighted. Each is thin, an estimated 10 μm to 30 μm in thickness, and semi-concentric (see back to plate 20B).

Cements with a meniscus morphology are also interpreted to have formed. Only one example of this type of cement was observed (plate 37), at 589.0 m in the Warwick reef, an area interpreted to be a beach setting. Inclusion-rich, dull luminescent cement post-dates non-luminescent pendant cements, fills in between crinoid fragments, and results in a rounded pore space. The remainder of the pore is subsequently plugged by a more brightly luminescent, zoned cement thought to be meteoric phreatic in origin. It is possible that the dull luminescence is the result of diagenesis in the strandline setting, where vadose and marine conditions exist, and fresh and marine waters mix. Meniscus, pendant and prismatic cements have been cited by James and Choquette (1984) as excellent criteria for evidence of vadose diagenesis.

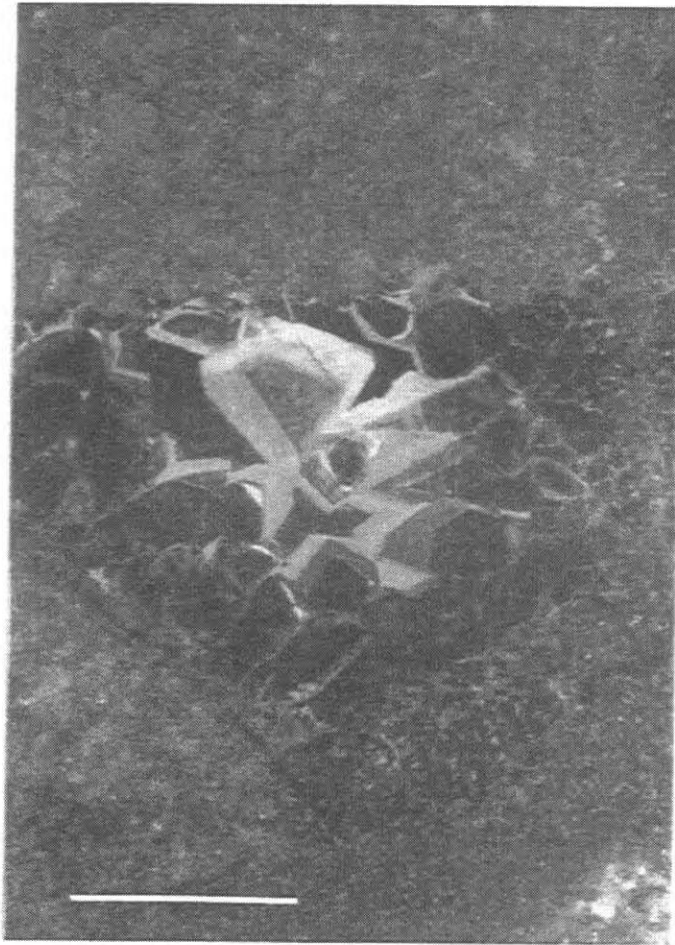
Cements precipitated under meteoric phreatic conditions in the pinnacle reefs are zoned, luminescent, equant, blocky crystals that coarsen toward the pore centre (plate 37). Mainly clear, inclusion-poor and iron-poor, individual crystals may attain sizes of 300 μm . The cements often post-date non-luminescent vadose cements, and plug irregularly shaped pores and pores within skeletal allochems. In places the cements form directly on isopachous fibrous marine cements.

Another form of meteoric phreatic cementation is epitaxial overgrowths on crinoids. These overgrowths are not found ubiquitously on all crinoids but only on those found below and near interpreted karst zones. A single crystal of clear, iron-poor, inclusion-poor calcite often

Plate 37: Vadose and meteoric phreatic cementation

Plate 37A: Thin section photomicrograph using cathodoluminescence showing interpreted meniscus calcite cements. Thin non-luminescent vadose cements are pendant from crinoid fragments (a). Brightly luminescent, inclusion rich cement follows and produces round pore (R). Zoned, brightly luminescent cement completes the occlusion. Sample is from strandline area, and the mixed vadose and marine waters may account for the luminescence observed. Bar scale approximates 500 μm . Imperial # 399, Warwick, 589.0m subsea.

Plate 37B: Thin section photomicrograph using cathodoluminescence of non-luminescent prismatic calcite cements of vadose origin and brightly luminescent blocky cements of meteoric phreatic origin. Cements are in chamber of Rugose coral and dull red luminescent dolomite rhombs are scattered throughout (E). Bar scale approximates 500 μm . Imperial # 399, Warwick, 644.9m subsea.



surrounds the entire crinoid fragment. Under cathodoluminescence, the overgrowths are brightly luminescent, zoned and often preceded by non-luminescent vadose cements. The cements may be then followed by equant, blocky calcite cements also of meteoric phreatic origin.

Another probable effect of meteoric diagenesis is the neomorphism of Mg-calcite allochems and cement to the more stable, low Mg-calcite phase. Cercone (1984) cites the presence of meteoric phreatic water as the cause of neomorphism of Mg-calcite cements in pinnacle reefs of the northern part of the Michigan Basin. James and Klappa (1983) evoke meteoric diagenesis to induce fabric specific dissolution of Mg-calcite cements and allochems. In this study, selected allochems such as cephalopods are made up of tiny, clear calcite crystals. The crystals are dully luminescent with similar characteristics to the neomorphosed fibrous marine cements.

4.4 Burial Diagenesis in Guelph Formation Pinnacle Bioherms

Burial diagenetic features found in the pinnacle reefs studied consist of physical features such as fractures, chemical compaction producing stylolites and an array of pore-occluding minerals including: coarse, euhedral scalenohedral calcite; saddle dolomite; iron-rich, blocky calcite; anhydrite; and halite. The evaporites constitute the overwhelming bulk of the burial minerals.

Stylolites are ubiquitous within the pinnacles and range from single, low-amplitude sutured seams to swarms of wispy stylolites. The single seams preferentially inhabit the cleaner, more skeletal facies while the wispy stylolites prefer more muddy and argillaceous facies. Little residue is associated with the seams and rarely does it exceed 1.0 mm thickness.

In almost all examples, the stylolites skirt around allochems. Calcite cements, dolomite rhombs and other features contained within the reefs are cross-cut. Only two samples showed stylolites cross-cutting allochems. Each stylolite was accompanied by dully luminescent, non-zoned, calcite cement probably derived from the allochem itself (see back to plate 10).

Choquette and James (1986) estimate that stylolites may form after only a few hundred metres of burial and are obvious by 1000 m burial.

Fracturing is not a common occurrence in the pinnacle reefs studied but fractures may be found in all facies types. Where present, fractures cross-cut all depositional fabrics, allochems and cements. Only late, burial cements are excluded and these either plug the fractures, in the case of salt or anhydrite, or grow as crystals, as is observed with saddle dolomite, scalenohedral calcite and iron-rich, blocky calcite cement.

Blocky, iron-rich calcite cement is the first burial cement to form. It consists of clear, coarse crystals, to an estimated maximum of 5.0 mm in size, that are a brilliant turquoise when stained. This cement is restricted to lower areas of the pinnacles, in the coral-stromatoporoid facies and crinoidal-skeletal wackestone facies, and, to the uppermost karsted area where it is found in numerous fractures that exist.

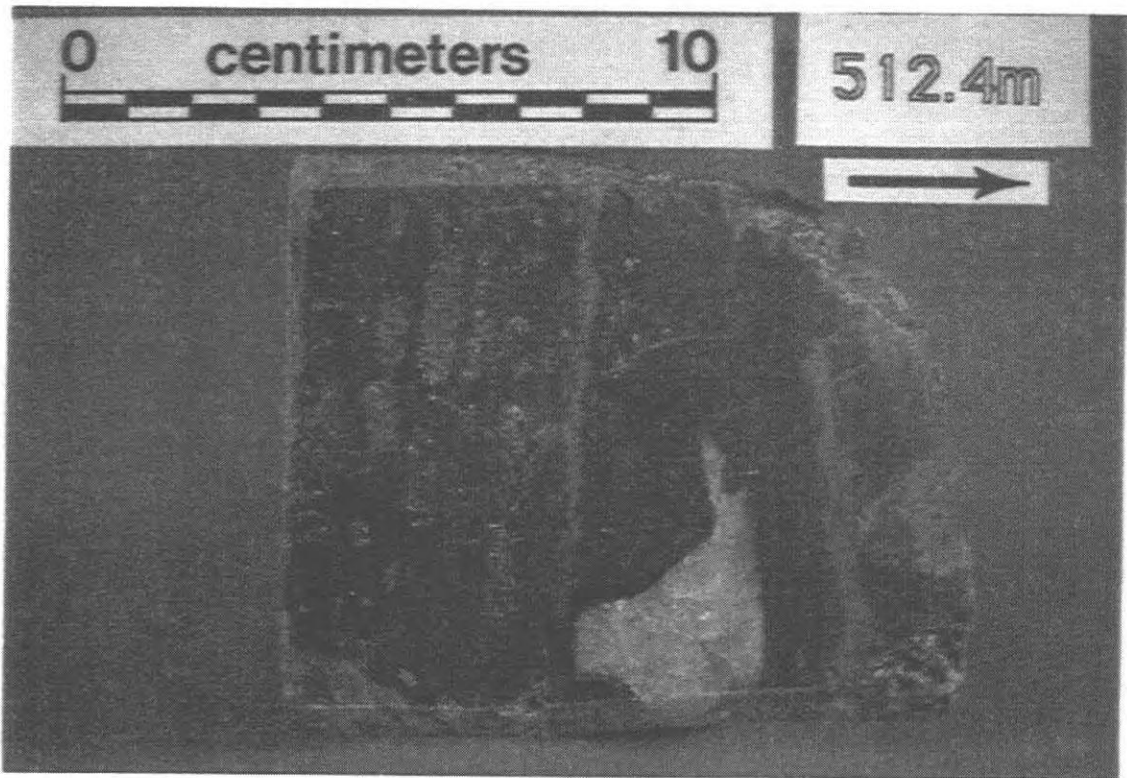
Like the meteoric phreatic cements, the blocky calcite occludes porosity and lines fractures or post-dates marine and meteoric phreatic cements. However, the dull mostly unzoned luminescence, its iron-rich nature, and anomalously depleted values of $\delta^{18}\text{O}$ (see section 4.6) allow it to be distinguished from the meteoric cements.

Euhedral, coarse white saddle dolomite crystals, from 2 mm to 4 mm in size, can be found lining fractures and pores (plate 38). Fracture and pore walls are commonly dark stained beneath the crystals, suggesting alteration by the fluids that emplaced the dolomite. The crystals, with their characteristic curved faces, are noticeably absent from the algal-brachiopod facies but otherwise can be found from the Lockport Formation upwards. Saddle dolomite crystals also show sweeping extinction and depleted $\delta^{18}\text{O}$ values (see section 4.6). Radke and Mathis (1980) gave evidence to imply that the formation of saddle dolomite was a late, burial diagenetic process and intimately associated with sulphate reduction processes. Aulstead and Spencer (1985) and Aulstead *et al.*, (1987) dispute the association of saddle dolomite with reduction processes, based on their data from fluid inclusions. Nevertheless, Radke and Mathis (1980) estimate that saddle dolomite formation occurs at temperatures

Plate 38: Burial diagenetic minerals

Plate 38A: Thin section photomicrograph using cathodoluminescence of large dullly luminescent saddle dolomite crystal (9) with curved face. Bar scale approximates 1mm. Union Rosedale 8-9-II-A, 616.1m subsea.

Plate 38B: Occlusion of pore space by later anhydrite. Note in the lower portion of the pore how needle laths of the anhydrite radiate into the brown mudstone. Union Rosedale 8-9-II-A.



between 60° and 150° C at depths of 1500 m to 4500 m. Burial estimations by Cercione (1984) place Michigan Basin pinnacles within this range.

Post-dating saddle dolomite emplacement, coarse euhedral iron-poor scalenohedral calcite crystals can be detected in all facies that are stratigraphically above the Lockport Formation. The crystals are up to 5.0mm long, have good terminations and most commonly are found in open pore spaces. Locally, growth in fractures was also noticed. Two places in the Rosedale and Terminus bioherms featured very coarse, white, poikilotopic, calcite cement plugging void space. In Rosedale, the cement is pre-dated by saddle dolomite and post-dated by salt. In Terminus it occurs alone, however it has dull luminescence and depleted values of $\delta^{18}\text{O}$ suggesting burial origin.

The final pore-occluding minerals consist of anhydrite and halite (plate 38). Volumetrically, these evaporite minerals make up an estimated 90 % of the burial, diagenetic minerals found in the pinnacle reefs, with halite being the most abundant. In some pinnacles such as Bayfield, this percentage is even higher.

In addition, both the halite and anhydrite may fill pore space following one or two generations of isopachous, fibrous, marine cement. Cercione and Lohmann (1986) have linked the minerals as late burial diagenetic events. It is not necessary to have a precursor cementation event prior to evaporite emplacement. Halite is also found selectively: within the individual corallites of *Favosites* and *Halysites* corals; between the dissepiments of solitary rugose corals; plugging fractures; within breccia; and filling solution created features.

Work by McCollough (1975) demonstrated that halite within the pinnacle reefs has the same bromide concentration as that from the A-1 Evaporite Formation. Additionally, halite within the overlying A-1 Carbonate Formation has bromide concentrations similar to the A-2 Evaporite Formation. Consequently this has led to much speculation on the timing of salt emplacement and suggests that salt emplacement could have occurred during the Late Silurian. However, the initial brine that precipitated the halite should have had a higher bromide concentration (Aulstead and Spencer, 1985) A later dissolution, mobilization and

recrystallization of the halite is possible and this allows for a wide time range concerning emplacement.

4.5 Dolomitization in the Lockport, Guelph and A-1 Carbonate Formations

Dolomitization takes many forms in the rocks included in the study area. While the pinnacle reefs themselves show varying degrees of dolomitization, the Lockport Formation is nearly completely dolomite and the A-1 Carbonate has been pervasively dolomitized.

The Lockport Formation displays two distinct types of dolomites. One consists of anhedral crystals that have selectively replaced the finer grained matrix, but not the allochems. The second dolomite is made up of well-developed euhedral crystals, up to 300 μm in size, that replace to partially replace skeletal allochems and can be fabric-destructive. These crystals show a non-luminescent final growth phase.

Shukla and Friedman (1983) report similar dolomite textures in the Lockport of New York State. They attribute their dolomite formation to: penecontemporaneous replacement of calcite and/or aragonite by clay-sized dolomite in association with evaporite minerals, and possible seawater-fresh water mixing which diagenetically replaced limestone and allochems. These authors report a third dolomite texture that reveals no precursor fabric. In this study, thin sections from the pinnacles show a third dolomite fabric when viewed under epifluorescence (Jeff Dravis, pers. comm., 1989) but this could not be positively identified under plane light.

Qing and Mountjoy, (1989) detail matrix dolomites to occur beneath and within Upper Devonian Keg River, Rainbow pinnacle buildups in Western Canada. These dolomites are thought to be replacive during mechanical compaction through burial. However, the lines of evidence used by Qing and Mountjoy (1989) to support dolomitization through burial, such as dolomite cross-cutting stylolites, were not similarly observed in the Michigan Basin pinnacles. Rather, the stylolites cross-cut the anhedral dolomites and the euhedral dolomite crystals.

Kendall (1989) explained that regional dolomitization of the strata of the Elk Point Basin in Western Canada is known to occur beneath the Prairie Evaporite Formation but not above. This may have resulted from the induced flow of water into and under the basin as created by evaporite deposition and dessicated conditions on the basin floor above. He further used this theory to explain the presence of an anomalous anhydritic shroud that envelops Elk Point Basin pinnacles and that occurs in an area of otherwise halite deposition. The flowing, dolomitizing water under the basin is perceived to have then travelled upward through the pinnacle reefs, which are thought to have created a permeability break in the basin floor. As these waters, rich in calcium from the dolomitization process emerged from the pinnacles, the surrounding water was freshened and anhydrite deposition induced rather than halite adjacent to the reefs. Kendall (1989) suggests that similar mechanisms may have been in place for the Michigan Basin.

However, while this theory, if applied to the Michigan Basin, may shed light on the regional dolomitization of the Lockport, it does not explain: (1) why there is not a complete shroud of anhydrite encasing the Guelph Formation pinnacles; (2) why some pinnacles remain limestone, and yet still have an association with the anhydrites of the A-1 Evaporite; (3) how dolomitizing fluids ascending the pinnacles were able to flow through the impermeable intervals created by subaerial exposure episodes; and, (4) where the volume of water necessary for such massive dolomitization originated.

The origin of the dolomites within the Lockport Formation is problematic. The karst surface, documented by this study to exist at the top of the formation, allows for the possible mixing of seawater and fresh water to create mixing-zone dolomitization. However, is it possible to form regionally extensive dolomites through mixing-zone processes? Also, the dolomites of the Lockport of the Michigan Basin lack the intimate association with evaporites to invoke the method of dolomitization described by Shukla and Friedman (1983). Although burial methods could account for the extensive nature of the dolomites, there is a lack of petrographic evidence to support dolomitization after shallow burial, as described for the

Rainbow buildups by Qing and Mountjoy (1989). Dolomitizing, hypersaline brines from A-1 Evaporite deposition may be one venue. Such a scenario has been documented for platform carbonates of the Miocene in Egypt (Coniglio *et al.*, 1989). In short, the mechanisms for the generation of the dolomites of the Lockport Formation are uncertain.

Within the pinnacle bioherms proper, dolomitization is indicated by: (1) saddle dolomite crystals; (2) randomly scattered, anhedral to euhedral, dolomite rhombs within recrystallized micritic lime mud; (3) crypto-crystalline dolomite associated with karsted areas; and, (4) anhedral to subhedral, replacive dolomite which occurs pervasively or in varying degrees of completion. The origin of the saddle dolomite crystals has already been linked to burial diagenesis in the preceding section.

Tiny, anhedral to euhedral, inclusion-rich dolomite rhombs ranging in size to an estimated maximum of 100 μm and are scattered throughout recrystallized lime mud areas. Just as the fibrous, isopachous marine cements are interpreted to originally have been Mg-calcite, the lime mud is presumed to have originally been Mg-rich micrite. The dolomite crystals are thought to result from the neomorphism of the Mg-rich micrite to a more stable, low-Mg form with the excess Mg forming dolomite crystals. This is similar to the recrystallization of the Mg-calcite, fibrous cements, to low-Mg cements containing micro-crystals of dolomite, that was cited previously.

In the Warwick reef, light grey crypto-crystalline dolomite occurs in small patches in close proximity to interpreted karsted areas. Although noticed by Pearson (1980), the link with subaerial exposure episodes was not made. In thin section the dolomite consists of inclusion-rich, anhedral rhombs that are estimated to be less than 30 μm in size. The spatial relationship of the dolomite with karsted areas and its patchy nature suggests that it is a product of subaerial exposure, possibly resulting from the mixing of meteoric and marine waters.

Dolomite occurs pervasively in the Bayfield and Wilkesport reefs and is known to occur in the majority of Michigan Basin pinnacles. Anhedral to subhedral, fabric-destructive dolomite crystals, up to approximately 100 μm in size, have cloudy centres, post-date marine and

meteoric phenomenon but are in turn post-dated by the effects of burial diagenesis. Fossil allochems that were low-Mg calcite in origin, such as brachiopods, remain largely unaffected by the dolomite. However, those allochems that were originally Mg-calcite, such as crinoids, show varying degrees of dolomite replacement.

Several authors have theorized as to the causes of pervasive dolomitization within Guelph Formation pinnacles. Sears and Lucia (1980) suggested that fresh water and seawater mixed as a meteoric lens lowered through the reefs during the final, major exposure episode. This idea has been supported by other authors (Pearson, 1980; Cercone, 1984).

However, Cercone and Lohmann (1986) point to the arid climate of the area and the small size of the pinnacles to argue against the model. They propose a schizohaline phreatic lens existed only at the base of the pinnacles during A-1 Evaporite deposition. They admit that their isotopic data support the theory of Sears and Lucia (1980) but suggest that recrystallization has resulted in slight $\delta^{13}\text{C}$ enrichment and therefore conclusive interpretations cannot be made from the data.

Jodry (1969) hypothesized that dolomitization resulted from the migration of connate fluids upward through the reef as off-reef strata were compacted. This may be correct for other pinnacles in the basin, however the ones examined in this study reveal that dolomitization seems to pre-date any burial diagenetic phenomenon.

That the dolomite appears to post-date marine and meteoric effects, yet pre-date burial effects, tends to support the findings of Sears and Lucia (1980). But this then raises several questions. Why are some pinnacles dolomitized, others partially dolomitized and still others remain as limestone? Can this be linked to the amount of porosity initially present as the lens was lowered through the reefs? Also, how was the lens able to pass through previously karsted areas where horizontal and vertical permeability and porosity is very low?

Within the A-1 Carbonate dolomite is found as anhedral, interlocked crystals to euhedral rhombs in more porous areas. The brown crystals are highly variable in their size but their origin is from refluxing of brines through the A-1 Carbonate during the deposition of A-2

Evaporites (Sears and Lucia, 1980). This has been confirmed by other authors (Pearson, 1980; Cercone, 1984; Cercone and Lohmann, 1986) who cite their own isotopic work. Why then, if brines moved through the A-1 Carbonate resulting in dolomitization, are some reefs such as Rosedale still limestone? The many questions raised emphasize the need for additional work concerning dolomitization of the pinnacle bioherms.

4.6 Analysis of Stable Isotope Data

A total of 56 samples were submitted for stable ^{13}C and ^{18}O isotope analysis at the Stable Isotope Laboratory, Department of Physics, at the University of Calgary. Of these samples, 41 were calcite and 15 dolomite. Sample number 2 as well as sample numbers 50 to 56 (see appendix) were lost at the laboratory. The results are displayed in figure 27, figure 28 and figure 29. The findings are expressed as a ratio, in parts per thousand, of both the $^{18}\text{O}:^{16}\text{O}$ and $^{13}\text{C}:^{12}\text{C}$ of the sample versus those of the PDB standard, a Cretaceous belemnite from the Carolinian Pee Dee Formation. Therefore:

$$\delta^{13}\text{C} = \frac{^{13}\text{C}:^{12}\text{C}_{\text{sample}} - ^{13}\text{C}:^{12}\text{C}_{\text{standard}}}{^{13}\text{C}:^{12}\text{C}_{\text{standard}}} \times 1000$$

and $\delta^{18}\text{O}$ is similarly expressed (Hudson, 1977).

Stable isotopes may be used to study diagenesis and thus are a valuable tool to compliment standard petrographic, core, cathodoluminescence and epifluorescence analytical techniques. It is thought that, allowing for fractionation, the isotopic values of cements and skeletal allochems reflect the isotopic values of the fluid that precipitated them or the fluids that subsequently modified them (Hudson, 1977). The ^{13}C isotope is influenced not only by the presence of hydrocarbons but more importantly, by the source of bicarbonate, be it from soils or from rock (Bathurst, 1975; Hudson, 1977; Moldovanyi and Lohmann, 1984). Cercone (1984) also states that for Michigan Basin pinnacle reefs, the migration pathway and rate of diagenetic

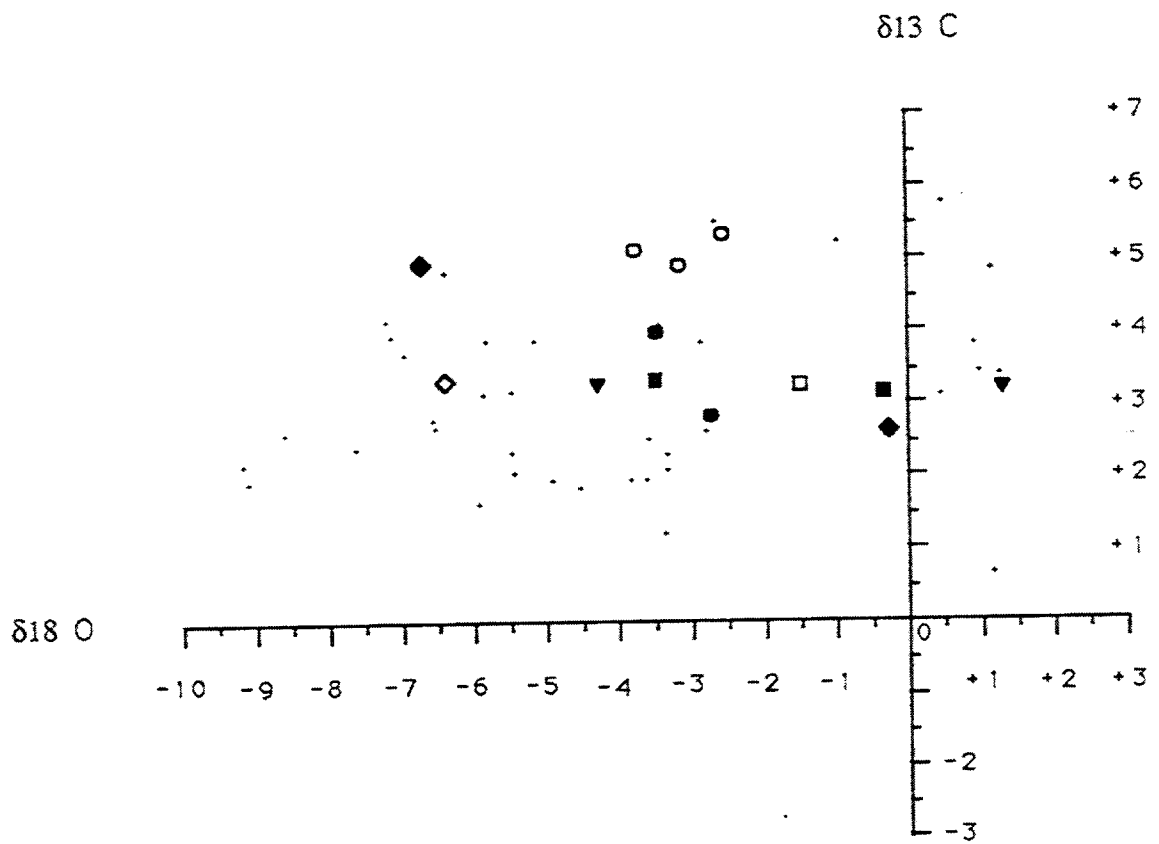
fluid flow exert control on carbon isotopes. The ^{18}O isotope has been shown to be affected by temperature and salinity (Hudson, 1977; Dickson and Coleman, 1980; Given and Lohmann, 1985). Bathurst (1975) notes that some organisms may preferentially enrich one isotope versus another. For the Silurian, the established value for marine precipitated calcite is $\delta^{18}\text{O} = -3$ to -4 (Wilkinson, 1982, Davies, 1977, James and Choquette, 1983).

Eleven different skeletal allochems from differing stratigraphic positions were sampled from the studied reefs and the isotopic results are shown in figure 27 (Appendix B). Additional data points occur as small "+" signs and show the isotopic results from all the other samples from this study. Data with the heaviest isotope values are often regarded as the best approximation of the original isotopic composition (James and Choquette, 1983). Only the calcitic crinoid sample from the Lockport Formation ($\delta^{18}\text{O} = -2.81$, $\delta^{13}\text{C} = 2.67$) is close to those values suggested by James and Choquette (1983) as being good approximates of the original calcite isotope signature for the Silurian. An additional calcitic crinoid sample taken from the Rochester Formation has similar $\delta^{18}\text{O}$ readings as the Lockport crinoid but with enriched $\delta^{13}\text{C}$. This is believed to reflect the influence of the higher organic content of the Rochester Shale.

Three coral samples show $\delta^{13}\text{C}$ values that range from 4.96 to 5.31 and $\delta^{18}\text{O}$ values ranging from -2.55 to -3.70 (figure 27). Each coral sample showed little evidence of cementation or the presence of sediment. Values for $\delta^{18}\text{O}$ that are similar to the Lockport crinoid sample but with slightly enriched $\delta^{13}\text{C}$ values. This suggests that the same diagenetic processes affected all of the corals and the enrichment of heavy carbon may result from neomorphism to low-Mg calcite or possibly from the influences of meteoric phreatic zone water. Hudson (1977) suggests that enrichment of $\delta^{13}\text{C}$ values occurs with depth in the meteoric phreatic zone.

Three other samples plot with $\delta^{13}\text{C}$ values similar to the Lockport crinoid, but with enriched $\delta^{18}\text{O}$. These samples, a brachiopod, a bryozoan and a stromatoporoid, were taken from areas interpreted to have been subaerially exposed and are closely associated with dolomites. The stromatoporoid is from the Lockport Formation and the bryozoan from close to the Lockport-Guelph contact. Land (1980) suggests that $\delta^{18}\text{O}$ dolomite is enriched relative to

Figure 27: $\delta^{13}\text{C}$ and $\delta^{18}\text{O}$ isotope values for skeletal samples from the six pinnacle reefs studied. Results are expressed in percent relative to the PDB standard. Small "+" signs show locations of other isotope samples from this study.



| | |
|-------------------|---|
| CORALS | ○ |
| CRINOIDS | ● |
| BRACHIOPODS | □ |
| BRYOZOANS | ■ |
| STROMATOPOROIDS | ◆ |
| ALGAE | ◇ |
| LOCKPORT DOLOMITE | ▼ |

$\delta^{18}\text{O}_{\text{calcite}}$ by an average of 3 ± 1 ‰. He notes however that others have cited values of 1 ‰ to 7 ‰. Both stromatoporoid and bryozoans have porous skeletons and the brachiopod contained dolomitic silt in its shell. Therefore, the enriched $\delta^{18}\text{O}$ values are interpreted to reflect the presence and $\delta^{18}\text{O}$ values of the dolomite.

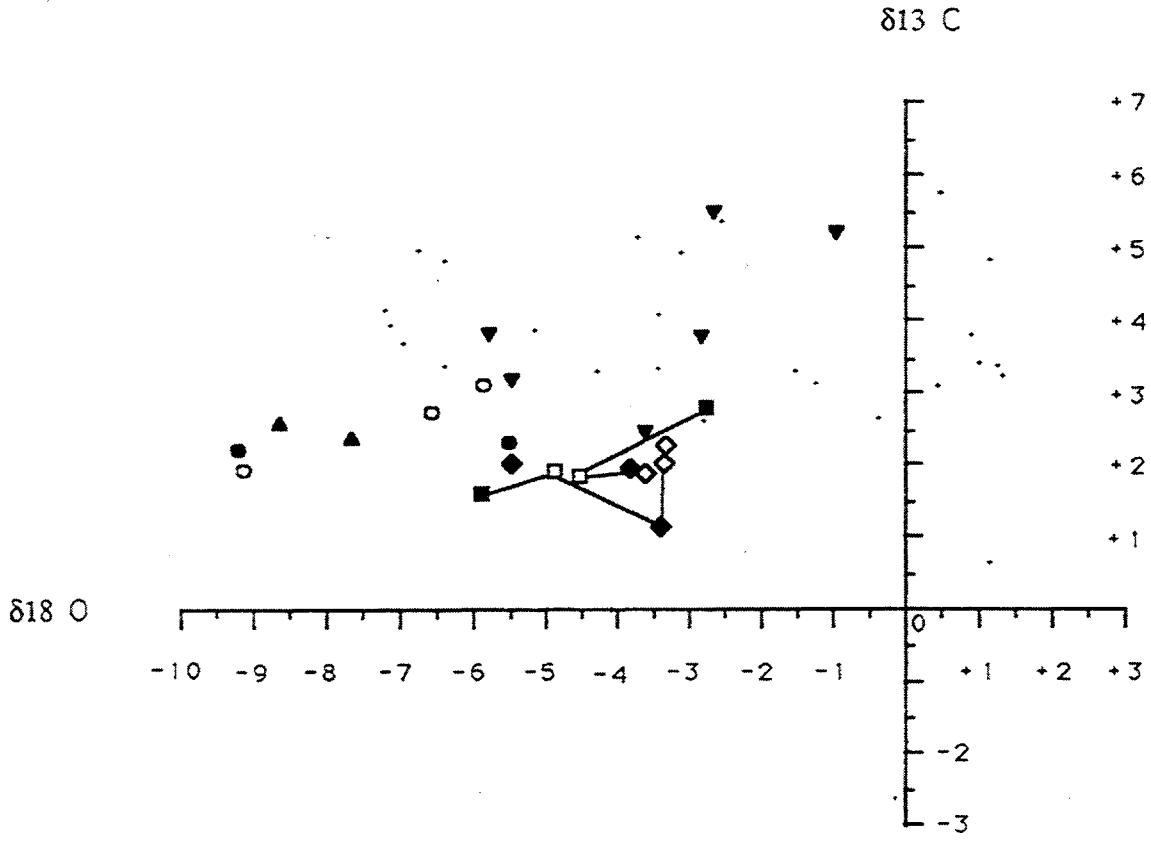
Lastly, two data points from a stromatoporoid and an algae show anomalously depleted $\delta^{18}\text{O}$. Both of these samples were taken from areas of the bioherms dominated by algae, but proximal to subaerial exposure surfaces. When data points from sampled algal crusts from exposure zones are examined (figure 29), these points also plot in the vicinity of the stromatoporoid and the algae. It is perceived that the depletion in $\delta^{18}\text{O}$ reflects association with exposure (Hudson, 1977).

Also included in figure 27 are two data points showing the isotopic values of dolomites from the Lockport Formation. One of these points plots in the vicinity of the values obtained for the Lockport crinoid despite being dolomite. The other shows a similar $\delta^{13}\text{C}$ value, but the $\delta^{18}\text{O}$ value is substantially enriched. This can be interpreted several ways. The high $\delta^{18}\text{O}$ reading is interpreted to reflect an enrichment in $\delta^{18}\text{O}$ due to dolomitization (Land, 1980). It may reflect hypersaline brines from the A-1 Evaporite that may have contributed to dolomitization (Shukla and Friedman, 1983). Such conclusions however, should not be based on one datum point.

Interpreted marine, meteoric and burial cements were sampled from all six reefs and the isotopic values are displayed in figure 28 (Appendix B). As with the preceding figure, the other sample data points are displayed as small "+" signs.

Fibrous marine cements were sampled primarily from the Warwick reef due to the availability of numerous multi-generation pore-filling cements. Two four-phase cement fills were analyzed. The cements, in general, are slightly depleted in both $\delta^{13}\text{C}$ and $\delta^{18}\text{O}$ readings, a trend noticed by Grimes (1988). Each sample from successive phases shows a progressive depletion of the $\delta^{18}\text{O}$ values. This is thought to represent the neomorphism of the cements to low-Mg calcite under the influence of meteoric waters and/or the precipitation of the cements to

Figure 28: $\delta^{13}\text{C}$ and $\delta^{18}\text{O}$ isotope values for cement samples from the six pinnacle reefs studied. Results are expressed in percent relative to the PDB standard. Lines connect successive zones of four zone pore filling cement (two sampled). Small "+" signs show locations of other isotope samples from this study.



| | |
|----------------------------------|---|
| ISOPACHOUS PORE FILLING CEMENT | |
| FIRST PHASE | ◇ |
| SECOND PHASE | ◆ |
| THIRD PHASE | □ |
| FOURTH PHASE | ■ |
| SADDLE DOLOMITE | ○ |
| DOG-TOOTH CALCITE | ● |
| IRON-RICH, CLEAR, BLOCKY CALCITE | ▲ |
| COARSE, WHITE, BLOCKY CALCITE | ▼ |

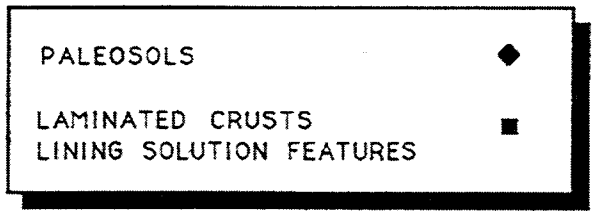
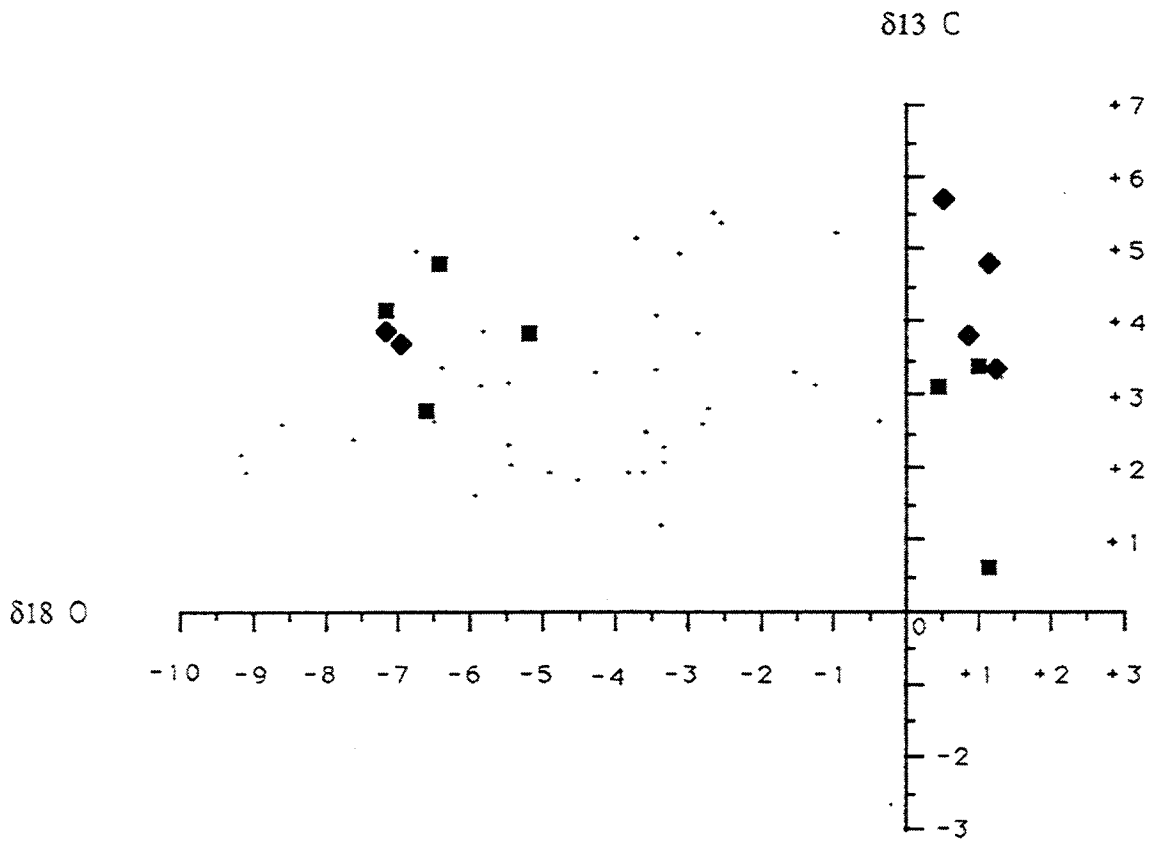
an increasingly closed, local fluid system. The range of the isotopic values is from 1.19 to 2.89 for $\delta^{13}\text{C}$ for and -2.74 to -5.90 for $\delta^{18}\text{O}$. These values are similar to those reported by Cercone (1984) for marine cements from Michigan Basin pinnacle reefs but with slightly enriched $\delta^{18}\text{O}$. It should be noted that one of the cements sampled produced a datum point that is anomalous when compared to the other marine cements. This sample, although calcite, did not effectively evolve in phosphoric acid over a period of three days prior to analysis. The resulting carbon and oxygen values are likely erroneous.

The other isotopes sampled are from: saddle dolomite; iron-rich, pore-filling calcite; coarse, euhedral, scalenohedral calcite; and coarse, white, pore-filling calcite sources. The saddle dolomite crystals sampled were single, euhedral crystals. Results from the iron-rich calcites, saddle dolomites and dog-tooth calcites show depletion of ^{18}O (figure 28). Values for $\delta^{18}\text{O}$ range from -5.86 to -9.19. This depletion is interpreted to represent the increase in temperature brought on by burial conditions. Of note is that the saddle dolomite samples and scalenohedral calcite samples seem to co-mingle yet form two distinct fields (figure 28). This suggests that the two fields may have formed under two different temperature regimes or by two different fluids. Analysis of additional samples is necessary to provide additional data points to illustrate this further.

The last cements to be analyzed are from interpreted meteoric phreatic sources. These cements define a large, broad field with $\delta^{13}\text{C}$ values ranging from 5.47 to 2.55 and $\delta^{18}\text{O}$ values ranging from -0.97 to -3.58 (figure 28). There is no apparent link to these data points, however the samples were taken from the immediate vicinity of an interpreted karst area and at different stratigraphic levels. It has been shown that most of the subaerial exposure surfaces cannot be stratigraphically correlated. Therefore, it is thought that the meteoric waters associated with these events are slightly different with respect to one another and react with the host carbonate differently. As such, the isotopic values are also different.

The last group of data is depicted in figure 29. These points represent the carbon and oxygen values of interpreted paleosols and caliche horizons, and laminated crusts taken from solution

Figure 29: $\delta^{13}\text{C}$ and $\delta^{18}\text{O}$ isotope values for paleosol and laminated crust samples from the six pinnacle reefs studied. Results are expressed in percent relative to the PDB standard. Small "+" signs show locations of other isotope samples from this study. Data on the left side of the graph represents isotopic values from limestone samples. Data on the right is from dolomite samples.



features (Appendix B). Noticeable is the enriched ^{18}O values affiliated with the dolomite samples taken from paleosols and caliche horizons and the variable $\delta^{13}\text{C}$ signatures. The oxygen variation is interpreted to reflect the enrichment of ^{18}O through dolomitization. This is further suggested when comparing the dolomite values with those of two calcite paleosols from the Rosedale reef. These samples show depleted ^{18}O values. The variations in $\delta^{13}\text{C}$ values are believed to depict the influence of the host carbonate rock with meteoric water of varying composition, or presence or lack of organic matter within the paleosol.

The other group of data points represents values from rinds and laminated crusts lining the walls of solution features. These points define a field (figure 29) with $\delta^{13}\text{C}$ ranging from 2.77 to 4.79 and $\delta^{18}\text{O}$ ranging from -5.18 to -7.21. These values are interpreted to reflect the depletion of ^{18}O associated with subaerial exposure.

In analyzing the isotopic compositions of meteoric cements and paleosols, few of the data follow established trends for meteorically influenced isotopes. These trends imply that, for the Late Paleozoic through to the present, $\delta^{13}\text{C}$ values should show depletion in the face of meteoric diagenesis (James and Choquette, 1984). It is thought that in the Silurian, the lack of development of organic plant life to provide isotopically light ^{13}C is responsible for the lack of agreement. Also, carbon isotope values may reflect influence by the carbonate (of marine origin) through which the meteoric water is flowing .

Cercione (1984) analyzed isotopes from a number of pinnacle reefs in the northern part of the Michigan Basin. Although her isotopic values varied between the different reefs, Cercione (1984) identified four groups with isotopic distribution. The isotopic values from this study in terms of allochems, cements and paleosols approximate the results of previous workers and do not fit the groupings of Cercione (1984). It has been shown that each of the pinnacles studied experienced a different combination of subaerial exposure events. Consequently, each pinnacle has a slightly different growth history, and because of differing amounts of meteoric diagenesis, different diagenetic histories. This, together with the variable isotopic results of

Cercone (1984), may suggest that the isotopic results obtained for a given reef may be somewhat unique to that reef and different from neighbouring reefs.

4.7 Relative Timing of Diagenetic Events

Each of the pinnacle reefs studied has evidence of multiple subaerial exposure surfaces and evidence of extensive meteoric diagenesis. Because exposure surfaces cannot be correlated among reefs, each reef has presumably experienced different karstic events. As such, the amount of meteoric diagenesis experienced by each reef is variable and therefore, the diagenetic history for each reef is different. Nevertheless, an overall, gross diagenetic sequence can be presented based upon all accumulated data from this study (figure 30, in pocket).

Since seafloor and meteoric diagenesis alternated during the growth of the pinnacle reefs, the various diagenetic sequences contained in each realm occur several times. Within the seafloor diagenetic environment, bioherm growth was an active process from the time of reef initiation to the final, growth-terminating karst event. It was however, interrupted several times by episodes of subaerial exposure. Synsedimentary cementation occurred with fibrous, Mg-calcite cements precipitated in the skeletal wackestone facies and the coral-stromatoporoid facies. In the algal-dominated facies, precipitation of high-Mg micrite was pervasive with minor amounts of fibrous calcite.

Superimposed throughout are the effects of meteoric diagenesis. Exposure resulted in karsting of the reef with paleosols and caliche restricted to the algal facies. Besides dissolution and the creation of porosity, vadose cements were precipitated. Exposure also allowed the creation of a fresh water phreatic zone. Within this zone epitaxial overgrowths developed on crinoids and coarse, equant, blocky cement occluded porosity. The meteoric phreatic zone is believed to be responsible for the neomorphism of Mg-calcite to calcite and possible dolomitization within the mixing zone. Subsequent transgression over the karst surface

resulted in renewed bioherm growth and additional seafloor diagenesis. Consequently, the entire bioherm is a series of stacked bioherm packages (Smith, 1984).

Following the subaerial exposure event that induced the termination of bioherm growth, burial of the reefs caused fracturing, compaction and staining by warm fluids. The growth of saddle dolomite crystals, scalenohedral calcite and blocky, iron-rich calcite followed, all within a regime of elevated temperature. Stylolites formed, cross-cutting most fabrics. Finally, first anhydrite and then halite were precipitated. The exact time of hydrocarbon migration into the pinnacles is unknown; however, Gill (1979) points out that several source rocks exist, including the A-1 Carbonate, inter-reef facies, and formations found below the Lockport Formation.

4.8 Summary

The six pinnacle reefs studied all exhibit evidence of diagenesis from the three diagenetic environments. Seafloor diagenesis takes the form of syndepositional cementation. Fibrous, isopachous calcite cement is prevalent in the skeletal wackestone and coral-stromatoporoid facies while micritic lime mud is found in more muddy and argillaceous areas.

Diagenesis in the meteoric realm features numerous karst surfaces and the formation of paleosols and caliche horizons. Cementation in the vadose zone includes pendant, prismatic and meniscus cements. The meteoric phreatic zone features crinoid overgrowths and blocky, equant pore-filling calcite. Because subaerial exposure occurred several times during reef growth and affected each pinnacle differently, each bioherm has a different growth history and different diagenetic history. Effects of meteoric diagenesis are superimposed upon those of the seafloor creating a series of stacked bioherm packages. Meteoric diagenesis is also believed to be responsible for the neomorphism of Mg-calcite and possible dolomitization in the mixing zone.

Burial of the pinnacles resulted in fracturing, and the growth of saddle dolomite, scalenohedral calcite and iron-rich calcite. Stylolitization and the emplacement of anhydrite and halite complete the burial diagenetic features observed.

A number of different replacive dolomite textures were found in the pinnacles as well as in the formations above and below. Some of the dolomite can probably be linked to an origin in the mixing zone, but most is of uncertain origin.

CHAPTER FIVE

Pinnacle Growth and Genesis

5.1 Overview

This chapter focuses on the growth history of Guelph pinnacle reefs in the Michigan Basin and the deposition of associated formations. It proposes that the vertical succession of facies that occur in the reefs reflects the response of the reef to the surrounding physical and chemical environment. In addition, several karst events are incorporated into the growth phases of the pinnacles. The possible cause of the cyclic deposition of the evaporites and carbonates of the Salina Group are briefly examined.

Theories by Sanford *et al.*, (1985) concerning pinnacle reef growth on tilted fault blocks are highlighted and then critically assessed using information obtained through this study. This results in a better understanding of the influence of small fault blocks on pinnacle development.

5.2 The Theory of Fault Control on Pinnacle Genesis

Mantek (1976) described the presence of numerous faults in the Michigan Basin and their potential for influencing reef genesis. This idea was refined considerably by Sanford *et al.*, (1985). These authors determined that cratonic basin inception and development was controlled by plate motion and related orogenic activity. Two main cycles of tectonic adjustment were identified including one, spanning from the late Precambrian to the late Paleozoic. This resulted in cratonic uplift along the axes of arches that criss-cross the continent in northeasterly and northwesterly directions (Sanford *et al.*, 1985). Cratonic basins, bounded by these axes formed as a result.

Sanford *et al.* , (1985) identified a very simple set of single, east-west trending fractures in the Bruce megablock compared to a more complex pattern in the Niagara megablock (figure 31). These two megablocks underlie all of southwestern Ontario and are thought to have moved independently of one another throughout the Paleozoic (Sanford *et al.* , 1985). They suggest that major fracture rejuvenation in the Bruce megablock in Ontario occurred in the late Middle Silurian to early Upper Silurian. They propose that pinnacles in the Michigan Basin "favoured fault line scarps and thus formed along the structurally higher segments of west and northwest trending tilted blocks" (Sanford *et al.* , 1985, p. 65). In addition, they indicate that these long linear fault scarps formed on the sea floor at the beginning of Guelph deposition and were prominent enough to locally control facies, initiation and depositional trends of biohermal growth (figure 31). Of note however, is that faulting had no apparent effect on the basinwide distribution of reef belts.


5.3 Stages of Reef Growth

From the facies identified within the Guelph Formation, five stages of reef growth can be interpreted which reflect environmental conditions and depositional processes. The first four stages reflect development of the reef and of the pinnacle morphology, and the final one was an erosional event that terminates bioherm growth. Because each pinnacle was subjected to different subaerial exposure events, the growth history of each individual pinnacle was different. A generalization reef growth history is presented here.


Development of an environment suitable for pinnacle reef growth began to take shape with deposition of the Lockport carbonates after deposition of the Rochester Shale. Brett (1983) interprets the Rochester Formation in western New York State to represent deposition on a sloping, muddy shelf in approximately 50 m of water. Periodic storms resulted in lag deposits of shelly allochems and suspension clouds depositing finer material.


Figure 31: Diagram showing the simple fracture pattern existing in the Bruce Megablock near Lake Huron and a more complicated pattern existing in the Niagara Megablock near Lake Erie. Growth of pinnacle and patch reefs on the elevated, tilted edges of the fault blocks is shown (From Sanford *et al.* 1985).

BARRIER REEF FACIES

 GREY & TAN DOLOSTONE
(80-100 METRES)

INTER-REEF FACIES

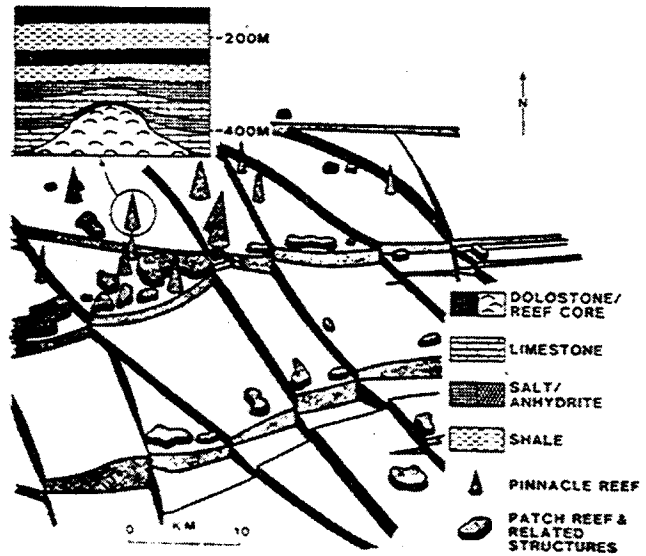
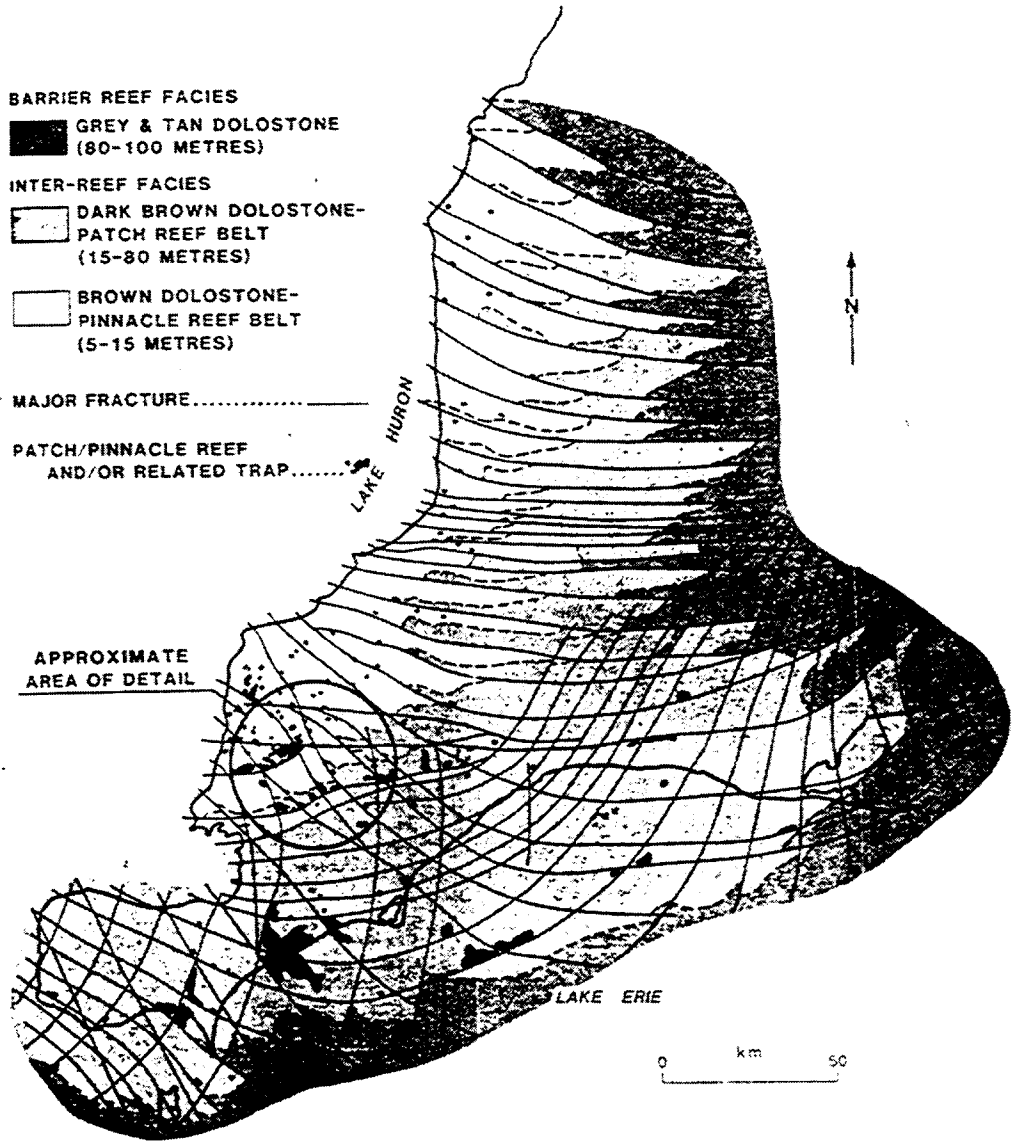
 DARK BROWN DOLOSTONE-
PATCH REEF BELT
(15-80 METRES)

 BROWN DOLOSTONE-
PINNACLE REEF BELT
(5-15 METRES)

MAJOR FRACTURE.....

PATCH/PINNACLE REEF
AND/OR RELATED TRAP.....

APPROXIMATE
AREA OF DETAIL



Paleogeographic reconstruction by Brett (1983, p. 963) does not show the Rochester Shale in the Michigan Basin. However, Sanford *et al.*, (1985) show the Rochester Formation of the Michigan Basin to connect with the Rochester of the Appalachian Basin studied by Brett (1983), by way of a channel across southwestern Ontario. This channel was bounded by portions of the Algonquin Arch, thought to be a positive feature from the Late Ordovician to Early Devonian (Sanford *et al.*, 1985). The arch eventually isolated the Michigan Basin, and Sanford *et al.*, (1985) show the Basin to substantially deepen away from the channel. Therefore, it is possible that the Rochester Shale of the Michigan Basin was deposited by the same mechanisms described by Brett (1983), but in a greater water depth than is envisioned for the unit in the Appalachian Basin.

The axis of the Algonquin Arch is thought to have shifted to the southeast during Lockport deposition and carbonates onlap the arch from both the Michigan Basin side and the Appalachian Basin side (Bailey, 1986). The Lockport Formation in the Appalachian Basin is interpreted to represent platform carbonate deposition in a shallowing-upward environment which vertically accreted subtidal to inter-tidal to supratidal facies (Shukla and Friedman, 1983). Environments in the Michigan Basin, however, is interpreted to be deeper as only subtidal facies were observed in the study area. Near the centre of the basin, a still deeper environment was the site of carbonate mud deposition (Mesoletta *et al.*, 1974) and the Lockport has a hematitic red colour (Huh *et al.*, 1977).

The appearance of corals and stromatoporoids in abundance as Lockport deposition continued suggests that the environment of deposition became more shallow and more hospitable for their growth. This may be due to the tectonic theory of Sanford *et al.*, (1985) or due to a general, basin-wide relative sea-level fall.

Sanford *et al.*, (1985) suggest that pinnacle reefs grew preferentially on the higher portions of active, tilted fault blocks. Such tilted blocks would be in shallower environments. However, reef organisms occur toward the top of the Lockport section under each pinnacle. Due to a lack of sufficient numbers of cores in inter-reef areas, it is unknown if the stromatoporoids also occur at

the same interval in inter-reef areas. In each instance, in the Payne, Rosedale and Warwick reefs, stromatoporoids first occur at 24.0 m, 23.8 m and 23.2 m above the top of the Rochester Formation respectively. For the tectonic theory to be correct, either all the fault blocks had to have tilted at approximately the same time to allow the organisms to first occur at the same interval or all the studied reefs had to have existed on the same tilted fault block. It appears that during Lockport Formation deposition, block fault movement had not yet occurred.

Rather, a general lowering of relative sea-level is favoured resulting in the growth of the stromatoporoids in more favourable conditions. This may be caused by shallowing and infilling due to a prograding, shallowing-upward, carbonate wedge of sedimentation (James, 1984). Alternatively, it may be caused by a slight thickening of the Lockport which results in a topographic high.

Near the Lockport-Guelph contact however, the irregular karst surface under each pinnacle reef suggests Lockport sediments must have been exposed by a lowering of sea-level in the basin. Appearance of reef organisms, and their subsequent reduction in number as the karst surface is approached, show evidence of the gradual shallowing. The top of the Goat Island Member in inter-reef areas also shows leaching and the effects of subaerial erosion. Therefore, it appears that the presence of the corals and stromatoporoids coincides with a lowering of sea-level that eventually karsted the top of the Lockport Formation.

In the past, the Guelph-Lockport contact surface under the pinnacles has been hard if not impossible to recognize (Bailey, 1986; Gill, 1979). Most workers however, have not examined a substantial number of reefs. It is proposed that this karst event best represents the Lockport-Guelph contact.

In outcrop, the Lockport-Guelph contact is placed arbitrarily at the first appearance of bituminous material (Winder, 1961; Bolton, 1957). However, in the subsurface there is no attempt at differentiating between the two units (Winder, 1961; Bolton, 1957; Sanford and Brady, 1955; Liberty and Bolton, 1966) and under the reefs, the bituminous material is absent. These authors refer to the contact as difficult to place or transitional.

There is a definite lithologic change across the surface from Lockport Formation lithology to that of Guelph Formation lithology (Figures 18 to 23). In addition, this exposure potentially affected the whole platform and provides a significant break between deposition of the Lockport and development of the pinnacle reefs and inter-reef Guelph facies.

Kahle (1988) describes the contact between the Lockport Dolomite and the Greenfield Dolomite in western Ohio as erosional with usually no to little (one to two inches) relief. The Greenfield is placed in the Salina Group by Droste and Shaver (1976). It overlies the Lockport-Guelph and is thought to be the equivalent of the A-2 Carbonate by Gill (1977). This example serves to illustrate that with so little relief possible across a major karst surface, the erosional surface such as the one between the Lockport and Guelph could easily go unrecognized by previous workers. James and Bone (1989) have shown that if there is little aragonite contained within an ancient carbonate, there may be little or no petrographic and geochemical evidence of subsequent karsting.

After the subaerial exposure event that produced karst at the top of the Lockport, relative sea-level in the Michigan Basin increased and the platform flooded. Pinnacle reef development began, possibly initiating on the very slight remnant highs of the karst terrain as the transgression occurred. Continued sea-level rise and platform flooding eventually allowed for the development of patch reefs in more marginward locations. The patch reefs, thought to exist on fault blocks also display the curious basin concentric distribution pattern of the pinnacles.

The crinoidal wackestone facies represents the initial stage of reef development as a silt mound evolved on the sea floor. This stage, combining pioneering of the substrate and colonization, begins the interpreted ecologic succession of reef development (Walker and Alberstat, 1975; James, 1979). Abundant crinoids, brachiopods, bryozoans and rugose corals attest to open marine conditions in a sea of warm, normal salinity water. Rugose corals and bryozoans probably grew as thickets on the crinoid and brachiopod debris and acted as bafflers or stabilizers. Tabular stromatoporoids, corals and algae (?) contributed as binders and

encrusters. Profusion of bryozoans versus corals suggests water that was somewhat deeper and less turbulent than in succeeding facies. This is also supported by the lack of abrasion observed in rugose corals. Large quantities of silt with stromatactis indicate not only low energy water conditions, but also that early marine cementation was as important as the binders in providing support for the fledgling mound.

The second stage of reef growth, that of the coral-stromatoporoid facies, differs from the preceding stage by virtue of a greater quantity of reef-building organisms. In addition, there is a more diverse faunal assemblage. Large tabulate corals and stromatoporoids act as frame-building organisms and provide a core for the reef to flourish. Varied coral types show some of the diversity of the emerging reef. There is an increase in ecologic niches as organisms such as brachiopods and crinoids belong to the dweller guild (Fagerstrom, 1988).

This expansion by the reef in terms of size and diversity suggests that living conditions for the organisms were very favourable with low chemical and physical stresses (James, 1983). The encrusting stromatoporoids and corals indicate that the reef was growing in shallow, more energetic water. Delicate organisms such as bryozoans are rare. Toppled corals and stromatoporoids suggest bioerosion and the layers of skeletal material suggest possible, periodic storm influence.

The shallow-water environment also places the reef close to sea-level where minor fluctuations left it intermittently exposed. However, few of these exposure surfaces can be correlated between reefs. Resubmergence after exposure resulted in renewed reef growth on the hard, unconformity surface left behind by the karst. James (1984) documents that after a karst event, renewed reef growth begins in a stage of diversification and that some workers erroneously see this as evidence of different stages of reef growth instead of recognizing unconformity bounded packages.

Other authors have observed a similar diversification stage in Michigan Basin reefs (Gill, 1977,1986; Pearson, 1980; Sears and Lucia, 1979, 1980; Mesoilella *et al.* , 1974). Although periodic exposure of Michigan Basin pinnacles has not been recognized by these other workers,

evidence from this study suggests that it occurred during the growth history of an individual pinnacle.

Continued accretion of the reef results in the development of the third stage of reef growth and the algal-brachiopod facies. This growth stage is markedly different from stage two in that there is very little diversity of organisms. Algae dominate, with minor brachiopods and other shelled organisms present. The algal wackestone facies represents the emergence of a dominant species type as chemical and physical conditions work to exclude other reef dwellers.

It is possible that this stage may represent very shallow, restricted subtidal to intertidal conditions, as several workers have suggested the presence of quiescent, lagoonal conditions on top of the bioherms as the pinnacles neared maturity (Gill, 1986; Cercone, 1984; Pearson, 1980). If so, then this facies should be encountered beneath, and associated with, each karst surface. However, this stage may also reflect changing, elevating salinity levels in the basin as a possible prelude to the onset of evaporite deposition of the Salina Group. Flank position cores also reveal algal-dominated facies, showing that their distribution was not restricted to the top of the reef. This suggests again that these facies may not solely result from lagoonal conditions on the reef top. Interpreted caliche crusts occurring in the algal facies of the Rosedale reef implies a semi-arid environment. Such an environment may have been in effect prior to the deposition of evaporites and consequently would have enhanced evaporation rates. Because of the distribution of the algal-dominated facies, its absence at karst surfaces, and the caliche horizons it contains, this facies is interpreted to reflect changing, elevating salinity levels.

The reefs now begin the fourth stage of growth, exemplified by the stromatolite boundstone facies. In this stage, further domination by algae occurs and the growth habit of the organisms was laminated. Few other creatures are present. James (1983) details similar life habits for organisms in the domination stage of reef growth. Presence of the stromatolites suggests that environmental conditions changed to even more restricted settings than for the previous phase

of reef growth. This may be the result of more pronounced lagoonal depositional sites on the top of the reef, it may result from further increases in salinity levels, or a combination of both.

As deposition of the stromatolites continued, the reef entered its final stage of growth. Although it was not a growing period *per se* for the reef, the karst stage does have a fatal effect on bioherm growth and an extraordinary karst fabric was superimposed on the established facies. The final karst event resulted in the termination of bioherm growth and the formation of conduits, breccias, pisoliths and caliche crusts. A green clay marks the top of the pinnacles.

To account for the exposure Gill (1977) and Briggs *et al.*, (1980) propose that water levels in the Michigan Basin suddenly dropped 100 m to 180 m, almost completely draining the basin, and that the resultant exposure karsted the pinnacles to their bases. This is based on the detected presence of a breccia, correlated to the tops of the reefs, that underlies the inter-reef A-1 Evaporite (Gill, 1977). However, other karst events during reef genesis could also account for that breccia, and the presence of the clasts does not translate to a complete draining of the Basin. Undoubtedly, sea-level dropped substantially, but did it fall up to 180 m swiftly in a single catastrophic and cataclysmic occurrence? The recognition of separate karst events occurring throughout pinnacle reef growth allows for other interpretations.

Rather, karst solution fabrics found throughout the reefs are interpreted to be separate events as few can be correlated. Additionally, core analysis reveals very low permeability and porosity in areas adjacent to interpreted exposure surfaces, and increased porosity and permeability in areas distal to the surfaces.

Coinciding with the fall in sea-level, exposure of the reefs, deposition of the A-1 Evaporite occurred (Gill, 1977; Huh *et al.*, 1977; Cercone 1984). Reasons for the drop in sea-level are uncertain. Gill (1977) suggests that in late Wenlockian to early Ludlovian time, intensive evaporation in the basin caused the sea to withdraw to the centre of the basin. Here, the new Salina Basin began to deposit evaporites in deep water and the topographic relief inherited from the preceding Guelph basin "was on the order of about 800 ft" (Gill, 1977, p. 1010). Nurmi

and Friedman (1977) suggest possible evaporation as the cause of the sea-level drop with dessication and shallow-water evaporite deposition following. Huh *et al.*, (1977) and Mesolella *et al.*, (1974) recognize the drop in relative sea-level but do not attempt to resolve it. Droste and Shaver (1977) hypothesize that the evaporites evolved in deep water and that sea levels remained uniformly high. However, deposition of shallow-water evaporites and interpreted drops in sea-level are not witnessed in adjacent carbonate settings such as the Wabush Platform in Indiana (Droste and Shaver, 1977; Cercone, 1988). Therefore, it appears that these phenomenon are restricted to the Michigan Basin.

In addressing the problem of the cyclic evaporites and carbonates of the Salina Group, previous authors have discussed how sea levels dropped and how salinity levels increased to result in deposition of the evaporite units. They do not however, address the problem of how the basin suddenly realized the higher sea levels and less saline waters necessary to deposit the carbonate units that follow.

Cercone (1988) suggests that evaporative sea-level downdraw may have been the cause of the drop. For this to have occurred, the Michigan Basin would have to have been isolated. This may have been possible since only two outlets for the basin are thought to have existed (Briggs *et al.* 1980) and both are close to the Algonquin Arch. Movement of the Bruce and Niagara megablocks was independent of one another throughout the Paleozoic (Sanford *et al.*, 1985) and this caused the axis of the Algonquin Arch to shift laterally (Bailey, 1986). A gradual shift in the Algonquin Arch during Guelph deposition could have resulted in the subsequent closure of the two outlets. A similar scenario has been suggested by Maiklem (1971) for the Elk Point Basin in the Devonian of Western Canada.

As the basin became isolated, water influx through the two outlets would gradually diminish and salinity levels increase. Eventually, the only recharge available would be through the barrier complex itself. Logan (1987) described an analogous situation with the Holocene MacLeod Basin and showed that replenishment of the basin was only a small fraction of the water lost through evaporation. As evaporation rates outstripped recharge rates, the

water in the basin would become even more saline. This overall increase in salinity may be reflected by the development of first the algal wackestone and then the stromatolitic boundstone facies as salinity increased further. As water levels continued to drop, the pinnacle reefs were exposed and evaporite deposition occurred in an isolated Michigan Basin. Hsü *et al.*, (1977) suggests similar drawdown and evaporation in the late Miocene of the Mediterranean.

After A-1 Evaporite deposition, rising sea levels and a decrease in salinity levels resulted in the A-1 Carbonate being deposited unconformably on top of the pinnacles. The algal mudstone and stromatolitic boundstone facies in the A-1 suggest that conditions were still harsh and restricted enough to exclude other fauna. In inter-reef areas the A-1 Carbonate is micro-laminated mudstone with some bioturbation and fecal pellets but no invertebrate fossils (Gill, 1977). Apparently, few organisms could tolerate this environment until sea levels covered the pinnacles once again. Then algae and stromatolites were able to live and flourish until the onset of A-2 Evaporite deposition.

The cause of the rise in sea-level is unknown. If the idea of an isolated basin and resulting drawdown is followed, then a breach of the surrounding barrier reef was necessary to allow for the influx of water into the basin. Or recharge rates into the basin would now have to outpace those of evaporation.

Following the deposition of the A-1 Carbonate, there was once again an exposure event before the onset of evaporite deposition (Gill, 1977). With large thicknesses of A-1 Evaporite and A-1 Carbonate lying underneath and helping to fill the basin, the now depositing A-2 Evaporite was able to cover the reefs and enshroud them in anhydrite.

The A-2 Evaporite and the overlying mudstones of the A-2 Carbonate once again show the highly cyclic nature of sea-level and salinity levels in the Michigan Basin during Cayugan time.

5.4 Discussion of Fault Control on Reef Genesis

The theory of fault block control of reef initiation and growth (Sanford *et al.*, 1985) fails to explain several trends noticed in the pinnacle reefs. When taken individually, none of these trends refutes the hypothesis. However, collectively certain aspects of the principle are cast into doubt.

Sanford *et al.*, (1985) are unable to explain why the pinnacle reefs grow in a near-concentric ring around the Michigan Basin. If initiation of growth was due to the higher topography offered by a tilted fault block and if these fault blocks are distributed throughout the Michigan Basin, then why are the pinnacles not distributed randomly throughout the basin, or in a linear or reticulate pattern?

The Lockport Formation itself disputes the block fault theory. Tilted block faults would cause noticeable variations in the thickness of the Lockport section. This unit however, is known to be relatively uniform in thickness (Gill, 1986). Thicknesses of the Lockport encountered in this study follow trends observed by Gill (1979) which show only a slight thinning toward the basin.

Reef-building organisms occur in the Goat Island Member of the Lockport Formation under the pinnacles at roughly the same stratigraphic level in the three cores that penetrate to the Rochester Formation? For this to occur: (1) the fault blocks had to have tilted previously and at the same time for the organisms to all occur at the same interval; (2) all the pinnacles studied must lie on the same fault block; or (3) fault block tectonism had not yet occurred. However, diagrams by Sanford *et al.*, (1985) show the blocks to be small and numerous blocks occur across the study area and southwestern Ontario (figure 31).

In addition, the karst surface at the base of the pinnacles, that is here proposed as the Lockport-Guelph contact, can be correlated among all the pinnacles studied. If fault blocks had been tilted prior to this event, then the karst surface should be found at different stratigraphic levels and varying degrees of reef development should be observed under the surface. That the

exposure surface occurs at the same level under each pinnacle, and that the same changes from platform carbonates to reef initiation are observed across the surface, suggests no movement prior to karsting.

It is however, important to consider that after karsting and prior to reef initiation, block fault movement may have occurred and that this movement may have triggered reef growth. Determination of the existence of any such movement would require a regional study incorporating many cores from many pinnacles. Again however, the movement of independent blocks cannot explain the ring of pinnacles around the basin. There remains the possibility that movement could have coincided with the post-karst transgression. This could create topographic highs for reef development and account for the concentric ring of pinnacles basinwide. Under such a scenario nonetheless, bioherm development might be also expected randomly in areas more toward the basin centre where water depths would still be relatively shallow. Such development is unknown and the overall timing of all events would have to be precise for the faults to account for both pinnacle initiation and distribution.

It appears from this study that there is no direct evidence linking initiation of the pinnacle reefs to the presence of fault blocks. Rather reefs developed after a subaerial exposure episode had left a correlatable karst surface on the top of the Lockport Formation. As sea-level transgressed the platform, some pinnacle reef growth may have been initiated on slightly elevated sections of the karst terrain and a momentary pause in the transgressive pulse may have allowed the organisms to populate an area around the basin that at the time provided suitable living conditions. This accounts for the ring-like belt of pinnacles in the basin more easily.

With further increases in relative sea-level, the pinnacles grew upwards and were easily able to keep pace with the relative rising water. This accounts for their high height versus size ratios as well as their steep dip angles on their flanks. By maintaining themselves in shallow-water, the reefs also were subjected to subaerial exposure repeatedly over their life-

spans. Landward, in response to the transgression and flooding, patch reefs developed, also in a concentric ring.

Previous authors (Sears and Lucia, 1979; Gill, 1986; Huh *et al.*, 1977; Pearson, 1980; Mesolella *et al.*, 1974) have theorized that the pinnacle reefs began as mud mounds on the sea floor that accreted toward sea-level as the basin subsided. At some time the mounds developed reefal facies. The question must be raised as to how mud accumulation could not only keep pace with relative sea-level increases, but overcome those increases and build up high enough above the seafloor to allow for population by reef-building organisms. Smaller pinnacles are thought to be mud mounds that were never able to fully develop and were consequently drowned (Bailey, 1986).

However, cores through shorter, smaller pinnacles show an ecologic succession of reef development similar to the larger reefs, but on a smaller, more compressed scale. This disputes the findings of Bailey (1986). In terms of reef genesis, it is not required that all the pinnacles initiate at the same time. Therefore, it is possible that these pinnacles are smaller because growth was initiated at a later time relative to the larger pinnacle reefs, and by block fault movement. This however again raises the spectre of why the pinnacles grow in a concentric ring. If later fault block movement could initiate growth and produce a smaller, shorter reef, and if there are block faults everywhere, then why are the pinnacles not distributed everywhere?

That most of these karst episodes cannot be readily correlated between all the pinnacles suggests that block fault movement did influence their subsequent development. Cores through the crest positions of three similar sized reefs, Rosedale, Warwick and Payne show little correlation between karst events. This tends to support the notion that fault blocks with independent movement did influence subsequent pinnacle reef growth, and in the case of smaller pinnacles initiated growth. The presence of the stromatolite boundstone at the top of the pinnacles in part suggests that when the final karst episode terminated bioherm growth, all the pinnacles, including the late starters were close to sea-level.

5.5 Summary

The theory by Sanford *et al.*, (1985) that tilted fault blocks governed the initiation of Guelph Formation pinnacle reefs does not adequately explain why the pinnacle reefs in the Michigan Basin grew in a near-concentric ring around the basin. Their hypothesis cannot account for the appearance of corals and stromatoporoids at the same stratigraphic level in three reefs studied with cores down to the Rochester, and the presence of a correlatable karst surface between the Lockport and Guelph Formations unless fault movement had not occurred prior to this time. Subsequent fault movement after karsting again does not adequately explain the distribution pattern of the reefs.

Instead it is proposed that most pinnacle genesis was initiated by a transgression after a regional exposure episode. Pinnacles may have developed on the incipient highs left by the karst terraine or may have flourished during a momentary pause in the transgressive phase itself. After initiation, the reefs kept pace with a rising sea-level by growing upwards and were subaerially exposed several times throughout their life-span. Only the lowermost karst surface, at the Lockport-Guelph contact, and the final bioherm terminating exposure episode at the top of the pinnacles can be correlated between all the reefs. That the other karst surfaces cannot be correlated between the reefs suggests that while fault blocks were not responsible for most reef initiation, these blocks did exert influence on subsequent reef development by way of differential movement. Smaller pinnacles show an ecologic succession similar to larger ones and thus are believed to have initiated at a later time due to fault block movement.

Block fault movement in the late Middle Silurian and early Upper Silurian is also interpreted as a possible mechanism by which the two inlets connecting the Michigan Basin to other waterways may have been closed. This gradual closure would have resulted in isolation of the basin and elevation of salinity levels. Salinity increases are possibly reflected in the emergence of the algal-brachiopod facies and stromatolitic boundstones as the dominant facies in the reef. With evaporation rates exceeding replenishment rates into the basin, sea

levels would fall and the pinnacles would be exposed one final time. This would be followed by evaporite deposition. Re-opening of the basin or a change in the evaporation rate-replenishment rate ratio would result in an influx of less saline marine waters. This might result in carbonate deposition with the restricted facies of the A-1 Carbonate covering the pinnacles.

Block fault movement resulting in closure, isolation, high evaporation rates and subsequent reopening of the basin is one possible explanation for the cyclic deposition of the evaporites and carbonates of the Salina Group. Other theories also invoke eustatic changes in sea-level to account for the Salina deposition. However, these sea-level changes are not observed outside the Michigan Basin, indicating that the Michigan Basin must have been independent.

CHAPTER SIX

Conclusions

Although the pinnacle bioherms of the Michigan Basin have been extensively examined by previous workers, this is the first detailed study of cores from several pinnacles from southwestern Ontario. Based on this study a number of original conclusions have evolved. These are presented below.

1. Pinnacle reef bioherms of the Michigan Basin experienced several episodes of subaerial exposure throughout their growth history. This finding is notably different from virtually all previous conclusions which allow for only one, bioherm-terminating, karst event.

2. Only two of the many exposure zones detected in the reefs can be correlated among all six pinnacles studied, the lowermost karst surface found at the base of each pinnacle and the final subaerial facies at the top. Remaining exposure zones cannot be correlated among all the pinnacles and this suggests that each pinnacle experienced a different growth history.

3. The lowermost karst surface forms the Guelph Formation-Lockport Formation contact at the base of each of the pinnacles studied. This contact had been considered to be transitional, gradational or impossible to detect. Changes occurring across the surface may include: (a) changes from rocks representative of the Lockport to those exemplary of the Guelph; (b) change from dolomite to limestone; and, (c) appearance of reef-building organisms.

4. That the Guelph-Lockport surface can be correlated between all six bioherms infers that the karst event may have been regional in its scope.

5. The following features suggest that block fault movement was not responsible for the initiation of pinnacle reef growth in the Michigan Basin: (a) near-uniform thicknesses of the Lockport Formation under the pinnacles; (b) the appearance of stromatoporoids in the Lockport at the same stratigraphic interval in three cores that penetrate to the Rochester Shale; (c) the

concentric distribution of the pinnacle reefs around the Basin; and, (d) the correlatable karst surface at the base of each pinnacle. A relative sea-level rise after karsting partially flooded the platform and is believed responsible for reef initiation and this explains the concentric nature of pinnacle distribution. Continued flooding of the platform initiated patch reefs, also in a concentric pattern, in more marginward locations.

6. Subaerial exposure surfaces found between the lowermost surface and uppermost karst facies cannot be correlated between all of the pinnacles. Therefore, it appears that any individual reef may or may not have experienced a given exposure episode. Thus, some mechanism, probably fault block movement, influenced the subsequent development of the pinnacles after initiation.

7. Smaller, more stunted pinnacle bioherms show an ecologic succession similar to the one documented in larger ones by previous workers, but with thinner facies units. This shows that the smaller pinnacles are not the result of continued accretion of mud mound material. Rather these are pinnacles that may have been initiated at a later time.

8. Diagenesis within the meteoric zone is much more extensive than previously reported. There is abundant evidence of vadose and meteoric phreatic phenomena in the pinnacle bioherms, such as pendant, prismatic and meniscus cements, and epitaxial overgrowths and blocky cements respectively. Meteoric cementation is found in close association with interpreted karst surfaces and is not found pervasively throughout the bioherms. This suggests that the final exposure event that terminated bioherm growth did not karst the pinnacles to their bases.

9. Replacive dolomitization within the pinnacle bioherms has a number of different textures that may or may not be present in a given pinnacle. This includes: (a) pervasive, anhedral, interlocked dolomite crystals; (b) crypto-crystalline dolomite associated with karst surfaces; and, (c) single randomly scattered dolomite rhombs. Two types of dolomite were recognized in the Lockport Formation: (1) anhedral and pervasive dolomite crystals throughout

the matrix of the Lockport; and (2) complete to partial replacement of skeletal allochems with euhedral rhombs. Dolomites in the A-1 Carbonate are anhedral to euhedral.

10. Dolomitization has a negative effect on the pinnacles in terms of the recognition of karst surfaces. Exposure surfaces with topographic irregularity associated with them are the most likely to be recognizable after dolomitization. Processes of dolomitization also negate meteoric cements and their luminescence.

11. Isotopic values from pinnacle bioherm samples reveal slightly different overall readings for $\delta^{13}\text{C}$ and $\delta^{18}\text{O}$ when compared to previous work. Whether due to different migration pathways for fluids affecting the pinnacles studied or the influence of the differing subaerial exposure events experienced by each reef, perhaps each pinnacle in the Michigan Basin has a somewhat different, isotopic signature all its own.

12. Additional bioherms should be analyzed to for the presence of subaerial exposure features and their correlation with the surfaces documented in this study. Specifically, the regional extent of the lowermost karst surface at the base of the pinnacles should be sought. Also, a study of pinnacles from across the Michigan Basin should be used to document the nature of block fault movement.

13. Implications of this study to hydrocarbon exploration and production are wide ranging. An alternative interpretation regarding the genesis of pinnacle reefs in the Michigan Basin is now possible. This identifies the need to re-assess previous depositional and diagenetic models. Recognition of karst surfaces and their associated reductions in porosity and permeability is essential to identifying barriers in hydrocarbon reservoirs.

References

- Allan, J.R., and Matthews, R.K., 1982, Isotopic signatures associated with early meteoric diagenesis: *Sedimentology*, v. 29, p. 979-817.
- Alling, H.L., and Briggs, L.L., 1961, Stratigraphy of Upper Silurian Cayugan Evaporites: *American Association of Petroleum Geologists Bulletin*, v. 45, p. 515-547.
- Archer, A.W., and Feldman, H.R., 1986, Microbioherms of the Waldron Shale (Silurian Indiana): Implications for organic framework in the Great Lakes area. *Palaios*, v. 1, p. 133-140.
- Aulstead, K.L., and Spencer, R.J., 1985, Diagenesis of the Keg River Formation, northwestern Alberta: fluid inclusion evidence: *Bulletin of Canadian Petroleum Geology*, v. 33, p. 167- 183.
- Aulstead, K.L., Spencer, R.J., and Krouse, H.R., 1987, Fluid inclusion and isotopic evidence of dolomitization, Devonian of Western Canada: *Geochimica et Cosmochimica Acta*, v. 52, p. 1027- 1035.
- Back, W., Hanshaw, B.B., Herman, J.S., and Van Driel, J.N., 1986, Differential dissolution of a Pleistocene reef in the groundwater mixing zone of coastal Yucatan, Mexico: *Geology*, v. 14, p. 137-140.
- Badiozamani, K., 1973, The dorag dolomitization model-application to the Middle Ordovician of Wisconsin: *Journal of Sedimentary Petrology*, v. 43, p. 965-984.
- Bailey, S.M.B., 1986, A new look at the development, configuration and trapping mechanisms of the Silurian Guelph reefs of Southwestern Ontario: *Ontario Petroleum Institute, 25th Annual Conference, Paper 14, 28 p.*
- Bainbridge, T.W., 1973, The sedimentology of a Silurian pinnacle reef in the Michigan Basin (unpublished B.Sc. thesis): *Queen's University, Kingston, Ontario, 52 p.*
- Bates, R.L., and Jackson, J.A., (eds.), 1980, *Glossary of Geology, Second Edition*: American Geological Institute, Falls Church, Virginia.
- Bathurst, R.G.C., 1959, The cavernous structure of some Mississippian *Stromatactis* reefs in Lancashire, England: *Journal of Geology*, v. 67, p. 506-521.
- Bathurst, R.G.C., 1975, *Carbonate sediments and their diagenesis*: Elsevier Scientific Publishing Co., Amsterdam, 658 p.
- Bathurst, R.G.C., 1982, Genesis of stromatactis cavities between submarine crusts in Paleozoic carbonate mud buildups: *Journal of the Geological Society of London*, v. 139, p. 165-181.
- Bogli, J., 1980, *Karst hydrology and physical speleology*: Springer-Verlag, Berlin and Heidelberg, 285 p.
- Bolton, T.E., 1957, Silurian stratigraphy and paleontology of the Niagara escarpment in Ontario: *Geological Survey of Canada Memoir 289*.
- Bourque, P.A., and Gignac, H., 1983, Sponge - constructed stromatactis mud mounds, Silurian of Gaspe, Quebec: *Journal of Sedimentary Petrology*, v. 53, p. 521-532.

Bourque, P.A., Amyot, G., Desroches, A., Gignac, H., Gosselin, C., Lachambre, G., and Laliberte, J.-Y., 1986, Silurian and Lower Devonian reef and carbonate complexes of the Gaspé Basin, Quebec—a summary: *Bulletin of Canadian Petroleum Geology*, v. 34, p. 452-489.

Brett, C.E., 1983, Sedimentology, facies and depositional environments of the Rochester Shale (Silurian: Wenlockian) in western New York and Ontario: *Journal of Sedimentary Petrology*, v. 53, p. 949-971.

Briggs, L.I., Gill, D., Briggs, D.Z., and Elmore, R.D., 1980, Transition from open marine to evaporite deposition in the Silurian Michigan Basin: *in* Nissenbaum, A., ed., *Hypersaline and evaporite environments*, Elsevier, Amsterdam, p. 253-270.

Caley, J.F., 1946, Paleozoic geology of the Windsor-Sarnia area, Ontario: Geological Survey of Canada, Memoir 240.

Cant, D.J., 1983, Subsurface facies analysis: *Geoscience Canada*, v. 10, p. 115-121.

Caughlin, W.G., Lucia, F.J., and McIver, N.L., 1976, The detection and development of Silurian reefs in Northern Michigan: *Geophysics*, v. 41, p. 646-658.

Cercione, K.R., 1984, Diagenesis of Niagaran (middle Silurian) pinnacle reefs, northwestern Michigan (unpublished Ph.D. thesis): University of Michigan, Ann Arbor, Michigan, U.S.A., 367 p.

Cercione, K.R., 1988, Evaporative sea-level drawdown in the Silurian Michigan basin: *Geology*, v. 16, p. 387-390.

Cercione, K.R., and Budai, J.M., 1985, Formation of geopetal diagenetic sediment by evaporite solution: evidence that not all crystal silt is vadose: *Society of Economic Paleontologists and Mineralogists Annual Mid-year Meeting Abstracts*, v. 2, p. 17.

Cercione, K.R., and Lohmann, K.C., 1985, Early diagenesis of Middle Silurian pinnacle reefs, Northern Michigan: *in* Cercione, K.R. and Budai, J.M., eds., *Ordovician and Silurian rocks of the Michigan Basin and its margins*: Michigan Basin Geological Society Special Paper No. 4.

Cercione, K.R., and Lohmann, K.C., 1986, Diagenetic history of the Union 8 pinnacle reef (Middle Silurian) Northern Michigan: *in* Schraeder, J.H., and Purser, B.H., eds., *Reef Diagenesis*: Springer Verlag, Berlin, p. 381-398.

Chafetz, H.S., McIntosh, A.G., and Rush, P.F., 1988, Fresh water phreatic diagenesis on the marine realm of recent Arabian Gulf carbonates: *Journal of Sedimentary Petrology*, v. 58, p. 433-440.

Chamberlain, T.C., 1877, *Geology of Wisconsin*. Wisconsin Geological Survey, v. 2, p. 93-405. [article not seen but cited by Shaver, R.H., 1989]

Chalkley, P., 1983, The sedimentologic correlation and history of the Fletcher Silurian pinnacle reef, in the eastern Michigan Basin (unpublished B.Sc. thesis): Queen's University, Kingston, Ontario, 52 p.

Cherns, L., 1982, Paleokarst, tidal erosion surfaces and stromatolites in the Silurian Eke Formation of Gotland, Sweden: *Sedimentology*, v. 29, p. 819-833.

Choquette, P.W., and James, N.P., 1986, Diagenesis 12: Limestones-the deep burial environment: *Geoscience Canada*, v. 14, p. 3-35.

Choquette, P.W., and James, N.P., 1988, Introduction to Paleokarst: *in* James, N.P., and Choquette, P.W., *eds.*, *Paleokarst*. Springer Verlag, New York, p.

Choquette, P.W., and Pray, L.C., 1970, Geologic nomenclature and classification of porosity in sedimentary carbonates: *American Association of Petroleum Geologists Bulletin*, v. 54, p. 207-250.

Churcher, P.L., and Dusseault, M.D., 1985, Clay mineralogy of two selected Silurian carbonate reservoirs in southwestern Ontario: Ontario Petroleum Institute 25th Annual Conference, Technical Paper no. 8, 21 p.

Coniglio, M., James, N.P., and Aissaoui, D.M., 1988, Dolomitization of Miocene carbonates, Gulf of Suez, Egypt: *Journal of Sedimentary Petrology*, v. 58, p. 110-119.

Coron, C.R. and Textoris, D.A., 1974, Non-calcareous algae in Silurian carbonate mud mounds, Indiana. *Journal of Sedimentary Petrology*, v. 44, p. 1248-1250.

Crowley, D.J., 1973, Middle Silurian patch reefs in Gasport Member (Lockport Formation), New York. *American Association of Petroleum Geologists Bulletin*, v. 57, p. 283-300.

Davies, G.R., 1977, Former magnesian calcite and aragonite submarine crusts in Upper Paleozoic reefs of the Canadian Arctic: a summary: *Geology*, v. 5, p. 11-15.

Davies, G.R., and Krouse, H.R., 1975, Carbon and oxygen isotopic composition of late Paleozoic calcite cements, Canadian Arctic archipelago-preliminary results and interpretation: *Geological Survey of Canada, Paper 75-1, Part 1*, p. 215-220.

Dawson, W.C., and Carozzi, A.V., 1985, Experimental fabric-selective porosity in phylloid-algal limestones (abs.): *American Association of Petroleum Geologists Bulletin*, v. 69, p.248.

Devaney, K.A., and Wilkinson, B.H., and Van Der Voo, R., 1986, Deposition and compaction of carbonate clinothems: the Silurian Pipe Creek Junior complex of east-central Indiana: *Geological Society of America Bulletin*, v. 97, p. 1367-1381.

Dickson, J.A.D., 1965, A modified staining technique for carbonates in thin section. *Nature*, v. 205, p. 587.

Dickson, J.A.D., and Coleman, M.L., 1980, Changes in carbon and oxygen isotope composition during limestone diagenesis: *Sedimentology*, v. 27, p. 107-118.

Dravis, J.J., and Yurewicz, D.A., 1985, Enhanced carbonate petrography using fluorescence microscopy. *Journal of Sedimentary Petrology*, v. 55, p. 795-804.

Droste, J.B., and Shaver, R.H., 1976, The Limberlost Dolomite of Indiana, a key to the great Silurian facies in the southern Great Lakes area: *Indiana Geological Survey Occasional Paper 15*, 21 p.

Droste, J.B., and Shaver, R.H., 1977, Synchronization of deposition: Silurian reef-bearing rocks on Wabush Platform with cyclic evaporites of Michigan Basin: *American Association of Petroleum Geologists Studies in Geology 5*, p. 93-109.

Droste, J.B., and Shaver, R.H., 1982, The Salina Group (Middle and Upper Silurian) of Indiana: Indiana Geological Survey Special Report 24, 41 p.

Dunham, R.J., 1962, Classification of carbonate rocks according to depositional texture. *in* Ham, W.E., *ed.*, Classification of carbonate rocks: American Association of Petroleum Geologists Memoir 1, p. 108-121.

Embry, A.F., and Kloven, J.F., 1971, A Late Devonian reef tract on northwestern Banks Island, North West Territories. *Bulletin of Canadian Petroleum Geology*, v. 19, p. 738-781.

Esteban, M., and Klappa, C.F., 1983, Subaerial exposure environment: *in* Scholle, P.A., Bebout, D.G., and Moore, C.H., *eds.*, Carbonate depositional environments: American Association of Petroleum Geologists Memoir 33, p. 1-54.

Fagerstrom, J.A., 1988, A structural model for reef communities. *Palaios*, v. 3, p. 217-220.

Folk, R.L., 1962, Petrography and origin of the Silurian Rochester and MacKenzie shales, Morgan County, West Virginia. *Journal of Sedimentary Petrology*, v. 32, p. 539-578.

Folk, R.L., 1965, Some aspects of recrystallization in ancient limestones. *in* Pray, L.C., and Murray, R.C., *eds.*, Dolomitization and limestone diagenesis—a symposium: Society of Economic Paleontologists and Mineralogists, Special Publication 13, p. 14-48.

Frank, J.R., Carpenter, A.B., and Ogelsby, T.W., 1982, Cathodoluminescence and composition of calcite cement in the Taum Sauk Limestone (Upper Cambrian) Southeast Missouri. *Journal of Sedimentary Petrology*, v. 52, p. 631-638.

Friedman, G.M., and Sanders, J.E., 1967, Origin and occurrence of dolostones. *in* Chillingar, G.V., Bissell, H.J., Fairbridge, R.W., *eds.*, Carbonate Rocks: Origin, occurrence and classification: Elsevier, Amsterdam, p. 267-348.

Gill, D., 1973, Stratigraphy, facies, evolution and diagenesis of productive Niagaran Guelph reefs and Cayuga sabkha deposits, the Belle River Mills gas field, Michigan Basin: unpublished Ph.D. Dissertation, University of Michigan, 276 p.

Gill, D., 1975, Cyclic deposition of Silurian carbonates and evaporites in Michigan Basin, discussion: *American Association of Petroleum Geologists Bulletin*, v. 59, p. 535-538.

Gill, D., 1977, Salina A-1 sabkha cycles and the Late Silurian paleogeography of the Michigan Basin. *Journal of Sedimentary Petrology*, v. 47, p. 979-1017.

Gill, D., 1979, Differential entrapment of oil and gas in Niagaran pinnacle reefs of Northern Michigan: *American Association of Petroleum Geologists Bulletin*, v. 63, p. 608-620.

Gill, D., 1986, Depositional facies of Middle Silurian (Niagaran) pinnacle reefs, Belle River Mills gas field, Michigan Basin, southeastern Michigan: *in* Roehl, P.O., and Choquette, P.W., *eds.*, Carbonate Petroleum Reservoirs, Springer Verlag, Berlin, p. 123-139.

Given, R.K., and Lohmann, K.C., 1985, Derivation of the original isotopic composition of Permian marine cements: *Journal of Sedimentary Petrology*, v. 55, p. 430-439.

Given, R.K., and Lohmann, K.C., 1986, Isotopic evidence for early meteoric diagenesis of the reef facies, Permian Reef-complex of West Texas and New Mexico: *Journal of Sedimentary Petrology*, v. 56, p. 183-193.

- James, N.P., and Bone, Y., 1989, Petrogenesis of Cenozoic, temperate water calcarenites, South Australia: A model for meteoric/shallow burial diagenesis of shallow-water calcite sediments. *Journal of Sedimentary Petrology*, v. 59, p. 191-203.
- James, N.P., and Choquette, P.W., 1983, Diagenesis 6: Limestones-the sea floor diagenetic environment: *Geoscience Canada*, v. 10, p. 162-179.
- James, N.P., and Choquette, P.W., 1984, Diagenesis 9: Limestones- the meteoric diagenetic environment: *Geoscience Canada*, v. 11, p. 161-194.
- James, N.P., and Choquette, P.W., 1988, *Paleokarst*, Springer Verlag, New York,
- James, N.P., Ginsburg, R.N., Marzalek, D.S., and Choquette, P.W., 1976, Facies and fabric specificity of early subsea cements in shallow Belize (British Honduras) reef: *Journal of Sedimentary Petrology*, v. 46, p. 523-544.
- James, N.P., and Klappa, C.F., 1983, Petrogenesis of Early Cambrian reef limestones: *Journal of Sedimentary Petrology*, v. 53, p. 1051-1096.
- Jodry, R.L., 1969, Growth and dolomitization of Silurian reefs, St. Clair County, Michigan: *American Association of Petroleum Geologists Bulletin*, v.52, p. 957-981.
- Kahle, C.F., 1974, Nature and significance of Silurian rocks at Maumee Quarry, Ohio, *in* Kesling, R.V., *ed.*, *Silurian reef-evaporite relationships: Michigan Basin Geological Society Field Conference Guidebook*, p. 31-54.
- Kahle, C.F., 1978, Patch-reef development and effects of repeated subaerial exposure in Silurian shelf carbonates, Maumee, Ohio, *in* Kesling, R.V., *ed.*, *Geological Society of America, North Central Section Guidebook*, p. 63-115.
- Kahle, C.F., 1988, Surface and subsurface Paleokarst, Silurian Lockport and Peebles Dolomites, Western Ohio: *in* James, N.P., and Choquette, P.W., *eds.*, *Paleokarst: Springer Verlag, New York*, p. 229- 255.
- Kendall, A.C., 1977, Fascicular optic calcite: a replacement of bundled acicular carbonate cement: *Journal of Sedimentary Petrology*, v. 47, p. 1056-1062.
- Kendall, A.C., 1989, Brine mixing in the Middle Devonian of Western Canada and its possible significance to regional dolomitization: *Sedimentary Geology*, V. 64, p. 271-285.
- Kobluk, D.R., 1984, A coastal paleokarst near the Ordovician-Silurian boundary, Manitoulin Island, Ontario: *Bulletin of Canadian Petroleum Geology*, v. 32, p. 398-407.
- Koepke, W.E., and Sanford, B.V., 1966, Silurian oil and gas fields of southwestern Ontario. *Geological Survey of Canada, Paper 65-30*.
- Liberty, B.A., and Bolton, T.E., 1966, *Geology of the Bruce Peninsula, Ontario: Geological Survey of Canada, Paper 65-41, 40 p.*
- Logan, B.W., Rezak, R., and Ginsburg, R.N., 1964, Classification and environmental significance of algal stromatolites: *Journal of Geology*, v. 72, p. 68-83.

- Goldhammer, R.K. and Elmore R.D., 1984, Paleosols capping regressive carbonate cycles in the Pennsylvanian Black Prince Limestone, Arizona: *Journal of Sedimentary Petrology*, v.54, p. 1124-1137.
- Grimes, D.J., 1988, Depositional models, subaerial facies, and diagenetic histories of the Rosedale and Fletcher reefs, southwestern Ontario: unpublished M.S.c. Thesis, Queen's University, 120p.
- Hall, J., 1839, Third annual report of the Fourth Geological District of the State of New York: New York State Geological Survey Annual Report Number 3, p. 287-339. [article not seen but cited by Brett, C.E., 1983].
- Hall, J., 1862, Report on the geological survey of the State of Wisconsin. Wisconsin Geological Survey, v. 1, 445 p. [article not seen but cited by Shaver, R.H., 1989].
- Hardie, L.A., 1987, Dolomitization: a critical view of some current views: *Journal of Sedimentary Petrology*, v. 57, p. 166-183.
- Harrison, R.S., and Steinen, R.P., 1978, Subaerial crusts, caliche profiles, and breccia horizons: comparison of some Holocene and Mississippian exposure surfaces, Barbados and Kentucky: *Geological Society of America Bulletin*, v. 89, p. 385-396.
- Havard, C., and Oldershaw, A., 1976, Early diagenesis in back-reef sedimentary cycles, Snipe Lake Reef-complex, Alberta: *Bulletin of Canadian Petroleum Geology*, v. 24, p. 27-69.
- Have, T., and Heijnen, W., 1985, Cathodoluminescence activation and zonation in carbonate rocks: an experimental approach: *Geologie en Mijnbouw*, v. 64, p. 297-310.
- Hill, J.V., 1966, Silurian reef carbonates: Ontario Petroleum Institute 5th Annual Conference, 21 p.
- Hudson, J.D., 1977, Stable isotopes and limestone lithification: *Journal of the Geological Society of London*, v. 133, p. 637-660.
- Huh, J.M., Briggs, L.L., and Gill, D., 1977, Depositional environments of pinnacle reefs, Niagara and Salina Groups, northern shelf, Michigan Basin, in Fisher, J.H., ed., *Reefs and Evaporites; Studies in Geology No. 5*, American Association of Petroleum Geologists Bulletin, p. 1-21.
- Hutt, R.B., MacDougall, T.A., and Sharp, D.A., 1973, Southern Ontario: in McCrossan, R.G., ed., *Future Petroleum Provinces of Canada: Bulletin of Canadian Petroleum Geology Memoir 1*, p. 411-441.
- James, N.P., 1972, Holocene and Pleistocene calcareous crust (caliche) profiles: criteria for subaerial exposure: *Journal of Sedimentary Petrology*, v. 42, p. 817-836.
- James, N.P., 1979, Facies models 8. Shallowing-upward sequences in carbonates: *Geoscience Canada*, v. 4, p. 126-136.
- James, N.P., 1983, Reefs: in Scholle, P.A., Bebout, D.G, and Moore, C.H., eds., *Carbonate depositional environments: American Association of Petroleum Geologists Memoir 33*, 345- 440.

Lohmann, K.C., 1988, Geochemical patterns of meteoric diagenetic systems and their application to studies of paleokarst. *in* James, N.P., and Choquette, P.W., eds., *Paleokarst*: Springer Verlag, New York, p. 58-80.

Lohmann, K.C., and Meyer, W.J., 1977, Microdolomite inclusions in cloudy prismatic calcites: a proposed criterion for former magnesium calcites: *Journal of Sedimentary Petrology*, v. 47, p. 1078-1088.

Longman, M.W., 1980, Carbonate diagenetic textures from near-surface diagenetic environments: *American Association of Petroleum Geologists Bulletin*, v. 64, p. 461-487.

Lowenstam, H., 1950, Niagaran reefs of the Great Lakes area: *Journal of Geology*, v. 58, p. 430-487.

Machel, H.G., 1985, Cathodoluminescence in calcite and dolomite and its chemical interpretation: *Geoscience Canada*, v. 12, p. 139-148.

Maiklem, W.R., 1971, Evaporative drawdown-a mechanism for water level lowering and diagenesis in the Elk Point Basin. *Bulletin of Canadian Petroleum Geology*, v. 19, p. 485-501.

Mantek, W., 1976, Recent exploration activity in Michigan: Ontario Petroleum Institute, 15th Annual Conference, 29 p.

Macqueen, R.W., and Ghent, E.D., 1970, Electron microprobe study of magnesium distribution in some Mississippian echinoderm limestones from western Canada: *Canadian Journal of Earth Science*, v. 7, p. 1308-1316.

McCullough, C.N. Jr., 1975, Origin of pore-filling salts in the Niagaran reefs of northern Michigan (abs.). *American Association of Petroleum Geologists Bulletin*, v. 59, p. 1737.

McGovney, J.E., Lehmann, P.J., and Sarg, J.F., 1982, Eustatic sea-level control of Silurian (Niagaran) reefs, Michigan Basin: *American Association of Petroleum Geologists Bulletin*, Abstracts with Program, p. 85.

Meadows, J.R., Churcher, P.L., Lawson, D.E., and Dusseault, M.B., 1986, Fletcher field: a Silurian patch/barrier reef-complex in southwestern Ontario (abs): Eastern Section Annual Meeting, *American Association of Petroleum Geologists Bulletin*, v. 70, p. 1069.

Mesolella, K.J., Robinson, J.D., McCormick, L.M., and Ormiston, A.R., 1974, Cyclic deposition of Silurian carbonates and evaporites in Michigan Basin: *American Association of Petroleum Geologists Bulletin*, v. 58, p. 34-62.

Mesolella, K.J., Robinson, J.D., McCormick, L.M., and Ormiston, A.R., 1975, Cyclic deposition of Silurian carbonates and evaporites in Michigan Basin: *American Association of Petroleum Geologists Bulletin*, v. 59, p. 538-542.

Meyers, W.J., 1974, Carbonate cement stratigraphy of the Lake Valley Formation (Mississippian), Sacramento Mountains, New Mexico. *Journal of Sedimentary Petrology*, v. 44, p. 837-861.

Meyers, W.J., and Lohmann, K.C., 1978, Microdolomite-rich syntaxial cements; proposed meteoric-marine mixing zone phreatic cements from Mississippian limestones, New Mexico: *Journal of Sedimentary Petrology*, v. 48, p. 475-488.

- Moldovanyi, E.P., and Lohmann, K.C., 1984, Isotopic and petrographic record of phreatic diagenesis: lower Cretaceous Sligo and Cupido Formations: *Journal of Sedimentary Petrology*, v. 54, p. 972-985.
- Mullins, H.T., Newton, C.R., Heath, K., and Van Buren, H.M., 1981, Modern deep-water coral mounds north of Little Bahamas Bank: Criteria for the recognition of deep water coral bioherms in the rock record. *Journal of Sedimentary Petrology*, v. 51, p. 999-1013.
- Narbonne, G.M., and Dixon, O.A., 1984, Upper Silurian lithistid sponge reef on Somerset Island, Arctic Canada: *Sedimentology*, v. 31, p. 25-50.
- Nurmi, R.D., and Friedman, G.M., 1977, Sedimentology and depositional environments of basin centre evaporites, Lower Salina Group (Upper Silurian) Michigan Basin: in Fisher, J.H., ed., *Reefs and evaporites—Concepts and depositional models: American Association of Petroleum Geologists Studies in Geology* 5, p. 23-52.
- Palonen, P.A., Booth-Horst, R., and Tanton, G., 1979, O.M.N.R. Oil and Gas Paper 2, 171p.
- Pearson, E.M., 1980, Sedimentology and diagenesis of the Warwick reef (Silurian), Lambton County, southwestern Ontario (unpublished M.Sc. thesis): University of Waterloo, Waterloo, Ontario, 250p.
- Petta, T.J., 1980, Silurian Pinnacle reef diagenesis—northern Michigan: effects of evaporites on pore-space distribution, in Halley R.B., and Loucks, G., eds., *Carbonate reservoir rocks: Notes for Society of Economic Paleontologists and Mineralogists Core Workshop No. 1*, p. 32-42.
- Pierre, C., and Rouchy, J.M., 1988, Carbonate replacements of sulphate evaporites in the Middle Miocene of Egypt: *Journal of Sedimentary Petrology*, v. 58, p. 446-456.
- Pierson, B.J., 1981, The control of cathodoluminescence in dolomite by iron and manganese: *Sedimentology*, v. 29, p. 797-817.
- Playford, P.E., 1980, Devonian "Great Barrier Reef" of the Canning Basin, Western Australia: *American Association of Petroleum Geologists Bulletin*, v. 64, p. 814-840.
- Pratt, B.R., 1982, Stromatolitic framework of carbonate mud-mounds: *Journal of Sedimentary Petrology*, v. 52, p. 1203-1227.
- Pray, L.C., 1958, Fenestrate bryozoan core facies, Mississippian bioherms, southwestern United States: *Journal of Sedimentary Petrology*, v. 28, p. 261-273.
- Prezbindowski, D.R., and Tapp, J.B., 1989, Aysmmetric dissolution textures as evidence of subaerial exposure. *Journal of Sedimentary Petrology*, v. 59, p. 835-838.
- Qing, H., and Mountjoy, E.W., 1989, Multistage dolomitization in Rainbow buildups, Middle Devonian Keg River Formation, Alberta, Canada. *Journal of Sedimentary Petrology*. v. 59, p. 114-126.
- Radke, B., and Mathis, M.L., 1980, On the formation and occurrence of saddle dolomite: *Journal of Sedimentary Petrology*, v. 50, p. 1149-1168.

Read, J.F., and Grover, J.R., 1977, Scalloped and planar erosion surfaces, Middle Ordovician limestones, Virginia: Analogues of Holocene exposed karst or tidal rock platforms. *Journal of Sedimentary Petrology*, v. 47, p. 956-972.

Richter, D.K., and Fuchtbauer, H., 1978, Ferroan calcite replacement indicates former magnesian calcite skeletons: *Sedimentology*, v. 25, p. 843-860.

Sandberg, P.A., 1983, Aragonite cements and their occurrence in ancient limestones: *Society of Economic Paleontologist and Mineralogists Special Publication No. 36*, p. 33-58.

Sanford, B.V., 1962, Sources and occurrences of oil and gas in the sedimentary basins of Ontario: *Proceedings of the Geological Association of Canada*, v. 14, p. 59-89.

Sanford, B.V., 1969, Silurian of southwestern Ontario: Ontario Petroleum Institute, Ninth Annual Conference, Technical Paper no. 5.

Sanford, B.V., and Brady, W.B., 1955, Paleozoic geology of the Windsor-Sarnia area, Ontario: Supplement to Memoir 240: *Geological Survey of Canada, Memoir 278*, 65 p.

Sanford, B.V., Thompson, F.J., and McFall, G.H., 1985, plate tectonics-a possible controlling mechanism in the development of hydrocarbon traps in southwestern Ontario: *Bulletin of Canadian Petroleum Geology*, v. 33, p. 52-71.

Sears, S.O., and Lucia, F.J., 1979, Reef growth model for Silurian pinnacle reefs, northern Michigan reef trend: *Geology*, v. 7, p. 299-302.

Sears, S.O., and Lucia, F.J., 1980, Dolomitization of northern Michigan Niagaran reefs by brine refluxion and fresh water seawater mixing: in Mazullo, S.J., and Zenger, D.R. *eds.*, Concepts and models of dolomitization: *Society of Economic Paleontologists and Mineralogists Special Publication No. 28*, p. 215-235.

Sharma, G.D., 1966, Geology of Peters reef, St. Clair County Michigan: *American Association of Petroleum Geologists Bulletin*, v. 50, p. 327-350.

Shaver, R.H., 1977, Silurian reef geometry-new dimensions to explore: *Journal of Sedimentary Petrology*, v. 47, p. 1409-1424.

Shaver, R.H., and Sunderman, J.A., 1989, Silurian seascapes: Water depth, clinotherms, reef geometry, and other motifs-a critical review of the Silurian reef model. *Geological Society of America Bulletin*, V. 101, p. 939-951.

Shaver, R.H., Sunderman, J.A., Mikulic, D.G., Klussendorf, J., McGovney, J.E.E., and Pray, L.C., 1983, Silurian reef and inter-reef strata as responses to a cyclical succession of environments, southern Great Lakes area: in *Field trips in Midwestern Geology*, Geological Society of America, 1983 annual meeting, Indianapolis, v. 1, p. 141-196.

Shukla, V., and Friedman, G.M., 1983, Dolomitization and diagenesis in a shallowing-upwards sequence: the Lockport Formation (Middle Silurian) New York State.: *Journal of Sedimentary Petrology*, v. 55, p. 703-717.

Smith, L., 1984, The Guelph-Lower Salina in southwestern Ontario: Subaerial exposure and episodic reef growth in a syn-erosional basin (abs): *Geological Association of Canada*, v. 9, p. 107.

Smith, L., Grimes, D.J., and Charbonneau, S.L., 1988, Karst episodes and permeability development, Silurian reef reservoirs, Ontario: in Milne, V.G., ed. Summary of Research, Ontario Geological Survey, Miscellaneous Paper 140, p. 124-132.

Smosna, R., and Warshauer, S.M., 1981, Rank exposure index on a Silurian carbonate tidal flat: *Sedimentology*, v. 28, p. 723-731.

Straw, W.T., 1985, Facies and depositional setting of the A-1 Carbonate (Silurian) in the Michigan Basin: in Cercone, K.R., and Budai, J.M., eds. Ordovician and Silurian rocks of the Michigan Basin and its margins: Michigan Basin Geological Society Special Paper No.4., p. 143-156.

Textoris, D.A., and Carozzi, A.V., 1964, Petrography and evolution of Niagaran (Silurian) reefs, Indiana: American Association of Petroleum Geologists Bulletin, v. 48, p. 397-426.

Textoris, D.A., and Carozzi, A.V., 1966, Petrography of a Cayugan (Silurian) stromatolite mound and associated facies, Ohio: American Association of Petroleum Geologists Bulletin, v. 50, p. 1375-1388.

Walker, K.R., and Alberstadt, L.P., 1975, Ecological succession as an aspect of structure in fossil communities: *Paleobiology*, v. 1, p. 238-257.

Wallace, M.W., 1987, The role of internal erosion and sedimentation in the formation of stromatolite mudstones and associated lithologies: *Journal of Sedimentary Petrology*, v. 57, p. 695-700.

Walls, R.A., Harris, W.B., and Nunan, W.E., 1975, Calcareous crust (caliche) profiles and early subaerial exposure of Carboniferous carbonates, northeastern Kentucky: *Sedimentology*, v. 22, p. 417-440.

Walls, R.A., Mountjoy, E.W., and Fritz, P., 1979, Isotopic composition and diagenetic history of carbonate cements in Devonian Golden Spike reef, Alberta, Canada: *Geological Society of America Bulletin*, v. 90, p. 963-982.

Wanless, H.R., 1979, Limestone response to stress: pressure solution and dolomitization: *Journal of Sedimentary Petrology*, v. 49, p. 437-462.

Wilkinson, B.H., 1982, Cyclic carbonate carbonates and Phanerozoic calcite seas: *Journal of Geological Education*, v. 30, p. 189-203.

Wilson, J.L., 1975, Carbonate facies in geologic history: Springer-Verlag, New York, 471 p.

Winder, C.G., 1961, Lexicon of Paleozoic stratigraphy, southwestern Ontario: University of Toronto Press, 121 p.

Wood, W.W., 1985, Origin of caves and other solution openings in the unsaturated (vadose) zone of carbonate rocks: a model for CO₂ generation: *Geology*, v. 13, p. 822-824.

Yanguas, J.E., and Dravis, J.J., 1985, Blue fluorescent dye technique of recognition of microporosity in sedimentary rocks. *Journal of Sedimentary Petrology*, v. 55, p. 600-602.

APPENDIX A: Core descriptions of studied wells

Colours described using the rock colour chart, Geological Society of America. In all instances white is N9.

Warwick Reef:

Imperial #399

Rochester Formation:

685.8 m to 680.9 m

The Rochester Formation is a dark grey to black (n3, n2, 5yr 2/1), calcareous to dolomitic shale. In places thin (2 to 3 cm) fossiliferous lenses are encountered which cause the unit to briefly grade to a wackestone or packstone. Equally, other areas are fossil poor. The fossiliferous areas are composed primarily of crinoid debris but brachiopod shells are also abundant, with minor constituents including trilobite and bryozoan fragments. These deposits may represent storm accumulations. The unit has a laminated appearance due to the abundance of shell layers and due to fissility. When dissolved in HCl, there is a strong sulphurous odour and the small amount of residue left behind suggests an argillaceous nature.

Pyrite can be found throughout. It appears as disseminated grains, as small patches, fills in burrows and rarely replaces small brachiopod particles. Porosity is very low and consists of small vugs (<1 mm, irregularly shaped and present where skeletal fragments have been partially removed. Dolomitization is patchy. It is micro to very finely crystalline and light grey in colour.

The contact with the overlying Lockport Formation is sharp and well-defined. It shows an irregular, undulatory surface and the patchy dolomitization abruptly terminates against the medium to dark grey (n5, n4) Lockport Formation. Small patches of pyrite are located below the contact. If the contact is an exposure phenomenon, it lacks any brecciation and was very brief. Due to the lack of any shallowing evidence, it is more probable is that it represents a marine hardground surface.

Lockport Formation (Gasport Member)

680.9 m to 676.0 m

The Lockport lowerdown is a medium to dark grey (n5, n4) sparsely fossiliferous wackestone that grades to a packstone in areas of skeletal fragment concentration. Conversely, there are small areas (up to 20 cm) that are more allochem poor and the unit grades downward to a mudstone.

Crinoid fragments are the most abundant skeletal fossil. They initially are very small, less than 1mm in diameter, but increase to 3 mm as the unit thickens. The largest fragment observed was 5 mm. Brachiopods are also plentiful, thin shelled and on average 3 mm in length. Small, horizontal, encrusting bryozoans (15 mm long and 2 mm wide) are also present. The shell fragments are held in a recrystallized mud, or rarely, a marine calcite. Shell fragments increase in number near the middle of the interval and a packstone texture is attained. At interval end the unit is again a wackestone. Porosity is low and primarily inter-crystalline. Some small vugs existed previously but these are less than 1 mm in size and are now filled with calcite spar. Stylolites are common, have low-amplitude and often are lined with pyrite or argillaceous matter. Pyrite is found as disseminated grains and in very small patches.

Dolomitization is more extensive than in the Rochester Formation. It is found in the mud matrix, is finely crystalline, light grey (n6), and may be due in part to bioturbation.

Dolomitization contributes most to any existing porosity. Rarely, white (n9) euhedral to anhedral fine dolomite crystals can be found plugging vugs. The upper 1m of the interval shows a high degree of dolomitization (finely crystalline) and only a few skeletal fossils, mainly crinoids and some brachiopods, are calcite. Because of the dolomitization the contact appears sharp.

676.0 m to 668.4 m

Overall, the interval is an argillaceous, light to medium grey (n6, n7), crinoidal, dolomitic wackestone that shows very small skeletal intervals and small mudstone intervals. Crinoids enlarge in size, obtaining sizes of up to 1.2 cm. Encrusting bryozoans are also present. They are thin, 1mm in thickness and average 20 mm long. Brachiopods see a size increase to about 6.0 mm long. Two lone, solitary rugose corals were observed at 669.6 m. They show evidence of transport, and are only 4.0 mm in diameter and 1.3 cm long (average). All organisms are held within a recrystallized mudstone. The average size of the allochems increases upwards through the interval.

Whispy stylolites are present in part, particularly in the more muddy sections where they skirt around skeletal allochems. Associated with the stylolites is pyrite. Also found in the muddy intervals is stromatactis. It features many of the usual characteristics, including flat to near flat floors and irregular roves. The stromatactis cavities all show a white (n9) isopachous lining of marine calcite cement growing perpendicular to the cavity wall with the cavity middle showing a second generation of cement. This growth is also calcite but is clear and contains rare disseminated pyrite grains.

Dolomite is confined to the matrix. It is very finely crystalline to micro-crystalline and is light grey in colour. Some dolomite however appears as coarse, white, euhedral, saddle crystals. It fills small voids and is the last cement to be grown. Little porosity remains due to the infilling by the marine cement. Where it is found it is primarily due to the tiny vugs and molds present. Very small amounts of inter-crystalline porosity can be found randomly within dolomites.

(Goat Island Member) ?

668.4 m to 653.2 m

Following a gradational contact covering approximately 1 m, there is a change to a light to medium grey (n6, n7), argillaceous crinoid-skeletal wackestone. Short intervals are coral and stromatoporoid rich. The interval shows abundant rugose corals by 654.3 m that show an increasing size up to 7 mm in diameter. Tabulate coral fragments also are abundant (*Favosites* sp. *Heliolites* sp. and *Halysites* sp.) and are oriented randomly. The fragments are 20 mm to 25 mm in size. Stromatoporoids, with a horizontal orientation and encrusting morphology appear at 657.7 m. Other skeletal allochems include brachiopods and bryozoans, also similar to the preceding interval. The bryozoans occupy various orientations, sometimes appearing as thickets, but most often provide good shelter porosity (subsequently filled with marine cement). Crinoids are 2 to 7 mm in diameter and in places are concentrated in lenses or beds.

Stromatactis is common in this interval but unlike the previous section, the infilling spar often consists of more than two generations. A white (n9) isopachous lining is followed by a light brown (5yr 6/4, 10yr 6/2) calcite lining which is then followed by a clear spar. Larger stromatactis cavities feature repetition of the white and brown cement layers. Some larger voids that are incompletely filled show that the marine cement is often botryoidal in morphology. Porosity is low with most former vugs and shelter cavities being completely infilled by marine cement. Where it does exist, porosity is mainly intra-fossil and found in corals. Vuggy and moldic porosity can be found and this occurs where skeletal organisms,

usually brachiopods, have been selectively leached. Thus molds and vugs are only a few millimetres in size. Inter-crystalline porosity is also present but in low amounts and is associated with dolomitization.

The mudstone matrix which supports and envelopes skeletal allochems is selectively dolomitized. As before, the dolomite is micro to very finely crystalline. White (n9), euhedral dolomite crystals up to 2 to 3 mm in size can be found in cavities occurring as a final pore-filling event. Stylolites are also common throughout the mud matrix. Recrystallization has occurred. This interval is assigned as the Goat Island Member on the basis of the increase in stylolites, the argillaceous nature of the unit and the gradual increase in allochems other than crinoids.

653.2 m to 649.8 m

A gradational contact is followed by a short interval of light grey (n7, n8), limey, dolomite mudstone to wackestone. Thin bryozoans (up to 1 mm) and tabular stromatoporoids are horizontally oriented, creating shelter porosity, and are associated with small tabulate coral fragments (*Favosites* sp.). The light grey dolomite mudstone shows thin 1 to 2 cm lenses of concentrated crinoid and brachiopod shell debris. Stromatactis is very evident and shows multiple generations of marine cement. In areas where cement does not completely fill a cavity euhedral, white (n9) dolomite crystals with curved faces complete the sequence. Stylolites are common. The unit very strongly resembles the underlying interval with the exception that fossil content is much lower. There is a gradational contact with the overlying interval.

649.8 m to 646.5 m

Interval is a crinoidal wackestone but after 10 cm changes for 1.1 m to a stromatoporoid-coral rudstone, light to medium grey (n6, n5) in colour. Minor amounts of crinoidal-skeletal debris are interspersed throughout. Rugose corals are abundant and up to 7 mm in diameter. Other corals are *Halysites* sp. and *Favosites* sp. fragments up to 15 mm in size and many have adapted an encrusting life habit. Stromatoporoids are both tabular and encrusting. There is a noticeable decrease in stromatoporoids after the short interval, however the rugose corals maintain their presence.

Crinoids are plentiful up to 5 mm in diameter as are brachiopod shell fragments. Bryozoans occur as before and provide shelter porosity. Brachiopods commonly show spar infill with or without geopetal fill. In places, the shells are concentrated into layers. All skeletal fragments are held within a light grey (n6) mud matrix. Marine calcite cement fills voids as multiple generations or it surrounds skeletal fragments.

Porosity is very low, moldic to vuggy but in places intra-fossil is present. The small voids occur where skeletal organisms have been partially removed or where calcite cement has incompletely filled a larger void. In places, stromatactis fabric is prevalent with a white (n9) calcite cement filling the characteristic pores. Larger pores show botryoidal calcite.

Dolomite is selective, being confined to the matrix and finer sediments. It is light grey (n7, n6) and micro-crystalline. Very coarse, white (n9), euhedral dolomite crystals occur in a couple of larger vugs and cavities where growth was unrestricted. It was a later event as it post dates calcite cements. Halite emplacement subsequently post dates the dolomite. The halite is clear with well-defined cubes up to 1 cm.

Stylolites are less common than before with horsetails being detected in part. Some pyrite is associated with these microstylolites.

At 646.5 m a very irregular surface exists, resembling a razor-sharp, cockling-like karst surface. Brachiopods and/or bivalves with cephalopods and accompanying rugose corals occur in a light grey (n6) limestone that shows selective dolomitization. This limestone is solutioned, abruptly terminated and overlain by marine calcite in multi-generation growths. Fingers of the limestone protrude into the cement from above, below and the sides. Small amounts of pyrite are noticeable below the surface.

Guelph Formation

646.5 m to 627.3 m

The interval begins as a light grey (n6) to light brown to buff (10 yr 6/2, 5y 7/2) coloured, crinoid wackestone for 7.0 m and then becomes a coral-stromatoporoid floatstone to rudstone with thin, crinoidal-skeletal wackestone to packstone intervals. Short intervals grade to a framestone higher up in the section. Corals are mainly *Coenites* (up to 1.0 cm diameter) and *Favosites* (averaging 4.0 cm in size), with fewer *Heliolites* and *Halysites*. Rugose corals are less abundant than in the previous interval but of similar sizes. Stromatoporoids are thin (1.0 cm), tabular and encrusting. In the shelly areas, crinoids are up to 5 mm in diameter as are brachiopod shell fragments. The brachiopods show a spar infill in part. There are much fewer bryozoans than before but they still provide shelter porosity. Shells are concentrated into layers as before. All skeletal fragments are held within a mud matrix that is patchily dolomitized to a light grey (n7) in places. Multi-generation marine calcite cement fills voids and it envelops skeletal allochems.

Minor tiny vugs represent the only porosity observed. These occur where calcite cement has failed to fill a once large void. Stromatactis is prevalent with a white calcite cement filling the characteristic pores. Larger pores also show a botryoidal cement morphology.

Dolomitization is patchily confined to the matrix . It is light grey (n7, n6) and micro-crystalline. Very coarse, late, white, euhedral dolomite crystals occur in a single vug. Whispy, horsetail stylolites are present but only in minor amounts. Some pyrite is associated with these microstylolites as before.

Around 635.5 m and after a gradational contact the unit shows a greater concentration of coral. The core changes to a light to medium grey (n6, n5) coral framestone with small floatstone to rudstone intervals. This interval is dominated by *Favosites* sp. which show good cementation (little intra-fossil porosity) to very poor cementation (very open corallites that are quite fragile). The corals are large with the maximum size unknown due to the small size of the core. They do however encrust and repeatedly grow ontop of one another. Many show a very thin, fine-grained, dark mud that fills chambers suggesting in situ growth. Borings are also found on the stromatoporoids present. Shelter porosity formed by the corals and stromatoporoids is infilled with a marine cement made up of multiple growth layers.

This calcite cement is isopachous in nature and white and beige (10yr 6/2) in colour. It fills cavities through successive cement layers or botryoids. In places it surrounds and envelops fragments. The banded cement is especially prominent where coral skeletons are scarce.

Locally, concentrations of associated skeletal matter includes; bivalves, brachiopods, crinoids, gastropods, cephalopods, and, coral and stromatoporoid fragments. These concentrations provide a base for coral growth. The stromatoporoids are infrequent in their occurrence but where present are thin (up to 7 mm), tabular and encrusting. Brachiopods may be to be spiriferids or atrypids. Allochems that resemble encrusting algae are also present.

Stylolites can be detected and in places contain small amounts of pyrite along with clay residue. Dolomitization is patchy as before and confined to the mud matrix. However the white euhedral dolomite crystals, present earlier, were not detected. The interval is recrystallized. Where allochems are scarce, muddy areas occur as small, thin layers. These layers separate coral growth into distinct packages and give a stacked appearance.

Overall porosity is poor. Some small vugs exist where marine calcite cement has not fully occluded a pre-existing vug. Good intra-fossil porosity occurs in selected *Favositid* corals and, rarely, small molds where brachiopods or molluscs have been removed.

627.3 m to 602.0 m

Following a gradational contact, this interval appears as a more consistent light grey (n6) to light brown (5yr 5/2), rugose and branching coral floatstone. Constituents remain somewhat similar to the underlying interval. The dominating tabulate corals are replaced by branching and rugose corals but not entirely excluded. The interval is briefly interrupted at 624.5 m and 609.0 m by a 15 cm thick, bryozoan-dominated packstone to grainstone. Also included are crinoids, brachiopods, molluscs and algae (?). Stromatoporoids are conspicuously rare throughout the interval with only a few thin, tabular organisms noticed.

Allochems are contained within a mudstone matrix that shows multi-generation marine calcite cement in former voids. The isopachous spar is white to cream colour (5y 8/4) but by the middle of the void it is clear and possibly dolomite. Botryoids leave small vugs where cementation is incomplete. Stromatactis is common. Extensive cementation at 624.5 m shows Coenites acting as the nuclei for the growth of cement botryoids.

Dolomitization is mainly confined to the muddy matrix. Fine-grained areas also show recrystallization. Porosity is low and mainly intra-fossil where tabulate corals are found. Interparticle porosity and small vugs occur in areas of concentrated skeletal debris where mud content is lower. In these areas, white, euhedral dolomite crystals with curve faces, multi-generation marine cement, bitumen, and scalenohedral spar help plug voids. Minor halite plugging is also noticeable as a final pore-filling event in these larger vugs (up to 30 mm x 15 mm).

The upper contact is gradational over about 3 m as faunal diversity decreases. Stromatoporoids are slightly more plentiful but are then overwhelmed by crinoids.

602.0 m to 578.1 m

The interval is a light grey (n6) coral floatstone that shows interruptions by skeletal packstones and grainstones where crinoids are concentrated and to wackestone where allochems are scarce. *Favosites* sp. and *Halysites* sp. are the corals present with some rugosans also. Stromatoporoids are thin, horizontal and encrusting types that show some borings. The skeletal intervals are to a maximum thickness of 15 cm. Allochems are contained within a micro-crystalline to very finely crystalline lime mud. The most plentiful organisms are crinoids. Other allochems include minor amounts of; brachiopods, bryozoans, corals and stromatoporoids fragments and algae. Bryozoans are also small and are of a branching variety. Also, where concentrated, allochems exhibit a rudimentary bedding with dips of 20-35° relative to the core sidewalls. Algal content begins to increase toward the top of the interval.

Calcite occludes pores as a blocky cement, or, in larger voids of 2 cm or greater, it appears as large 5 mm to 7 mm dog tooth crystals. Where it plugs pores, the calcite cement is multi-generation and often associated with stromatoporoids or bryozoans. The calcite is locally present in muddy areas as is the stromatactis. Euhedral saddle dolomite rhombs are also found in larger cavities but these are not as common as the calcite and postdate it. There appears to be very minor salt and anhydrite plugging both of which post-date the latest dolomites. Drilling mud may have removed additional salt and anhydrite.

Porosity is low and mainly interparticle. In those areas where cement is not pervasive, minor moldic and vuggy porosity remains. Intra-fossil porosity is locally present in corals. Small amounts of well-developed fracture porosity occur in places and show an associated dog tooth calcite (eg. 600m). Calcite crystal size increases with the increase in fracture width.

From 597.0 m to 598.6 m the core shows the effects of exposure. The medium grey (n5) wackestone is crosscut by a subvertical solution feature. A 2 mm thick, dark brown (5y 3/2, 5yr 2/1), isopachous fringe lines the original, scalloped rock, and shows an undulatory surface. The fill within this feature is very coarsely crystalline, buff calcite and clear spar that appears to contain some skeletal debris. Some minor pyrite concentrations are noticeable in this area and down to 598.0 m.

578.1 m to 570.6 m

This interval is a light grey (n6) to light brown (5yr 4/1) algal-brachiopod wackestone that shows sporadic, small zones of algal-skeletal packstone. The algae has an encrusting morphology and is contained within a very finely crystalline, recrystallized lime mud. Other accessory allochems are markedly missing with brachiopods being the notable exception. The brachiopods are up to 1 cm long and 6 to 7 mm wide, perhaps *Pentamerus sp.* Remaining allochems noticed include very small crinoids and thin (5 mm) encrusting stromatoporoids. The amount of allochems increases toward a proposed minor karst surface at 570.0 m.

Dolomite is still a minor constituent of the rocks and produces a light grey (n7) mottling. Porosity is low and is in the form of small vugs and molds.

At 571.0 m a small breccia zone is encountered of 0.5 m. Clasts up to 3 cm by 2 cm in size occupy a subvertical cavity within the core. Some clasts contain skeletal fragments while others are laminated and may be to be sections of broken pisoliths. These are all contained within a recrystallized mud matrix. Overtop of the breccia lies a thin 1 cm crust of very finely crystalline dolomite. Hydrocarbon staining has imparted a medium to dull brown colour but weathered, irregularly shaped, chalky blebs are scattered throughout. Small molds exist as does good interparticle porosity. Some larger vugs are also present and these show a late stage scalenohedral calcite.

570.6 m to 563.9 m

Interval is a light to medium (5yr 4/1, 5yr 4/4, 5yr 3/4), brown algal-brachiopod dolomite wackestone that is both oil stained and bitumen impregnated. A fine to very finely crystalline dolomite is pervasive and has obliterated many details. Crystals occur as to be anhedral to euhedral.

Minor brachiopod shell debris is scattered throughout. The brachiopods are similar to the underlying interval. Also present in minor amounts, is a finely crystalline, white calcite which lines and occludes pores within the wackestone and creates a stromatactis fabric. In places there are laminations suggesting possible algal stromatolite boundstones. The laminations are wavy or undulating and a fenestral fabric exists where there has been preferential dissolution.

The interval shows good inter-crystalline porosity due to dolomitization and there is an abundance of solution vugs up to 1.5 cm in size. Because of the dolomite lithology, the contact between the overlying and underlying intervals is sharp.

563.9 m to 536.1 m

This interval is characterized by a light to medium brown (5yr 4/1, 5yr 4/4, 5yr 3/4) algal-brachiopod wackestone. The main difference from the preceding interval is a lithologic change from dolomite to limestone. Encrusting algae dominate the interval but encrusting, thin (3.0 cm) stromatoporoids are also plentiful. Some globular morphologies were also noticed. Fragmented Favositid corals occur randomly scattered throughout. The corals are poorly preserved and show salt infilling. As in the lower unit, brachiopods are the main shell fossil with similar sizes observed. Crinoids however are rare to near non-existent. In their place, gastropods, bivalves, and ostracods (?) occur. The allochems are held within a fine-grained recrystallized lime mud matrix.

Isopachous marine cement is common. It is white to cream-coloured (5yr 8/4) and lines cavities, imparting a stromatactis fabric. In other areas it lines fossil fragments. Where no cement is present, salt acts as a pore occluder. It does not however act in conjunction with calcite cement.

Porosity is variable but overall it is good. Vugs up to 2.0 cm are obvious with some showing moldic remains of a former skeletal resident. The very fine-grained, lime mud areas have

small amounts of inter-crystalline porosity. Salt effectively plugs many molds and vugs, mainly in the corals and rarely in the brachiopods. It shows a preference for larger pores.

Dolomitization has reverted back to being a minor constituent. Where present it is patchy and confined to the matrix. There is a complete absence of saddle dolomite crystals. Few stylolites were noticed, but a number of fractures are present.

A possible karst fabric is found at 544.7 m. Here a small grike filled with grey-brown (5yr 6/1) dolomite mudstone crosscuts the core and the algal wackestone. The dolomite can be traced downward for 0.3m where it abruptly terminates with a very irregular contact against a light brown-light grey (n6, 5yr 4/1) algal-skeletal packstone. A thin 1 mm to 1.5 mm microlaminated crust exists between the dolomite and the original rock. Enhanced porosity in the form of vugs and molds is present

536.1 m to 531.8 m

Following a gradational contact, the new interval is a dark brown to chocolate brown to light brown (5yr 2/2, 5yr 3/4), finely laminated algal-stromatolite boundstone. In places where laminations are faint to scarce, the rock is an algal mudstone. Individual laminae are from 0.1 mm to 0.3 mm thick and alternate from light to dark colour.

This interval shows some meteoric effects. Small solution vugs and molds up to 1 cm in size are present with minor inter-crystalline porosity. Calcite crusts (5 mm to 7 mm thick) occur scattered throughout the section. The top of these crusts is hard and well lithified with the immediate underlying material somewhat softer. Vugs in places show a fine-grained, laminated silt lining their floors. Dog tooth calcite abuts into the remaining void.

Dolomitization is relatively minor, being patchy and associated more with the meteoric phenomenon and the muddy intervals. Some low-amplitude, sutured seams were noticed. A number of small fractures also exist. They attain a maximum width of 1.5 cm and are salt plugged.

531.8 m to 525.8 m

The preceding unit grades quickly into a thoroughly brecciated and karsted section. A large solution cavity is cut within the medium to dark brown (5yr 2/2, 5yr 3/4) algal stromatolite boundstone. Angular clasts of stromatolites up to 7 cm by 2 cm are contained within a dark brown (5yr 2/2) mud matrix. Mudstone clasts also add to the collapse breccia. Finer sized clasts are found lower down where the cavity is more narrow with larger clasts found in well solutioned areas. This results in both clast-supported and matrix-supported rock. All clasts are randomly oriented. In muddy areas, clasts show a tiny dark rind, while in clast-supported areas a white calcitic halo rims clasts. Remnants of broken and smashed pisoliths are also present.

Limestone predominates but small patches are solely dolomite. White, euhedral saddle dolomite crystals can also be found jutting into voids. Porosity varies from near non-existent with the rock tight, to highly porous and gutted. Porosity types are inter-crystalline and vuggy with some minor fracture porosity. Calcite cement has occluded some pores, sometimes acting in conjunction with later salt. Elsewhere, pores that escaped calcite cementation are now sealed solely with salt.

The dark brown nature of the matrix begins to change into reddish brown (10r 3/4) higher up. By the top of the section, traces of a green shale (5gy 5/2, 5gy 3/2, 10 gy 3/2) capping the reef can be found.

A-1 Carbonate Formation

525.8 m to 503.8 m

Following the unconformity with the underlying Guelph Formation, the Salina Group A-1 Carbonate Formation overlies the pinnacles. It consists of a dark brown to chocolate brown (5y 2/2, 5y 3/4), coralline algal, dolomite mudstone for 11.7 m followed by a tan to gold brown (5y 6/4), laminated algal-stromatolite, dolomite boundstone for the remainder of the interval. A fine mottling is noticeable and separates minor limestone from dolomite. The algal laminites alternate from dark brown to tan in colour. The tan layer is thickest (approximately 1 mm) with dark laminae being about 0.2 mm to 0.5 mm. Laminae are also coarsest at the bottom of the interval and are increasingly finer toward the top. The laminae range from rare horizontal to a more prevalent wavy to crinkly morphology.

Porosity is moderate to very good and is primarily inter-crystalline. Some fenestral porosity exists between the stromatolite layers and small vugs (< 1 cm) may be brachiopod or ostracod remnants. Euhedral dolomite crystals protrude into the vugs. The minor limestone areas are tight with only a small amount of inter-crystalline porosity. A great number of vugs show plugging by halite. The salt occurs without being preceded by dolomite or calcite growth.

The last few meters of the interval shows traces of individual anhydrite lathes, randomly oriented, and up to 1 cm long by 2 mm wide.

A-2 Evaporite

503.8 m to 502.0 m

An unconformable erosional contact leads to the anhydrite of the A-2 Evaporite Formation. It consists of nodular, folded, felted and enterolithic anhydrite that is blue to blue-white (5b 8/2, 5b 6/2) in colour. Interspaced within the anhydrite are wispy stringers of gold-brown (5y 6/4) dolomite. This helps provide a chickenwire texture in places.

A-2 Carbonate Formation

502.0 m to 501.4 m

This short, initial unit is a light to medium grey (n6, n5), argillaceous shale. It shows regular, planar laminations, is fissile and dolomitic.

501.4 m to 495.0 m

The interval is a micro to very finely crystalline, light grey to olive grey (n7, 5y 6/1), argillaceous, mottled dolomite. There is scattered pyrite, hydrocarbon staining and burrowing throughout. Porosity has vugs to 1 cm by 1 cm subsequently salt plugged and good inter-crystalline porosity. The halite is not preceded by either dolomite or calcite cements in vugs.

Imperial #619

Guelph Formation

585.5 m to 580.3 m

The interval is an olive-brown (5y 5/6) skeletal wackestone. Many of the allochems have been leached away resulting in enhanced porosity. Rugose corals, brachiopods and minor crinoids have been selectively removed to create vugs up to 1.5 cm in size. Remaining allochems are held within a recrystallized lime mud. Former vugs over 1.5 cm are now salt plugged. The intensive, dissolutioned look of the rock makes identification difficult. An appearance much

like popcorn is common. Little dolomite is present, confined to small patches in the matrix. Hydrocarbon staining imparts a gold-tan (5y 6/4) colour and oily smell.

580.3 m to 579.4 m

The core shows a small subvertical solution feature cut through light grey to light brown (n6, 10yr 6/2) dolomitic limestone. Sides of the feature show scalloping and a thin 1 mm black rind is patchily present. The feature is plugged by massive (up to 3 cm) salt crystals. This karst surface may be linked to the porosity noticed in the preceding interval.

579.4 m to 571.8 m

The interval is a coral-bryozoan floatstone to wackestone that is light brown to olive (10yr 6/2, 5y 5/6) in colour. The bryozoans are branching types and 0.5 cm in diameter and up to 3.0 cm long. Approximately, 60 % are enveloped by a thin isopachous layer of olive to cream-coloured (5y 6/1, 5y 7/2) calcite. Tabulate corals were not noticed. Rather small fronds of *Coenites* are plentiful with the 'flowers' about 1.0 cm in diameter. Like the bryozoans, they are also cement enveloped. Rugose corals are also present. They are up to 0.5 cm in diameter and are preferentially leached. Allochems are held by a recrystallized lime mud.

In places, skeletal fossils are plentiful, especially brachiopods (up to 1.0 cm in size). Many of the brachiopods are also leached. Thin, tabular stromatoporoids complete the major identifiable allochems. Overall porosity is good as allochems show leaching to some degree. The exceptions being the bryozoans and the corals. Molds and vugs are up to 1.0 cm on average. Several former pores were larger (up to 2.0 cm) however these are now salt filled. Compared to previous depths, there is more stromatactis fabric. The former voids are small, averaging about 1.5 cm along their floors, and are filled with a cream-coloured marine cement.

Dolomitization is slightly more pronounced than in the previous sections as the core has more muddy layers (ie. 578.5 m to 578.8 m and 572.7 m to 573.0 m) and more overall mud content. Where present, dolomitization is patchy and has left the core light grey in colour. Only a single saddle dolomite crystal, for the whole interval, was noticed at 574.5 m.

571.8 m to 553.8 m

A gradational contact over several metres results in a light brown to olive (10 yr 6/2, 5y 5/6) coloured coral-stromatoporoid floatstone to framestone to rudstone. It features large, tabulate Favositid corals that are larger than the core diameter. These have good inter-crystalline porosity. rugose corals up to 4.0 cm long by 1.0 cm in diameter are also included but they show leaching in most cases. Stromatoporoids vary from thin encrusters up to 2.0 cm thick to more bulbous encrusters up to 6.0 cm thick. There is abundant skeletal debris throughout including fragments of brachiopods, gastropods, trilobites (?) and crinoids. Bryozoans are found in small numbers in the lower portions of the interval. Algae is a minor allochem initially, but by the top of the core algae appears to be dominant. Within these algal areas a stromatactis fabric is evident.

Many of the skeletal allochems have been leached with subsequently one or two generations of isopachous marine cement infilling. In some instances, there is a small amount of sediment on the floor of the former void. A final emplacement of clear salt occludes many pores. Large vugs do remain open and their highly irregular shape suggests that stromatoporoids may have initially occupied the site. What porosity remains is largely due to small vugs and inter-crystalline porosity. Pores < 0.5 cm remain open while most of the larger are filled. Dolomitization is patchy and matrix confined. Some fine-grained mudstone layers are present and these are now more dolomite rich. These thin dolomite layers at 565.1 m to 564.8 m, 561.4 m to 560.8 m, and 556.6 m to 556.9m give the interval a sectioned, stacked look.

Imperial #407

Guelph Formation

622.1 m to 611.4 m

The core initially starts in a coral-stromatoporoid floatstone to framestone to rudstone that is light brown to light grey (n6, 10tr 6/2) in colour. Favositid corals are numerous with pieces up to 8.5 cm thick. The smaller stromatoporoids are usually 3.0 cm to 4.5 cm long on average and 2.0 cm to 3.0 cm thick. Both the corals and stromatoporoids mutually encrust one another. *Coenites* sp. and rugose corals were noticed. All are contained within a recrystallized lime mud.

The effects of solutioning of allochems has made only the larger constituents readily identifiable. Consequently, it is difficult to recognize the smaller skeletal fragments. It appears that brachiopods, crinoids, gastropods, trilobites and algae (?) are present. Vugs are to a maximum of 2.0 cm by 1.5 cm with almost all major ones (> 0.75 cm) being salt plugged.

Some minor compaction features in the form of stylolites are present. They are single stylolites with a low-amplitude, wavy, residue-less appearance. Dolomite was noticed in only one locality from 617.5 m to 616.8 m. It is crypto-crystalline to very finely crystalline and may be lime mud originally. Rare saddle dolomite can be found in places, predating salt.

611.4 m to 609.0 m

This interval is very similar to the preceding one featuring a light brown to light grey (10yr 6/2, n6) coral-stromatoporoid floatstone to framestone. However the core has been intensely solutioned resulting in a popcorn-like appearance. Skeletal organisms are as before but almost all have been leached away to leave large (up to 4.0 cm), irregularly shaped vugs and smaller molds. Salt emplacement has again occluded porosity in larger vugs and it post-dates saddle dolomite crystals. The salt shows evidence of solutioning also, probably the result of drilling.

609.0 m to 608.6 m

Abruptly overlying the solutioned area is a small zone of light grey to light brown (10yr 6/2, n6) breccia. It has irregular, undulatory upper and lower contact surfaces. Clasts are less than 1.0 cm in size and the interval is slightly pyritic

608.6 m to 601.4m

Atop the sharp contact, there is a return to the coral-stromatoporoid floatstone to rudstone that is light grey to light brown (10yr 6/2, n6) in colour. Skeletal organisms are slightly more robust looking than in lower sections, but are of the same fauna types. Corals and stromatoporoids are noticeably absent in the one metre section above the bottom contact. Here, there is an abundance instead of shelly organisms with brachiopods dominating over crinoids and gastropods. Porosity is mainly inter-crystalline but some small, salt filled, former vugs exist. No calcite or dolomite is associated with the salt. Rare saddle dolomite crystals are randomly placed in several vugs. This constitutes the only noticed dolomite.

601.4 m to 600.8 m

After another sharp contact a small, poorly lithified almost chalky zone exists. It features small (<5 mm) clasts of medium-crystalline dolomite held within a more calcareous matrix.

The light grey to tan-gold (n6, 5y 6/4) coloured unit has good pinpoint porosity and minor salt filled former vugs that are not larger than 5 mm in size.

600.8 m to 586.0 m

The interval is a medium brown to tan-gold (5yr 3/4, 5y 6/4) algal-brachiopod wackestone with accessory solitary, rugose corals and small, thin, tabular to bulbous, encrusting stromatoporoids. Coral, brachiopod and stromatoporoid content is greater in the lower portions of this section. Here, the observed sizes of each had the rugosans being 1.5 cm long and the stromatoporoids double that. Rarely, tabulate and branching corals are present. Algae appears to be of a branching variety and is found in a patchily dolomitic, recrystallized lime mud. Accompanying the algae is a stromatactis-like fabric, however instead of a carbonate cement, salt is the pore filler.

Brachiopods have been selectively removed and they leave small vugs and molds up to 5 mm in size. In large solution vugs, well-developed large salt crystals plug and nearly occlude porosity. Up to 90 % of all voids are subsequently salt plugged. No saddle dolomite was noticed.

586.0 m to 585.8 m

Across an abrupt contact, a small weathered zone is located. Here, a 20 cm chalky, poorly lithified, calcified mud is medium to chocolate brown (5yr 2/2, 5yr 3/4) in colour. Small pellet-like clasts about 2mm in size are plentiful. Not as plentiful are small, wavy, low-amplitude, single stylolites.

585.8 m to 572.1 m

Another sharp contact results in a return to a, medium brown (5yr 2/2), algal-brachiopod wackestone similar to lower sections of the core. Abundant small stromatactis cavities (maximum 4.0 cm floor length) exist and most are now filled with a single generation of cream-coloured (5y 8/4) calcite. In those instances where the calcite did not occlude porosity, salt finishes the plugging. Few stylolites were observed and they are wispy. Dolomitization is patchy and matrix confined.

572.1 m to 570.0 m

Gradational contact to a light grey to olive to light (n6, 5y 5/6) brown, well-developed to faintly laminated, algal stromatolite, dolomite boundstone. The laminations are approximately 0.5 mm to 1.3 mm in thickness and range from wavy to sub-horizontal. Some fenestral porosity exists but most has been destroyed by salt emplacement. Stylolites are common but not abundant and single wispy seams trace along laminae.

570.0 m to 566.9 m

Core sharply reveals a karst breccia infilling a solution cavity cut into the pre-existing algal boundstone. It features clasts that are medium brown (5yr 3/4) in colour, contained in a darker brown (5y 2/2) mud matrix. The highly brecciated, randomly aligned clasts were originally stromatolites, pisoliths and caliche crusts. Clasts as large as the core width are common with smaller pieces located at the bottom of the interval. Single stylolites dart around the clasts which also feature thin, dark coloured rinds. The green shale, noticed in other cores was not observed. Porosity is very low and the core is dolomitized to a high degree.

A-1 Carbonate Formation

566.9 m to 537.1 m

Unconformably overlying the karst zone, this interval begins as a burrowed algal wackestone for 17.5 m and then becomes a medium brown to tan (5yr 3/4, 5y 6/4), algal dolomite boundstone. The small section to 566.4 m is chocolate brown (5yr 3/4) and appears to be coralline algae. This however is rapidly replaced by faintly, then well laminated algal-stromatolite boundstone. The laminations are planar-horizontal to crinkly to undulatory in places and range from 0.5 mm to 1.5 mm in thickness. The thickest laminations are tan coloured and dips up to 15° are common.

Porosity varies from very good fenestral and inter-crystalline to very poor. Any pore that is larger than 5 mm is salt sealed with no precursor carbonate cement. Rare vugs show very well-developed salt crystal faces. Stylolites are common but not plentiful.

A-2 Evaporite Formation

537.1m to 535.5 m

The upper section of the core is a blue to blue-white nodular (5b 6/2, 5b 8/2), felted, enterolithic and rarely, chicken-wire anhydrite. Whisps of gold to tan (5y 6/4) coloured, crypto-crystalline dolomite exists within the anhydrite. Nodules average 1 to 2 cm in size.

Rosedale Reef

Union Enniskillan 8-9-II A

Rochester Formation

666.6 m to 661.7 m

The Rochester Formation is a dark grey to medium grey (n2,n3,n4), dolomitic to calcareous shale. Thin 2.0 cm to 3.0 cm beds of skeletal material cause wackestone sections. Most of the debris is tiny crinoid material averaging 1.0 mm to 2.0 mm in diameter. Some very thin shelled brachiopods and trilobites are also present as well as unknowns. Other areas are skeletal poor. The formation is laminated and fissile in the lower part of the core, but it tightens considerably near its contact with the Lockport Formation.

Pyrite is common, being found as disseminated grains, replacing brachiopods and lining and replacing burrows. There is extensive pyrite concentrations at the Rochester-Lockport contact. Dolomitization is patchy throughout and is micro-crystalline to very finely crystalline. Skeletal allochems remain calcitic. The upper contact is sharp, irregular and undulatory. Some pyrite can be found adjacent to and above the contact, in the Lockport. The upper few centimetres of the Rochester changes to an olive (5y 6/1) colour and bioturbation is possible. Given the lack of any solid evidence of shallowing, the contact is interpreted to be a marine hardground.

Lockport Formation (Gasport Member)

661.7 m to 646.8 m

The Lockport begins as a dark brown to blackish (n2, 5yr 2/1) mudstone, but changes in less than 1 m to a light grey to medium grey (n5, n6), crinoidal, dolomite wackestone. Small sections up to 4.0 cm thick grade upward to packstones or grainstones where crinoids have been

deposited in thin sheets. Other small sections grade down to mudstone where allochems are scarce. Crinoids are small and starved looking. They attained a maximum observed size of 4.0 mm in diameter. Brachiopods that accompany the crinoids are also small (3.0 mm to 4.0 mm) and thin shelled. Scattered larger specimens, possibly Pentamerids can be found.

The interval has a mottled look. This may be due to bioturbation or the effects of different sizes of dolomite crystals. Pyrite is scattered throughout as disseminated grains. Dolomitization is complete with only allochems retaining any calcite precursors. Two distinct crystal morphologies were observed, consisting of a fine-grained, anhedral, matrix dolomite and a less common dolomite of larger euhedral rhombs.

There is good inter-crystalline porosity with small vugs up to 2.0 mm where shelly organisms have been leached away. Rarely, larger vugs of 3.0 cm by 2.0 cm can be found. These vugs have a few saddle dolomite rhombs inside and large broad laths of celestite (?). The laths are up to 4.0 mm wide by 1.0 cm long. Only the larger vugs show the dolomite and celestite crystals. In places, intermediate sized vugs have a fine-grained, beige dolomite mudstone infilling. Where this infill has not been complete, salt occludes the remaining porosity. This gives a stromatactis-like fabric, but without the marine calcite cement.

Stylolites are not very common but can be up to 1.0 mm thick with small clay accumulations and some scattered pyrite. Porosity decreases toward the upper contact and allochem content drops off.

Goat Island Member

646.8 m to 628.5 m

Following a gradational contact, the Goat Island Member displays the same characteristics as the Gasport but with an increase in stylolites and argillaceous content. The interval is a light to medium grey (n6, n5), crinoidal to skeletal, dolomite wackestone that changes in places to a packstone. Initially, crinoids are a similar size to those in the Gasport, but by the top of the member, they are up to 2.0 cm in diameter. Stromatoporoids occur at 637.6 m and they are thin (< 1.0 cm) tabular types. Other varieties also are present. They are bulbous to hemispherical (5.0 cm thick), show distinct laminae and pillars, and encrust. Fracturing of the thin stromatoporoids and boring of the bulbous ones is common. A dolomite mud infills the holes. Reef-building organisms are not detected from 630.6 m up to the section top. Bryozoans are found in significant numbers by 632.8 m. Each 2.0 to 3.0 mm thick bryozoan creates a small shelter cavity that is filled with fine-grained dolomitic mud of cement spar. However, by the top of the section, the bryozoans have also decreased in number.

Brachiopods constitute another plentiful allochem. They are up to 1.0 cm long and may be Pentamerids. Solitary rugose corals occur at 632.2 m and initially are 5.0 mm in diameter. Favosites, Coenites and Halysites are also present.

Stylolites are highly visible in the Goat Island. They occur in concentrated horizontal swarms and lend a nodular effect to the core. Minor clays are concentrated along the stylolites. Porosity is low and inter-crystalline. The core is finely crystalline dolomite, but is calcareous by 637.9 m. At 634.9m, the unit becomes limestone with a trace of dolomite and a light grey to olive (5y 6/1) colour dominates. At 628.5 m, the section abuts against a spectacular karst feature that represents the top of the Lockport.

628.5 m to 625.8 m

This section consists of a massive solution conduit carved into the existing skeletal packstone and an associated karst breccia that infills the lower cavity. The country rock is similar to the underlying section. Allochems are plentiful and bryozoans are more efficient at providing shelter porosity. One time pores are sealed by; a white isopachous calcite cement, the isopachous cement and a later clear spar, or a double isopachous layer and either clear spar

or anhydrite. The cements are governed by pore size with the larger pores requiring the three cement event. All of this is overshadowed by the karst cavity.

The lower reaches of the conduit terminates against a sutured, stylolitized contact. Below the contact, solution features are not obvious. Above the stylolite, a small 1.0 cm to 4.0 cm grike contains skeletal material, collapse breccia and cement fragments. This grike widens upward and the clasts are contained in a combination of white, coarsely bladed anhydrite and a fine-grained mud. The cavity widens to encompass the entire core and shows excellent solutioning and scalloping of the conduit walls. All pre-existing fabrics have been truncated. Stylolites trace their routes to the edge of the cavity and stop.

A 1.0 mm to 3.0 mm, isopachous, marine cement lines the conduit in places and is excluded in others. Following the cement, a turquoise (5b5/6) anhydrite completely seals the grike. The cavity narrows again around 626.7 m and anhydrite content drops off. The exact top of the feature is unknown as main pipe moves away laterally and disappears.

Dolomite is negligible in this zone. Some rare vugs and molds of brachiopods and rugose corals exist and these have late scalenohedral calcite wedges protruding into the small void.

Guelph Formation

625.8 m to 613.0 m

The Guelph begins as a light grey to light brown (n6, 10 yr 6/2), skeletal wackestone made up of crinoids, bryozoans, brachiopods, rugose corals and thin (6.0 mm to 7.0 mm) encrusting stromatoporoids. The allochems start out small, but attain sizes similar to those in the underlying Goat Island and are contained in a recrystallized lime mud. The bryozoans, 1.0 mm to 4.0 mm thick, are the primary allochems and line the walls and roves of pores. Rugose corals are up to 1.0 cm wide and 3.5 cm long. Coenites appear by 617.1 m. Stromatactis is prevalent with most cavities showing marine, calcite cement fills. Marine cement also radiates outward from many bryozoans, Coenites and rugose corals. Only a single cement event was noticed as clear spar was not found. About 20 % of all pores remain partially open, having botryoidal cements that do not occlude. Very minor salt completes some cavities.

Small fractures can be found throughout the interval. They have a white, bladed anhydrite fill or late saddle dolomite crystals inside. The fractures are a later phenomenon as they cross-cut and truncate allochems and the abundant stylolites. The saddle dolomite was the only dolomite observed. Porosity is only fair due to the marine cement. Many corals show intra-fossil porosity and vugs to 1.0 cm can be found, but pores are poorly connected.

From 622.1 m to 620.3 m, a rugose floatstone interrupts the wackestone facies. The solitary corals are up to 2.0 cm in diameter and 6.0 cm long. Where they contact a pore, the rugosans show a marine calcite growing radially from them.

613.0 m to 604.8 m

This interval represents a very gradual change from a skeletal wackestone to a light grey (n6, n7) to buff (5y 7/2) coloured stromatoporoid-coral floatstone. Only thin stromatoporoids are initially present with the more common bryozoans, crinoids, brachiopods and rugose corals. However, by the section end, stromatoporoids, Favosites, Halysites and Coenites are the more noticeable organisms. Allochem sizes are similar to the underlying interval. Stromatactis is common through most of the unit but is absent by the top. Thin layers of skeletal material are present consisting mainly of brachiopod and crinoid debris.

Very noticeable in this section is the remnants of a potential karst event. Beginning at 612.2 m, a light brown (10yr 6/2) to chocolate brown (5yr 3/4) sediment fills former vugs. It is very fine-grained and surrounds allochems. By 610.8 m, a fine breccia criss crosses the core filling a small solution feature. It is composed of irregularly shaped clasts up to 1.0 cm in size, derived from the wall rock. A later, light blue-white (5b 8/2) calcite cement helps fill the

cavity. The silt and breccia reappear several times to the top of the interval. Stylolites are very common as they circumvented each clast. Minor salt plugging accompanies the breccia. Pyrite is common in places. The top of the cavity has a three event fill. Very coarse, white, poikilotopic calcite is followed by large 1.0 mm to 2.0 mm saddle dolomite crystals and a final salt plugging event.

604.8 m to 581.6 m

Following the gradational contact, the reef shows a core of light to medium grey (n6,n5) coral-stromatoporoid floatstone to framestone to rudstone. The relative amounts of stromatoporoids versus corals varies and at times the interval is more stromatoporoid dominated.

Initially, the unit is muddy and the encrusting stromatoporoids and corals are not bigger than 4.0 cm long. Brachiopods, bryozoans and rugose corals are also found. Stylolites are common and show well-defined single sutures.

By 599.8 m, stromatoporoids are mainly bulbous varieties and up to 15 cm thick. Favosites, Coenites, Heliolites and Halysites make up the corals present and many occur in situ. Individual Favosites up to 9.0 cm were observed, and, Coenites thickets and Halysites are up to 12 cm high. Throughout the interval, thin beds (up to 1 m, but averaging 10 cm) of mud, crinoids, bryozoans and brachiopods interrupt the coral growth. These beds are often grainstones and show some leaching of allochems. A recrystallized lime mud is the associated matrix.

Porosity varies within the unit. Corals show good intra-fossil porosity. Stromatoporoids and bryozoans created shelter porosity, but this has been occluded in most instances by an isopachous white calcite cement and a follow-up clear spar. The leaching of organisms has left many vugs and molds averaging 2.0 cm to 3.0 cm in size. These pores may be cemented shut by calcite cement, occluded by salt, occluded by calcite and then salt or they may remain open.

Dolomite was limited to plugging numerous small fractures that jut into the core and to several pores that have euhedral, saddle dolomite crystals. It is possible that some dolomite is contained within the matrix of the interval especially more muddy areas. Stylolites are common as sutured seams. In more muddy areas, small swarms of stylolites are found. However, the largest observed amount of clay along any stylolite was 2.5 mm.

581.6 m to 571.2 m

The coral-stromatoporoid facies show a gradational change over a few meters to a combination light grey (n6, n7) to buff (5y 7/2) coloured, coral-stromatoporoid floatstone and skeletal packstone. Porosity is increased greatly and continues to increase upward to 575.5 m. Skeletal debris is made up of brachiopods mainly, but crinoids, gastropods, bivalves, algae, bryozoans, corals and stromatoporoids are also present in number. Allochems show abrasion due to transport and stromatoporoids are overturned and fractured. Moldic porosity is rare but vugs of up to 3.0 cm by 2.0 cm are common. Many vugs show a salt plugging as do fractures. This suggests that salt plugging was a later event. Marine cement, pre-empting the salt, is absent or has been removed. A red-brown (10yr 4/6) silt remains in some cavities and is within some salt crystals. The interval begins to tighten at 575.5 m. Dolomite was not found. Stylolites are present as low-amplitude, single sutured seams. They have little clay associated with them.

The upper contact is sharp and across a stylotized surface. Above the stylolite, salt plugging is absent. For 0.3 m above the stylolite, a small zone of weathered corals and stromatoporoids show solutioning, abrasion and fracturing. A large (5.0 cm), open, subvertical, solution feature tops off the unit.

571.2 m to 556.6 m

The core now shows a light brown (10yr 6/2) to tan coloured algal-brachiopod wackestone. In places, the interval grades up to a packstone for short distances. The interval is dominated overall by algae. In places, other organisms are prevalent but not abundant. Solitary rugose corals, Coenites, Favosites and broken stromatoporoid fragments are up to 3.0 cm in size. All are surrounded by a recrystallized lime mud. The allochems show solutioning and the effects of bioerosion. Brachiopod molds are common and up to 1.2 cm long. Porosity is generally low but short intervals show vugs to 2.0 cm and molds (see 564.5 m to 559.0 m). Dolomitization and saddle dolomite was unnoticed. Stylolites are randomly placed and are low-amplitude, wispy to sutured types with small amounts of clay.

At 558.7 m, the unit begins to turn a light grey (n6, n7). Small, open fractures occur and most allochems have been solutioned away. By 557.5 m, the unit is tight and irregular surfaces can be found.

A 7.5 cm laminated, very slightly dolomitic, mudstone caps the section. There is only a very slight dip to the laminations. A 3.0 mm, purple (5p 2/2) deposit, of unknown origin, exists at the base of the mudstone. The mudstone is topped by a 3.0 mm to 4.0 mm cream-coloured (5y 8/4) crust. This crust is itself brecciated in places and clasts are found lower down in the mudstone. Atop the cream-coloured crust, a very calcareous, chalky and porous layer sits and it too has been dragged downward and mixed with the fine breccia. Some white to cream-coloured (5y 8/4) gypsum is also associated with the feature. The cap appears to be an exposure phenomenon.

556.6 m to 553.5 m

Overlying, is a tan (5y 6/4) to medium brown (5yr 3/4), algal-brachiopod mudstone to wackestone. Small brachiopods accompany the algae and when leached leave vugs and molds up to 1.0 cm in size. Solitary corals up to 7.0 mm in diameter, and rarer crinoids to 5.0 mm are also found. Well-developed bryozoan thickets occur. White marine calcite infills former cavities and creates stromatactis. Rarely, when cementation is not complete, larger vugs show a botryoidal calcite cement morphology. Stromatoporoids begin to occur by the interval top. Dolomite was not observed. The section is muddy and single seam stylolites are common.

553.5 m to 547.9 m

There is a gradational change to a short section of light grey (n6, n7), coral-stromatoporoid floatstone to rudstone. The interval consists of displaced Favosites tabulate coral pieces. Most are 3.0 cm to 4.0 cm in size however, some pieces are to 10 cm. Stromatoporoids are equally plentiful and like the corals, most show evidence of abrasion. Some stromatoporoids are encrusters. Brachiopods, bryozoans, algae and rare crinoids accompany the reef allochems and are contained in a medium brown to chocolate brown (5yr 3/4) recrystallized mud.

There is good intra-fossil porosity within the corals, and brachiopods have left small vugs and molds to 1.0 cm. Dolomitization is rare and confined to the matrix in patches. It may contribute to the small amounts of inter-crystalline porosity.

547.9 m to 545.6 m

The core gradationally changes to a medium brown (5yr 3/4), skeletal wackestone. Bryozoans are plentiful as are small Halysites chains, Coenites, brachiopods and rare crinoid pieces. Large, bulbous, encrusting stromatoporoids to 10 cm high, and with borings, are found. Porosity is low as most all vugs and molds show a multi-generation isopachous cement that occludes porosity. Some vugs do remain partially uncemented and these show an isopachous cement rind followed by scalenohedral calcite crystals. Corals have some intra-fossil porosity. The cemented cavities resemble stromatactis but without the internal floor sediment.

Stylolites are common and limited to mud areas. They skirt around allochem but do not cross-cut them. Dolomite was unobserved.

This interval is capped abruptly by a dipping (35°), laminated mudstone, light brown (10yr 6/2) in colour. A thin, dark rind coats portions of the top of the mudstone, while the remainder is coated by a cream-coloured (5y 8/4) rind. Atop the rinds, an 8 cm breccia containing angular clasts can be found. The clasts consist of rind fragments, stromatoporoids pieces, mudstone clasts and pieces of the laminated mudstone from below. The breccia is topped by a sharp, thin (1.0 mm to 3.0 mm) black rind. Lastly, a laminated mudstone 6.0 cm thick, completes the section. This mudstone is similar to the first except that the laminations are near-horizontal. A sharp, stylolitic contact on the top of the second mudstone shows an algal wackestone overlying.

It is possible that this feature may be a storm feature, however, the lack of graded bedding and the presence of laminated mudstone clasts much higher in the breccia suggests another genesis. The rinds and laminated muds may represent a karst exposure surface and subsequent soil development.

545.6 m to 540.0 m

After the stylolitic contact, the core returns to being a medium brown (5yr 3/4), algal-brachiopod wackestone to algal mudstone. Accessory allochems are brachiopods and small crinoids and bryozoans are present but scarce. Pellets are also an accessory allochem. Rare, thin stromatoporoids and tabulate corals up to 7.5 mm are found. Some allochem have been leached away to leave one time vugs, but these are now filled with an isopachous marine cement that creates stromatactis. Nevertheless, despite the low porosity, some vugs to 1.5 cm still exist. Brachiopod moldic porosity is on the order of 5.0 mm. Dolomite was not observed again.

Several thin, laminated crusts occur throughout the interval. Up to 1.0 cm in thickness, they occur at; 562.1 m, 573.3 m, 572.4 m, and 571.8 m. With the lack of any exposure evidence these features most likely are marine in origin. Due to the muddy nature of the interval, stylolites are more pronounced. Very little clay residue is associated with them however. Mainly, they are wispy seams.

This brief interval is also capped by a possible exposure feature. A medium brown (5yr 3/4), horizontally laminated mudstone approximately 5.0 cm thick, drapes on top of the underlying algal facies. A 2.0 cm lens, chalky, poorly lithified and made up of breccia clasts and anhydrite blades, sits on top of the mudstone, separated from it by a thin, cream-coloured (5y 8/4) crust. The small clasts may have been part of the crust that were ripped up. An additional laminated mudstone rests on top of the lens. These laminations are curved, not of regular thickness, and in places are irregularly shaped. This 5.0 cm mudstone is topped off by a white to cream-coloured (5y 8/4) crust which is also irregular in shape. Stylolites are found along major lamination contacts and between the mudstone-lense contacts. Several laminations in the second mudstone show abrupt displacement. This may be a possible settling phenomenon as not all laminations above the disruption are themselves offset.

540.0 m to 534.9 m

The core returns abruptly to a medium brown (5yr 3/4), algal-brachiopod wackestone to mudstone. Thin shelled brachiopods are more common than in the previous interval and are up to 1.0 cm in size. Small tabulate corals and possibly ostracods are present. Pellets are plentiful. The unit becomes light grey (n6, n7) by 537.1m. Larger vugs and molds show a white, isopachous cement that leaves much open pore space. Scalenoedral calcite crystals follow. Smaller pores show the same isopachous lining but here the pore is occluded. Consequently, porosity is somewhat low. Dolomite was not detected.

A short zone of collapse breccia is found at the top of the section. Small clasts averaging 1.0 cm, but as large as 3.0 cm long axis, clog a small subvertical solution feature. This zone is probably related to the overlying karst zone.

534.9 m to 531.9 m

Following the short exposure zone, the core reveals faint laminations and appears to be an algal-stromatolite boundstone. The light grey (n6, n7) laminations are horizontal and very regular in their spacing (averaging 1.0 mm thickness). Dolomite was not noticed and porosity is restricted to small amounts of fenestral. Stylolites trace their paths along the laminations.

531.9 m to 525.6 m

The reef now begins to show evidence of its final growth-ending exposure phase. Initially, leaching of the algal boundstone to algal wackestone results in irregular surfaces and cross-cut fabrics. The interval is light grey (n6, n7) to tan (5y 6/4) with short medium brown (5yr 3/4) areas. The section has good stromatolite growth which is cross-cut with a mudstone matrix holding small breccia clasts. The stromatolites show good couplets of light and dark laminae form 0.5 mm to 1.5 mm thick. By 529.4 m, the unit is heavily stylotized with up to 2.0 mm of clay concentrated along the seams. The core becomes argillaceous and has a higher organic content. At 529.0 m, a massive solution pipe containing a slurry of eroded debris and breccia clasts occurs. Pieces of broken stromatolite up to 8.0 cm long are mixed together in a mudstone matrix. Broken pisolith clasts made up of concentric laminations are included along with fragmented caliche crusts. Walls of the conduit are coated with algal laminations and crusts.

Regular stromatolite growth resumes by 526.1 m with large laterally linked hemispheroids. This illustrates that either the conduit is winding or that the stromatolites re-established themselves only to be further pulverised. Their growth laminae are nearly horizontal by 525.9 m when further exposure results in their brecciation and destruction. Again broken clasts of stromatolite are found but these are contained in a green shale (5gy 5/2, 5gy 3/2, 10 gy 3/2). The shale abruptly ends at 525.6 m

A-1 Carbonate Formation

525.6 m to 513.6 m

The A-1 Carbonate is a light brown (10yr 6/2) to chocolate brown (5yr 3/4), algal, dolomite mudstone to wackestone. It lacks any laminations and may be coralline algae caused. Porosity is good as numerous small vugs and molds of brachiopods and/or ostracods leave pores up to 5.0 mm in size. Additional porosity is due to inter-crystalline porosity. Areas of high porosity have additional minor amounts of anhydrite laths. The growth patterns of the algae and colour differences cause a mottled texture in the core. Traces of dolomite can be found in the light brown component. Very wispy, stylolite seams are common.

513.6 m to 503.2 m

The core gradationally changes to a light brown (10yr 6/2) to light grey (n6, n7), stromatolite, dolomite boundstone. Alternating light and darker laminae mimic one another and curves, dips and irregularities are translated through many generations. The laminations are gently dipping and may be to be laterally linked hemispheroids. The interval shows excellent porosity from fenestral, vuggy and inter-crystalline sources. Individual vugs are to 1.0 cm and unplugged. Short muddy intervals where porosity is tight are randomly scattered. The section is dolomitic in part and stylolites follow laminae.

A small exposure surface occurs at 506.7 m as blue-white (5b 6/2, 5b 3/2) anhydrite fills large vugs. Pieces of stromatolite breccia are in the anhydrite and a small amount of silt floors the cavity. Other small brecciated surfaces occur randomly and suggest dessications surfaces.

A-2 Evaporite

503.2 m to 501.7 m

Unconformably overlying the A-1 Carbonate is the anhydrite of the A-2 Evaporite. Nodular blue to blue-white (5b 6/2, 5b 8/2) anhydrite contains whisps of tan (5y 6/4) to gold coloured dolomite mud. The contact with the A-1 Carbonate is sharp. Minor enterolithic, chickenwire and felted textures are present. Porosity is near zero.

A-2 Carbonate

501.7 m to 499.6 m

The A-2 Carbonate begins as a light grey (n6, n7) to tan (5y 6/4) coloured, recrystallized mudstone. Buff (5y 7/2) coloured whisps of dolomite can be found similar to the underlying A-2 Evaporite. Solution features such as vugs are salt filled. In part, the unit is argillaceous and minor rip up clasts can be found.

499.6 m to 498.3 m

The core shows a short return to a stromatolitic boundstone. This section has very little porosity. Laminations are angled and consist of dark laminae of approximately 0.1 mm to 0.5 mm separated by beige (5y 6/4) laminae of approximately 0.1 mm to 0.3 mm thicknesses. The unit becomes more argillaceous and passes gradationally into the overlying unit. Dolomitization is patchy and random.

498.3 m to 494.4 m

The core finishes with a dark olive to light grey (5y 6/1) mudstone. It is argillaceous, laminated and almost fissile. Coarser terrigenous looking material is noticeable. Low-amplitude stylolites following the laminations enhance the layered effect. There is good clay concentrations along the stylolites. The mudstone commonly has rip up clasts.

Terminus Reef

Ram #2

A-1 Carbonate

498.6 m to 488.3 m

The entire core and interval consists of a finely laminated, algal-stromatolite dolomite, boundstone that is light (10yr 6/2) to medium brown (5yr 3/4) or olive to tan (5y 6/4)-gold in colour. Laminations are wavy to crinkly and are presumed to be of the LLH variety, although the narrow core diameter precludes positive identification. The stromatolites show alternating light and dark layers with the lighter ones being an approximate average of 0.5 mm thick and the dark ones up to 1.0 mm thick. There is very good fenestral porosity and the stromatolites shows evidence of cracking and shrinkage. Fibrous, acicular, white anhydrite laths are scattered in part but are especially concentrated around 493.5 m. The core is stained by dead hydrocarbons and is quite smelly.

Ram #4

Lockport Formation (Goat Island Member)

599.2 m to 593.6 m

The interval is a highly stylolitic, crinoidal, dolomite wackestone that is light grey (n6, n7) in colour. Crinoids are to 4.0 mm in diameter and are accompanied by brachiopods, thin (5.0 mm to 7.5 mm), tabular stromatoporoids and minor solitary and Halysites (?) corals. Mottling becomes quite noticeable near the section top.

Dolomitization is pervasive throughout the matrix and possibly the allochems also. The unit is quite stylolitic, mainly with wispy horsetails, although some sutured seams with up to 1.0 mm of clay residue are present. Porosity is poor up to 596.5 m, then good pinpoint porosity and small vugs up to 3.0 mm in size are abundant.

From 593.7 m to 593.6 m a pyritized, crustal surface is found. It abruptly truncates existing depositional facies, is extremely tight in the area of the surface with porosity development to 596.5 m. This surface may represent a hardground or more likely it represents the karst surface observed in other wells and previously undocumented. The core changes colour across the contact from light grey (n6, n7) to olive-light brown (5y 5/6).

Guelph Formation

593.6 m to 591.9 m

The Formation begins briefly as an olive-light brown (5y 5/6) coloured, brachiopod-crinoid, dolomite packstone to wackestone. The brachiopods are up to 7.5 mm in size and the crinoids to 6.0 mm in diameter. Stromatoporoids and corals are present only as fragments and it appears that the stromatoporoids are thin tabular varieties and the corals are rugosans. Unit appears to be reef talus as allochems show evidence of transport and tumbling.

591.9 m to 571.5m

This interval is similar in composition to the last unit however there is an immediate change to a light (10y 6/2) to medium brown (5yr 3/4), mottled colour. The rock is a dolomite, skeletal wackestone grading to packstone and mudstone. It is dominated by small whole brachiopods, brachiopod fragments, crinoids, trilobites and bryozoans. Corals and stromatoporoids are again as fragments with the corals appearing more to be Coenites than rugosans. Sizes are similar to the preceding section with some abraded stromatoporoid fragments being up to 2.0 cm x 2.0 cm.

The interval is dirty and argillaceous and this is reflected in the number of stylolites present. Small horsetail stylolites are plentiful and, in places, sutured seams. Where shells are concentrated, the interval shows extensive leaching of allochems with open molds and vugs to 0.75 cm in size. In places, the rock takes on a popcorn-like appearance. Muddier sections are dolomitized, stylotized and tight. No salt plugging was observed and no saddle dolomite crystals noticed.

571.5 m to 565.1 m

The core changes gradationally to a light brown (10yr 6/2) to light grey (n6, n7), mottled, algal wackestone. There is minor stromatolite development with fibrous, white to cream-coloured (5y 8/4), marine cement infilling. Two small, thin beds or lenses of brachiopod debris were noticed. Each is 4.0 to 5.0 cm in thickness and are found at 569.1 m and 566.9 m.

Only a small amount of dolomite was observed and it is very finely crystalline, matrix confined. There is good pinpoint porosity throughout and small micro vugs of up to 1.0 mm where brachiopod shells once existed. Larger vugs are now spar filled

565.1 m to 560.5 m

After a gradational change, the rock is now a light grey (n6, n7) to cream-coloured (5y 8/4), laminated, algal boundstone that features dips of 10° to 15°. The laminations are evenly spaced and approximately 1.0 mm in thickness. Sutured stylolites with very low amplitudes trace their way along lamination boundaries. In places, these are cross-cut by sutured seams with much larger amplitudes. Dolomitization was unnoticed and porosity, mainly fenestral is fair at best. Small clusters of acicular, anhydrite needles in sunburst patterns are found from 561.7 m upward.

560.5 m to 559.3 m

The interval is a severe karst facies showing broken pisolith, mudstone and algal boundstone clasts irregularly oriented and contained in a dark brown (5yr 2/2) to medium brown (5yr 3/4) mudstone. The mudstone clast mixture fills large solution cavities carved into the existing algal facies. Dolomitization is patchy but not selective. Stylolites are common and porosity near non-existent. The top 7.0 cm shows a trace of green clay.

A-1 Carbonate

559.3 m to 551.1 m

The A-1 Carbonate is a horizontally laminated to slightly dipping, algal stromatolite dolomite boundstone with thin intervals of brachiopod wackestone. Where boundstone, the laminations are wavy to crinkly, light brown (10yr 6/2) to light grey (n6, n7) in colour and about 0.5 mm in thickness. In wackestone areas, the unit shows shells of brachiopods, with gastropods (?) and/or ostracods (?). These randomly scattered 5.0 cm to 6.0 cm layers, are light brown (10yr 6/2) in colour, associated with pellets and are more limey than the boundstone areas. Dolomitization is extensive. Stylolites where present follow the laminations. Porosity is fair, fenestral and inter-crystalline.

551.1 m to 550.2 m

The algal-dominated facies are abruptly overlain by a thin chocolate brown (5yr 3/4), bioturbated dolomite mudstone. The unit appears unfossiliferous. Some wispy stylolites with up to 1.0 mm of clay residue are present.

550.2 m to 545.6 m

As abruptly as the mudstone truncated the algal facies, it is internally sharply overlain by a return to skeletal packstones and algal-stromatolite boundstones, light grey (n6, n7) to medium grey (n4, n5) in colour. In this interval, the packstones are more plentiful than the boundstones. The unit is very porous with inter-crystalline, vuggy and moldic (ostracods ?) porosity.

Ram # 5

Lockport Formation (Goat Island Member)

592.5 m to 585.0 m

The interval is a crinoidal, finely-crystalline dolomite, wackestone with abundant skeletal allochems. Unlike other examples of the Goat Island, this section is tan (5y 6/4) to gold in colour as it is oil stained and smelly. Minor amounts of corals and stromatoporoids are present in the lower 3.0 m but the double effect of the hydrocarbons and dolomitization makes identification difficult. Corals are to be solitary species and stromatoporoids are thin tabular types. The rock shows abundant stylotization with wispy swarms dominating. Porosity is good and inter-crystalline.

At 585.2 m, a highly irregular karst surface abruptly truncates the dolomite wackestone. The feature shows solutioned and eroded clasts and the overlying lithology is limestone. Solution features within the Lockport show a fill made up of material from above. Relief along the surface of the core is up to 4.5 cm. Above the contact Favosites corals and stromatoporoids are plentiful, while immediately below they are absent.

Guelph Formation

585.0 m to 534.3 m

Following the abrupt contact, the core shows a very consistent set of facies for 51m. Except for small intervals of skeletal wackestones, packstones and grainstones, the rock is a tan (5y 6/4) to buff (5y 7/2) coloured coral-stromatoporoid floatstone to framestone. The section alternates between stromatoporoid and coral domination. Favosites are abundant with sizes from 2.0 cm to 7.0 cm. Coenites are also plentiful and may be 7.5 mm in diameter, while rugose corals are up to 1.0 cm in diameter and 5.0 cm long. Both the rugose and branching corals are leached. Stromatoporoids are thin encrusters up to 2.0 cm thick or bulbous types up to 8.0 cm thick.

Small sections are skeletal in nature with brachiopod packstones and grainstones. Many of the brachiopods (*Pentamerus* ?) have been leached away and only molds up to 2.0 cm remain. Some minor crinoids, bryozoans, pellets, algae and trilobites (?) are also included. The interval begins skeletal in nature for 5.1 m before becoming coral and stromatoporoid favourable.

Little dolomitization was observed. Porosity is good throughout and is intra-fossil in corals, moldic where brachiopods and rugose corals once existed, and vuggy. Stylolites are not abundant or conspicuous.

A number of irregular surfaces cut across the core randomly. At 541.3 m a grike like structure weaves across the core for 3 m. This solution feature is filled with a red-brown laminated crust that is chalky in selective areas. The bottom of the cavity shows a very fine-grained, light brown (10yr 6/2) silt or mud.

Another series of fine-grained, light brown (10yr 6/2) silt features is found at 574.9 m. Here, a number of stromatactis-like cavities are filled with a possible vadose silt. At 578.8 m an irregular surface with a very sharp prominence is overlain by a dark finely crystalline mud which infills fractures.

A micro-laminated, very hard dolomite mudstone is found at 581.9 m. This thin 1.5 cm layer is poorly lithified in places and chalky. A feature very similar in appearance and thickness was observed in the Ram #3 well also drilled into the Terminus reef.

534.3 m to 519.6 m

After a 5 cm thick laminated crust, a tan (5y 6/4) to beige to light brown (10yr 6/2) coloured, algal wackestone exists for 16 m. In places, the algal-dominated unit gives way to thin skeletal-pellet packstone layers with abundant brachiopods (to 7.5 mm). The section is stylolitic with whisps and swarms as well as low-amplitude, sutured seams.

Little dolomite was observed. Porosity is good with vugs to 1.0 cm in size. More muddy areas show stromatactis with one to two generations of cream-coloured (5y 8/4) spar infilling.

The contact with the coral-stromatoporoid zone shows a thin cream-coloured (5y 8/4), hardpan-like crust capping a softer, very finely laminated, dark brown mudstone. Similar features were noticed at 532.3 m and 530.2 m.

The top 2.4 m of this interval sees a change to a tan-cream-coloured (5y 6/4, 5y 8/4), algal-stromatolite boundstone. Laminations are thin (1.0 mm) but evenly spaced. Little dolomite was noticed and stylolites are plentiful.

519.6 m to 518.5 m

Capping the top of the algal unit is a karst area similar to other cores is present as a large subvertical solution feature cross cuts the core. Broken, twisted clasts of pisoliths, stromatolite and caliche are held within a medium to dark brown (5yr 3/4, 5yr 2/2) mud matrix that fills the solution conduit. Porosity is negligible and dolomite is patchy and minor. Only traces of green shale (5gy 5/2, 5gy 3/2, 10 gy 3/2) are present.

A-1 Carbonate

518.5 m to 499.0 m

After the karstic contact, the A-1 Carbonate shows a light brown (10yr 6/2) to tan (5y 6/4), algal mudstone to occur for 6.0 m. following this pervasively dolomitized and highly porous facies, algal stromatolite dolomite boundstone makes up the remainder of the section. Laminations are about 1.0 mm to 0.5 mm in thickness and are wavy, crinkly or horizontal in nature. Very good fenestral and inter-crystalline porosity is present. Large, acicular anhydrite laths up to 3.0 cm long are randomly scattered and rarely an anhydrite nodule is observed. Stylolites are plentiful and they follow the laminations in the boundstone.

Wackestone areas have a high shell content that may be ostracods or gastropods. These have left numerous molds. Porosity is good being moldic, vuggy and inter-crystalline.

A-2 Evaporite

499.0 m to 497.4 m

A blue to blue-white (5b 6/2, 5b 8/2), nodular anhydrite sits on top of the carbonate. In places has an enterolithic and chicken wire texture. Whisps of gold to tan (5y 6/4), finely crystalline dolomite are scattered throughout. Porosity is near zero. A single stromatolite is found in the middle of the section showing horizontal laminations.

Ram #3

Lockport Formation (Gasport Member)

602.0 m to 600.2 m

Lower portion of the core consists of a light grey (n6, n7), crinoidal, dolomite wackestone that is argillaceous in part. Portions of the unit are undolomitized. Crinoids make up the bulk of the allochems and initially they are 1.0 to 2.0 mm in diameter, increasing to 4.0 mm by the interval end. Brachiopods and trilobite fragments also accompany the crinoids. Two, thin, tabular stromatoporoids occur by the section end. They are less than 5.0 mm in thickness, show borings and fractures now sediment filled. Porosity is low and is inter-crystalline.

Stylolites are minor and where present they are singular, sutured seams. Very little clay content is observed along the seams. Towards the top of the unit, the stylolites increase in number and occur in swarms. In places they cross-cut the thin stromatoporoids. With the

increase in stylolites, there is an increase in clays and organics. Hence the core now appears medium grey (n4, n5).

Goat Island Member

600.2 m to 587.0 m

Following a gradational contact, the core is now a medium grey (n4, n5), crinoidal, dolomite packstone that also is skeletal in part. The crinoids are up to 1.4 cm in diameter and they show a layered effect as if accumulated by storm action. In places, a crinoid grainstone is apparent. Stromatoporoids are more plentiful. They are thin and tabular, encrusting other stromatoporoids or they are bulbous, not in situ and up to 4.0 cm thick. The stromatoporoids show borings as before, that are now filled with a dark grey micrite or lime mud. By 593.2 m, the stromatoporoids are difficult to detect. Halysites corals are also evident.

This interval features more muddy areas and the unit is more argillaceous. These areas have more stylolites and are slightly nodular. The stylolites are in swarms with little clay residue associated with an individual stylolite. Muddy areas also are bioturbated.

The Goat Island has abundant dolomite but it does not seem to be selective. Porosity is low. In the area around 587.5 m, the unit lightens and becomes olive-light brown (10yr 6/2) to medium brown (5yr 3/4) in colour. Mottling is observed and pyrite is found along stylolites.

From 587.2 m to 587.0 m, core recovery is shoddy, however, a karstic fabric is observed. A small conduit shows plugging by coarse white calcite. Angular clasts of country rock up to 1.0 cm by 1.0 cm float in the calcite fill. Feature may be of tectonic origin, however, sides of cavity are solutioned and allochems in the area do not show tectonic influences.

Guelph Formation

587.0 m to 583.4 m

The Guelph Formation begins as a light brown (10yr 6/2), skeletal wackestone for 3.6 m. Small brachiopods up to 1.0 cm are the main allochem with solitary rugose corals up to 4.0 mm in diameter being the second most plentiful organism. Many allochems have been leached leaving small molds and vugs to 1.0 cm in size. In addition to the vugs and molds, porosity is also inter-crystalline. Some minor, random salt plugging occurs. The interval is still argillaceous and consequently, horsetail stylolites are common. Dolomite is present in patches but is not pervasive.

From 583.7 m to 583.4 m, the Guelph is made up of weathered and abraded reef detritus with irregular surfaces. Above the contact, the core is limestone and very vuggy.

583.4 m to 548.3 m

Following the sharp contact, a buff (5y 7/2) to light brown (10yr 6/2) coloured, coral-stromatoporoid floatstone dominates. The relative abundance of corals versus stromatoporoids varies with each taking turns at being the prevalent organism. Small (3.0 to 6.0 cm) intervals of skeletal wackestone, packstone and grainstone are also noticeable. Favositid corals up to 8.0 cm in size encrust stromatoporoids and in turn are encrusted. Coenites and Heliolites were observed but these are minor relative to the Favosites. Coral content drops off significantly from 554.5 m upward. Stromatoporoids are mainly tabular encrusters up to 3.0 cm thick and 4.0 cm long, however, some bulbous types are present. The bulbous varieties are overturned and not in situ. The skeletal intervals are dominated by brachiopods, but molluscs, crinoids, trilobites and algae (?) are also included. All are contained by a lime mud matrix.

In places, the core shows good cementation by isopachous calcite cement and a stromatolitic fabric is evident. Other areas are highly gutted with the core having a popcorn appearance. Overall, porosity is good with corals having intra-fossil porosity. Vugs up to 3.0 cm in size are

common with some to 6.0 cm and brachiopods have frequently left molds. Many molds show internal structure. Entire corals and stromatoporoids have been removed in places.

Dolomitization of the rock was not observed, nor was any saddle dolomite. Stylolites are minor, occurring mainly as single sutured seams. Only in muddy wackestone areas does the core show any stylolite swarms.

Throughout the interval irregular surfaces are present as in Ram # 5. Many are the result of bioeroded or storm eroded reef debris filling voids and cavities that were present in the living reef. However, some of the surfaces are erosional and similar surfaces were noticed in the Ram # 5 core. At 574.2 m, a small zone showing an irregular surface and coated with a laminated "crust" is noticeable. A 1.0 cm thick micro-laminated dolomite mudstone crosscuts the core at 562.3 m. In places, this mud is poorly lithified while in others it is very hard. The sides of the cavity containing the mud show evidence of solutioning. This feature was also observed in the Ram #5 core. Higher up, from 554.5 m to 553.0 m a thin, subvertical solution feature is present. It is filled with dark microlaminated mudstone and a cream-coloured (5y 8/4), poorly lithified, chalky material (gypsum?). There is some minor salt associated with the feature and it abruptly halts against a thin crust. Overlying is a light grey (n6, n7) wackestone.

548.3 m to 531.3 m

Over a gradational change, the reef changes to a algal wackestone. Corals, stromatoporoids and skeletal organisms decrease in both number and diversity. The corals cease from 542.1 m upward. The interval is chocolate brown (5yr 3/4) in colour. With the decrease in skeletal allochems, vuggy and moldic porosity also decreases. Former large vugs show a white to cream-coloured (5y 8/4) isopachous cement which lends a stromatolite fabric. Rare vugs to 0.5 cm are still present but porosity is now inter-particle.

Dolomite was not detected. Stylolites are plentiful, possibly reflecting the more muddy nature of the rock. The stylolites are found in swarms as well as single, sutured seams. A number of thin, laminated mudstone intervals are randomly scattered in the upper part of the unit. These mudstone lenses are a maximum of 4.5 cm thick and are found at 535.8 m, 535.4 m, 533.7 m and 532.3 m. It is uncertain if they are paleosols as have been noticed in other reefs.

531.3 m to 527.9 m

Over a gradational change, the core is now a laminated, algal stromatolite boundstone. It alternates between dark brown (5yr 2/2) and tan (5y 6/4) coloured laminae ranging in thickness from 0.5 mm to 1.1 mm. The laminations are wavy and crinkly as in other cores and porosity is fenestral and inter-crystalline in nature. Dolomite is present but not pervasive. Single stylolites with very low amplitudes follow the laminae.

527.9 m to 523.5 m

The algal facies are abruptly ended by the massive karst exposure present in all pinnacles. A vertical solution conduit is filled with collapse breccia and broken clasts of mudstone, stromatolite and pisoliths. All are held within a dark brown (5yr 2/2) mud matrix. The largest clast observed was 2.0 cm along its long axis. Porosity is non-existent and dolomite confined to random patches. The green clay noticed on top of other pinnacles was not noticed in Ram #3.

A-1 Carbonate

523.5 m to 502.0 m

Initially, the A-1 Carbonate begins as an chocolate brown (5yr 3/4), algal mudstone for 7.2 m. Few allochems are noticeable as the core is thoroughly dolomitized. Small vugs and molds

to 6.0 mm possibly once ostracods or brachiopods give some evidence of shelly organisms as well as providing additional porosity.

The A-1 is then typified by laminated algal-stromatolite dolomite boundstone that shows random, thin (15 cm) beds of skeletal debris. The skeletal allochems are brachiopods, ostracods or gastropods. The interval is light brown (10yr 6/2) to chocolate brown (5yr 3/4) featuring wavy to crinkly to near-horizontal laminations of 0.3 mm to 1.3 mm thicknesses. Each laminae mimics the underlying one.

Porosity is good and mainly inter-crystalline and fenestral, although some small vugs exist in the skeletal areas. Stylolites are very common and single seams follow the trace of individual laminae. In the skeletal areas, stylolites are in swarms. Laths of anhydrite are randomly distributed from 513.5 m upward. By 507.4 m, rare anhydrite nodules are found. They are a maximum of 1.0 cm by 2.0 cm in size.

A-2 Evaporite

502.0 m to 501.1 m

The upper 1.9 m of the core corresponds to the A-2 Evaporite unit. White-blue (5b 8/2), nodular, and enterolithic anhydrite contains wisps of tan (5y 6/4)-gold dolomite. Small clasts of stromatolite float in the anhydrite.

Wilkesport Reef

Imperial Sombra 14-XIII

Lockport Formation (Gasport Member)

665.1 m to 653.7 m

The Gasport Member consists of light grey (n6, n7), crinoidal dolomite wackestone. The crinoid fragments are small and up to 3.5 mm in diameter. Small brachiopods accompany the crinoids and have thin shells. On average, the shells are 4.0 mm long. Small scattered disseminated grains of pyrite are found randomly in the interval.

Dolomitization is pervasive through the Gasport with most allochems remaining as calcite. No saddle dolomite was noticed. Porosity is mainly inter-crystalline. Small vugs up to 3.0 mm in size occur where a shelly allochem has been removed. Stylolites are common and about 1.0 mm thick.

Goat Island Member

653.7 m to 634.0 m

The Goat Island Member is a light grey (n6, n7), dolomite wackestone dominated by crinoids but with abundant skeletal material. The ossicles are up to 1.5 cm in size. Small, very thin, tabular encrusting stromatoporoids occur at 641.5 m and are scattered in part to 639.2 m. Also scattered are brachiopods up to 5.0 mm long, trilobites and molluscs. Only a few random solitary corals were observed and only as fragments. Porosity is inter-crystalline and fair, but becomes quite low by 635.5 m. Stylolites are common, resulting in a nodular appearance. The stylolites are wispy and in swarms. Some clay residue is concentrated along major stylolites. Dolomitization is pervasive.

The upper contact is sharp and erosional. Across an irregular boundary, there is a sudden increase in coral and stromatoporoid content and a marked increase in porosity. The light grey (n6, n7) lithology of the Lockport gives way to the light brown (10yr 6/2) of the Guelph. The degree of dolomitization decreases. Minor amounts of pyrite are found beneath the surface. This contact seems to correspond to the karst event noticed in other cores.

Guelph Formation

634.0 m to 605.9 m

After the abrupt contact, the Guelph Formation is a tan (5y 6/4) to light brown (10yr 6/2), coral-stromatoporoid, dolomite floatstone. However, it begins for 3.1 m as a crinoid and skeletal wackestone to packstone. Several layers of skeletal packstone to grainstone interrupt the reef builders. Favosites, Coenites and solitary rugose corals are the most plentiful organisms. They are however, much smaller than those observed in other reef cores, with the tabulates being only 3.0 cm in size and the rugosans 7.5 mm in diameter. Stromatoporoids are mainly thin encrusters although some bulbous and hemispherical types were noticed. The coral and stromatoporoid content decreases toward the top of the unit. Skeletal intervals are composed of brachiopods, crinoids, cephalopods, molluscs, trilobites and algae (?). Minor bryozoans also are included.

Porosity is poor initially but overall it is good throughout. Many stromatoporoids are leached away leaving vugs and molds up to 3.0 cm in size. Brachiopods and bivalves leave vugs and molds up to 1.3 cm and some show good internal structure. Porosity is mainly vuggy or moldic with inter-crystalline porosity associated with dolomite. Corals show intra-fossil porosity. Most large (>1.3 cm) pores are subsequently salt plugged with no precursor cement. Some vugs and molds show large anhydrite or celestite (?) laths up to 1.0 cm long.

The interval begins as limestone but by 619.0 m it is dolomite. Allochems remain calcitic. Stylolites are single, sutured seams and are not overly abundant.

605.9 m to 586.4 m

Following a gradational contact the Guelph is made up of a dark brown (5yr 2/2) to medium brown (5yr 3/4), algal, dolomite wackestone. Some skeletal allochems accompany, mainly brachiopods, but also bivalves and minor amounts of bryozoans. Most are less than 1.0 cm in size. Pellets also are plentiful. Several tiny, white blebs were noticed and are enigmatic, possibly calcispheres. Many shelled organisms have been leached away to leave one time vugs and molds, now filled with spar.

Porosity varies from good to poor and is vuggy, moldic and inter-crystalline. The inter-crystalline pores are found in areas of dolomitization. Approximately 75 % of the unit is dolomite. The unit is also stylolitic with single seams and wispy swarms common. Salt is not as prevalent as in the previous interval and is confined to the larger vugs and molds (1.5 cm).

An interpreted karst zone occurs at 593.4 m. Here a solution feature with irregular, scalloped walls contains randomly oriented clasts of wackestone that are coated with a thin, 1.0 mm to 2.0 mm, black rind. The feature has subsequently been filled with spar and anhydrite.

586.4 m to 583.4 m

Over a gradational contact, the algal wackestone is succeeded by a laminated, algal-stromatolite, dolomite boundstone. The unit is medium to dark brown (5yr 2/2) with some laminae being light brown (10yr 6/2) to tan (5y 6/4) coloured. Each individual laminae is up to 1.0 mm thick and they are more horizontal than wavy or crinkly. Porosity is poor and inter-crystalline or very minor fenestral where present. Stylolites trace along laminae as before.

583.4 m to 577.6 m

The algal boundstone is abruptly terminated by a massive subaerial exposure episode. Solution vugs contain broken skeletal fragments and pisoliths, smashed stromatolites, and remnants of laminated crusts randomly oriented. Fragments are up to 5.0 cm long by 2.0 cm and show a thin, black rind coating them. All clasts are held within a dark brown (5yr 2/2) dolomite mudstone. Stylolites are very common, skirting the outside of clasts. Some fracturing is evident. Porosity is near zero as any remaining karst created porosity was sealed by a white calcite spar.

A-1 Carbonate

577.6 m to 557.2 m

Unconformably overlying the exposure episode is the gold-brown (5y 6/4) algal stromatolite, dolomite boundstone of the A-1 Carbonate. Initial areas show a chocolate brown (5yr 3/4), algal dolomite mudstone to burrowed dolomite mudstone for 4.7 m. Porosity is good throughout and mainly inter-crystalline. Some small vugs and molds exist possibly once being brachiopods, ostracods or molluscs.

The interval is dolomite and this makes recognition of algal laminations difficult. However, the laminations are wavy or near-horizontal and attain maximum thicknesses of about 1.0 mm. The unit is also stylotized throughout with single, sutured seams and horsetail swarms common.

A-2 Evaporite

557.2 m to 554.1 m

A thicker A-2 Evaporite unit was encountered in this core. Solution features in the underlying A-1 Carbonate are filled with a blue to blue-white (5b 6/2, 5b 8/2) anhydrite. The anhydrite is mainly nodular although chicken-wire and felted textures were observed. Small, thin whisps of gold to tan (5y 6/4) coloured dolomite are common in the anhydrite.

Bayfield Reef

Bluewater Oil and Gas Porter #1

Lockport Formation (Goat Island Member)

592.2 m to 586.4 m

The Goat Island is a light grey (n6, n7), mottled, stylolitic, crinoidal to skeletal, dolomite wackestone. Crinoids are 3.0 mm to 5.0 mm in diameter, with modest size increases upward. Small, bryozoans also occur and are 3.0 mm to 4.0 mm thick and 1.2 cm to 1.5 cm long. Stromatoporoids, Halysites, solitary corals and Coenites are noticeable to the top 1.3 m of the section where they then are absent. The stromatoporoids are thin, tabular and encrusting while the corals are a maximum of 1.0 cm in diameter. Porosity is fair due to the finely crystalline dolomite that is pervasive. Stylolites are abundant with swarms causing a nodular effect. The interval is argillaceous overall.

Guelph Formation

586.4 m to 563.3 m

The contact between the Goat Island and the Guelph is shape, undulatory and abrupt. It lacks the more obvious erosional features found in other reefs at this stratigraphic level. However, its sharpness, the change of colour and faunal dissimilarities, and minor amounts of pyrite are of note when comparing it to the other pinnacles.

Overall, this section is a tan (5y 6/4) to olive brown (5y 5/6), stromatoporoid-coral dolomite floatstone to rudstone with abundant skeletal wackestone layers throughout. Tabular, encrusting stromatoporoids outnumber the corals. The stromatoporoids reach a maximum thickness of 3.5 cm, while tabulate corals are up to 4.0 cm. Branching stick corals are also plentiful.

The amount of skeletal material at the base of the section is less than in other reefs with only 2.4 m of crinoid, bryozoan, brachiopod and other skeletal debris present. By 566.6 m the unit is tan (5y 6/4) in colour and the proportion of skeletal debris (crinoids, brachiopods, bivalves, trilobite (?) and algae) has increased relative to the reef builders.

Porosity is good overall and varies from inter-crystalline in lower sections to micro vugs and molds (3.0 mm to 4.0 mm) with the increase in skeletal allochems higher up. Salt plugging is common and only the smaller vugs remain open. Some pores show a stromatactis fabric while others show initial calcite spar followed by salt occlusion. A third variety has salt plugging with no precursor cements. Dolomitization is pervasive and only select organisms remain as calcite. Stylolites are common throughout. In lower parts of the section they occur as wispy seams but by 580.1 m they are mainly low-amplitude, single sutured seams.

563.3 m to 549.6 m

After a gradational contact, the unit is now a skeletal packstone to stromatoporoid floatstone. The relative abundance of corals has decreased dramatically. Stromatoporoids are thin encrusting types as before, however, apart from solitary corals, the remainder of the allochems are crinoids, brachiopods, molluscs, rare bryozoans, trilobites and algae. The upper 1.1 m of the interval marks a return of large tabulate corals.

Dolomite is thorough as before and it overprints most fabrics and features. Porosity is fair with salt plugging throughout. Small vugs and molds of brachiopods and molluscs less than 5.0 mm remain open. Stromatoporoids create shelter porosity but most has been occluded by salt. Stylolites are common but not readily detectable.

A small, possibly erosional feature was detected at 559.9 m. Here, a subvertical cavity traces an irregular contact as it cross cuts through the reef core. The sides of the cavity are solutioned and they are coated with a dark brown (5yr 2/2) rind. Small 2.0 cm to 3.0 cm clasts contained within the cavity are also coated. Acicular needles of anhydrite are also present.

549.6 m to 540.1 m

Over a gradational contact, the core changes to a dolomite brachiopod grainstone and dolomite skeletal packstone, buff (5y 7/2) in colour. Tabulate corals that appeared at the top of the previous interval are randomly present along with Coenites (?). Stromatoporoid content is reduced. The main skeletal constituents are brachiopods. They are up to 2.0 cm long and frequently are leached away. Molluscs (?) are also present. The upper 2.2 m is more muddy and argillaceous and a stromatactis fabric is evident.

Porosity is good throughout as shelly organisms are leached away. Vugs to 4.0 cm are rare with the average vug being approximately 2.0 cm. Vugs in grainstone areas have an isopachous, calcite cement lining while those in more muddy areas show a dark, isopachous rind. Salt plugging occurs as a late event post-dating the calcite cement. The rock is dolomitized thoroughly and many organisms are only ghosts. Stylolites are rare except in the

more muddy and argillaceous areas. Here, they occur as single sutured seams or as swarms. Little clay residue was observed accompanying the stylolites.

540.1 m to 538.6 m

Following a gradational contact, a short interval of dolomite coral framestone was observed. The section is solely Favositid corals with a buff (5y 7/2) to olive (5y 5/6) colour. The corals occupy the entire core and little matrix is present as they grow on top of one another. There is good intra-fossil porosity throughout, with only a minor amount of salt plugging of individual hexes. Rarer still is anhydrite plugging. As with the rest of the core, dolomite is pervasive.

538.6 m to 533.1 m

The coral framestone gradually grades to an olive-buff (5y 7/2) coloured coral floatstone with a skeletal packstone distributed through the interval. The corals are much smaller than before (up to 3.5 cm) and are solitary and tabulate types. The packstones show brachiopods and possibly bivalves, but the organisms are less than 1.5 cm in size. Packstone areas show extensive leaching of allochems and many highly irregular surfaces. Larger cavities are selectively salt plugged or have thin, isopachous cement rinds. Only smaller vugs of less than 7.5 mm remain open. There is good inter-crystalline porosity due to the extensive dolomitization.

533.1 m to 530.0 m

Reef growth is abruptly truncated by the massive karst episode occurring at the top of all pinnacle reefs. An olive to medium brown (5yr 3/4) breccia fills solution conduits within an algal-brachiopod mudstone to algal-stromatolite boundstone. Clasts are composed of mudstone, broken crusts and stromatolite pieces. Dark rinds coat most grains and all are contained within an olive brown (5y 5/6) mud and anhydrite. Stylolites skirt around grains, never cross-cutting. The entire section is dolomite and only traces of green clay (5gy 5/2, 5gy 3/2, 10gy 3/2) were observed.

A-1 Carbonate

530.0 m to 527.6 m

Lying unconformably on top of the karst facies, the A-1 Carbonate is a dark brown (5yr 2/2), algal mudstone. The unit is dolomite. Faint laminations (?) are overprinted by the dolomitization of the core. Unlike the other examples of the A-1 Carbonate, porosity in the Bayfield core is low. High percentages of inter-crystalline porosity existed but most have been occluded by salt. Large vugs to 4.0 cm can be found and these show only partial salt fills. Few skeletal fossils were observed with possible ostracods or brachiopods present in small numbers. The dolomite overprint makes their identification difficult. Where detectable, laminations are very thin.

Payne Reef

Imperial Payne #4

Rochester Formation

762.9 m to 757.1 m

The Rochester is a medium grey (n4, n5), argillaceous, dolomitic to calcareous shale. The unit ranges from thinly bedded, fissile, unfossiliferous sections to massive, highly fossiliferous beds. Crinoids are the most noticeable organism but they are tiny (3.0 mm diameter) and show the adverse conditions. Brachiopods were also found. They are up to 15 mm long and are very thin shelled. Many are pyritized. Pyrite is also found as disseminated grains below the contact. Porosity is very low to non-existent. The contact with the overlying Lockport Formation is distinct and very irregular. In the absence of any shallowing phenomenon, it is viewed as a submarine hardground.

Lockport Formation (Gasport Member)

757.1 m to 745.2 m

Following the sharp contact, the unit is a light grey (n6), crinoidal, dolomite wackestone. Crinoids range from 1.0 mm to 10 mm and are more plentiful upward. Minor thin shelled brachiopods and bryozoans were also observed. The brachiopods are a maximum of 4.0 mm long and the bryozoan fragments are 12 mm long. Small grains of disseminated pyrite are scattered throughout.

Porosity is very low with only a small amount of inter-crystalline porosity remaining. Other porosity in the form of tiny vugs and molds (< 1.0 mm) is salt or calcite sealed. Stylolites are common but not overly abundant. They form single, low-amplitude lines that have up to 1.0 mm of clay residue. Dolomitization is complete and the dolomite is crypto-crystalline to finely-crystalline.

Goat Island Member

745.2 m to 727.6 m

The change from the Gasport to the Goat Island is a gradational one and results in an increase in argillaceous material. The interval is a light grey (n6, n7), crinoidal wackestone that grades in places to skeletal dolomite packstone. In places, an olive green colour compliments the grey.

Lower portions of the section are mainly crinoidal, with ossicles up to 15 mm in diameter. By 733.1 m, thin, tabular stromatoporoids and rare bulbous varieties are found. Tabulate corals averaging 1.0 cm in size are common as does *Coenites* and, in part, *Halysites*. They occur in situ as small amounts of mud sit on their septa. Rugose corals up to 6.0 mm in diameter, thin shelled brachiopods, molluscs, trilobites (?) and bryozoans complete the observed organisms.

The unit is finely-crystalline dolomite and has good inter-crystalline porosity. Corals show intra-fossil porosity, while brachiopods and other shelled organisms have been leached to leave molds and vugs of up to 4.0 mm. The Goat Island is highly stylolitic and has a nodular or banded effect due to the swarms of stylolites. In places, the concentration of stylolites causes a medium brown (5yr 3/4) colour.

The upper contact at 727.6 m is sharp and abrupt. An irregular, erosional surface marks a change from the light grey (n6, n7) skeletal wackestone to a medium brown (5yr 3/4) to light brown (10yr 6/2) crinoidal wackestone. Allochem content with the exception of the crinoids is suppressed for several meters. Minor disseminated pyrite is found below the contact.

Guelph Formation

727.6 m to 713.1 m

Overlying the erosion surface, the Guelph begins as a medium (5yr 3/4) to light brown (10yr 6/2) to buff (5y 7/2), crinoidal, dolomite wackestone for 3.2 m. Crinoids are up to 10 mm in

diameter. A gradational contact shows an increase in both the number and diversity of organisms. An olive green (10y 6/2) colour marks the onset of a coral-stromatoporoid dolomite floatstone to rudstone. Corals include Favosites, Coenites Heliolites and solitary rugose corals. Stromatoporoids are thin, up to 1.0 cm, and encrusting. Bryozoans, brachiopods, crinoids and bivalves complete the observed fauna. Both the bryozoans and the stromatoporoids create shelter porosity but this has been plugged by calcite cement, leaving stromatactis.

Porosity is fair due to vugs and molds from leached shelly allochems. Inter-crystalline porosity is also important due to the extensive dolomitization of the reef. Stylolites are single sutured seams that randomly cross-cut the core. They have a maximum of about 1.0 mm of clay residue.

713.1 m to 698.9 m

The interval is a coral-stromatoporoid dolomite floatstone that has abundant skeletal material as packstones and is separated from the lower interval by a gradational change. Most of the brachiopods, bivalves, crinoids, corals, stromatoporoids and pellets (?) that make up the section have been leached away. Consequently, porosity is enhanced, with vugs to 1.5 cm. Crinoid content increases toward the lower contact with the coral-stromatoporoid floatstone. Dolomitization is complete and is micro-crystalline. Hydrocarbon staining and smell is prevalent and a brown colour results. The lower 6 m shows light blue (5b 6/2) anhydrite plugging of pores.

698.9 m to 673.6 m

The core changes gradationally to limestone and facies-wise to an olive coloured (10y 6/2), coral floatstone. Stromatoporoids are few and corals are tabulate and large (up to 12 cm thick). Also present and large, are brachiopods, to 2.5 cm. Few other organisms were noticed as the core is stained with hydrocarbons. Little dolomite was detected either as a matrix replacement or as saddle dolomites. Porosity is variable. Corals show most of their chambers filled with marine cement. The large brachiopods have been preferentially leached away to leave large vugs and molds. However, by 695.6 m the section is tight and stromatactis is found. The stromatactis have a dark, isopachous rind along the cavity walls before calcite cementation. Stylotization is minor and single seam.

At 688.2 m, the colour of the core changes to a medium brown (5yr 3/4) to medium grey (n4, n5). Corals still dominate, but the skeletal content is greater. Thin intervals could be classed as skeletal packstones. There is an increase in the number of single stylolites, and algae (?) may now be present in numbers.

673.6 m to 671.2 m

The core is now sharply cut by a solution cavity feature. Both the overlying and underlying units contrast across the irregular surfaces. Clasts up to 1.5 cm, slightly elongated are contained in a dark brown (5yr 2/2) mudstone. Wavy and laminated crusts coat some parts of the cavity walls but not others. The actual cavity can be found down to 672.1 m, but enhanced porosity, leached allochems and a popcorn appearance to the core continue to 673.6 m. Dolomite is patchily present and is micro-crystalline. Porosity is enhanced below the karst surface with vugs to 1.0 cm. Crusts can also be detected to 673.6 m. Stylolites are common.

671.2 m to 619.4 m

Atop the karst surface, a medium brown (5yr 3/4) to light brown (10yr 6/2), algal-brachiopod mudstone to wackestone is the dominant facies. Brachiopods are the most plentiful accessory allochem, but pellets, bivalves, echinod plates, and, rare solitary corals and stromatoporoids are also present. In several areas the algal wackestone is interrupted by

skeletal debris that forms thin (4.0 cm to 9.0 cm thick) packstone to grainstone units. Dolomite was not detected.

Porosity is however, mainly inter-crystalline and fair. Small vugs range in size from 3.5 mm to 7.0 mm and some show a calcite lining or fill. The interval can be very stylolitic in areas where mud and argillaceous content is high. Higher in the section, at 638.1m, the colour becomes darker and branching corals occur. They are slender, being only 6.0 mm in diameter and disappear after 3.1 m. The upper four meters of the section show faint, horizontally laminated structures, possibly algal-stromatolite boundstone. The dark colour of the core obscures the majority of the laminations which are less than 1.0 mm thick.

The interval is cross-cut by two potential karst areas. The first from 651.9 m to 653.0 m is a subvertical solution feature that contains a dark brown (5yr 2/2) mudstone infill. Within the mud are coated clasts and brecciated fossil fragments. The cavity walls are irregular and scalloped. Stylolites are common.

The second feature is at 627.1 m. Here, a solution cavity is filled with a blue-green fibrous anhydrite containing randomly oriented clasts. The clasts are small, up to 1.0 cm in size. Both the clasts and the walls of the cavity are coated with a dark rind. Possibly the same solution feature is found at 629.9 m as a clast bearing blue-green anhydrite is found in a solution cavity.

A major karst surface terminates the algal facies at 619.5 m.

619.5 m to 617.5 m

Reef growth is terminated by the karst episode found on top of all pinnacles. Here, the section is bleached to a light brown (10yr 6/2) colour and subvertical solution cavities hold brecciated clasts of dark brown (5yr 2/2) mud and stromatolite clasts. The clasts show evidence of abrasion and some are smashed. Small amounts of vuggy porosity can be found and based on shape may have been gastropods originally. Dolomite is present but not pervasive. Stylolites circumvent clasts and are very common.

The upper 10 cm of the karst area is infilled and capped by an olive coloured shale, similar to other pinnacles.

A-1 Carbonate

617.5 m to 611.4 m

Unconformably overlying the Guelph, the A-1 Carbonate begins as a chocolate brown (5yr 3/4), algal mudstone for 5.8 m and then changes to an algal-stromatolite dolomite boundstone. The interval is completely dolomitized and laminations are only faint. They are crinkly to near-horizontal. Inter-crystalline porosity is outstanding as the section has been severely leached in addition to the dolomite effect. Bivalves, brachiopods or ostracods leave small vugs and molds up to 7.5 mm. Many cavities display a "weathered rind" that isopachously lines their walls. Cream-coloured (5y 8/4) anhydrite is a common accessory although it doesn't occlude porosity. By 611.4 m, the anhydrite is nodular with small blebs up to 1.5 cm.

Appendix B: Carbon and Oxygen Isotope Results

| sam # | reef | fm | depth | taken from | miner | $\delta^{13}\text{C}$ | $\delta^{18}\text{O}$ |
|-------|------------|----------|--------|---|----------|-----------------------|-----------------------|
| 1 | Payne | Guelph | 644.7m | rugose coral | calcite | 5.05 | -3.70 |
| 2 | Payne | Lockport | 741.6m | dolomitized platform | dolomite | | |
| 3 | Payne | Guelph | 650.1m | white coarse cement | calcite | 5.47 | -2.68 |
| 4 | Terminus | Guelph | 562.4m | laminated paleosol | dolomite | 5.78 | 0.55 |
| 5 | Terminus | Guelph | 587.2m | coarse white calcite with breccia clasts | calcite | 3.85 | -5.70 |
| 6 | Terminus | Guelph | 555.7m | tabulate coral | calcite | 4.96 | -3.16 |
| 7 | Terminus | Guelph | 549.4m | halysites | calcite | 5.31 | -2.55 |
| 8 | Terminus | Lockport | 595.7m | stromatoporoid | calcite | 2.64 | -0.32 |
| 9 | Terminus | Guelph | 561.1m | paleosol | dolomite | 4.70 | 1.17 |
| 10 | Terminus | Guelph | 527.0m | paleosol with rubble in karst area | dolo | 3.73 | 0.98 |
| 11 | Terminus | Guelph | 559.6m | laminated crust or paleosol | dolomite | 3.37 | 1.27 |
| 12 | Wilkesport | Lockport | 658.9m | dolomitized platform | dolomite | 3.25 | 1.28 |
| 13 | Wilkesport | Guelph | 596.8m | coarse calcite | calcite | 3.75 | -2.78 |
| 14 | Wilkesport | Guelph | 593.6m | solution cavity with rind and anhydrite fill | dolomite | 0.66 | 1.18 |
| 15 | Baysfield | Guelph | 531.9m | dolomite in solution feature | dolomite | 3.03 | 0.43 |
| 16 | Baysfield | Guelph | 531.7m | solution cavity, rind with clasts | dolomite | 3.41 | 1.00 |
| 17 | Warwick | Guelph | 609.1m | botryoidal calcite- 2nd pore fill | calcite | 2.00 | -5.38 |
| 18 | Warwick | Guelph | 589.7m | coarse clear calcite | calcite | 2.66 | -8.63 |
| 19 | Warwick | Guelph | 571.9m | calcite cement in breccia zone | calcite | 3.17 | -5.50 |
| 20 | Warwick | Guelph | 598.6m | coarse white calcite | calcite | 5.21 | -0.97 |
| 21 | Warwick | Guelph | 598.6m | buff calcite cement in solution feature | calcite | 2.55 | -3.58 |
| 22 | Warwick | Guelph | 600.2m | dog tooth calcite | calcite | 2.29 | -9.19 |

| | | | | | | | |
|----|----------|-----------|--------|------------------------------------|----------|------|-------|
| 23 | Warwick | Guelph | 624.5m | bryozoan | calcite | 3.33 | -3.46 |
| 24 | Warwick | Guelph | 597.0m | coarse calcite in cavity | calcite | 3.94 | -5.18 |
| 25 | Warwick | Guelph | 608.5m | dog tooth calcite | calcite | 2.17 | -5.44 |
| 26 | Warwick | Guelph | 534.5m | laminated crust | calcite | 4.16 | -7.21 |
| 27 | Warwick | Guelph | 652.7m | white saddle dolo | dolomite | 2.72 | -6.50 |
| 28 | Warwick | Guelph | 571.3m | algal laminated crust | calcite | 4.79 | -6.45 |
| 29 | Warwick | Guelph | 624.5m | 1st ph pore cement | calcite | 1.94 | -3.52 |
| 30 | Warwick | Guelph | 624.5m | 2nd ph pore cement | calcite | 1.97 | -3.77 |
| 31 | Warwick | Guelph | 624.5m | 3rd ph pore cement | calcite | 1.82 | -4.53 |
| 32 | Warwick | Guelph | 624.5m | 4th ph pore cement | dolomite | 2.89 | -2.74 |
| 33 | Warwick | Guelph | 632.9m | 1st ph pore cement | calcite | 2.01 | -3.25 |
| 34 | Warwick | Guelph | 632.9m | 2nd ph pore cement | calcite | 1.19 | -3.41 |
| 35 | Warwick | Guelph | 632.9m | 3rd ph pore cement | calcite | 1.98 | -4.93 |
| 36 | Warwick | Guelph | 632.9m | 4th ph pore cement | calcite | 1.63 | -5.90 |
| 37 | Rosedale | Rochester | 664.8m | crinoid | calcite | 3.99 | -3.44 |
| 38 | Rosedale | Lockport | 637.9m | crinoid | calcite | 2.67 | -2.81 |
| 39 | Rosedale | Guelph | 627.3m | fibrous calcite in sol'n cavity | calcite | 2.25 | -3.39 |
| 40 | Rosedale | A-1 Carb | 524.9m | coralline algal carbonate | dolomite | 3.39 | -6.36 |
| 41 | Rosedale | Lockport | 659.6m | dolomitized platform | dolomite | 3.22 | -4.21 |
| 42 | Rosedale | Guelph | 611.1m | brachiopod/dolo silt | calcite | 3.23 | -1.50 |
| 43 | Rosedale | Guelph | 626.7m | bryozoan | calcite | 3.11 | -0.33 |
| 44 | Rosedale | Guelph | 626.7m | saddle dolomite | dolomite | 3.05 | -5.86 |
| 45 | Rosedale | Guelph | 609.7m | late clear calcite | calcite | 2.32 | -7.67 |
| 46 | Rosedale | Guelph | 545.6m | calcite paleosol, with clasts | calcite | 3.96 | -7.06 |
| 47 | Rosedale | Guelph | 608.4m | saddle dolomite | dolomite | 1.95 | -9.14 |
| 48 | Rosedale | Guelph | 546.8m | stromatoporoid | calcite | 4.93 | -6.67 |
| 49 | Rosedale | Guelph | 533.7m | algal laminated crust | calcite | 2.77 | -6.56 |
| 50 | Rosedale | Guelph | 540.1m | calcite in paleosol | calcite | 3.62 | -6.93 |
| 51 | Rosedale | Guelph | 556.9m | calcite in paleosol | calcite | | |
| 52 | Rosedale | Guelph | 608.4m | vadose silt | calcite | | |
| 53 | Rosedale | Guelph | 610.8m | vadose silt | calcite | | |
| 54 | Rosedale | Guelph | 527.5m | caliche | calcite | | |

| | | | | | |
|----|----------|--------|--------|----------------------------------|---------|
| 55 | Rosedale | Guelph | 627.9m | clear calcite final pore fill | calcite |
| 56 | Rosedale | Guelph | 627.9m | 1st phase pore fill | calcite |

Blank values indicate sample lost at U. of C. laboratory.

CONVERSION FACTORS FOR MEASUREMENTS IN ONTARIO GEOLOGICAL SURVEY PUBLICATIONS

| Conversion from SI to Imperial | | | Conversion from Imperial to SI | | |
|--------------------------------|----------------------|------------------------------|--------------------------------|------------------------|-----------------|
| <i>SI Unit</i> | <i>Multiplied by</i> | <i>Gives</i> | <i>Imperial Unit</i> | <i>Multiplied by</i> | <i>Gives</i> |
| LENGTH | | | | | |
| 1 mm | 0.039 37 | inches | 1 inch | 25.4 | mm |
| 1 cm | 0.393 70 | inches | 1 inch | 2.54 | cm |
| 1 m | 3.280 84 | feet | 1 foot | 0.304 8 | m |
| 1 m | 0.049 709 7 | chains | 1 chain | 20.116 8 | m |
| 1 km | 0.621 371 | miles (statute) | 1 mile (statute) | 1.609 344 | km |
| AREA | | | | | |
| 1 cm ² | 0.155 0 | square inches | 1 square inch | 6.451 6 | cm ² |
| 1 m ² | 10.763 9 | square feet | 1 square foot | 0.092 903 04 | m ² |
| 1 km ² | 0.386 10 | square miles | 1 square mile | 2.589 988 | km ² |
| 1 ha | 2.471 054 | acres | 1 acre | 0.404 685 6 | ha |
| VOLUME | | | | | |
| 1 cm ³ | 0.061 02 | cubic inches | 1 cubic inch | 16.387 064 | cm ³ |
| 1 m ³ | 35.314 7 | cubic feet | 1 cubic foot | 0.028 316 85 | m ³ |
| 1 m ³ | 1.308 0 | cubic yards | 1 cubic yard | 0.764 555 | m ³ |
| CAPACITY | | | | | |
| 1 L | 1.759 755 | pints | 1 pint | 0.568 261 | L |
| 1 L | 0.879 877 | quarts | 1 quart | 1.136 522 | L |
| 1 L | 0.219 969 | gallons | 1 gallon | 4.546 090 | L |
| MASS | | | | | |
| 1 g | 0.035 273 96 | ounces (avdp) | 1 ounce (avdp) | 28.349 523 | g |
| 1 g | 0.032 150 75 | ounces (troy) | 1 ounce (troy) | 31.103 476 8 | g |
| 1 kg | 2.204 62 | pounds (avdp) | 1 pound (avdp) | 0.453 592 37 | kg |
| 1 kg | 0.001 102 3 | tons (short) | 1 ton (short) | 907.184 74 | kg |
| 1 t | 1.102 311 | tons (short) | 1 ton (short) | 0.907 184 74 | t |
| 1 kg | 0.000 984 21 | tons (long) | 1 ton (long) | 1016.046 908 8 | kg |
| 1 t | 0.984 206 5 | tons (long) | 1 ton (long) | 1.016 046 908 8 | t |
| CONCENTRATION | | | | | |
| 1 g/t | 0.029 166 6 | ounce (troy)/ ton (short) | 1 ounce (troy)/ ton (short) | 34.285 714 2 | g/t |
| 1 g/t | 0.583 333 33 | pennyweights/ ton (short) | 1 pennyweight/ ton (short) | 1.714 285 7 | g/t |

OTHER USEFUL CONVERSION FACTORS

| | <i>Multiplied by</i> | |
|--------------------------------|----------------------|-------------------------------|
| 1 ounce (troy) per ton (short) | 20.0 | pennyweights per ton (short) |
| 1 pennyweight per ton (short) | 0.05 | ounces (troy) per ton (short) |

Note: Conversion factors which are in bold type are exact. The conversion factors have been taken from or have been derived from factors given in the Metric Practice Guide for the Canadian Mining and Metallurgical Industries, published by the Mining Association of Canada in co-operation with the Coal Association of Canada.

3268
ISSN 0826-9580
ISBN 0-7778-1225-8

OFR 5850

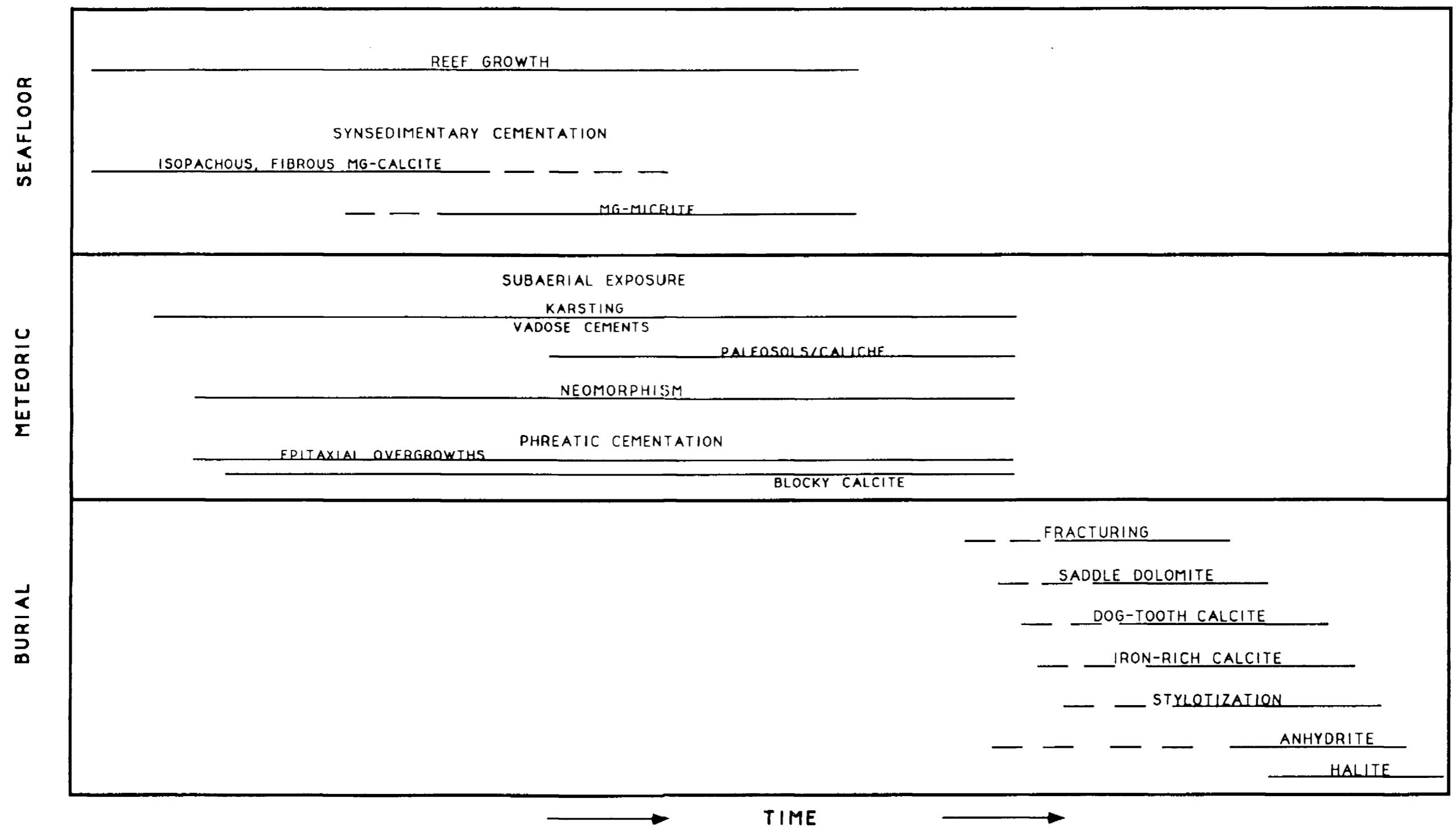


Figure 30: Generalized diagram showing the relative timing of diagenetic events from the three diagenetic environments. Because of alternating reef growth and subaerial exposure, seafloor and meteoric diagenesis are shown to act simultaneously. Burial diagenesis post-dates both seafloor and meteoric but may have started lower down in the pinnacles while the tops are still exposed. Diagram not to scale. Please see text for discussion.

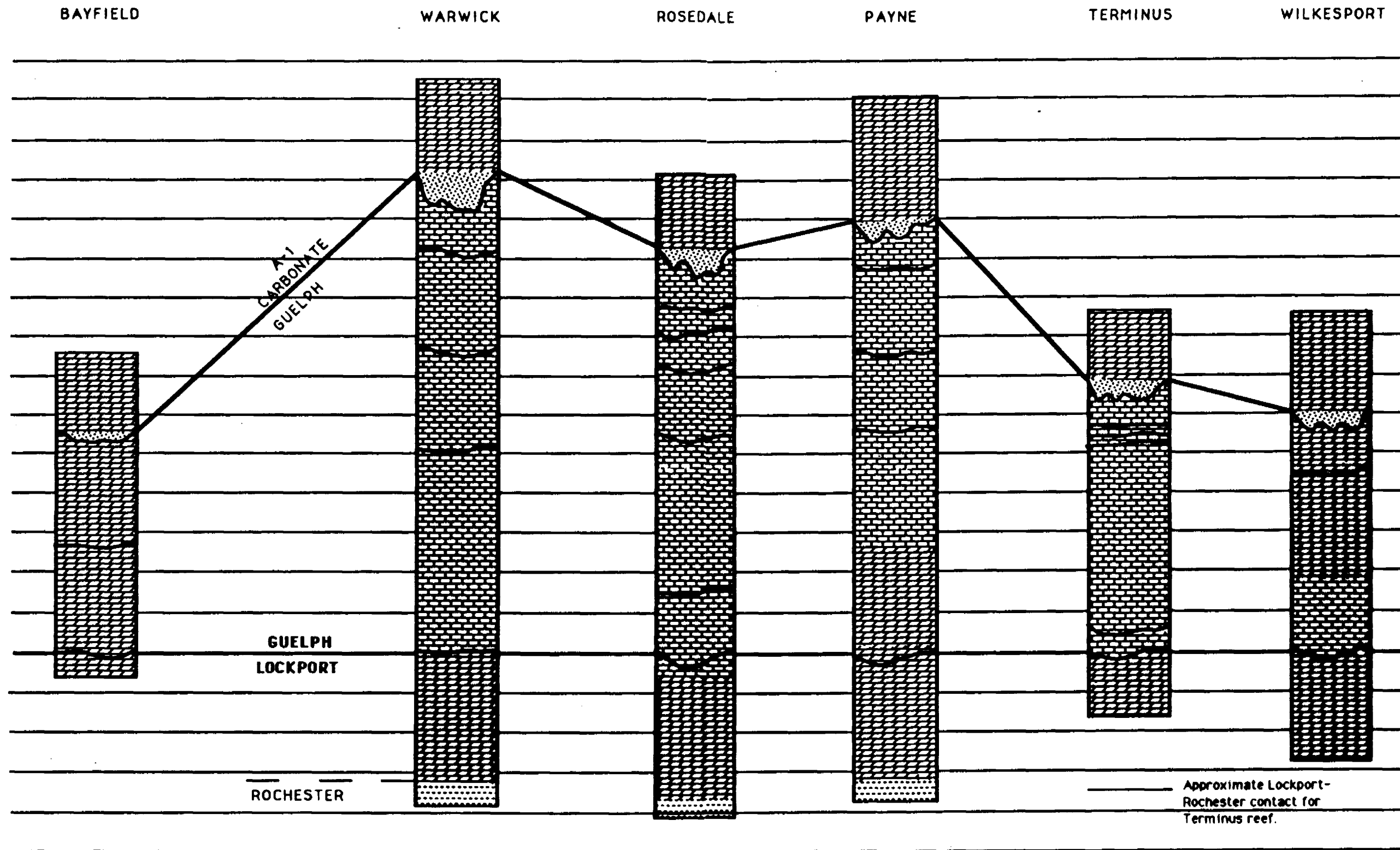


FIGURE 25: Correlation of detected exposure surfaces between all six pinnacle reefs using the top of the first karst event as a datum. Thick lines represent subaerial exposure features that can be identified in all pinnacles. Thin lines represent 10 m of vertical section. Only the first and last exposure events can be correlated between all six pinnacle bioherms. Vertical scale is 1 cm = 10 m. The top of the Rochester Formation in the Terminus pinnacle was obtained using data from the Ram # 6 core.

OFR 5850

PAYNE

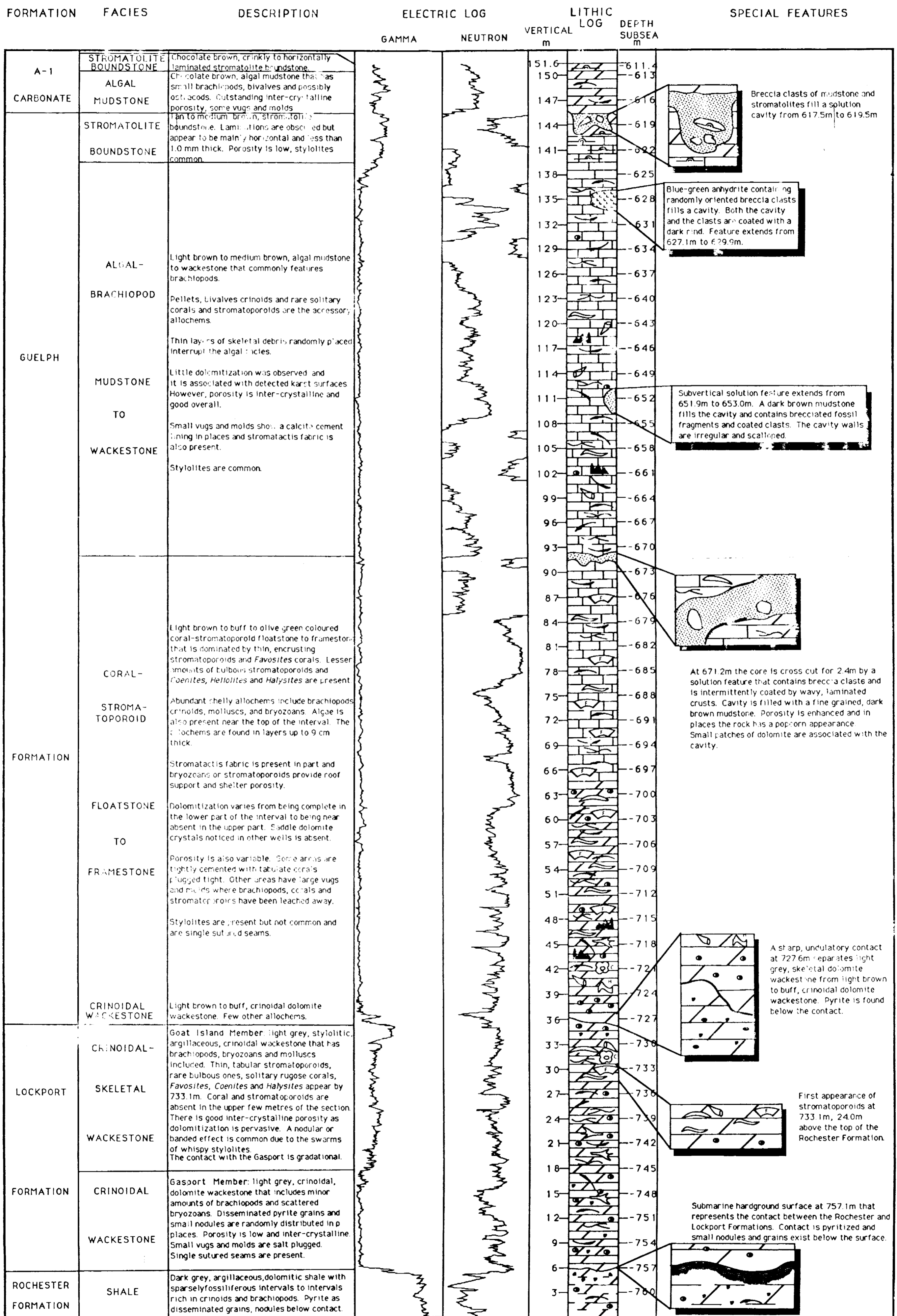


Figure 24: Lithologic column for the Payne pinnacle reef bioherm based on data from the Imperial Payne # 4 well. Electric log response and subaerial exposure features are also shown.

OFR 5850

WILKESPORT

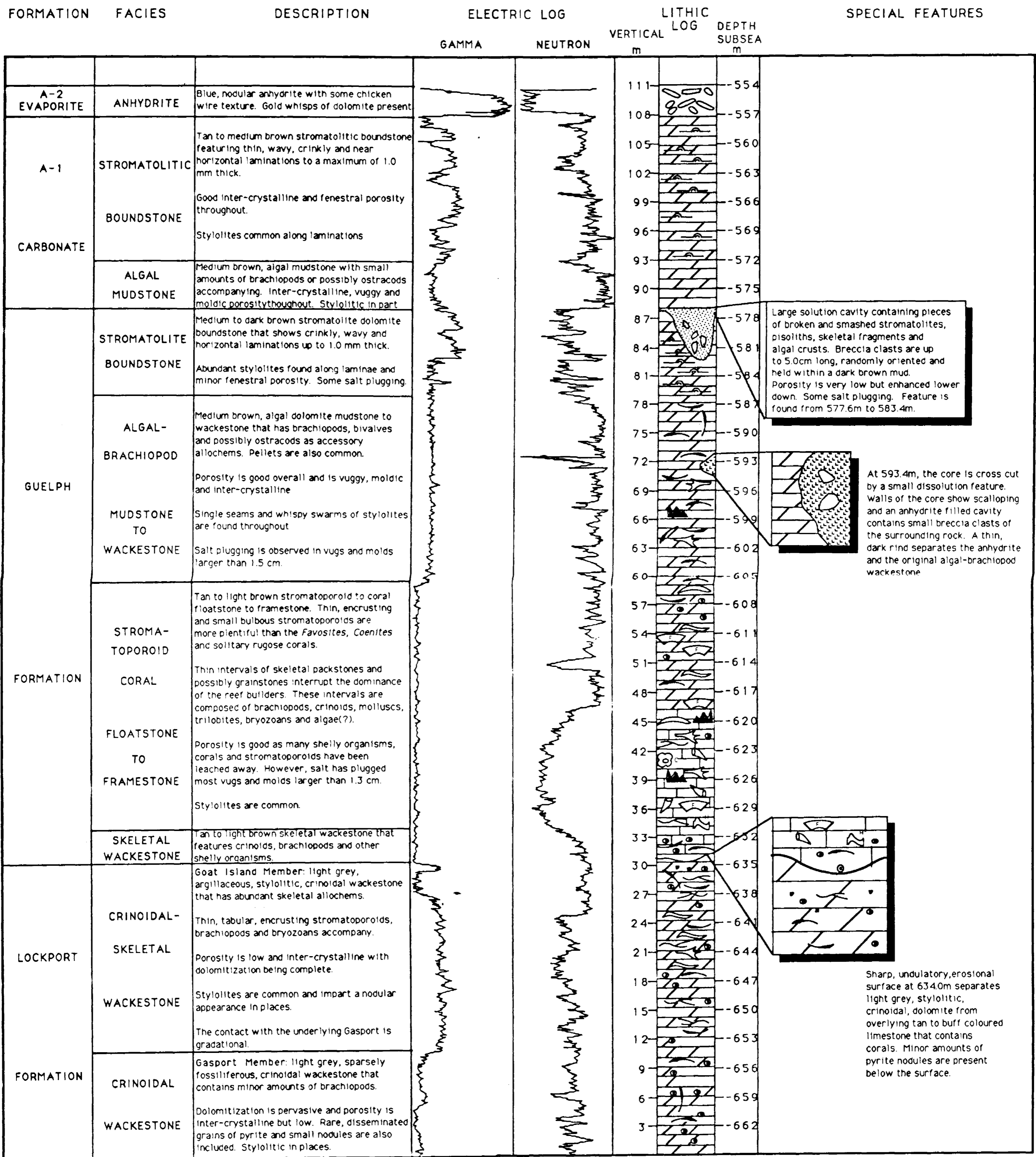


Figure 23: Lithologic column for the Wilkesport pinnacle reef bioherm based on data from the Imperial Sombra 4-14-13 well. Electric log response and subaerial exposure features are also shown.

OFR 5850

BAYFIELD

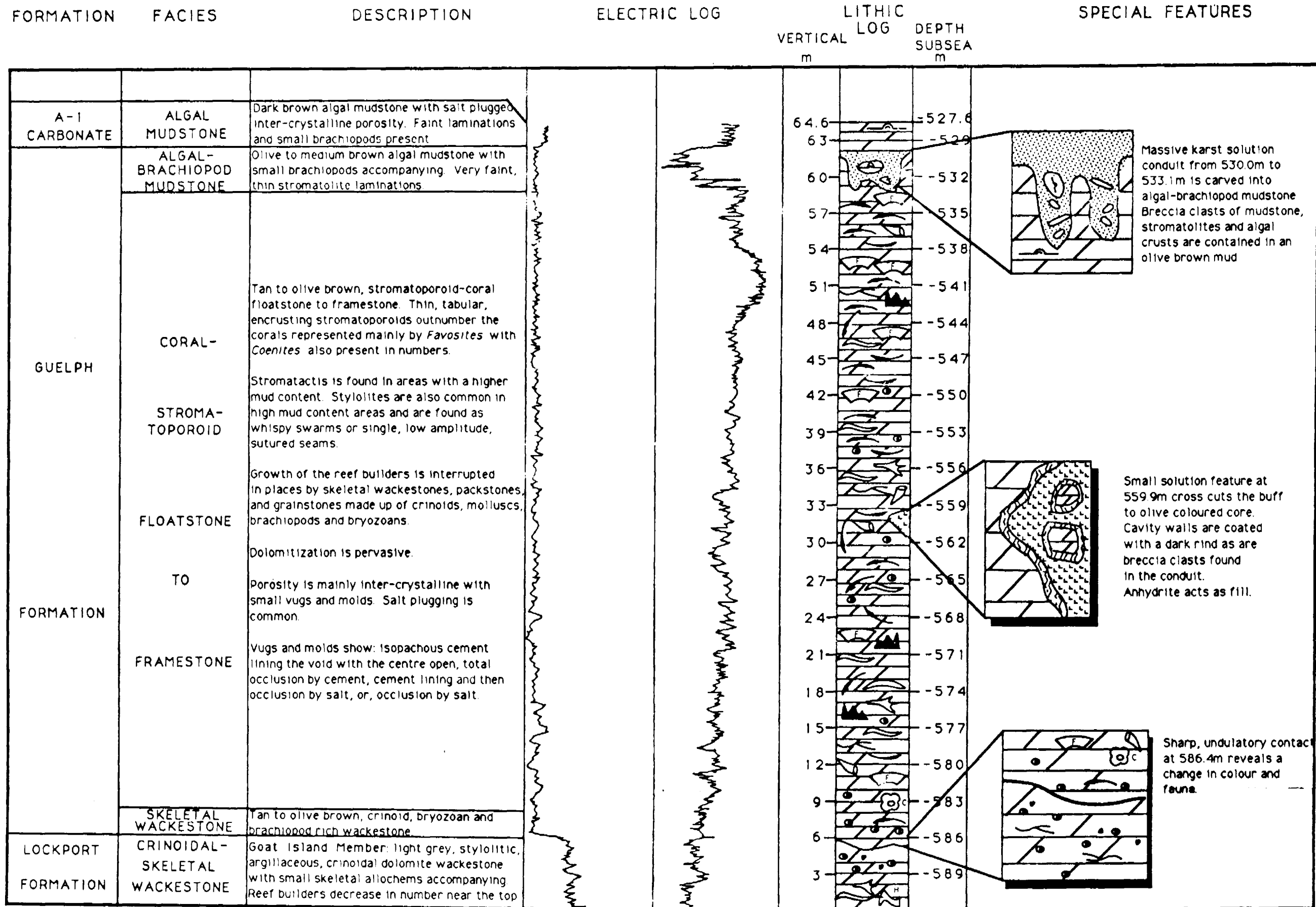


Figure 22: Lithologic column for the Bayfield pinnacle reef bioherm based on data from the Bluewater-Imperial Porter No. 1 well. Electric log response and subaerial exposure features are also shown

OFR 5850

TERMINUS

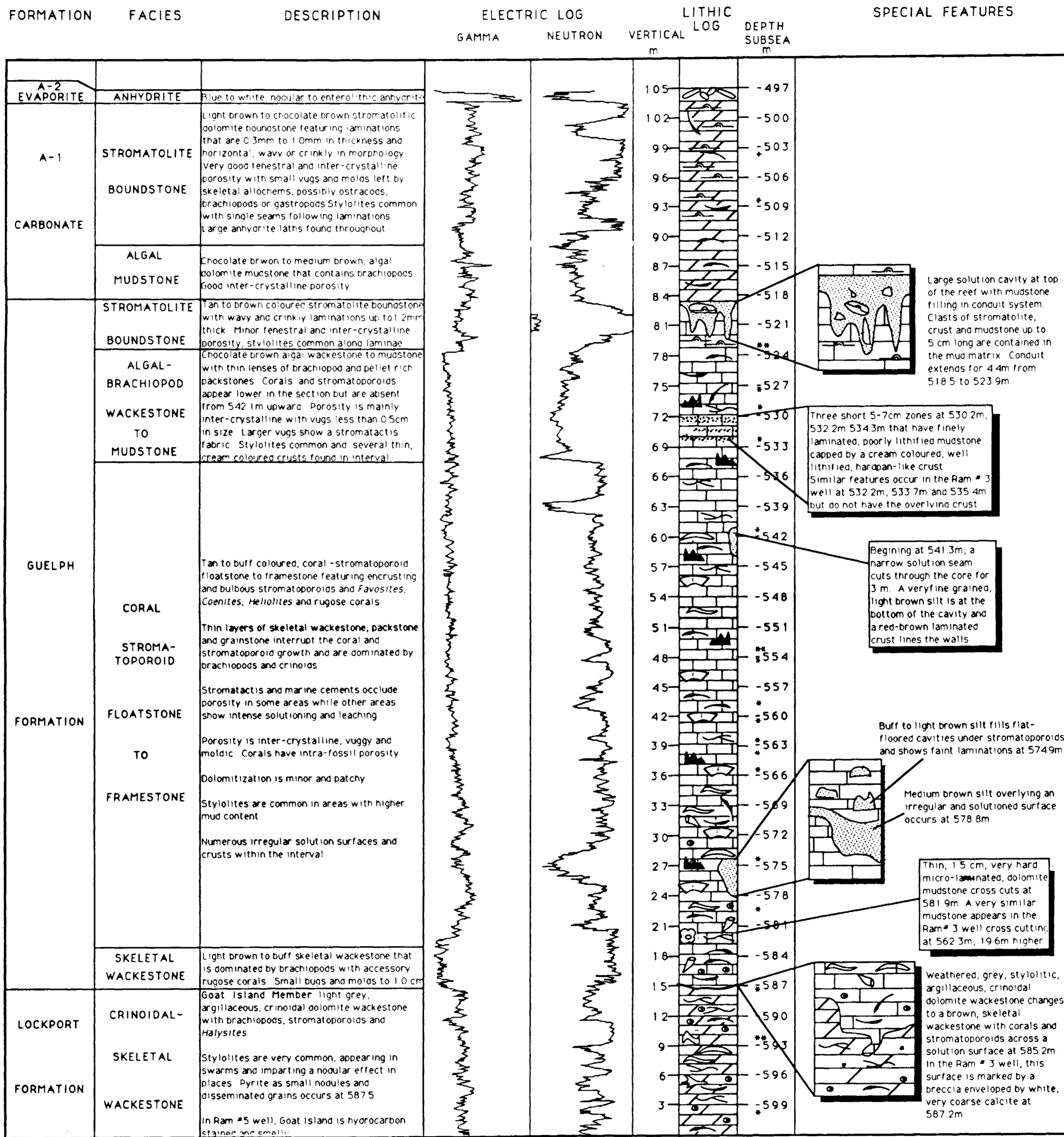


Figure 21: Lithologic column for the Terminus pinnacle reef bioherm based on data from the Ram # 5 and Ram # 3 wells. Electric log response and subaerial exposure features for the Ram # 5 well are also shown.

OFR 5850

ROSEDALE

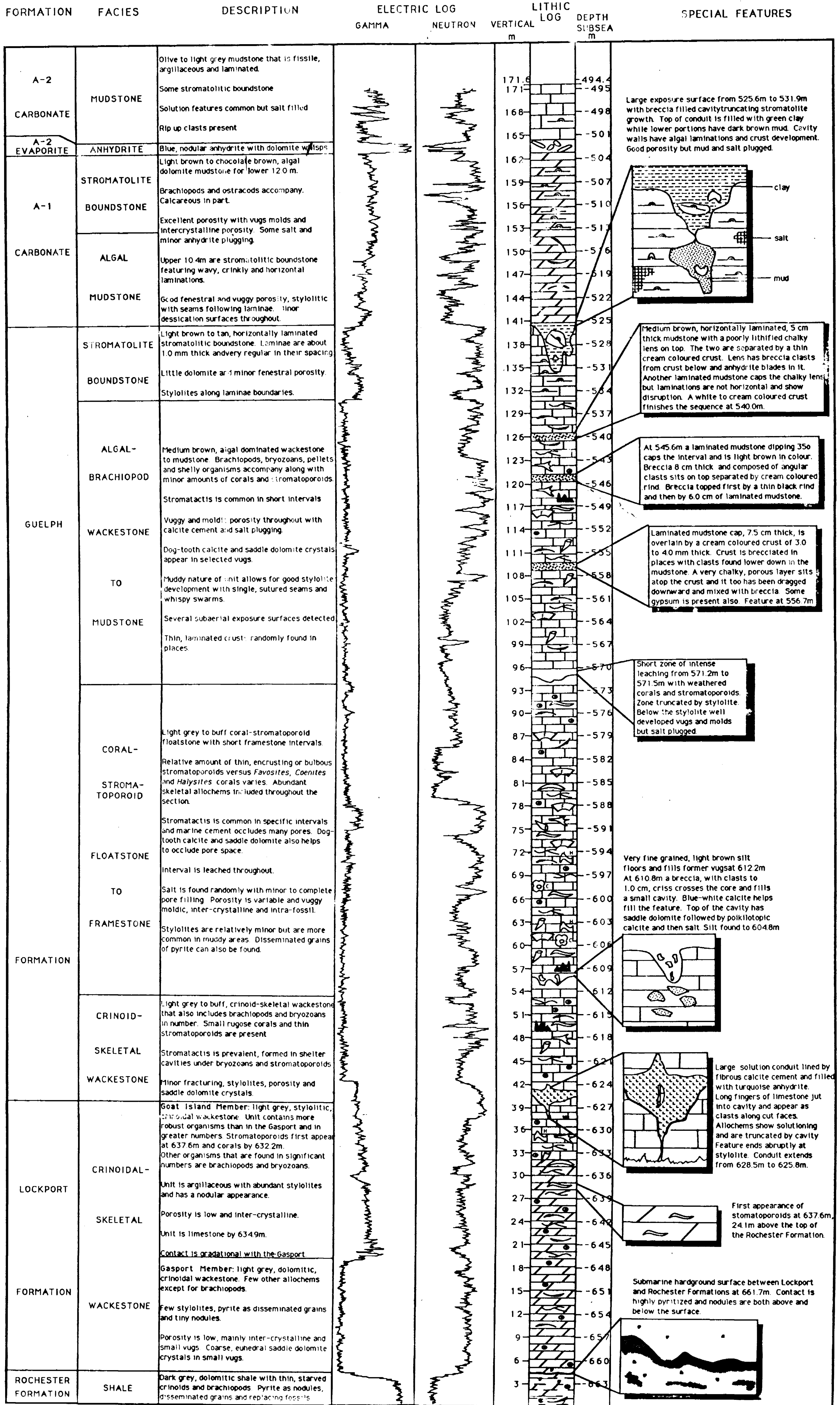


Figure 20: Lithologic column for the Rosedale pinnacle reef bioherm based on data from the ... (text partially obscured) ... features are also shown

OFR 5850

